Pharmaceutical Analysis of Polyamines and Aminoglycosides

Buranaphalin, Sawanya

Award date:
2009

Awarding institution:
University of Bath

Pharmaceutical Analysis of Polyamines and Aminoglycosides

Sawanya Buranaphalin

A thesis submitted for the degree of Doctor of Philosophy

University of Bath

Department of Pharmacy and Pharmacology

April 2009

Abstract

Methods for polyamine derivatization with a panel of extrinsic fluorophores followed by HPLC with fluorescence and UV absorption detection have been developed. Four fluorophores were examined using polyamines and aminoglycosides. *o*-Phthalaldehyde (OPA) and fluorescamine are selective fluorophores that only react with primary amines; 9-fluorenylmethyl chloroformate (FMOC Cl) and dansyl chloride react with both primary and secondary amines. Reaction and HPLC conditions were optimized with each of the above fluorophores using a series of model mono- and diamines and then applied to natural and semi-synthetic polyamines. The amines that have been investigated are natural di- and polyamines: putrescine, cadaverine, spermidine, spermine, thermospermine, aminoglycosides: kanamycin, paramomycin, neomycin, and synthetic polyamine conjugates *e.g.* N^4,N^9-dioleoylspermine, N^1-cholesteryl spermine carbamate. The resultant derivatives were confirmed by off-line high resolution electrospray ionization mass spectrometry (HR ESI MS).

The results show that the synthesis of polyamine derivatives in quantitative yield depends on the time of reaction, the temperature and the ratio of fluorophore reagent. Linearity of derivatization was calculated and regression coefficients ranged from 0.968 to 0.999 with good reproducibility. HR ESI MS analysis of the reaction products demonstrated complete derivatization of both primary and secondary amino groups with dansyl and FMOC fluorescence derivatives and of primary amine groups for OPA and fluorescamine derivatives. Under the ionization conditions used the dansyl derivatives showed, in addition to monovalent ions $[M+H]^+$, divalent cations $[M+2H]^{2+}$ because this chromophore contains a basic amine that can be easily protonated. FMOC derivatives gave prominent $[M+Na]^+$ ions. The OPA derivatization reaction is rapid, but the products have poor stability. The derivatization with fluorescamine gave multiple products with glucosamine due to the presence of a chiral centre in the fluorophore. The relative quantum yields of the polyamine-fluorophore derivatives were examined to determine the effect of intramolecular fluorescence quenching. Dansylation is the fluorescent derivatization method of choice.

Acknowledgements

I am really thankful to my supervisors Dr. Ian S. Blagbrough and Dr. Michael G. Rowan for their valuable guidance, supervision and support all through the years of this work without which this work would not have been possible.

I thank the research and technical staff at the University of Bath: Jo Carter, Kevin Smith, Don Perry and Rod Murray. I am also grateful to Dr. Timothy J. Woodman, for his help with the detailed NMR spectroscopy, Christian Rehbein, for his help with HR-ESI-MS, and Ade Olatokun for his help in computer-related problems.

I also gratefully acknowledge the Royal Thai Government and the Collaborative Research Networks for the financial support.

I thank all my colleagues in 5W 3.14 laboratory: Dr. Osama Ahmed; Dr. Daniel Furkert; Dr. Benjamin Greedy; Dr. Francessca Giuntini who have helped me when I have had chemistry problems; Dr. Mostafa Soltan who kindly provided his synthesized chemicals; Dr Noppadon Adjimatera; Dr. Pilan Saensuk and Supattra Rungsimakan who encouraged me, and also Dr. Soad Bayoumi; Manal Elmasry; Abdelkader Metwally; and Yuxi Chen. I also thank my housemate Dr. Adriana Ibrahim who gave me a lot of encouragement.

Finally, I would especially like to thank my family, for their love, tolerance, vital encouragement, tremendous help and infinite patience.

Abbreviations

Å	angstrom
aq	aqueous
^{o}C	degrees Celsius
CNLSD	condensation nucleation light scattering detector
COSY	correlated spectroscopy
DCM	dichloromethane
DEPT	Distortionless Enhancement by Polarization Transfer
DNS Cl	dansyl chloride
e.g.	*exempli gratia*, for example
ELISA	enzyme-linked immunosorbent assay
et al.	*et alii*, and others
etc.	*et cetera*, and so forth)
FMOC Cl	9-fluorenylmethyl chloroformate
GC	gas chromatography
h	hour
HPLC	high performance liquid chromatography
HR-ESI-MS	high resolution-electrospray ionization-mass spectrometry
Hz	Hertz
i.e.	*id est*, that is
IR	infrared
J	coupling constant
λ_{ex}	excitation wavelength
λ_{em}	emission wavelength
λ_{max}	wavelength at maximum absorption
LC-MS	liquid chromatography-mass spectrometry
µ, µm	micron, micrometre
mM	millimolar
M	molar
MCE	mercaptoethanol
Me	methyl
MeCN	acetonitrile
µL	microlitre
mL	millilitre
mp	melting point

M.W.	relative molecular weight
m/z	mass over charge
nm	nanometre
NMR	nuclear magnetic resonance
ODC	ornithine decarboxylase
ODS	octadecyl silane
OPA	*o*-phthaladehyde
ppm	part per million
RIA	radio immunoassay
Rt	retention time
RP-HPLC	reverse phase-high performance liquid chromatography
TLC	thin layer chromatography
UV	ultraviolet
v/v	volume by volume

Contents

	Page
Abstract	ii
Acknowledgements	iii
Abbreviations	iv
Contents	vi
Chapter 1: Introduction	1
1.1 Polyamines - general introduction	1
1.2 Occurrence of polyamines in biological materials	4
1.3 Physical properties	9
1.4 Biological roles and pharmacological effects of polyamines	12
1.5 Analysis of polyamines	14
1.6 Aims of the study	18
Chapter 2: Experimental	19
2.1 Materials and general methods	19
2.2 *o*-Phthalaldehyde (OPA)/mercaptoethanol (MCE) derivatization	22
2.3 *o*-Phthalaldehyde (OPA)/mercaptoethanol (MCE)/9-fluorenylmethyl chloroformate (FMOC) derivatization	30
2.4 Fluorescamine derivatization	31
2.5 9-Fluorenylmethyl chloroformate (FMOC Cl) derivatization	33
2.6 Dansylation derivatization	41
2.7 Synthesis of thermospermine	49
2.8 Purification of intermediates	55
2.9 Analysis of thermospermine and spermine	56
Chapter 3: Selective polyamine derivatizations	59
3.1 Primary amine-*o*-phthalaldehyde/mercaptoethanol (OPA/MCE) derivatization	59
3.2 Primary amine-fluorescamine derivatives	92
Chapter 4: Derivatization of primary and secondary amines with 9-fluorenylmethyl chloroformate (FMOC Cl)	104
Chapter 5: Derivatization of primary and secondary amines with dansyl chloride	134
Chapter 6: Thermospermine synthesis	172
General conclusions	220
References	229
Appendix	245

CHAPTER 1: INTRODUCTION

1.1 Polyamines - general introduction

Polyamines, the diamines putrescine (1,4-diaminobutane), cadaverine (1,5-diaminopentane), the triamine spermidine (*N*-(3-aminopropyl)-1,4-diaminobutane) and the tetraamine spermine (*N*,*N*^{1}-bis-(3-aminopropyl)-1,4-diaminobutane), are non-protein nitrogenous bases that are ubiquitous in living organisms (Seiler *et al*., 1978). Although they were discovered many years ago, are relatively unfamiliar to most investigators because they have no striking or acute pharmacological effects, and because the significance of their presence was not known. In recent years, several observations and many analytical studies have shown the occurrence of polyamines in various species of living organism such as in bacteria, in plants and in animal tissues (Hamana *et al.*, 1992, 1993, 1994). Polyamines constitute a group of cell components that are important in biochemical processes, mainly in cell proliferation and cell differentiation (Bauza *et al.*, 1995). As they are polybasic in nature, polyamines have a high affinity for cellular polyanions. Indeed, there is increasing interest in the actions of polyamines on polynucleic acids, as the polyvalent cations titrate poly(anionic) phosphate.

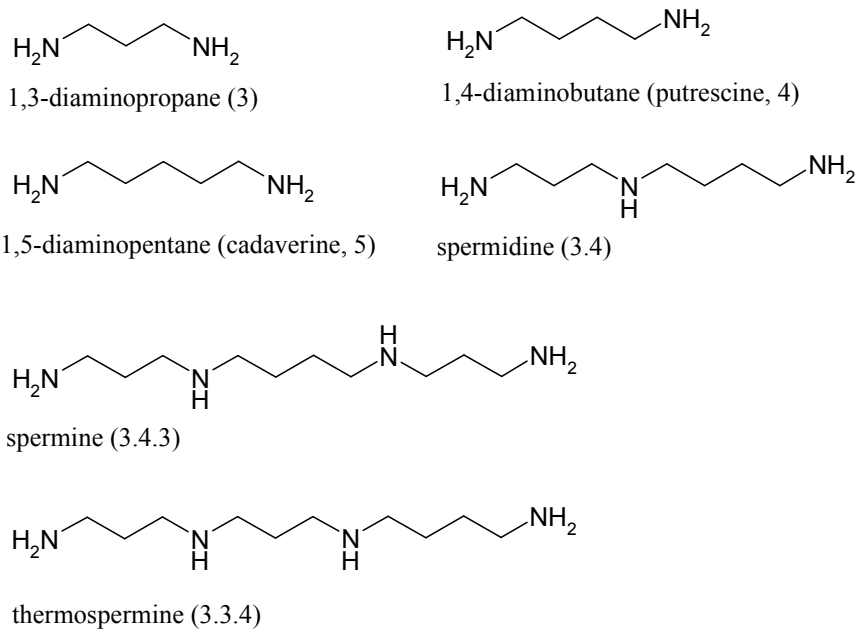

Figure 1.1 Naturally occurring di- and polyamines (the nomenclature reflects the methylene count in the spacing between nitrogen atoms).

The separate classification of polyamines and monoamines is based on the fact that the two types of compounds exhibit a number of quite different characteristics. The polyamines are, in the main, linear aliphatic molecules. The polymer-like nature of polyamines has led to an abbreviated way of denoting their structures. The molecule starts with a primary amino group (H_2N-) link to a chain of methylene groups (-CH_2-) interspersed with secondary amino group (-NH-) and terminates with another primary amino group (-NH_2); the structure can be described simply by denoting the number of carbons between each amino group. Thus putrescine is shown as 4, spermidine 3.4, spermine 3.4.3, its regioisomer thermospermine 3.3.4 etc. The structures of some simple linear naturally occurring di- and polyamines are shown in Figure 1.1.

In 1678, the early period of the Scientific Revolution, Antoni van Lewenhoeck examined various fluids include samples of human semen with the aid of a microscope. He reported the existence of motile sperm (spermatozoa) in semen (Lewenhoeck, 1678) and described crystals that formed when left to cool. These crystals are now known to be spermine phosphate which is a source of a semen-like odour (Rosenheim, 1924). From the early period, it was believed that the compound spermine was uniquely present in human semen. There were several experiments and observations during this period, various names were given to the crystals. In 1878, Schreiner described spermine as a substance present in many mammalian tissues not only in semen and he was the first to identify the crystals correctly as spermine phosphate (Schreiner, 1878). In the period of 1923 to 1927, the correct chemical structure of spermine was established, determined and confirmed by synthetic spermine (Dudley *et al.*, 1924, 1925, 1926; Rosenheim, 1924; Wrede *et al.*, 1923, 1924, 1925, 1926, 1927). The diamines' history is shorter than that of spermine. 1,4-Diaminobutane (putrescine) and 1,5-diaminopentane (cadaverine) were first described in decomposing animal material, in cadavers by Brieger in 1885 (Middlebrooks *et al.*, 1988), and in urine of cystinuric patients (Bremer and Kohne, 1971). The structures were established by comparison with synthetic diamines.

Due to their p*K*a values, putrescine, cadaverine, spermidine and spermine are di- and polycations under physiological conditions and exhibit net charges close to 2^+, 2^+, 3^+ and 4^+, respectively. The polyamines form complexes, especially with polyanionic compounds *i.e.* RNA and DNA and with nucleic acid containing structures and membranes. Spermidine and spermine are particularly flexible and have charge distribution along the whole molecule, thus facilitating greater interaction with the negatively charged backbone of DNA (Teti *et al.*, 2002). This reduces the net charge and increases the conformational stability of the molecules (Liquori *et al.*, 1967). These interactions form the basis for the role of polyamines

in cell metabolism at the replication, transcriptional, and post-transcriptional levels. Their involvement in processes related to cell growth and cell differentiation has attracted much interest recently. There is also evidence suggesting a role for polyamines in programmed cell death (Hawell *et al.*, 2002). As polyamines are synthesized by amino acid decarboxylation reactions which consume H^+, polyamine accumulation may function as part of a homeostatic mechanism to keep intracellular pH at a constant value. Rapidly growing tissues usually have higher amounts of polyamines and they have stimulating effects on DNA, RNA and protein synthesis. Conversely, severe depletion of polyamines reduces growth in mammalian cells (Gugliucci, 2004).

Polyamines are reported to have a role in the prevention of nerve damage and duodenal mucosal repair. Spermine has been recommended for the treatment of human prostate cancer separately and in combination with other anticancer drugs (Ernestus, 2001). One report indicated the functions of the polyamines as growth factors; antioxidants; stabilizers of DNA, RNA, membranes; metabolic regulators; nutrients and second messengers (Ekegren, 2005). Spermidine and spermine bind to the phosphate backbone of poly-nucleic acids. This interaction is mostly based on electrostatic interactions between positively charged ammonium groups of the polyamines and the negatively charged phosphates of the poly-nucleic acids. Spermine is an important reagent widely used to precipitate DNA in molecular biology protocols. Spermidine and spermine are derivatives of putrescine which is produced from L-ornithine by the action of ornithine decarboxylase (ODC). Spermidine and spermine levels are also affected by the rate of conversion of their respective precursors, putrescine and spermidine. Also, it is known that the reverse conversions of spermine into spermidine, and spermidine into putrescine are also important (Khuhawar, 2001).

Early polyamine research was concentrated in the field of cancer and relatively little polyamine research was neuroscience related. However, further research revealed the existence of uptake and release mechanisms for brain polyamines, as seen with other substances more commonly accepted as neurotransmitters (Ekegren, 2004). Polyamines also play a regulatory role in cellular calcium homeostasis and have a metabolism that is deregulated in response to cerebral trauma or ischaemia (Moinard, 2005).

In most cells polyamines are the products of a highly regulated biosynthetic pathway. It is not clear whether the elaborate regulation of polyamine synthesis is a consequence of their essential roles in cellular differentiation and development, or part of a defence mechanism to prevent over accumulation of compounds that are toxic in excess (Sairam and Tyagi, 2004). In addition to their biosynthetic capability, many cells also process transport systems for

polyamines that respond to intracellular polyamine levels, and other stimuli, and are regulated by mechanisms that are at present incompletely defined.

The widespread occurrence of a variety of polyamine-oxidizing enzymes in animals, plants, bacteria and fungi results in the formation of aminoaldehydes as intermediates. These compounds containing one or more amino groups that will be positively charged at physiological pH, and an aldehyde functional groups are highly reactive. Aminoaldehydes have been shown to be cytotoxic to a wide variety of cell types (Yu, 2003). It is not yet clear whether these compounds have any biological function or are merely unstable and rapidly degraded intermediates in the polyamine catabolic pathway.

Intracellular polyamine concentrations vary throughout the cell cycle. An increase in polyamine synthesis is a very early event in cell proliferation and takes place before any increase in protein or nucleic acid synthesis. Thus, the polyamine biosynthetic pathway presents an attractive target in tumour and proliferative disease chemotherapy (Jänne *et al.*, 2004; Wallace and Niiranen, 2007). Inhibitors of polyamine biosynthesis have been used successfully in the treatment of some protozoan diseases such as African trypanosomiasis (Heby *et al.*, 2007).

Adequate intracellular levels of polyamines are necessary for optimal growth and replication of animals, plants, bacteria, fungi, protozoa, and probably all living organisms (Jänne *et al.*, 1978; Tabor and Tabor, 1984; Wallace *et al.*, 2003; Luo *et al.*, 2009). Polyamines influence the transcriptional and translational stages of protein synthesis, interact with the nucleic acids, stabilized membranes, alter intracellular free calcium, and have important neurophysiological functions (Bernsteina and Müller, 1995). Fruit-ripening and flower-setting processes in plants are modulated by polyamines (Toumadje and Richardson, 1988).

1.2 Occurrence of polyamines in biological materials

The three most commonly occurring natural polyamines are putrescine, spermidine, and spermine, together with 1,3-diaminopropane and cadaverine. One or more of these compounds are present in every living cell. All have been found in eukaryotes, but spermine is rare in prokaryotes or might be replaced by thermine (norspermine, 3.3.3) and thermospermine (3.3.4). In addition to spermine, spermidine and putrescine, a large number of other linear, and some branched-chain, polyamines have been detected in mammalian tissues and excreta, or in plants, bacteria and microorganisms (Hamana *et al.*, 1993, 1994).

Polyamine moieties are constituents of many compounds found in plants and insects. Putrescine, spermidine or spermine containing alkaloids are found in many plants, non-proteinaceous spider and wasp toxins, and glutathionyl-spermidine conjugates in some pathogenic microorganisms (Bollinger, 1995).

Polyamines in animal tissues

The highest concentrations of spermidine and spermine in animal tissues are found in the pancreas, prostate, and human semen (Bolliger, 1935; Dudley *et al.*, 1924, 1927; Harrison, 1931, 1933; Rosenthal, 1958; Wrede, 1925). The polyamines in human semen are largely in the seminal plasma, rather than in the spermatozoa. The concentration of diamines is very low in animal tissues, and they are accordingly difficult to determine with accuracy or specificity. However, several reports have shown the presence of diamines in animal tissues. 1,3-Diaminopropane has been found in rat and guinea pig liver, and in human semen (Weaver and Herbst, 1958). 1,4-Diaminobutane has been found in the pancreas (Fischer and Bohn, 1957) and liver (Weaver and Herbst, 1958) of several species, in ox lung, in bovine brain, in pig brain, in human semen, in pupae and caterpillars of the silkworm (Weaver and Herbst, 1958). 1,5-Diaminopentane was found in liver. Although most of the polyamines in animal tissues are present as free amines, some minor components are present in conjugated form *e.g.* conjugates of spermine and 1,3-diaminopropane with phenolic acids are found in the venoms of certain species of spider and wasp as acylpolyamines (Figure 1.2) (Schafer *et al.*, 1994, Chesnov *et al.*, 2002). Spider *Paracoelotes birulai* produced venoms which contained guanidine derivative PA 3334G (Figure 1.3) (Chesnov *et al.*, 2002). The first polyamine alkaloid with the 1,4-diguanidinobutane moiety is Stellettadine A (Figure 1.4), obtained from a marine sponge *Stelletta* sp. (Tsukamoto *et al.*, 1996).

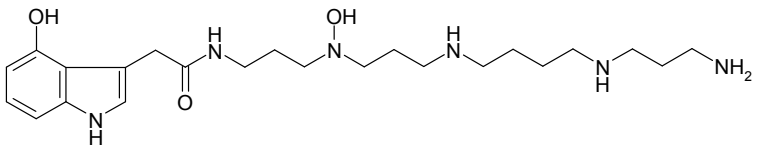

Figure 1.2 A spider venom acylpolyamine

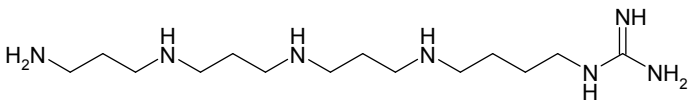

Figure 1.3 Guanidine derivative of polyamine (PA 3334G)

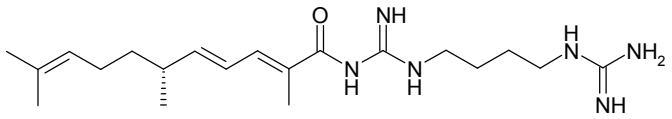

Figure 1.4 Stellettadine A

The functions of polyamines in animals are reported (Thomas and Thomas, 2003; Childs *et al.*, 2003; Umekage and Ueda, 2006) as the essential regulators of growth, gene transcription and ribosome-mediated translation.

Polyamines in microorganisms

A very large number of papers have been published on polyamines in a variety of microorganisms such as bacteria and yeast (Tabor and Tabor, 1985; Bachrach, 1961; Dubin and Rosenthal, 1960). The polyamines concentrations of the various bacteria vary with the pH and other cultural conditions for instance gram-positive organisms contained trace or no of polyamines, while high concentration of polyamines were formed in gram-negative organisms (Herbst, 1958). The composition of the culture medium played important role in bacteria uptake, since many organism take up amines from the medium, which results in intracellular content of both the free amines and derivatives (Tabor *et al.*, 1958; Dubin and Rosenheim, 1960). The presence of high concentrations of polyamines in bacteria even when grown on a minimal glucose-salts medium support the concept that these amines are important biological compounds, rather than just a result of detoxification (Silverman and Harris, 1943).

The most abundant polyamines in bacteria are putrescine and spermidine. Cadaverine is also present but less abundant. Thermospermine, an isomer of spermine was found in thermophillic bacterium *Thermus thermophilus* (Oshima, 1979), in Halophilic archaeum *Halobacterium cutirubrum* (Carteni-Farina *et al.*, 1985), in *Agrobacterium* (Hamana *et al.*, 1989), in *Paracoccus denitrificans* (Hamana *et al.*, 1990). There are also a large number of polyamine alkaloids from the skeleton of 1,5-diaminopentane (cadaverine), spermidine and spermine alkaloids. Incorporating a cadaverine backbone, Terragines A-E (Figure 1.5) were isolated from *Streptomyces lividans* (Wang *et al.*, 2000).

Various functions of bacteria polyamines have been reported (Wortham *et al.*, 2007) such as they are the components of outer membrane of gram-negative bacteria, they are important in acid resistance, they play significant role for cellular differentiation, etc.

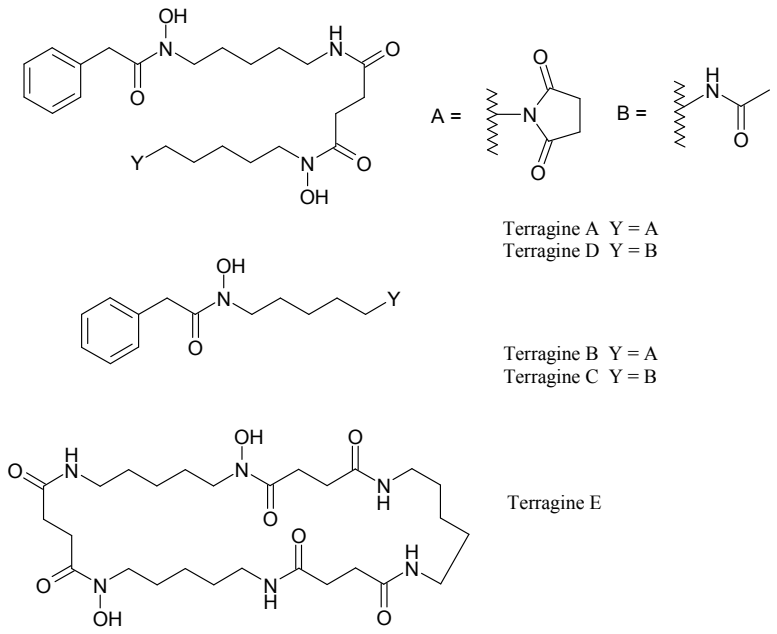

Figure 1.5 Terragines A-E

Polyamines in plants

In plants, putrescine (4), spermidine (3.4), spermine (3.4.3) are concerned as the core portions of ubiquitous polyamines. Cadaverine (5) and thermospermine (3.3.4) are also present in legumes *e.g.* from *Pisum sativum* and *Vicia sativa* (Hamana *et al.*, 1991). However, the less common polyamines such as polyamine (3.3), (3.5), (4.4), (3.3.4.3.3) also found in some alkaloids. Polyamines in plants have been suggested that they play important roles in morphogenesis, growth, embryogenesis, organ development, leaf senescence and stress response (Kumar *et al.*, 1997, Walden *et al.*, 1997, Malmberg *et al.*, 1998, Bouchereau *et al.*, 1999, Liu *et al.*, 2000). Most of compounds from putrescine core are N^1,N^4-diacylputrescine such as hemileptagline (N^1,N^4-bis-(3-(methylthio) propenoyl)putrescine (Figure 1.6) (Saifah *et al.*, 1999), pyramidatine (Figure 1.7) from Aglaia species (Saifah *et al.*, 1993, 1998). These compounds exhibit cytotoxin and antiviral activities. Previously, sulfur-containing amides had been reported as the constituents of the genus Glycosmis of the Rutaceae (Greger *et al.*, 1993). The putrescine alkaloid magnolamide (Figure 1.8), with a substituted pyrrole unit, was isolated by Yu *et al.* (1998) and was synthesized by Dong *et al.* (2002). Many of the polyamine alkaloids reported as cinnamoyl, coumaroyl, caffeoyl, feruloyl, and sinapoyl derivatives of putrescine ((Figure 1.9), spermidine and spermine such as N^1,N^4,N^9-tricoumaroylspermine and N^1,N^4,N^9,N^{12}-tetracoumaroylspermine (Figure 1.10). These compounds are believed to prevent photodamage to nucleic acids during the aerial transport of the pollen.

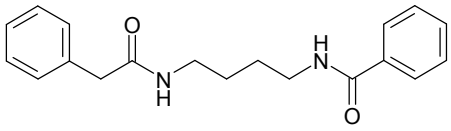

Aglaiduline

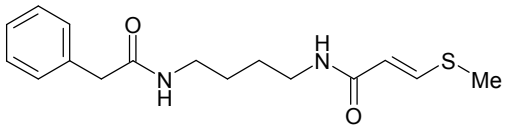

Aglaithioduline

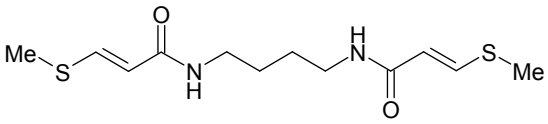

Aglaidithioduline (Hemileptagline)

Figure 1.6 Hemileptagline

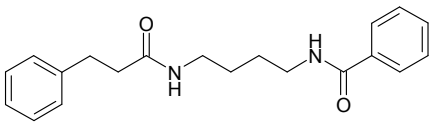

Figure 1.7 Pyramidatine

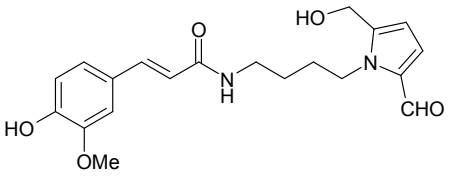

Figure 1.8 Magnolamide

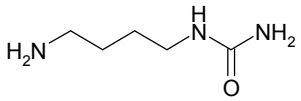

Carbamoylputrescine

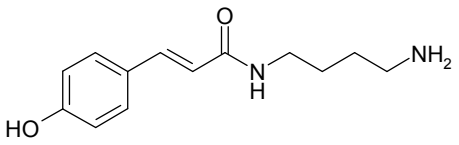

4-Coumaroylputrescine

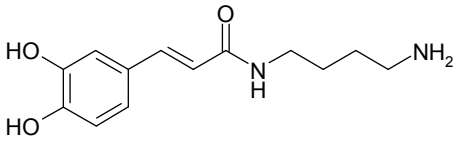

Caffeoylputrescine

Figure 1.9 Putrescine-backbone alkaloids in plants.

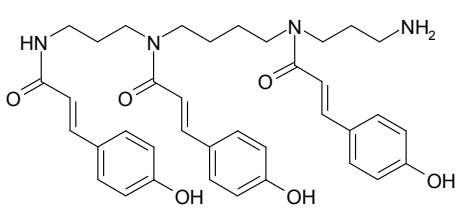

N^1,N^4,N^9-Tricoumaroylspermine

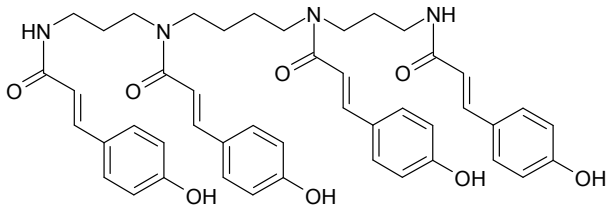

N^1,N^4,N^9,N^{12}-Tetracoumaroylspermine

Figure 1.10 N^1,N^4,N^9-Tricoumaroylspermine and N^1,N^4,N^9,N^{12}-tetracoumaroylspermine

1.3 Physico-chemical properties

Due to the proximity of at least two N-atoms in their structures, polyamines show reactivity that are distinctively different from those of monoamines. Polyamines are small molecular mass molecules, polybasic, water soluble and at physiological pH many of the amino groups are protonated and carry a positive charge. The distinctive names given to the diamines, putrescine and cadaverine, relate to the odour of the free volatile amines, which lack volatility and odour when they exist as their cationic salts. Appropriate combinations of pH and solubility of the amines and their salts in aqueous and organic media were exploited early in the isolation and estimation of the polyamines. The loss of the proton from the protonated amine at alkaline pH generating the free amine is crucial in the isolation and analysis of the natural polyamines.

Basicity and pK_a values of amines

Table 1.1 pK_a values of polyamines by potentiometry (Palmer and Powell, 1974).

Polyamines	pK_a
Putrescine	10.80, 9.63
Spermidine	10.95, 9.98, 8.56
Spermine	10.94, 10.12, 9.04, 7.97

The pK_a values of the various amines in the polyamines have been estimated by a variety of methods. Palmer and Powel (1974) studied pK_a of polyamines by potentiometric titration using glass electrodes (Table 1.1). The initial protonations are on the sterically more accessible (less hindered) primary amines even though secondary amines are more basic. Whereas uncharged amines can frequently penetrate lipid-containing membranes by diffusion (Guarino and Cohen, 1979), charged amines, including the quaternary ammonium

salts, do not cross membranes easily, if at all, in most cellular environments. The other technique used instead of glass electrode potentiometric measurement is spectroscopic, nuclear magnetic resonance (NMR) spectroscopy. By potentiometric titration and by NMR chemical shift measurements, the pK_a values of polyamines were determined (Table 1.2). From ^{13}C-NMR studies it was concluded that in spermidine, the inner secondary amine is protonated only after the complete protonation of the primary amines. Both primary nitrogens appeared to be protonated simultaneously, despite attachment to aliphatic chains of different length. The amine protonation is affected by the length of an intervening aliphatic chain. For spermidine and spermine, the initial protonations are on the primary amines. The uncharged amino groups appeared at values above pH 9.5 (Kimberly and Goldstein, 1981).

Table 1.2 pK_a values of spermidine by difference measurements

Polyamine	pK_a by ^{15}N-NMR (Takeda *et al.*, 1983)	pK_a by ^{13}C-NMR (Takeda *et al.*,1983)	pK_a by ^{1}H-^{13}C NMR (Onash *et al.*, 1984)
Spermidine	11.56, 10.80, 9.52	11.88, 10.77, 9.60	11.02, 10.02, 8.75

Table 1.3 pK_a values of diamines (Martell *et al.*, 1997).

Diamine	pK_a	ΔpK_a	ΔK_a
1,2-Diaminoethane (2)	9.89, 7.08	2.8	630
1,3-Diaminopropane (3)	10.56, 8.76	1.8	63
1,4-Diaminobutane (4)	10.72, 9.44	1.28	19
1,5-Diaminopentane (5)	10.78, 9.85	0.93	8.5
1,6-Diaminohexane (6)	10.97, 10.09	0.88	7.6

The comparison of pK_a values on the series of diamines (Table 1.3), triamines (Table 1.4) and tetramines (Table 1.5) have been reported (Martell *et al.*, 1997). For diamines, the difference between the pK_a of the first and second protonation is 2.8 log unit (K_a = 630) for 1,2-diaminoethane (2) (Table 1.3). Then this difference is dramatically reduced in (3) (ΔpK_a = 1.8 log unit, ΔK_a = 63) which means that the propylenic spacer between the terminal primary amine groups reduces significantly the electrostatic repulsion between both sites. This effect is much smaller when ΔpK_a is compared between (3) and (4), when one methylene group was added, and also clearly when more methylene groups are added in the chain to (5), and no such difference of ΔpK_a occurs between (5) and (6). The reduced effect of more spatially distant amine groups is reflected in higher pK_a values (Table 1.3).

Triamines present two kinds of amines, primary at the end and secondary in the middle of the molecule. In triamine, the change of an ethylenic chain by a propylenic (from 2.2 to 2.3) increases the basicity by more than two orders of magnitude. In 2.2, the p*K*a represents two relatively high values and one much lower while the other triamines show a set of two high p*K*a values with one intermediate or three high p*K*a values as the function of the length of the hydrocarbon chains between the nitrogen atoms.

Table 1.4 p*K*a values of triamines (Martell *et al.*, 1997).

Triamine	p*K*a
3-Azapentane-1,5-diamine (2.2)	9.84, 9.02, 4.23
3-Azahexane-1,6-diamine (2.3)	10.21, 9.17, 6.10
3-Azaheptane-1,7-diamine (2.4)	10.65, 9.42, 6.71
4-Azapentane-1,7-diamine (3.3)	10.65, 9.57, 7.69
4-Azaoctane-1,8-diamine (3.4, spermidine)	10.89, 9.81, 8.24

Table 1.5 p*K*a values of tetraamines (Martell *et al.*, 1997).

Tetraamine	p*K*a
2.2.2	9.74, 9.07, 6.59, 3.27
2.3.2	10.08, 9.26, 6.88, 5.45
3.2.3	10.53, 9.77, 8.30, 5.59
3.3.3	10.46, 9.82, 8.54, 7.21
3.4.3 (spermine)	10.80, 10.02, 8.85, 7.96

Tetraamines present two distinct kinds of nitrogen atoms, two primary amines at both ends and two secondary amines at the central part of the chain. From Table 1.5, the trends of protonation present two large basicity constants and two intermediate values in (2.3.2) while in (3.2.3) shows three large constants and one intermediate. However, in (2.2.2) the effect of repulsion effect of protonated nitrogens separated by ethylenic chains make three groups of pK_a values, the first is intermediate (9.74, 9.07), the second is small (6.59) and the last is low (3.27) which is from the fourth protonation. The polyamines (3.3.3) and (3.4.3) show a group of higher pK_a values due to the propylenic or butylenic chains which reduce the electrostatic repulsion more than the (shorter) ethylenic chains.

1.4 Biological roles and pharmacological effects of polyamines

Polyamines and nucleic acids

Polyamines have been shown to have an important role in cell division and their amount increases dramatically under conditions of high cell division for instance tumor growth, cystic fibrosis and pregnancy (Russel and Durie, 1978). As the polyamines carry multiple positive charges *in vivo* due to protonation of the polyamine groups, they will interact with negatively charged polynucleic acid and it has been estimated that a large amount of the polyamines present in the cell are associated to DNA or RNA (Watanabe *et al.*, 1991). Polyamines have been shown to induce DNA condensation and to stabilize compact forms of DNA (Bloomfield, 1991, Gosule *et al.*, 1976, Raspaud *et al.*, 1999). DNA often occurs in compact forms, *e.g.* in chromatin of eukaryotes and in sperm and phage heads, thus it is possible that polyamines are largely responsible for the stabilization of these compact DNA phases. It is believed that the primary targets for polyamine binding are the charged DNA phosphates (Deng *et al.*, 2000).

Polyamines as the microbial growth factors

The first study was those of Herbst *et al.* (1958) on *Hemophilus parainfluenzae 7901*. In the absence of added polyamine no growth occurs on a purified medium. Growth is obtained upon addition of small amounts of 1,3-diaminopropane, 1,4-diaminobutane or any one of about twenty other synthetic derivatives of these diamines, including spermidine and spermine. Sneath (1995) described a mutant of *Aspergillus nidulans* that has an absolute requirement of 1,4-diamonobutane. Several other compounds, including spermine, ornithine, arginine, lysine, 1,3-diaminopropane and 1,5-diaminopentane are ineffective, and only a small growth response is found with spermidine. The occurrence of a mutant with this specific growth requirement for 1,4-diaminobutane indicate that 1,4-diamonobutane or a derivative has an essential function in the cell.

Stabilization of bacterial spheroplasts and protoplasts by polyamines.

The discovery of the stabilization of osmotically fragile bacteria by small amounts of spermine indicated that in some unknown way spermine affects the strength of the bacterial cell wall or membrane. This work was demonstrated by Tabor (1962) by treating *E. coli* with lysozyme and ethylenediaminotetraacetate in a 20% sucrose medium; the bacteria are converted to spheroplasts (spheroplast is a cell from which the cell wall has been almost

completely removed) that lyse if the osmotic pressure is lowered. Protection against lysis is afforded by 0.001 M spermine, spermidine, $CaCl_2$, quinacrine or streptomycin; comparable concentrations of KCl, NH_4Cl, $MgCl_2$, ornithine, lysine or 1,4-diaminobutane are inactive. Spermine has a protective effect also on spheroplasts of *E. coli* produced by penicillin treatment and protoplasts of *Micrococcus lysodeikticus* made by treatment with lysozyme. The striking aspect of these results is the low concentration of spermine (0.001 M) needed to prevent lyse, compared to the 0.5 M sucrose usually used. The interior of cell has a higher osmotic pressure than the external medium; the cell is prevented from swelling even in distilled water by the rigidity of its cell wall. When the wall is damaged by lysozyme or its synthesis is inhibited by penicillin this restraint is absent and the spheroplast swells until its membrane ruptures, lyse occurs. The 0.5 M sucrose prevents lysis by raising the osmotic pressure of the environment to that of the contents of the spheroplast. Spermine in a concentration of 0.001 M does not increase the osmotic pressure significantly and therefore presumably acts by strengthening the spheroplast membrane.

Antimicrobial effects

Growth of several bacteria and yeast is inhibited by the polyamines; however, this effect varies in different species. At pH 7, *S. aureus* is killed by spermine at 5 x 10^{-4} M, while 0.01 M is necessary to kill *E. coli* (Razin and Rozansky, 1957). A competitive inhibitory effect between the penetration of basic amino acids and the corresponding diamines (of similar chain length) was observed in *Bacterium cadaveris* (Mandelstam, 1956). Various polyamines conjugated to cholesterol, cholenic acid and bile acids have been reported (Geall *et al.*, 2000, Karigiannis, 2000). Some of these sterol-polyamine conjugates exhibit antimicrobial (Kim, 2000, Kikuchi *et al.*, 1997, Jones *et al.*, 1996, Sadownik *et al.*, 1995) and anti-trypanosomal activity (Khabnadideh *et al.*, 2000). The isolation, structural determination, and characterization of a water-soluble cationic steroid from the dogfish shark, *Squalus acanthias*, called squalamine exhibits potent antimicrobial activity against fungi, protozoa, and both Gram-negative and Gram-positive bacteria (Figure 1.11) (Moore *et al.*, 1993).

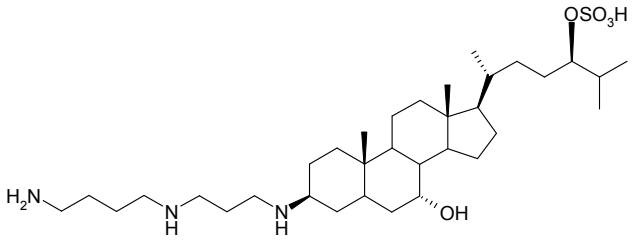

Figure 1.11 Squalamine

1.5 Analysis of polyamines

Polyamines content of cells and body fluids are in the range of 0.05–500 μmol/10^{12} cells and 0.05 – 15 μmol/L. The analysis of polyamines had been performed with almost all available techniques: thin-layer and paper and liquid chromatography, electrophoresis, immunochemical methods, enzymatic methods, high-performance liquid chromatography (HPLC) and gas chromatography (GC). The difficulties experienced in attempting to identify and measure the amount of polyamines in biological materials follow from three characteristics: their size as they are low-molecular-mass aliphatic amines, the low concentrations in which they are present, and that their only reactive centres are the amino groups which make them high basicity and strong adsorption on solid surfaces. Thus methods for polyamine analysis must include procedures to extract, and perhaps concentrate, the polyamines; to separate them from other amino-containing compounds (such as amino acids), and from each other; to convert them into colour or fluorescence derivatives; to identify them; and then to make quantitative measurements. All available methods have definite limitations and there is still no simple, specific method for the quantitative determination of the various polyamines. It is usually necessary to carry out one or more preliminary steps to separate the polyamines from each other and from other cellular materials.

Analytical methods for polyamines

1. Thin-layer chromatography (TLC)

TLC has been used extensively for preliminary identification and semiquantitative of polyamines. TLC is not very precise and specific technique. However, it is simple, rapid and can be used without sophisticated equipment. In these procedures, the amines are usually detected with a ninhydrin spray (Shirahata *et al.*, 1983) or by derivative formation of primary and secondary amines with dansyl chloride (5-dimethyl aminonaphthalene-1-sulfonyl chloride) (Seiler and Wiechmann, 1965, Boffey *et al.*, 1974, Fleisher *et al.*, 1975, Heby *et al.*, 1978, Beyer *et al.*, 1983, Wettlaufer, 1988, Madhubala, 1998). TLC is an easy way to determine polyamines in tissue extracts and cell extracts (Madhubala, 1998). Different solvent systems were evaluated for their ability to separate biogenic amines after dansylation by TLC and detected by fluorescence densitometry at 330 nm (Lapa-Guimarães *et al.*, 2004). Recently, calcium sulphate ($CaSO_4$) coated TLC plates were used for the analysis of aliphatic polyamines without derivatization for separation of six di- and polyamines (ornithine, citrulline, putrescine, cadaverine, spermidine and spermine) (Khan, 2006).

2. Immunoassays

The immunoassays which were used for the determination of polyamines are Radio Immunoassay (RIA) and Enzyme-Linked Immuno Sorbent Assay (ELISA). Both techniques provide high sensitivity, require small tissue samples and allow multiple analyses in parallel. Moreover there is no need to derivatize the samples. Nevertheless, a major problem is the specificity of the antibody produced the inability to obtain antibodies against putrescine and also the hazard of handling radioactive reagent in the RIA. The early efforts to produce antibody of spermine had resulted in somewhat less specific antispermine that processed cross-reactivity with spermidine (Bartos *et al.*, 1975). Enzyme immunoassay which employed two antibodies against spermine and spermidine was developed by Fujiwara, proved to be non-specific again cross-reaction problems were present (Fujiwara *et al.*, 1983).

3. Gas-liquid chromatography and Gas-chromatography-mass spectrometry

Methods of analysis of polyamines by using GC were introduced in 1969 (Brooks *et al.*, 1969). GC of non-derivatized polyamines is not very popular and not very successful because of their polar characteristics which present many problems of loss on the column, tailing patterns of elution, difficulties of improvements, non-reproducible. GC is not as often used for the determination of polyamines as liquid chromatography. One of the main problems with GC is that sample introduction as aqueous phase is undesirable, which causes problems with serum and urine samples. Moreover, the presence of non-polar contamination in biogenic samples makes difficulty for detection by GC. However, a GC method for non-derivatized polyamines was developed to separate and detect polyamines in different organs (Beninati *et al.*, 1977). By using trifluoroacetylacetone as a derivatizing reagent for polyamines improved the sensitivity of putrescine and cadaverine quantification in the serum of cancer patients (Khuhawar *et al.*, 1999). The use of capillary columns instead of packed columns increased the sensitivity of GC systems and gives reproducible results. Polyamines and acetylpolyamines were analysed simultaneously this minimized the problems of adsorption and reduced the analysis-time (Dorhout *et al.*, 1997). Further developments in GC analyses comprised both pre-purification and derivatization procedure improvements. Derivatisation usually necessitates isolation of analytes in a water and salt free form. Nevertheless, polyamine analyses by GC remained time-consuming and unattractive so GC has been become neglected probably because of initially laborious pre-purification. The pre-purification were carried out by extraction with alkaline butanol (Beninati *et al.*, 1977), trichloroacetic acid (Fujihara *et al.*, 1983, Emonds *et al.*, 1983, Khuhawar *et al.*, 1999), cation-exchange chromatography (Rattenbury *et al.*, 1979, Slemr *et al.*, 1984) or adsorption with silica gel (McGregor *et al.*, 1976, Yamamoto *et al.*, 1982, Muskiet *et al.*, 1984, Jiang, 1990, Dorhout *et al.*, 1997). The derivatizations performed with isobutyloxycarbonyl

(Bakowski *et al.*, 1981), pentafluoropropionyl (Rattenbury *et al.*, 1979), ethyloxycarbonyl (Yamamoto *et al.*, 1982, 1984), trifluoroacetyl (Jiang, 1990; Khuhawar *et al.*, 1999) or heptafluorobutylryl derivatives (Fujihara *et al.*, 1983; Muskiet *et al.*, 1984; van den Berg *et al.*, 1986; Dorhout *et al.*, 1997).

GC systems can also be coupled with more selective detector methods such as MS which will give the powerful separation and identification technique. Polyamines can be determined more selectively by applying isotopic labelled standards (Smith *et al.*, 1977). GC-MS was used for determination of hair polyamines as hair is the noninvasive biosample (Choi *et al.*, 2000). At present capillary GC seems more suitable for profiling of polyamines because of its higher number of theoretical plates and its easy convertibility to GC-MS.

4. High-performance liquid chromatography (HPLC)

HPLC with on-line detection is the most common applied profiling method for polyamines. Cation-exchange and reversed-phase high performance liquid chromatography require pre- or post-column derivatization, followed by UV-VIS spectrophotometric or fluorimetric detection. An HPLC method for polyamines was first reported by Samejima in 1976 (Samejima *et al.*, 1976). Chromatographic separation of polyamines is based on hydrophobic interactions of the residual part of the molecule; therefore retention of non-derivatized polyamines is not easy on standard reversed-phase chromatographic columns. However, there was a method described based on this principle (Fransson *et al.*, 1990). The method was not sensitive and only applicable to high concentrations. The separation of non-derivatized polyamines is easily performed with ion-chromatography. There are three methods of operation; (cat) ion-exchange, ion-pair and ion-exclusion chromatography. The first two, ion-exchange chromatography and ion-pair chromatography are more popular than ion-exclusion chromatography for the separation of biogenic polyamines (Molnar-Perl, 2005). The strong electrostatic interaction between the two or more protonated amines of the analytes and the anionic fixed charged of the ion-exchange chromatography stationary phase cause strong analyte retention. Thus, high concentrations of counter ion in the eluent are required to elute the polyamines. The specific detection of non-derivatized polyamines after ion-exchange chromatography was done by a condensation nucleation light scattering detector (CNLSD) (Sadain *et al.*, 1999). Another interesting approach to directly detect non-derivatized polyamines is LC-MS which is sensitive and selective due to the mass chromatograms. However, an LC-MS with ion exchange systems is expensive, and not easy for quantification purposes. The methods mentioned above were carried out by non-derivatization reaction of polyamines, however, ion-chromatography with selective post-column derivatization reaction is a very popular method to separate and detect polyamines

(Suzuki *et al.*, 1990, Conca *et al.*, 2001, Vidal-Carou *et al.*, 2003). OPA (*o*-phthalaldehyde) is most often used as the post-column detector. Polyamine-ninhydrin is another post-column derivatization of choice (Bremer *et al.*, 1971; Gehrke *et al.*, 1974). Pre-column derivatization is another alternative way to determine polyamines. Some advantages of this technique over post-column derivatization are as follows: the pre-column derivatization is not related to the mobile phase so unlike the post-column derivatization, the reaction conditions can therefore be chosen freely; the rates of the reactions are not usually limiting, whereas slow reaction can cause serious mixing and reaction-volume problems in post-column derivatization; the pre-column derivatization can be use as a pre-clean-up step; selective reagents and extraction procedures can result in the easy elimination of much interference of reagents in contrast to reaction after separation; pre-column derivatization can improve the sensitivity and it uses small amounts of expensive derivatization reagents and achieves short analysis times.

Pre- or post-column derivatisation with fluorogenic reagents became popular because of their superior sensitivity compared with those that introduce UV-VIS absorbing moieties. Pre-column derivatisation with DNS Cl in aqueous solution, followed by reversed-phase HPLC/fluorimetry is a widely employed method for polyamines in tissue and body fluids. Other examples of pre-column reactions to fluorophores are those with fluorescamine, OPA/MCE and OPA/ethanethiol. Cation-exchange HPLC with post column OPA/ME fluorimetry is another option. A number of pre-column derivatisation techniques have been developed for HPLC with UV-VIS spectrophotometric detection. They include reaction with benzoyl chloride, *p*-toluenesulfonyl chloride (tosyl chloride), 2,4-dinitrofluorobenzene, 4-fluoro-3-nitrobenzotrifluoride, quinoline-8-sulfonyl chloride and 4-dimethylaminoazo-benzene-4-sulfonyl chloride (dabsyl chloride).

5. Mass spectrometric methods

MS methods can simultaneously separate and identify polyamines on the basis of the difference of their mass without use of column (Furuumi *et al.*, 1998). A quadrupole MS with ionspray ionization interface (ISI-Q MS) was the first one used to determine polyamine concentrations in rat tissues (Xu *et al.*, 2002). Recent progress in MS has made it possible to use a time-of-flight mass spectrometer with electrospray ionization interface (ESI-TOF MS), which is more sensitive and provides a higher resolution (Samejima *et al.*, 2007).

1.6 Aims of the study

This study attempts to determine accurate and simple assays for a wide range of polyamines by optimizing the derivatization methods and increasing the sensitivity of polyamine detection by HPLC using four typical fluorescent chromophores: *o*-phthalaldehyde/ mercaptoethanol (OPA/MCE), fluorescamine, 9-fluorenylmethyl chloroformate (FMOC Cl) and dansyl chloride (DNS Cl) for pre column derivatization and using HR-ESI-MS to confirm the structures of the derivatives. Intramolecular and intermolecular interactions that might influence the sensitivity of fluorescence detection have also been investigated. The synthesis of the spermine (3.4.3) regioisomer, thermospermine (3.3.4) has been carried out in order to investigate the methods to separate and quantify these two isomers by RP-HPLC.

The objectives of this research are:

1. To study the analytical pharmaceutical chemistry related to polyamines and aminoglycosides which are difficult to analyze using current protocols. In this research we will use fluorescence spectroscopy (of *e.g. o*-phthalaldehyde/mercaptoethanol, fluorescamine, FMOC and dansyl derivatives) and the efficiency of poly-derivatization (and the quantification of such polyamine-fluorophore conjugates), detailing the potential for the regioselective, fluorescent derivatization of basic amines.

2. To investigate the chromatographic and spectroscopic characterization of these derivatives of polyamines and aminoglycosides, from a variety of natural product sources, concentrating on those which contain several amine functional groups: 2 (as found in putrescine and cadaverine), 3 (spermidine), 4 (spermine, kanamycin), 5 (paramomycin), up to 6 (neomycin).

3. To investigate reactions which selectively convert primary and secondary amines into fluorescent derivatives. Then to develop suitable chromatographic procedures using fluorescence detection to resolve and quantify these amine derivatives. The parent polyamines are of interest as novel vectors in non-viral gene delivery. The intermediates involved in their synthesis such di- and polyamines lack any useful chromophores and therefore they are intrinsically hard to analyse, to detect and especially to quantify.

4. To synthesize thermospermine (4.3.3) and then to analyse it in the presence of spermine (3.4.3) by making deuteriated and fluorescent derivatives which can be easily and practically separated by RP-HPLC, ultimately working towards a quantitative analysis.

CHAPTER 2: EXPERIMENTAL

2.1 Materials and general methods

Chemicals, reagents, and solvents were purchased from Fisher and Sigma-Aldrich, all in GPR grade, unless otherwise stated and were used without further purification unless specified. Water refers generally to distilled water or to Milli-Q-water for HPLC. Concentrated acids and bases were diluted in aqueous solution unless otherwise stated and pH adjustments were monitored by pH meter model CCM C625 combined conductivity/pH meter, WPA Linton, Cambridge, UK.

Typical extraction or reaction work-ups ended with the organic solution being dried over anhydrous magnesium sulfate, filtered, and then evaporated to dryness under reduced pressure. Solvents were evaporated with a rotary evaporator (Büchi rotavapor) using a vacuum pump (Vacuubrand PC 2001 vario) with a pressure control (Vacuubrand CVC 2^{II}) and a variable temperature water bath (Büchi water bath).

Flash column chromatography (Still *et al.*, 1978) was generally performed on silica gel 60 (Merck, 0.040-0.063 mm, 230-400 mesh ASTM, pH 6.5-7.5 for a 10% suspension) or on activated standard grade, neutral, acidic and basic (Brockmann I) alumina gels (Sigma-Aldrich, 58Å, ~150 mesh). The column was packed in an open-glass column with an appropriate solvent that could achieve a satisfactory resolution on TLC. Solvent ratios are v/v unless otherwise stated. The progress of the elution was followed by collecting fractions from the eluate, concentrating and monitoring by analytical TLC, HPLC, NMR and HR-ESI-MS.

Analytical TLC was performed on commercial aluminium-backed plates pre-coated with silica GF_{254} 60 in 0.25 mm thickness and commercial aluminium-backed plates pre-coated with aluminium oxide GF_{254} 60 neutral purchased from Merck. TLC samples were applied as solutions in methanol. The four mobile phase systems (ratios in v/v/v) used to monitor the reaction are given in Table 2.1.

TLC plates were subjected to a single development to a height of approx. 5 cm in saturated vapour conditions. Compounds were visualized by drying the plate and dipping in (or spraying with) a freshly prepared solution of ninhydrin (1.0 g) in a mixture of 95% methanol (50 mL) and glacial acetic acid (10 mL) followed by heating for ~3 min. The amine and polyamine components were visible as purple spots on a white background.

Table 2.1 TLC mobile phase systems for monitoring thermospermine synthesis.

system 1	dichloromethane: methanol = 10:1
system 2	dichloromethane: methanol = 4:1
system 3	dichloromethane: methanol: ammonium hydroxide = 10:5:1
system 4	dichloromethane: methanol: ammonium hydroxide = 20:10:1

Ultraviolet (UV) spectra were measured in methanolic solution using a Perkin-Elmer UV/VIS spectrophotometer Lambda EZ201. Infrared (IR) spectra were recorded from anhydrous KBr discs or NaCl plates using a Perkin-Elmer RX 1 FT-IR instrument.

Fluorescence studies were carried out with a Perkin-Elmer LS 50B Luminescence Spectrometer (λ_{ex} and λ_{em} for different chromophores as in Table 2.2) using a 1 cm path length, 3 mL glass cuvette, slit width 5 nm. An IBM compatible personal computer was used for data collection, using FL Winlab (Perkin-Elmer) software.

Table 2.2 λ_{ex} and λ_{em} of different chromophores.

Chromophore	λ_{ex} (nm)	λ_{em} (nm)
Dansyl derivatives	330	510
OPA/MCE derivatives	340	450
FMOC derivatives	264	310
Fluorescamine derivatives	390	486

The high performance liquid chromatography (HPLC) instrument consisted of a solvent delivery system equipped with a Jasco PU-980 Intelligent HPLC pump (Ishikawa-cho, Japan) and monitored by a Jasco UV-1575 variable wavelength ultraviolet detector and Waters 470 fluorescence detector in series. HPLC detection was typically by UV with the λ_{max} the same as the λ_{ex} of fluorescence for typical fluorophores in Table 2.2. Chromatograms were recorded on a Goerz Metramatt SE 120 recorder with chart speed at 1 cm/min. All columns used were commercially pre-packed reversed phase HPLC columns, purchased from Phenomenex Inc. Analytical column: Phenomenex hypersil ODS C18 5µ 150 x 4.60 mm, Phenomenex luna C18 5µ 150 x 4.60 mm, Phenomenex luna C8 5µ 150 x 4.60 mm with guard column H1-5C18 were used for the analytical separation procedures. Samples were dissolved in mobile phase and filtered though a 17 mm diameter SYR Filter Nylon 0.45 µm before injection using a 20 µL Rheodyne injection loop. All mobile phase

mixtures were pumped at a flow rate of 1 mL/min and at 20^{o}C. The column was washed using the chosen solvent for 20 min or until a stable base line was obtained.

Table 2.3 Mobile phase for HPLC experiments

Chromophore type	Mobile phase (%v/v)
OPA/MCE derivatives	Acetonitrile (MeCN) : Milli-Q-water (40:60, 60:40, 65:35, 70:30, 80:20, 85:15, 90:10)
	Methanol : Milli-Q-water (70:30)
OPA/MCE/FMOC derivatives	Acetonitrile (MeCN) : Milli-Q-water (65:35, 70:30, 80:20, 85:15)
FMOC derivatives	Acetonitrile (MeCN) : Milli-Q-water (40:60, 50:50, 60:40, 65:35, 70:30, 80:20, 85:15)
	Methanol : Milli-Q-water (40:60, 70:30)
Fluorescamine derivatives	Acetonitrile (MeCN) : Milli-Q-water (40:60, 50:50, 60:40, 65:35, 70:30, 80:20, 85:15)
	Methanol : Milli-Q-water (40:60, 70:30)
	Acetonitrile (MeCN) : Methanol: Milli-Q-water (85:10:5)
Dansyl chloride derivatives	Acetonitrile (MeCN) : Milli-Q-water (40:60, 50:50, 60:40, 65:35, 70:30, 80:20, 85:15)
	Acetonitrile (MeCN) : Milli-Q-water: Formic acid (90:10:1, 60:40:0.1, 60:40:2.5)
	Methanol : Milli-Q-water (70:30)
	Acetonitrile (MeCN) : Methanol: Milli-Q-water (20:65:15)
Semi-preparative column	Acetonitrile (MeCN) : Milli-Q-water (70:30, 40:60)

Semi-preparative column: Phenomenex gemini 10 µ C18 110A 250 x 10 mm; guard column: Phenomenex gemini 5 µ C18 10 x 10 mm. Samples were dissolved in pure organic solvent or dissolved in mobile phase and filtered by 17 mm SYR Filter Nylon 0.45 µm before

injection onto HPLC using a 100 μL loop. Acetonitrile: Milli-Q-water (70:30, 40:60) was used as the mobile phase at flow rate 5 mL/min.

All the HPLC experiments were performed using isocratic elution. HPLC grade methanol and acetonitrile were purchased from Fisher and filtered through a Whatman® Nylon membrane prior to use. The acidic solution (0.1% formic acid) was filtered through Milli-Q Plus PF. The aqueous mobile system was shaken vigorously and then degassed on a Decon ultrasonicator for 30 min before use. The mobile phases that have been used are shown in Table 2.3.

NMR spectra were obtained on either JEOL GX 270 (operating at 270 MHz for ^{1}H and 67.8 MHz for ^{13}C) or a JEOL EX 400, Varian Mercury VX 400 (operating at 400 MHz for ^{1}H and 100.8 MHz for ^{13}C) spectrometer, in solution of $CDCl_3$ (~0.5 mL) unless otherwise stated. Chemical shifts values are recorded in part per million (ppm) on the δ scale. Spectra were referenced internally using either the residual solvent resonance for ^{13}C or to TMS (0.0 ppm) for ^{1}H. COSY and DEPT spectra were all recorded using automated programmes. Coupling constants are reported in Hertz (Hz, absolute values) and the multiplicities abbreviated as: s (singlet), d (doublet), t (triplet), q (quartet), quin (quintet) and m (multiplet). The abbreviation br (broad) is used to indicate significant broadening due to rapid exchange or unresolved fine coupling. The format used for reporting ^{1}H NMR spectra is: chemical shift (integration, multiplicity, coupling constant and assignment).

High Resolution-Electrospray ionization-Mass Spectrometry (HR-ESI-MS) was performed on a BRUKER DALTONICS micrOTOF instrument in the Department of Pharmacy and Pharmacology, University of Bath.

2.2 *o*-Phthalaldehyde (OPA)/Mercaptoethanol (MCE) derivatization

Optimization of derivatization conditions

The optimizations of derivatization conditions were done by:

1. Optimisation the pH of borate buffer to the OPA/MCE reagent using the series, pHs 4.0, 4.5,5.0, 5.5, 6.0, 6.5, 7.0, 8.3, 9.3 and 10.5.
2. Optimisation of the molar ratio of OPA/MCE reagent to sample solution.
3. Optimization of the mole ratio of MCE (mM) to 1 mM of OPA, using the series, 1.4, 2.8, 5.7, 10.0, 11.4 and 17.0.
4. Optimisation of the reaction time using the series, 1, 5, 10, 20, 30, 40, 50, 60 and 80 min.

5. Optimisation of the condition for maximum stability of the derivatives of amine-OPA/MCE at 20^{o}C and 1^{o}C.
6. Optimization the mobile phase for HPLC by using different ratio of acetonitrile: Milli-Q-water range from 40:60, 70:30, 80:20, 85:15, 90:10 (% v/v).

Optimization the pH of borate buffer

OPA/MCE reagent

The OPA/MCE reagents were prepared at least 90 min before use and stored no longer than 3 days in the refrigerator (4^{o}C). The stock solution of OPA contained 0.75 g of OPA in 50.0 mL methanol is referred to below as methanolic OPA solution.

The mole ratio of [OPA]:[MCE] = [1:10] was obtained by mixing, in order of listing, 2.5 mL methanolic OPA, 2.0 mL borate buffer (at various pH, using the series, pHs 4.0, 4.5,5.0, 5.5, 6.0, 6.5, 7.0, 8.3, 9.3 and 10.5) and 200 µL MCE and completed with methanol up to 10.0 mL.

Borate buffer solution

Borate buffer pH 4.0 -10.5 (Ref Appendix I E, A69, British Pharmacopoeia 1988)
A series of borate buffer (200 mM) from pH 4.0 to 10.5 was prepared by the following procedure. To 50 mL of a solution containing 0.6189 g of boric acid and 0.7456 g of potassium chloride, 20.0 mL of 0.2 M sodium hydroxide was added. The pH was adjusted by addition of boric acid solution or sodium hydroxide solution using a pH meter measure the pH then diluting to 200 mL with water.

Sample solution

Sample solutions of amines were prepared with distilled water at the concentration of 5.0 mM. Ethylamine and 1-butylamine were used in the optimisation the pH of borate buffer.

100 µl of 5 mM ethylamine and 100 µL of 200 mM borate buffer solution pH 4.0, 4.5, 5.0, 5.5, 6.0, 6.5, 7.0, 8.3, 9.3, and 10.5 were pipetted into 10 glass vials and mixed well. 100 µL of OPA/MCE reagent = [1:10] was added to each vial and left to react for 1 min. Then this solution was injected onto the HPLC. All the steps were repeated with 1-butylamine.

HPLC system

Column:	Phenomenex hypersil C18 5µ 150 x 4.60 mm.
Mobile phase:	Acetonitrile: Milli-Q-water (60:40) the mobile phase was filtered through a 0.45 µm nylon membrane filter under vacuum and degassed in an ultrasonic bath for 30 min, used at a flow rate of 1 mL/min.
Detection	Fluorescence detection at OPA wavelength λ_{ex} = 340 nm, λ_{em} = 450 nm. UV detector at λ_{max} = 340 nm.

Optimization for the mole ratio of MCE to 1 mM of OPA

OPA/MCE reagent

The OPA derivative reagent was prepared by dissolving 0.134 g of OPA into 5.00 mL methanol, then adding MCE in series of 100, 200, 400, 700, 800, 1200 µL, which is equal to the mole ratio of [OPA]:[MCE] = [1:1.4], [1:2.8], [1:5.7], [1:10], [1:11.4] and [1:17.0] respectively and then diluting to 25.0 mL with borate buffer (pH 10.5).

Borate buffer solution

Borate buffer pH 4.0-10.5 (Ref Appendix I E, A69, British Pharmacopoeia 1988).
A series of Borate Buffers (200 mM) 10.5 was prepared by the following method: to a 50 mL of a solution containing 0.6189 g of boric acid and 0.7456 g of potassium chloride, 20.0 mL of 0.2 M sodium hydroxide was added. The pH was adjusted by addition of boric acid solution or sodium hydroxide solution using a pH meter to measure the pH then diluting to 200 mL with water.

Sample solution

1-Butylamine (5.0 mM in distilled water) was used in the optimisation the mole ratio of OPA/MCE reagent composition.

1. 100 µL of 5 mM 1-butylamine and 100 µL of 200 mM borate buffer solution pH 10.5 were pipetted into 6 glass vials and mixed well.
2. 100 µL of OPA/MCE reagent [1:1.4], [1:2.8], [1:5.7], [1:10], [1:11.4] and [1:17.0] was added to each vial left to react for 1 min then injected onto HPLC.

HPLC system

Column:	Phenomenex hypersil C18 5µ 150 x 4.60 mm.
Mobile phase:	Acetonitrile: Milli-Q-water (60:40) the mobile phase was filtered through a 0.45 µm nylon membrane filter under vacuum and degassed in an ultrasonic bath for 30 min, used at a flow rate of 1 mL/min.
Detection	Fluorescence detection at OPA wavelength λ_{ex} = 340 nm, λ_{em} = 450 nm. UV detector at λ_{max} = 340 nm.

Optimizing the mole ratio of OPA/MCE to amines

OPA/MCE reagent

The OPA derivative reagent was prepared by dissolving 0.268 g of OPA in 5.00 mL methanol, then adding MCE in series of 1.4 mL, which is equal to the mole ratio of [OPA]:[MCE] = [1:10] and then diluting to 25.0 mL with borate buffer (pH 10.5). The concentration of OPA is 80 mM, then this solution was diluted by borate buffer (pH 10.5) to obtain the concentration series of 1 mM, 5 mM, 10 mM, 20 mM and 40 mM.

Sample solution

1-Butylamine (5.0 mM in distilled water) was used in the optimisation of the mole ratio of OPA/MCE reagent composition, derivatized as follows: 100 µL of 5 mM 1-butylamine and 100 µL of 200 mM borate buffer solution pH 10.5 were pipetted into 6 glass vials and mixed well. 100 µL of OPA/MCE reagent concentration at 1, 5, 10, 20, 40 or 80 mM was added to each vial and left to react for 1 min. After 1 min, this solution was injected onto HPLC.

HPLC system

Column:	Phenomenex hypersil C18 5µ 150 x 4.60 mm.
Mobile phase:	Acetonitrile: Milli-Q-water (60:40) the mobile phase was filtered through a 0.45 µm nylon membrane filter under vacuum and degassed in an ultrasonic bath for 30 min, used at a flow rate of 1 mL/min.
Detection	Fluorescence detection at OPA wavelength λ_{ex} = 340 nm, λ_{em} = 450 nm. UV detector at λ_{max} = 340 nm.

Stability of amines-OPA/MCE derivatives:

After the procedure had been optimized, the following OPA derivative reagent was used routinely, prepared by dissolving OPA (0.134 g) in 5.00 mL methanol, then adding MCE (700 μL) which is equal to the mole ratio of [OPA]:[MCE] = [1:10] and then diluting to 25.0 mL with borate buffer (pH 10.5). The concentration of OPA = 1 mmol, in 25 mL = 40 mM. The reagent was kept in the refrigerator (4^{o}C) and used within 7 days.

Sample solution

The following amines were prepared as aqueous solutions at a concentration of 1 mM: ethylamine, 1-butylamine, 1,4-diaminobutane, 1,5-diaminopentane, 1,7-diaminoheptane. 100 μl of 1 mM ethylamine and 100 μl of 200 mM borate buffer solution pH 10.5 were pipetted into a glass vials and mixed well. Then 100 μl of OPA/MCE reagent (routine working reagent) was added to each vial left to react for 1 min and this solution was injected onto HPLC at 5, 10, 20, 30, 60, 70, 80 and 90 min (after reaction time). All the steps were repeated with other four amines.

Temperature and stability of the derivatives

An aqueous solution of 1,4-diaminobutane (100 μL, 1 mM) was derivatized with borate buffer solution (100 μL, 200 mM, pH 10.5), pipetted into 2 glass vials and mixed well. 100 μL of OPA/MCE reagent (routine working reagent) was added to each vial, left to react for 1 min, then one vial was kept at 1^{o}C and the other at 20^{o}C. After reaction, the solutions were injected after 5, 10, 20, 30, 60, 70, 80 and 90 min onto HPLC.

HPLC system

Column:	Phenomenex hypersil C18 5μ 150 x 4.60 mm.
Mobile phase:	Acetonitrile: Milli-Q-water (70:30) the mobile phase was filtered through a 0.45 μm nylon membrane filter under vacuum and degassed in an ultrasonic bath for 30 min, used at a flow rate of 1 mL/min.
Detection	Fluorescence detection at OPA wavelength λ_{ex} = 340 nm, λ_{em} = 450 nm. UV detector at λ_{max} = 340 nm.

Polyamines-OPA/MCE derivatives

Sample solution

Amine solutions (concentration from 0.2-1 mM, 100 µl) were prepared. The following amines were investigated: ethylamine, 1-butylamine, 1,4-diaminobutane, 1,5-diaminopentane, 1,7-diaminoheptane, 1,8-diaminooctane, 1,9-diaminononane, 1,12-diaminododecane, spermidine, spermine, N^4,N^9-didecanoyl spermine, N^4,N^9-dilinoleoyl spermine, glucosamine, kanamycin and neomycin.

Derivatization method

1 100 µL of 5 mM 1-butylamine and 100 µL of 200 mM borate buffer solution pH 10.5 were pipetted into 6 glass vials and mixed well.

2 100 µL of OPA/MCE reagent (routine working reagent) was added to each vial left to react for 1 min.

3 After 1 min, this solution was injected onto HPLC.

HPLC system

Column:	Phenomenex hypersil C18 5µ 150 x 4.60 mm.
Mobile phase:	Acetonitrile: Milli-Q-water (40:60, 70:30, 80:20, 90:10) the mobile phase was filtered through a 0.45 µm nylon membrane filter under vacuum and degassed in an ultrasonic bath for 30 min, used at a flow rate of 1 mL/min.
Detection	Fluorescence detection at OPA wavelength λ_{ex} = 340 nm, λ_{em} = 450 nm. UV detector at λ_{max} = 340 nm.

Calibration curve obtained from amine-OPA/MCE derivatives

Sample solution

1-Butylamine, 1,4-diaminobutane, 1,5-diaminopentane, 1,7-diaminoheptane, spermidine and kanamycin over the concentration range 0.01 – 10 mM were examined to obtain the calibration curves.

Derivatization method

1 100 µL of various concentration of 1-butylamine and 100 µL of 200 mM borate buffer solution pH 10.5 were pipetted into 6 glass vials and mixed well.
2 100 µL of OPA/MCE reagent (routine working reagent) was added to each vial left to react for 1 min.
3 After 1 min, this solution was injected onto HPLC.
4 All the steps were repeated with other models (1,4-diaminobutane, 1,5-diaminopentane, 1,7-diaminoheptane,spermidine, kanamycin).
5 A plot of peak area versus the concentration of amines was obtained with R^2 at least 0.99 using Microsoft excel.

HPLC system

Column:	Phenomenex hypersil C18 5µ 150 x 4.60 mm.
Mobile phase:	Acetonitrile: Milli-Q-water (40:60, 70:30, 90:10) the mobile phase was filtered through a 0.45 µm nylon membrane filter under vacuum and degassed in an ultrasonic bath for 30 min, used at a flow rate of 1 mL/min.
Detection	Fluorescence detection at OPA wavelength λ_{ex} = 340 nm, λ_{em} = 450 nm. UV detector at λ_{max} = 340 nm.

Measurement of relative fluorescence yield experiment

Sample solution

The model amines: 1-butylamine, 1,4-diaminobutane, 1,5-diaminopentane, 1,7-diaminoheptane were used at a concentration of 0.01-0.1 mM.

1 The sample amines were derivatized by using routine working reagent of OPA/MCE by varying the concentration of amine samples from 0.01 to 0.1 mM.
2 This solution was injected onto HPLC.
3 A comparison of fluorescence yields of the model series was obtained by comparison between the peak area of fluorescence intensity and peak area of UV absorbance.
4 A plot of fluorescence intensity against absorbance and the FI/UV equation was obtained.

HPLC system

Column:	Phenomenex hypersil C18 5µ 150 x 4.60 mm.
Mobile phase:	Acetonitrile: Milli-Q-water (70:30) the mobile phase was filtered through a 0.45 µm nylon membrane filter under vacuum and degassed in an ultrasonic bath for 30 min, used at a flow rate of 1 mL/min.
Detection	Fluorescence detection at OPA wavelength λ_{ex} = 340 nm, λ_{em} = 450 nm. UV detector at λ_{max} = 340 nm.

OPA/MCE derivatives of a series of non-viral gene therapy (NVGT) vectors

10 mM of N^4,N^9-didecanoyl spermine was dissolved in 1 mL of methanol then diluted to 5 mL with distilled water.
10 mM of N^4,N^9-dilinoleoyl spermine was dissolved in 1 mL of methanol then diluted to 5 mL with distilled water.

1 100 µL of N^4,N^9-didecanoyl spermine and 100 µL of 200 mM borate buffer solution pH 10.5 were pipetted into a glass vials and mixed well.
2 100 µL of OPA/MCE reagent (routine working reagent) was added to each vial left to react for 1 min.
3 After 1 min, this solution was injected onto HPLC.
4 All the steps were repeated with another model (N^4,N^9-dilinoleoyl spermine).

HPLC system

Column:	Phenomenex hypersil C18 5µ 150 x 4.60 mm.
Mobile phase:	Acetonitrile: Milli-Q-water (90:10) the mobile phase was filtered through a 0.45 µm nylon membrane filter under vacuum and degassed in an ultrasonic bath for 30 min, used at a flow rate of 1 mL/min.
Detection	Fluorescence detection at OPA wavelength λ_{ex} = 340 nm, λ_{em} = 450 nm. UV detector at λ_{max} = 340 nm.

OPA/MCE derivatives of Aminoglycosides

Sample solutions of aminoglycosides kanamycin and neomycin were prepared with distilled water the concentration range 1.0 – 10.0 mM.

Optimizing the reaction time of OPA/MCE to kanamycin

1 100 μL of 1 mM kanamycin and 100 μL of 200 mM borate buffer solution pH 10.5 were pipetted into 4 glass vials and mixed well.
2 100 μL of OPA/MCE reagent (routine working reagent) was added to each vial left to react for 1, 10, 35, 45 min.
3 After the reaction time, these solutions were injected onto HPLC.

Optimizing the mole ratio of OPA/MCE to amines

1 100 μL of 1 mM kanamycin and 100 μL of 200 mM borate buffer solution pH 10.5 were pipetted into 7 glass vials and mixed well.
2 100 μL of OPA/MCE reagent concentration 1 mM, 2 mM, 4 mM, 5 mM, 10 mM, 15 mM and 25 mM. was added to each vial left to react for 10 min.
3 After 10 min, this solution was injected onto HPLC.
4 All steps were repeated with another model (neomycin).

HPLC system

Column:	Phenomenex hypersil C18 5μ 150 x 4.60 mm.
Mobile phase:	Acetonitrile: Milli-Q-water (40:60) the mobile phase was filtered through a 0.45 μm nylon membrane filter under vacuum and degassed in an ultrasonic bath for 30 min, used at a flow rate of 1 mL/min.
Detection	Fluorescence detection at OPA wavelength λ_{ex} = 340 nm, λ_{em} = 450 nm. UV detector at λ_{max} = 340 nm.

High Resolution-Electrospray ionization-Mass Spectrometry (HR-ESI-MS)

The expected molecular masses of some of the amine-OPA/MCE derivatives were confirmed by collection of the peak eluent and examination by HR-ESI-MS.

2.3 *o*-Phthalaldehyde (OPA)/Mercaptoethanol (MCE)/9-fluorenylmethyl chloroformate (FMOC Cl) derivatization

A two step derivatization process was performed by applying the OPA/MCE reagent followed by FMOC Cl reagent. By this method, molecules that contained both primary and

secondary amines such as spermidine and spermine should be fully labelled at their primary amines by OPA/MCE and their secondary amines by FMOC. Use the working OPA/MCE as described previously. FMOC Cl was in dissolved acetonitrile (4 mM). Amine samples: Spermidine, spermine (concentration from 0.1 mM-1 mM, 10-100 μL).

Derivatization procedure

100 μL Amine solution was rapidly mixed with 100 μL OPA/MCE reagent (routine working reagent) at 20°C. After 2 min (+/- 20 s), 100 μL of FMOC reagent was added and left for 2 min, then 50 μL were injected onto the HPLC. A blank was performed without amine.

HPLC system

Column:	Phenomenex hypersil C18 5μ 150 x 4.60 mm.
Mobile phase:	consisted of acetonitrile: Milli-Q-water (65:35, 70:30, 80:20, 85:15) the mobile phase was filtered through a 0.45 μm nylon membrane under vacuum and degassed, used at a flow rate of 1 mL/min.
Detection	Fluorescence detection at FMOC wavelength λ_{ex} = 264 nm, λ_{em} = 310 nm and at OPA wavelength λ_{ex} = 340 nm, λ_{em} = 450 nm.

2.4 Fluorescamine derivatization

A stock solution of fluorescamine was prepared by dissolving 0.2 g fluorescamine in 10 mL of acetonitrile. To 50 mL of a solution containing 0.6189 g of boric acid and 0.7456 g of potassium chloride add 36.85 mL of 0.2 M sodium hydroxide, adjust pH to 9.5 and dilute to 200 mL with water. Borate buffer pH 9.5 (Ref Appendix I E, A69, British Pharmacopoeia 1988). Using 1-butylamine, 1,4-diaminobutane, 1,5-diaminopentane, 1,7-diaminoheptane, serial dilutions of amine samples in water were prepared from concentration 0.1-2 mM, 0.1 mL, added 0.4 mL of 0.4 a borate buffer (pH 9.5), 0.1 mL of water and 0.5 mL of fluorescamine solution. The solution was left to react at 20°C for 5 min then injected onto the HPLC.

HPLC system

Column:	Phenomenex luna C18 5μ 150 x 4.60 mm.

Mobile phase: consisted of methanol: Milli-Q-water (40:60, 50:50, 70:30) the mobile phase was filter through a 0.45 μm nylon membrane filter under vacuum and degassed, used at a flow rate of l/min.

Detection Fluorescence detection at fluorescamine wavelength, λ_{ex} = 390 nm, λ_{em} = 486 nm. UV detector at λ_{max} = 390 nm.

Measurement of relative fluorescence yield experiment

Model amines: 1-butylamine, 1,4-diaminobutane, 1,5-diaminopentane, 1,7-diaminoheptane were dissolved in water to a concentration of 0.01- 0.1 mM. A comparison of fluorescence yields of the model series of amines was carried out by the following procedure:

1. The relevant HPLC peak was collected over 10 – 20 injection (depending upon the intensity of the peak).
2. The identity and stability of the product were confirmed by HR-ESI-MS.
3. A series of dilutions was prepared using the HPLC mobile phase: acetonitrile: Milli-Q-water (70:30).
4. Absorbance at λ_{ex} was measured by UV-VIS spectrophotometer and fluorescence intensity λ_{em} was measured by spectrofluorometer for each compound.
5. For each compound a plot of Fluorescence Intensity against Absorbance was prepared.

Fluorescamine and glucosamine

A stock solution of fluorescamine was prepared by dissolving 0.2 g fluorescamine in 10 mL of acetonitrile. Amine sample: glucosamine (0.2 mM). Borate buffer pH 9.5 (Ref Appendix I E, A69, British Pharmacopoeia 1988). To 50 mL of a solution containing 0.6189 g of boric acid and 0.7456 g of potassium chloride add 36.85 mL of 0.2 M sodium hydroxide, adjust to pH 9.5 and dilute to 200 mL with water.

Derivatization procedure

1. 100 μL of 2 mM glucosamine in aq. solution and 0.4 mL of borate buffer (pH 9.5), were pipetted into a glass vial and mixed well.
2. 0.5 mL of fluorescamine solution was added and left to react at 20^{o}C for 5 min.
3. This solution was injected onto the HPLC.

HPLC system

Column:	Phenomenex luna C18 5µ 150 x 4.60 mm
Mobile phase:	consisted of methanol: Milli-Q-water (30:70) the mobile phase was filter through a 0.45 µm nylon membrane filter under vacuum and degassed, used at a flow rate of 1 mL/min.
Detection	Fluorescence detection at fluorescamine wavelength, λ_{ex} = 390 nm, λ_{em} = 486 nm. UV detector at λ_{max} = 390 nm.

The expected molecular masses of some of the amine-fluorescamine derivatives were confirmed by collection of the peak eluent and examination by HR-ESI-MS.

2.5 9-Fluorenylmethyl chloroformate (FMOC Cl) derivatization

Optimization of the FMOC Cl derivatization method

The optimization was done by:

1. Optimisation of the reaction time.
2. Optimisation of the concentration of FMOC Cl reagent.
3. Optimization for the effect of pH of borate buffer
4. Methods to stop the reaction of FMOC Cl.
5. Optimization of the mobile phase for HPLC by using different ratio of acetonitrile: Milli-Q-water range from 60:40, 70:30, 80:20, 85:15 (%v/v), using C-18 Phenomenex luna analytical reverse phase column.
6. Stability of amine-FMOC derivatives.

FMOC Cl solution was prepared by dissolving FMOC Cl reagent in acetonitrile to obtain the concentration series of 1, 2, 4, 6, 8, 10 and 40 mM. The amines for optimization procedure were 1-butylamine (monoamine) and 1,5-diaminopentane (diamine). Both were prepared at the concentration of 1mM in Milli-Q-water.

Buffer preparation

A series of borate buffers pH 4.0–10.5 (200 mM) was prepared by adding 20.0 mL of 0.2 M sodium hydroxide to 50 mL of a solution containing 0.6189 g of boric acid and 0.7456 g of potassium chloride. The pH was adjusted to the required value by the addition of a solution

of boric acid or sodium hydroxide and using a pH meter measure the pH, then diluting to 200 mL with water (Ref Appendix I E, A69, British Pharmacopoeia 1988).

Optimization of the reaction time

1. 100 µL of 1 mM 1-butylamine and 100 µL of 200 mM borate buffer solution pH 9.0, were pipetted into 8 glass vials and mixed well.
2. 100 µL of 4 mM FMOC Cl reagent was added to each vial and left to react for 1, 5, 10, 20, 30, 40, 50 and 60 min.
3. At the appropriate time, 50 µL of 20 mM L-alanine solution (L-alanine 0.018 g in 10 mL of acetonitrile) was added to stop the reaction and left for another 5 min.
4. 100 µL of methanol was added to the vial and mixed well using a vortex mixer.
5. 200 µL of this solution was diluted with methanol to 1.00 mL.
6. This solution was injected onto HPLC.
7. All the steps were repeated with another model (1,5-diaminopentane).

Optimisation of the concentration of FMOC Cl reagent

1. 100 µL of 1 mM 1-butylamine (and then 1,5-diaminopentane) and 100 µL of 200 mM borate buffer solution pH 9.0, were pipetted into 8 glass vials and mixed well.
2. 100 µL of 1, 2, 4, 6, 8 and 10 mM FMOC Cl reagent were added to separate vials and left to react for 5 min.
3. After 5 min, 50 µL of 20 mM alanine solution was added to stop the reaction and left for another 5 min.
4. 100 µL of methanol was added to the vial and mixed well using a vortex mixer.
5. 200 µL of this solution was diluted with methanol to 1.00 mL.
6. This solution was injected onto the HPLC.

Optimization for the effect of pH of borate buffer

1 100 µL of 1 mM 1-butylamine and 100 µL of 200 mM borate buffer solution pH 4.0, 4.5, 5.0, 5.5, 6.0, 6.5, 7.0, 8.0, 8.5, 9.0, 9.5, 10.0 and 10.5 were pipetted into 13 glass vials and mixed well.

2 100 µL of 4 mM FMOC Cl reagent was added to each vial left to react for 5 min.

3 After 5 min, 50 µL of 20 mM alanine solution was added to stop the reaction and left for another 5 min.

4 100 μL of methanol was added to the vial and mixed well using vortex mixer.

5 200 μL of this solution was diluted with methanol to 1.00 mL.

6 This solution was injected onto HPLC.

7 All the steps were repeated with another model (1,5-diaminopentane).

Methods to terminate the reaction of FMOC Cl

Three main methods of termination of the reaction and removal of the excess FMOC Cl were investigated. In method 1, the excess of FMOC was removed by the reaction with alanine 100 mM. Method 2 removed the excess of FMOC Cl by extraction of amine-FMOC derivatives with pentane after derivatization. Method 3 used glacial acetic acid to stop the reaction at the desired time by acidifying the medium mixture.

Eight experiments were designed to examine and compare the methods to terminate the reaction of FMOC Cl as:

Experiment 1 Control experiment

1. 100 μL 5 mM 1-butylamine and 100 μL of 200 mM borate buffer pH 9.5 were placed in a glass vial.
2. 100 μL 10 mM FMOC Cl reagent was added and left to react for 5 min.
3. 200 μL methanol was added to this solution, and mixed well.
4. 200 μL was taken and diluted by 800 μL mobile phase [acetonitrile: Milli-Q-water, (70:30)]. This was injected onto the HPLC.

Experiment 2 Termination of the reaction with alanine

1. 100 μL 5 mM 1-butylamine and 100 μL of 200 mM borate buffer pH 9.5 were placed in a glass vial.
2. 100 μL 10 mM FMOC Cl reagent was added and left to react for 5 min.
3. 100 μL 100 mM alanine solution was added and left for 1 min then 100 μL methanol was added to this solution.
4. 200 μL was taken and diluted by 800 μL mobile phase [acetonitrile: Milli-Q-water (70:30)]. This was injected onto the HPLC.

Experiment 3 Termination of the reaction with glacial acetic acid

1. 100 μL 5 mM 1-butylamine and 100 μL of 200 mM borate buffer pH 9.5 were placed in a glass vial.
2. 100 μL 10 mM FMOC Cl reagent was added and left to react for 5 min.
3. 100 μL glacial acetic acid was added and left for 1 min then 100 μL methanol was added to this solution.
4. 200 μL was taken and diluted by 800 μL mobile phase [acetonitrile: Milli-Q-water (70:30)]. This was injected onto the HPLC.

Experiment 4 Termination of the reaction with alanine and glacial acetic acid

1. 100 μL 5 mM 1-butylamine and 100 μL of 200 mM borate buffer pH 9.5 were placed in a glass vial.
2. 100 μL 10 mM FMOC Cl reagent was added and left to react for 5 min.
3. 100 μL 100 mM alanine solution was added and left for 1 min then 100 μL glacial acetic acid was added and left for 1 min.
4. 200 μL was taken and diluted by 800 μL mobile phase (acetonitrile: Milli-Q-water (70:30)]. This was injected onto the HPLC.

Experiment 5 Termination of the reaction by extraction with pentane

1. 1 mL of 5 mM 1-butylamine and 1 mL of 200 mM borate buffer pH 9.5 were placed in a glass vial.
2. 1 mL of 10 mM FMOC Cl reagent was added and left to react for 5 min.
3. This solution was extracted with pentane 3 x 5 mL.
4. The pentane phase was combined and evaporated.
5. 5 mL of methanol was used to dissolve the residue.
6. 200 μL of this solution was taken and diluted by 800 μL mobile phase [acetonitrile: Milli-Q-water (70:30)]. This was injected onto the HPLC.

Experiment 6 Termination of the reaction with alanine and extraction with pentane

1. 1 mL of 5 mM 1-butylamine and 1 mL of 200 mM borate buffer pH 9.5 were placed in a glass vial.
2. 1 mL of 10 mM FMOC Cl reagent was added and left to react for 5 min.

3. 1 mL 100 mM alanine solution was added and left for 1 min.
4. This solution was extracted with pentane 3 x 5 mL.
5. The pentane phase was combined and evaporated.
6. 5 mL of methanol was used to dissolve the residue.
7. 200 μL of this solution was taken and diluted by 800 μL mobile phase [acetonitrile: Milli-Q-water (70:30)]. This was injected onto the HPLC.

Experiment 7 Termination of the reaction with glacial acetic acid and extraction with pentane

1. 1 mL of 5 mM 1-butylamine and 1 mL of 200 mM borate buffer pH 9.5 were placed in a glass vial.
2. 1 mL of 10 mM FMOC Cl reagent was added and left to react for 5 min.
3. 1 mL glacial acetic acid was added and left for 1 min (pH of the solution = 3.35).
4. This solution was extracted with pentane 3 x 5 mL.
5. The pentane phase was combined and evaporated.
6. 5 mL of methanol was used to dissolve the residue.
7. 200 μL of this solution was taken and diluted by 800 μL mobile phase [acetonitrile: Milli-Q-water (70:30)]. This was injected onto the HPLC.

Experiment 8 Termination of the reaction with alanine and glacial acetic acid then extraction with pentane

1. 1 mL of 5 mM 1-butylamine and 1 mL of 200 mM borate buffer pH 9.5 were placed in a glass vial.
2. 1 mL of 10 mM FMOC Cl reagent was added and left to react for 5 min.
3. 1 mL 100 mM alanine solution was added and left for 1 min then 1 mL glacial acetic acid was added and left for 1 min (pH of the solution = 3.05).
4. This solution was extracted with pentane 3 x 5 mL.
5. The pentane phase was combined and evaporated.
6. 5 mL of methanol was used to dissolve the residue.
7. 200 μL of this solution was taken and diluted by 800 μL mobile phase (acetonitrile: Milli-Q-water (70:30)]. This was injected onto the HPLC.

Calibration curve of amine-FMOC derivatives

Preparation of sample solutions

Amine samples were ethylamine, 1-butylamine (monoamine), 1,4-diaminobutane, 1,5-diaminopentane, 1,7-diaminoheptane, piperidine, piperazine, spermidine, spermine (polyamine), kanamycin, neomycin (aminoglycosides)

Stock solutions of sample were prepared by dissolving the suitable amount of each in Milli-Q-water. A range of concentrations from 1 mM – 10 mM were prepared from the stock solution by dilution with Milli-Q-water. All solutions were stored in the dark at 2^{o}C.

Working Method for FMOC derivatization

1. 1 mL of sample solution and 1 mL of 200 mM borate buffer pH 9.5 were placed in a glass vial.
2. 1 mL of 40 mM FMOC Cl reagent was added and left to react for 5 min.
3. 1 mL 100 mM alanine solution was added and left for a further 1 min.
4. This solution was extracted with pentane 3 x 5 mL.
5. The pentane phase was combined and evaporated.
6. 5 mL of methanol was used to dissolve the residue.
7. 200 μL of this solution was taken and diluted by 800 μL mobile phase [acetonitrile: Milli-Q-water (70:30)].
8. This was injected onto the HPLC.
9. A calibration curve of each amine-FMOC derivative was plotted.

HPLC system

Column:	Phenomenex luna C18 5μ 150 x 4.60 mm.
Mobile phase:	Methanol: Milli-Q-water (60:40, 70:30, 80:20, 85:15) the mobile phase was filtered through a 0.45 μm nylon membrane filter under vacuum and degassed in an ultrasonic bath for 30 min, used at a flow rate of 1 mL/min.
Detection	Fluorescence detection at FMOC wavelength, λ_{ex} = 264 nm, λ_{em} = 310 nm. UV detector at λ_{max} = 264 nm.

Stability of amine-FMOC derivatives

1. 1 mL of 1 mM of 1-butylamine was reacted with 1 mL 4 mM FMOC Cl reagent for 5 min in the presence of 1 mL of 200 mM borate buffer pH 9.5.
2. The reaction was terminated by reaction with alanine and extraction with pentane (as in Experiment 7) then after pentane phase was combined and evaporated, 5 mL of methanol was used to dissolve the residue.
3. This solution was injected onto HPLC at various times from 5-70 min then stored the sample at 20^{o}C, and injected at day 2, day 3, day 4, day 5, 1 week and 2 weeks. Measure the peak area.

Measurement of relative fluorescence yield

Sample solution:

The amines: 1,5-diaminopentane, 1,7-diaminoheptane, piperidine, piperazine and spermidine were dissolved in water. A comparison of fluorescence yields of the model series of amines was carried out by the following procedure:

1. The relevant HPLC peak was collected over 10 – 15 injection (depending upon the intensity of the peak).
2. The identity and stability of the product was confirmed by HR-ESI-MS.
3. A series of dilutions was prepared using the HPLC mobile phase [acetonitrile: Milli-Q-water (70:30)].
4. Absorbance at λ_{ex} and fluorescence intensity λ_{em} was measured for each compound.
5. For each compound a plot of Fluorescence Intensity against Absorbance was prepared.

Analysis of spermidine and spermine as their hexahydropyrimidine derivatives

***N*-(4-Aminobutyl)hexahydropyrimidine**

Spermidine was converted into *N*-(4-aminobutyl)hexahydropyrimidine by the reaction with formaldehyde.

1. Spermidine 1.0 g. (6.88 mmol) in a 100-mL round bottomed flask was dissolved in distilled water (25 mL). The solution was cooled to 5^{o}C.
2. Aqueous formaldehyde (0.5 mL of 37% solution: 1 equiv.) was slowly added to the cold solution.

3. The mixture was stirred for 1 h at 20°C.
4. The aqueous layer was saturated with solid sodium chloride (NaCl) and extracted four times with chloroform.
5. The combined chloroform extracts were dried ($MgSO_4$) filtered and concentrated to dryness by evaporator.
6. Dilution to the desired concentration.

After this the FMOC derivative was prepared by the standard method.

1,4-(Dihexahydropyrimidine) butane

Spermine was converted into 1,4-(dihexahydropyrimidine) butane by the reaction with formaldehyde.

1. Spermine 1 g. (4.95 mmol) in a 100-mL round bottomed flask was dissolved in distilled water (25 mL). The solution was cooled to 5°C.
2. Aqueous formaldehyde (1 mL of 37% solution: 2 equiv.) was slowly added to the cold solution.
3. The mixture was stirred for 1 hr at 20°C.
4. The aqueous layer was saturated with solid sodium chloride and extracted four times with chloroform.
5. The combined chloroform extracts were dried ($MgSO_4$) filtered and concentrated to dryness.

FMOC derivatives of experimental non-viral gene therapy (NVGT) vectors

Stock solutions of samples N^4,N^9-didecanoyl spermine, N^4,N^9-didodecanoyl spermine and the synthetic intermediate diphthalimido-4,9-diazadodecane were prepared by dissolving the suitable amount of each in methanol. A range of concentrations from 1 mM–10 mM were prepared from the stock solutions by dilution with methanol. These were derivatized with FMOC using the standard method.

HPLC system

Column: Phenomenex luna C18 5µ 150 x 4.60 mm.

Mobile phase: consisted of methanol: Milli-Q-water (85:15) the mobile phase was filter through a 0.45 µm nylon membrane filter under vacuum and degassed in an ultrasonic bath for 30 min at a flow rate of 1 mL/min.

Detection Fluorescence detection at FMOC wavelength, λ_{ex} = 264 nm, λ_{em} = 310 nm. UV detector at λ_{max} = 264 nm.

FMOC derivatization of aminoglycosides

Stock solutions of samples (kanamycin, paramomycin) were prepared by dissolving the suitable amount of each in Milli-Q-water. A range of concentrations from 1 mM–10 mM were prepared from the stock solution by dilution with Milli-Q-water.

1. 1 mL of sample solution and 1 mL of 200 mM borate buffer pH 9.5 in glass vial.
2. 1 mL of 40 mM FMOC Cl reagent was added and left to react for 5 min.
3. 1 mL 100 mM alanine solution was added and left for a further 1 min.
4. This solution was extracted with pentane 3 x 5 mL.
5. The pentane phase was combined and evaporated.
6. 5 mL of methanol was used for dissolve the derivative.
7. This solution was pipetted 200 µL and diluted by 800 µL mobile phase to get 1mL. Injected onto the HPLC.

HPLC system

Column: Phenomenex hypersil C18 5µ 150 x 4.60 mm

Mobile phase: consisted of methanol: Milli-Q-water (60:40) the mobile phase was filter through a 0.45 µm nylon membrane filter under vacuum and degassed in an ultrasonic bath for 30 min, used at a flow rate of 1 mL/min.

Detection Fluorescence detection at FMOC wavelength, λ_{ex} = 264 nm, λ_{em} = 310 nm. UV detector at λ_{max} = 264 nm.

2.6 Dansylation derivatization

Stability of Dansyl chloride (DNS Cl) reagent

1. DNS Cl was prepared in series of concentrations from 0.1 to 0.8 mM in acetone.
2. These solutions were injected onto HPLC (5 replicates).
3. A calibration curve was plotted.

HPLC conditions

Column:	Phenomenex luna C18, 150 mm x 4.6 mm. i.d. cartridge column (5 μm particle size) with guard column, H1-5C18.
Mobile phase:	Acetonitrile: Milli-Q-water (70:30) at a flow rate of 1.00 mL/min.
Detector:	Waters Fluorescence detector 470 at λ_{ex} = 330 nm and λ_{ex} = 510 nm Jasco UV detector at λ_{max} = 330 nm.

Blank-DNS reaction

1. 1 mL of Milli-Q-water and 1 mL of saturated sodium carbonate solution were placed in a glass vial.
2. 1 mL of 10 mM DNS Cl reagent (in acetone) was added and left at 60^{o}C for 15 min.
3. The excess of DNS Cl was removed by 20 mM alanine solution, then the reaction was left for 5 min at 20^{o}C.
4. This solution was extracted with toluene 3 x 5 mL.
5. The toluene phase was combined and evaporated.
6. 2 mL of mobile phase [acetonitrile: Milli-Q-water (70:30)] was used to dissolve the residue. This was injected onto the HPLC.
7. The peaks were eluted by HPLC, collected and then analyzed by HR-ESI-MS.

HPLC conditions

HPLC column:	Phenomenex luna C18, 150 mm x 4.6 mm. i.d. cartridge column (5μm particle size) with guard column, H1-5C18.
Mobile phase:	Methanol: Milli-Q-water (70:30) at a flow rate of 1.00 mL/min.
Detector:	Waters Fluorescence detector 470 at λ_{ex} = 330 nm and λ_{ex} = 510 nm. Jasco UV detector at λ_{max} = 330 nm.

HPLC condition establishment of mobile phase

In order to optimize the mobile phase for HPLC condition, the following mobile phases were used:

Acetonitrile: Milli-Q-water (60:40)
Acetonitrile: Milli-Q-water (70:30)

Acetonitrile: 0.1 % formic acid in Milli-Q-water (60:40)

Acetonitrile: 2.5 % formic acid in Milli-Q-water (60:40)

Methanol: acetonitrile: Milli-Q-water (65:20:15)

Selection of the excitation and emission wavelengths of amine-DNS derivatives

The amines: 1-butylamine, 1,5-diaminopentane, 1,7-diaminoheptane, 1,8-diaminooctane, piperidine, piperazine, spermidine and spermine were examined by collecting the HPLC eluate after dansylation.

Method

1. 1 mL of sample solution (concentration at 2 mM) and 1 mL of saturated sodium carbonate were placed in glass vial.
2. 1.00 mL of 10 mM DNS Cl in acetone was added.
3. The reactant solution was incubated in a water bath for 15 min at 60^{o}C
4. This solution was extracted with toluene 3 x 2 mL.
5. The toluene phase was combined and evaporated to dryness.
6. The residue was dissolved with 5 mL of methanol.
7. This solution was injected onto HPLC and the eluent of the amine-DNS derivatives were collected and confirmed by HR-ESI-MS.
8. The excitation and emission wavelengths of these elutes of amines-DNS derivatives were determined by using Hitachi Fluorescence F-2000 spectrophotometer and methanol was used as the blank.

Optimization of DNS Cl derivatization method

Method 1 Without removing the excess of DNS Cl

The reaction solution consisted of 1.0 mL DNS Cl (5-40 mM) in acetone, 1.00 mL of sample solution (1-5 mM) and 1.0 mL of saturated sodium carbonate. The reactant solution was incubated in a water bath for 15 min at 60^{o}C. This solution was injected directly without any procedure to remove the excess DNS Cl.

Method 2 With alanine to remove the excess DNS Cl

This derivatization method was based on the work of Minocha and Long (Minocha and Long, 2004). To 1.0 sample solution, 1.0 mL of saturated aqueous of Na_2CO_3 was added to give a pH of 9-10 and then 1.0 mL DNS Cl solution was added. The vials were capped, vortexed and incubated in a water bath at 60°C. After 15 min, aqueous L-alanine (0.5 mL, 10 mg/ mL) was added to react with the excess of DNS Cl, followed by further 5 min incubation. The amine-DNS derivatives were extracted with toluene (3 x 4.0 mL), and the toluene phase evaporated to dryness under vacuum. Methanol (7.0 mL) was added and vortexed for 2 min to redissolve the amine-DNS derivatives. At this stage in the final development of dansylation method, mobile phase 2.0 mL was used to redissolve the amine-DNS derivative. The products were filtered through a 0.45 μm nylon syringe filter to remove particulate matter before being injected onto the HPLC column. Blank HPLC runs were conducted using the procedure above without the amines.

In all these methods, dansylation was performed in dark since the derivatives are light sensitive. The solution of DNS Cl in acetone can be stored for 2 weeks at 4^{o}C in the dark. After the dansylation reaction, the sample was kept in the dark or in dark vials.

Optimization of DNS Cl derivatization method

The aims of optimization condition of DNS derivatization (dansylation) were:

1. Optimization of the pH of buffer for DNS Cl reaction with amines.
2. Optimization of the ratio of molarity of DNS Cl reaction with amines.
3. Optimization of the reaction time of DNS Cl with amines.
4. Optimization of the temperature of DNS Cl of the reaction.

Optimization of the pH of buffer for DNS Cl reaction with amines

1. Method 2 was used to derivatize 1 mM 1-butylamine with 10 mM DNS Cl reagent using borate buffer at various pHs from 4.5-10.5.
2. The vials were incubated at 60^{o}C for 15 min.
3. Toluene 3 x 5 mL was used to extract the DNS derivatives, then the combined organic phase was evaporated to dryness.
4. The residue was dissolved with 2 mL methanol.
5. This solution was injected onto HPLC.

Comparison between borate buffer pH 10.5 and saturated sodium carbonate

1. Method 2 was used to derivatize 1 mM 1-butylamine with 10 mM DNS Cl reagent with borate buffer pH 10.5 and another vial was prepared in the same way but used saturated sodium carbonate.
2. The vials were incubated at 60^{o}C for 15 min.
3. Toluene 3 x 5 mL was used to extract the DNS derivatives, then the combined organic phase was evaporated to dryness.
4. The residue was dissolved with 2 mL methanol.
5. This solution was injected onto HPLC.

Optimization of the reaction temperature of dansylation

1. Method 2 was used to derivatize 1 mM 1-butylamine with 10 mM DNS Cl reagent with 1 mL saturated sodium carbonate.
2. The vials were incubated at various temperatures from 20, 40, 60, and 80^{o}C for 15 min.
3. Toluene 3 x 5 mL was used to extract the DNS derivatives, then the combined organic phase was evaporated to dryness.
4. The residue was dissolved with 2 mL methanol. This solution was injected onto HPLC.

Optimization of the reaction time of dansylation

1. Method 2 was used to derivatize 1 mM 1-butylamine with 10 mM DNS Cl reagent with 1 mL saturated sodium carbonate.
2. The vials were incubated at various times from 1, 5, 10, 15, 20, 30, 40, 50 and 60 min at 60^{o}C.
3. Toluene 3 x 5 mL was used to extract the DNS derivatives, then the combined organic phase was evaporated to dryness.
4. The residue was dissolved with 2 mL methanol. This solution was injected onto HPLC.

Optimization of the concentration ratio of DNS Cl for dansylation

For the optimization for DNS Cl concentration, DNS Cl solution of concentration range from 1 to 100 mM was reacted with 1 mM solutions of ethylamine, 1-butylamine,

phenylethylamine, 1,4-diaminobutane, 1,7-diaminoheptane, piperidine, piperazine, spermidine.

1. Method 2 was used to derivatize these amines with various concentrations of DNS Cl reagent 1-100 mM, 1 mL saturated sodium carbonate was used to adjust the pH.
2. The vials were incubated at 60^{o}C for 15 min.
3. Toluene 3 x 5 mL was used to extract the DNS derivatives, then the combined organic phase was evaporated to dryness.
4. The residue was dissolved with 2 mL methanol. This solution was injected onto HPLC.

General derivatization of amines

DNS Cl reagent was prepared in acetone (2 concentrations, 10 mM prepared by dissolving 20 mg of DNS Cl in 10 mL acetone and 148 mM by dissolving 40 mg in 10 mL acetone).

An alanine solution was prepared from 100 mg of L-alanine dissolved in 10 mL of Milli-Q-water to give a concentration of 112 mM.

Amines examined were: 1-butylamine, 1,4–diaminobutane, 1,5-diaminopentane, 1,6-diaminohexane, 1,7-diaminoheptane, 1,8-diaminooctane, 1,9-diaminononane, 1,12-diaminododecane, piperidine, piperazine, 1,4-diaminobutanol, 1,5-diaminopentanol, spermidine, spermine, thermospermine, N^4,N^9-didecanoyl spermine, N^4,N^9-dihexadecanoyl spermine, N^1,N^{12}-di-trifluoroacetyl- spermine, N^1,N^4,N^9-tri-*t*-Boc-spermine derivative, N^4,N^9-digeranoyl spermine, N^4-decanoyl-N^9-cholesteryl carbamate spermine, N^4,N^9-Oleoyl spermine and N^4,N^9-Dioctadecanoyl spermine. Amine samples were dissolved in water from 0.1 mM – 15 mM

Amines for calibration curves

The following amines were used to construct a calibration curve over the concentration range 0.2-1 mM, all were in 5 replicates: ethylamine, 1-butylamine, 1,4-diaminobutane, 1,7-diaminoheptane, 2-phenylethylamine, piperidine, piperazine, spermidine, glucosamine, kanamycin. Most of the semi-synthetic non-viral gene therapy agents and their synthetic intermediates are not soluble in water, so some drops of methanol were routinely added to help dissolution before they were dissolved in water otherwise the reaction was performed in dichloromethane.

Conditions for the separation of N^4,N^9-oleoyl spermine and N^4,N^9-dioctadecanoyl spermine:

1. 1 mL of 10 mM Samples (MKS pH = 9.07, Lipogen pH = 8.81) + 1 mL sat. Na_2CO_3 (pH 11.20) pH mixture = 11.96 (MKS C18) and pH = 11.91 (Lipogen).
2. Added DNS (2 mL of 70 mM DNS), left 30 min at 60°C.
3. Extract with toluene 3 x 5 mL, and evaporate.
4. Redissolved with 1 mL acetonitrile: 1% formic acid in Milli-Q-water (90:10).
5. Inject onto HPLC column C 8, acetonitrile: 1% formic acid in Milli-Q-water (90:10).

HPLC conditions

HPLC column:	Phenomenex luna C18, 150 mm x 4.6 mm. i.d. cartridge column (5µm particle size) with guard column, H1-5C18
Mobile phase:	Acetonitrile: Milli-Q-water (85:15, 90:10, 95:5), used at flow rate of 1.00 mL/min.
Detector:	Waters fluorescence detector 470 at λ_{ex} = 330 nm and λ_{ex} = 510 nm. Jasco UV detector at λ_{max} = 330 nm.

Aminoglycosides

Aminoglycosides (1 mL of 10 mM, glucosamine, kanamycin) were reacted with 1 mL sat. Na_2CO_3 and DNS reagent (2 mL of 70 mM DNS) was added, left for 30 min at 60°C, then extracted with toluene (3 x 5 mL), and evaporated. The residue was redissolved with 1 mL 40% MeCN in water. This solution was injected onto HPLC.

HPLC conditions:

HPLC column:	Phenomenex luna C18, 150 mm x 4.6 mm. i.d. cartridge column (5µm particle size) with guard column, H1-5C18
Mobile phase:	Acetonitrile: Milli-Q-water (40:60), used at flow rate of 1.00 mL/min.
Detector:	Waters Fluorescence detector 470 at λ_{ex} = 330 nm and λ_{ex} = 510 nm Jasco UV detector at λ_{max} = 330 nm

Measurement of relative fluorescence yield experiment:

The dansylation method 2 was applied to these amines: 1-butylamine, 1,4-diaminobutane, 1,7-diaminoheptane and spermidine.

Derivatization method to obtain the monoDNS derivatives and diDNS derivatives

For diamines such as 1,4-diaminobutane both the mono- and di-DNS derivatives were prepared for a study of relative quantum yield. To obtain the diDNS derivatives of the diamines, method 3 was used. To obtain the monoDNS derivatives of diamines, the concentration of DNS Cl used was reduced to below 10 mM. This yielded both mono- and diDNS derivatives which were easily resolved by HPLC and collected separately.

HPLC conditions:

HPLC column:	Semi-preparative column: Phenomenex Gemini 10 μ C18 110A 250 x 10 mm; Guard column: Phenomenex Gemini 5 μ C18 10 x 10 mm.
Mobile phase:	Methanol: Milli-Q-water (70:30), used at flow rate of 5.00 mL/min.
Injection Volume:	100 μL
Detector:	Waters Fluorescence detector 470 at λ_{ex} = 330 nm and λ_{ex} = 510 nm Jasco UV detector at λ_{max} = 330 nm.

After collection of the peak of amine-DNS derivative, the expected molecular weight of the product was confirmed by HR-ESI-MS.

To measure the relative fluorescent yield of each product the following procedure was used. The UV-VIS absorbance spectrum of the solvent background for the chosen sample was recorded and the absorbance at the excitation wavelength to be used was noted. The fluorescence spectrum of the same solution in the 10 mm fluorescence cuvette was recorded.

Increasing concentrations of each sample of the five solutions were analyzed and a graph of integrated fluorescence intensity vs. absorbance was plotted. The slopes of the graphs obtained are proportional to the quantum yield of the different samples.

2.7 Synthesis of thermospermine

Method 1 Thermospermine was synthesized from spermidine using the method of Ganem and Chantrapromma (1983) following the scheme shown in Figure 2.1.

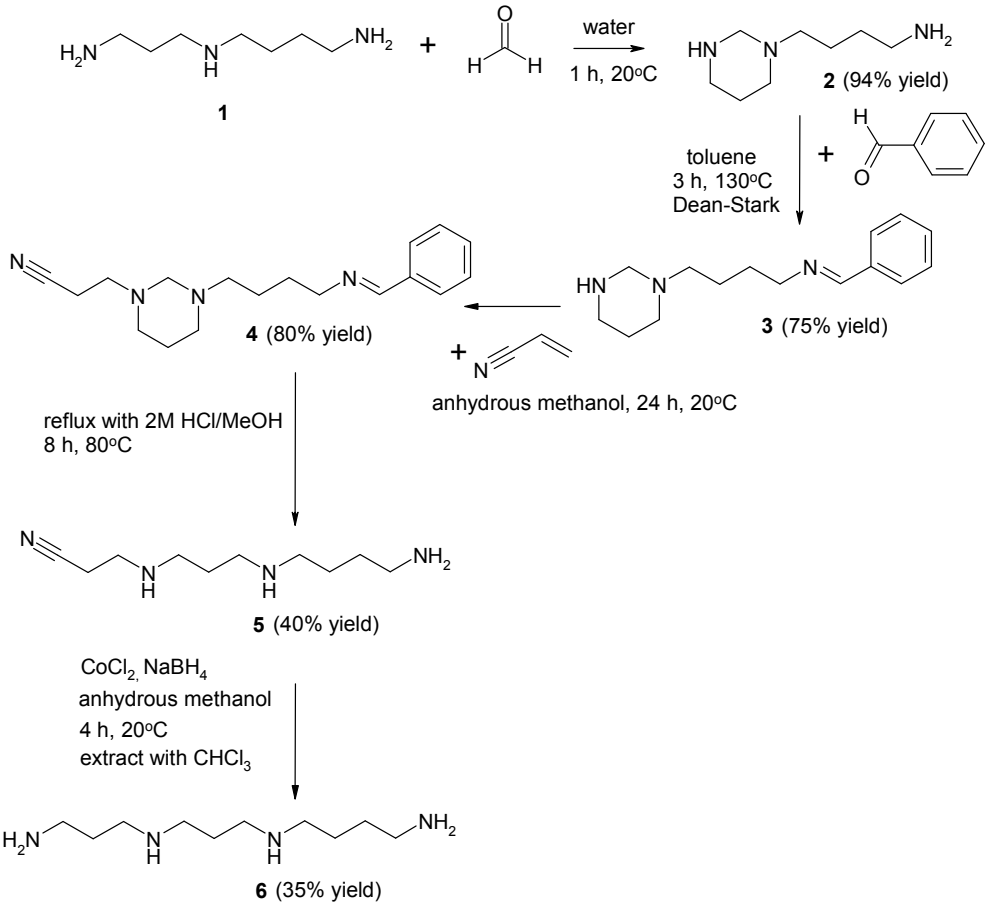

Figure 2.1 Scheme of thermospermine synthesis.

1. *N*-(4-Aminobutyl) hexahydropyrimidine (2)

Spermidine (**1**) 9.0 g (62 mmol), was dissolved in distilled water (225 mL) and the solution cooled to 5°C under N_2. 37% Aqueous solution of formaldehyde (4.52 mL) (0.9 equiv.) was added dropwise then the solution was stirred for 1 h at 20°C. The aqueous layer was saturated with solid NaCl and extracted four times with $CHCl_3$. The combined $CHCl_3$ extracts were dried ($MgSO_4$) filtered and concentrated to dryness, giving *N*-(4-aminobutyl) hexahydropyrimidine (**2**) (94%, 9.2 g) as a waxy white solid. TLC (dichloromethane: methanol: ammonia (20: 10: 1), detection by ninhydrin) $R_t = 0.1$.

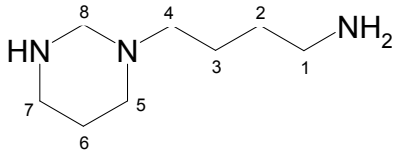

δ_H ($CDCl_3$) (400 MHz) 3.298 (2H, s, C(8)H_2), 2.732 (2H, m C(1)H_2), 2.643 (2H, m, C(7)H_2), 2.626 (2H, m, C(4)H_2), 2.172 (2H, m, C(5)H_2), 1.985 (1H, s, NH), 1.536 (2H, p, C(3)H_2), 1.410 (4H, m, C(2)H_2, C(6)H_2).

δ_C ($CDCl_3$) (100 MHz) 24.151, 26.957, 31.471, 41.716, 44.997, 52.943, 55.236, 69.736. $C_8H_{19}N_3$ requires M.W. = 157.1579, HR-ESI-MS: m/z $[M+H]^+$ = $C_8H_{20}N_3$ requires 158.1657, found = 158.1630.

2. 4-(*N*-Benzylideneaminobutyl) hexahydropyrimidine (3)

N-(4-Aminobutyl) hexahydropyrimidine (**2**) 2.50 g. (15.90 mmol) was dissolved in toluene (30 mL). Benzaldehyde (1.69 g, 15.90 mmol) was added and the mixture was refluxed at 130^{o}C for 3 h using a Dean-Stark apparatus to remove water azeotropically. After removal of the solvent, the *N*-(4-aminobutyl)hexahydropyrimidine (**2**) with its primary amine protected as a benzylidine derivative, 4-(*N*-benzylideneaminobutyl) hexahydropyrimidine (**3**) was obtained as colourless oil (2.95g, 75%).

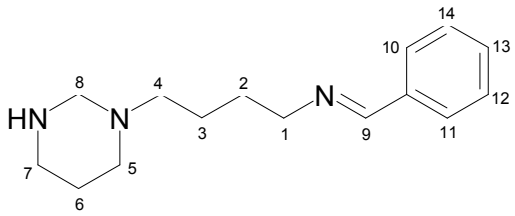

δ_H ($CDCl_3$) (400 MHz) 8.235 (H, s, C(9) H), 7.680 (2H, m, C(10)H, C(11)H), 7.374 (3H, m, C(12)H, C(13)H, C(14)H), 3.584 (2H, t, C(1)H_2), 3.071 (2H, s C(8)H_2), 2.547 (2H, t, C(7)H_2), 2.476 (2H, t, C(4)H_2), 2.336 (2H, t, C(5)H_2), 1.671 (2H, m, C(3)H_2), 1.578 (4H, m, C(2) H_2, C(6)H_2).

$C_{15}H_{23}N_3$ requires M.W. = 245.1892, HR-ESI-MS: m/z $[M+H]^+$ = $C_{15}H_{24}N_3$ requires 246.1970, found = 246.1945.

3. N^1-(*N*-Benzylidene-(1-hexahydropyrimidinebutyl)-N^3-propionitrile (**4**)

4-(*N*-Benzylideneaminobutyl) hexahydropyrimidine (**3**) 2.44 g (9.9 mmol) was dissolved in anhydrous methanol (15 mL) then acrylonitrile (0.66 mL, 9.9 mmol) was added dropwise with stirring under N_2. After 15 h, more acrylonitrile (0.5 mL) was added and stirring continued for 9 h, then concentrated under reduced pressure to yield N^1-(*N*-benzylidene-(1-hexahydropyrimidinebutyl)-N^3-propionitrile (**4**) (2.39 g, 80%).

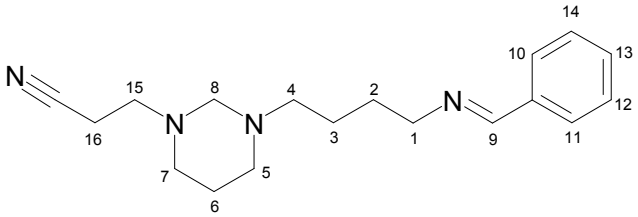

δ_H ($CDCl_3$) (400 MHz) 8.3 (H, s, C(9) H), 7.7 (2H, m, C(10)H, C(11)H), 7.4 (3H, m, C(12)H, C(13)H, C(14)H), 3.6 (2H, t, C(1)H_2), 3.5 (2H, s C(8)H_2), 3.2 (2H, t, C(16)H_2), 2.7 (2H, t, C(15)H_2), 2.3 (4H, t, C(5)H_2, C(7)H_2), 2.5 (2H, t, C(4)H_2), 1.6 (2H, m, C(2)H_2), 1.6 (2H, m, C(6)H_2), 1.5 (2H, m, C(3) H_2).

$C_{18}H_{26}N_4$ requires M.W. = 298.2157, HR-ESI-MS: m/z $[M+H]^+$ = $C_{18}H_{27}N_4$ requires 299.2236, found = 299.2201.

4. Deprotection of the N^1-(*N*-benzylidene-(1-hexahydropyrimidinebutyl)-N^3-propionitrile (**4**) to give 12-amino-4,8-diaza-dodecanenitrile (**5**)

A solution of N^1-(*N*-benzylidene-(1-hexahydropyrimidinebutyl)-N^3-propionitrile (**4**) (0.665 g, 2.23 mmol) in 2M HCl-methanol (15 mL) was heated under reflux at 80^{o}C for 8 h. After evaporation of methanol under reduced pressure, the resulting residue was redissolved in water (4mL) and extracted with diethyl ether (3x 15 mL) to remove benzaldehyde. The aqueous layer was alkalinized with 20% NaOH (8 mL) and extracted with $CHCl_3$. The $CHCl_3$ extracts were dried ($MgSO_4$), filtered and concentrated to yield 12-amino-4,8-diaza-dodecanenitrile (**5**) (0.17 g, 40%).

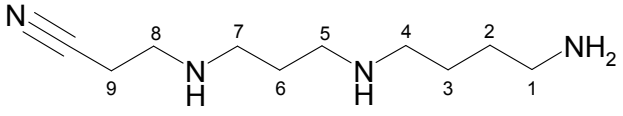

δ_H ($CDCl_3$) (400 MHz) 2.86 (2H, t, C(9) H_2), 2.76 (6H, m, C(4)H_2, C(5)H_2, C(7)H_2), 2.66 (2H, m, C(8)H_2), 2.48 (2H, m, C(1)H_2), 1.55 (4H, m, C(2)H_2, C(6)H_2), 1.45 (2H, m, C(3)H_2).

$C_{10}H_{22}N_4$ requires M.W. = 198.1844, HR-ESI-MS: m/z $[M+H]^+$ = $C_{10}H_{23}N_4$ requires 199.1923, found = 199.1923.

5. Thermospermine

An ice-cold solution of 12-amino-4,8-diaza-dodecanenitrile (**5**) (0.150 g, 0.76 mmol) in dry methanol (15 mL) was mixed with $CoCl_2 \cdot 6H_2O$ (0.360 g, 1.52 mmol); then $NaBH_4$ was added in portions (0.286 g, 10 equiv.). After the addition was complete, stirring was continued for 3 h at 20°C. The reaction mixture was acidified with 3M HCl and stirred until the black precipitate (Co_2B) dissolved. After concentration *in vacuo*, the resulting aqueous solution was alkalinized with 30% NaOH and extracted with $CHCl_3$, to give the desired thermospermine (**6**) (0.05 g, 35%).

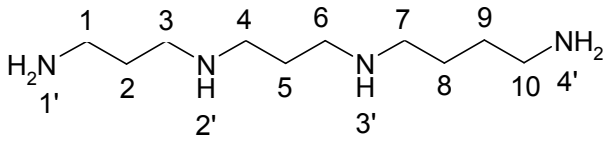

δ_H ($CDCl_3$) (400 MHz) 2.740 (4H, m, C(1)H_2, C(10)H_2), 2.645 (8H, m, C(3)H_2, C(4)H_2, C(6)H_2, C(7)H_2), 2.180 (H, s, N(2′)H), 2.150 (H, s, N(3′)H), 1.654 (2H, m, C(2)H_2), 1.610 (2H, m, C(5)H_2), 1.562 (2H, m, C(9)H_2), 1.424 (2H, m, C(8)H_2).

δ_C ($CDCl_3$) (100 MHz) 24.504, 27.538, 31.867, 40.580, 42.181, 47.967, 48.585, 48.691, 49.971.

$C_{10}H_{26}N_4$ requires M.W. = 202.2157, HR-ESI-MS: m/z $[M+H]^+$ = $C_{10}H_{27}N_4$ requires 203.2236, found = 203.2236.

Method 2 By protection of *N*-(4-aminobutyl) hexahydropyrimidine (2) with phthalimide: the scheme shown in Figure 2.2.

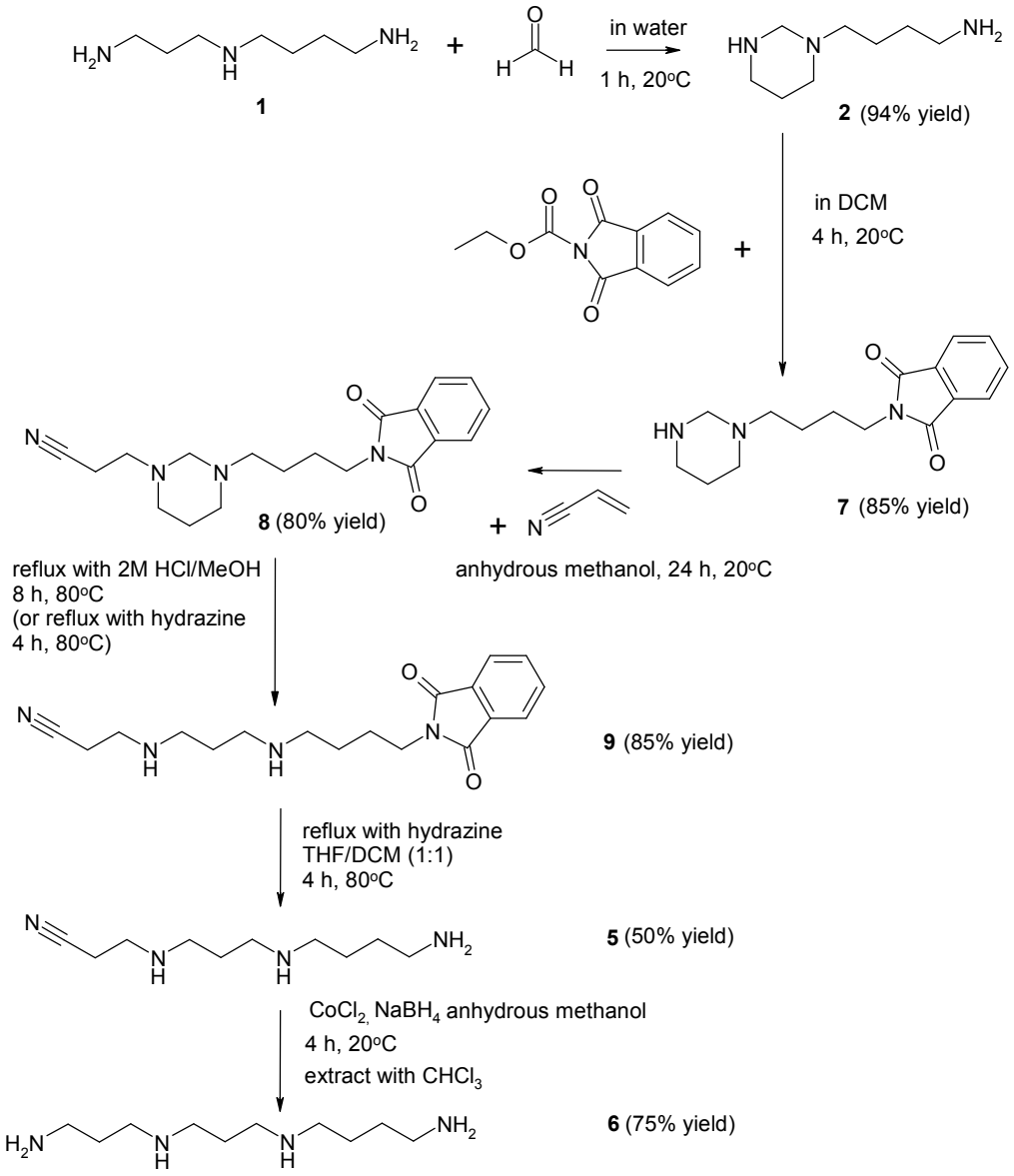

Figure 2.2 Scheme of thermospermine synthesis by method 2.

1. 2-(*N*-Butylhexahydropyrimidine) isoindoline-1,3-dione (7)

N-(4-Aminobutyl)hexahydropyrimidine (**2**) 2.50 g. (15.90 mmol) was dissolved in dichloromethane (30 mL). A solution of N-carbethoxyphthalimide 15.90 mmol in dichloromethane (10 mL), was added and stirred for 3 h at 20°C to obtain 2-(*N*-butylhexahydropyrimidine) isoindoline-1,3-dione (**7**) (3.8 g, 85%).

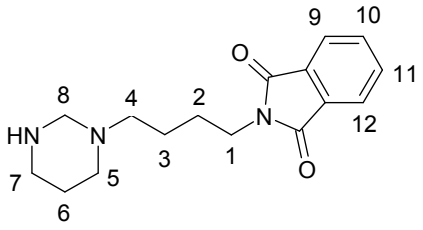

δ_H ($CDCl_3$) (400 MHz) 7.846 (2H, m, C(10) H, C(11)H), 7.814 (2H, m, C(9)H, C(12)H), 4.101 (2H, s, C(8)H_2), 3.703 (2H, t, C(1)H_2), 3.204 (2H, t C(7)H_2), 3.015 (2H, t, C(4)H_2), 2.898 (2H, t, C(5)H_2), 1.912 (2H, quin, C(3)H_2), 1.824 (2H, quin, C(2)H_2), 1.695 (2H, quin, C(6) H_2).

$C_{16}H_{21}N_3O_2$ requires M.W. = 287.1634, HR-ESI-MS: m/z $[M+H]^+$ = $C_{16}H_{22}N_3O_2$ requires 288.1712, found = 288.1699.

2. 2-(*N*^{1}-Butylhexahydropyrimidine)-isoindoline-1,3-dione-*N*^{3}-propionitrile (8)

The amine (**7**) 2.44 g (9.9 mmol) was dissolved in dry methanol (15 mL) then acrylonitrile (0.66 mL, 9.9 mmol) was added dropwise with stirring under N_2. After 15 h, more acrylonitrile (0.5 mL) was added and stirring continued for 9 hr. Methanol was removed under reduced pressure to yield 2-(*N*^{1}-butylhexahydropyrimidine)-isoindoline-1,3-dione-*N*^{3}-propionitrile (**8**) (2.00 g, 80%).

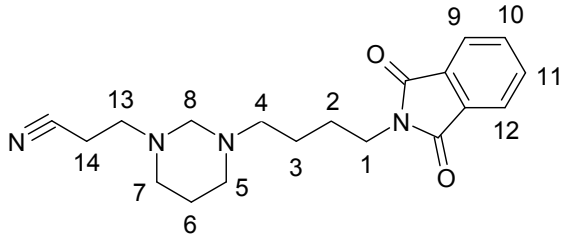

δ_H ($CDCl_3$) (400 MHz) 7.804 (2H, m, C(10) H, C(11)H), 7.691 (2H, m, C(9)H, C(12)H), 3.659 (2H, m, C(8)H_2), 3.659 (2H, t, C(1)H_2), 2.863 (2H, t, C(14)H_2), 2.732 (2H, m, C(13)H_2), 2.683 (2H, m, C(4)H_2), 2.490 (4H, m, C(5)H_2, C(7)H_2), 1.850 (2H, quin, C(3)H_2), 1.683 (2H, quin, C(2)H_2), 1.567 (2H, m, C(6) H_2).

3 12-(1,3-Dioxoisoindolin-2-yl)-4,8-diaza-dodecanenitrile (9)

A solution of (8) (0.665 g, 2.23 mmol) in 2 M HCl-methanol (15 mL) was heated under reflux at 80^{o}C for 8 h. Evaporation of the methanol gave a white solid which was redissolved in water (4 mL). The aqueous solution was alkalinized with 20% (w/v) NaOH (8

mL) and extracted with $CHCl_3$. The $CHCl_3$ extracts were dried ($MgSO_4$) and concentrated to yield 12-(1,3-dioxoisoindolin-2-yl)-4,8-diaza-dodecanenitrile (**9**) (0.56 g, 85%).

4 Removal of the phthalimide group to give 12-amino-4,8-diaza-dodecanenitrile (5)

A solution of amine (**9**) in 40 mL of CH_2Cl_2/THF (1:1) was treated with hydrazine monohydrate (1.0 mL) and heated under reflux for 4 h at 80°C. The solvent was evaporated to dryness under reduced pressure to yield 12-amino-4,8-diaza-dodecanenitrile (**5**) (0.30 g, 50%).

5 Simultaneous removal of phthalimide and hexahydropyrimidine from (8) to give 12-amino-4,8-diaza-dodecanenitrile (5)

A solution of amine (**8**) in 40 mL of CH_2Cl_2/ THF (1:1) was treated with hydrazine monohydrate (2 mL) and heated under reflux for 4 h at 80°C. The solvent was evaporated to dryness under reduced pressure to yield the 12-amino-4,8-diaza-dodecanenitrile (**5**) (0.42 g, 75%).

2.8 Purification of intermediates

Silica gel column chromatography (Merck, 40–63 μm, 230–400 mesh ASTM, pH 6.5–7.5) was used to purify the products from steps **(7)** of the thermospermine preparation. The column was packed in an open-glass tube with dichloromethane. The samples were dissolved in methanol, then applied to the column in a minimum volume. The column was eluted with a mixture of dichloromethane: methanol: ammonia solution (10:5:1). The progress of the elution was followed by collecting fractions (50 mL), concentrating and monitoring by analytical TLC, HPLC, NMR and HR-ESI-MS. Semi-preparative HPLC column: Phenomenex Gemini 10 μ C18 110A 250 x 10 mm; Guard column: Phenomenex Gemini 5 μ C18 10 x 10 mm. HPLC mobile phase used for separation was acetonitrile in Milli-Q-water (40:60) with amine (**7**) dissolved in methanol.

2.9 Analysis of thermospermine and spermine

Hexahydropyrimidine derivative of spermine

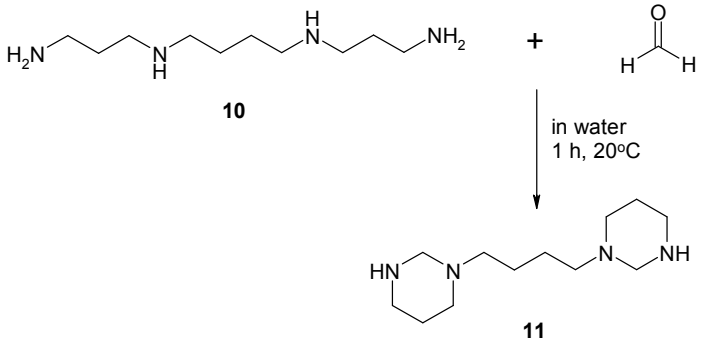

Spermine (**10**) 0.09 g (0.445 mmol), was dissolved in distilled water (25 mL) and the solution cooled to 5°C under N_2. 37% Aqueous solution of formaldehyde 0.1 mL (2 equiv.) was added dropwise then the solution was stirred for 1 h at 20°C. The aqueous layer was saturated with solid NaCl and extracted four times with $CHCl_3$. The combined $CHCl_3$ extracts were dried ($MgSO_4$), filtered and concentrated to dryness, giving the dihexahydro-pyrimidine ring derivative of spermine, 1,4-(dihexahydropyrimidine)butane (**11**).

1,4-(dihexahydropyrimidine) butane (**11**) ($C_{12}H_{26}N_4$, M.W. = 226.2157,) HR-ESI-MS: expected m/z $[M+H]^+$ ion = 227.2236 , found = 227.2217.

Hexahydropyrimidine derivative of thermospermine

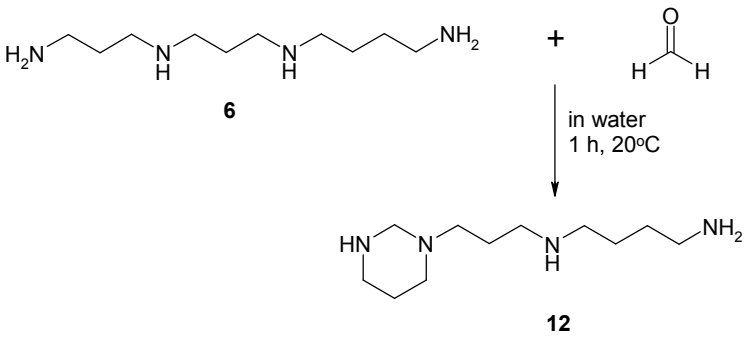

Thermospermine (**6**) 0.09 g (0.445 mmol), was dissolved in distilled water (25 mL) and cooled to 5°C under N_2. An aq. solution of formaldehyde (37%, 0.1 mL, 2 equiv.) was added dropwise then the solution was stirred for 1 h at 20°C. The aqueous layer was saturated with solid NaCl and extracted four times with $CHCl_3$. The combined $CHCl_3$ extracts were dried

($MgSO_4$), filtered and concentrated to dryness, giving the hexahydropyrimidine ring derivative of thermospermine, 1-(hexahydropyrimidine)-4-aza-aminooctane (**12**)

1-(Hexahydropyrimidine)-4-aza-aminooctane (**12**) ($C_{11}H_{26}N_4$, M.W. = 214.2157,) HR-ESI-MS expected m/z $[M+H]^+$ ion = 215.2236, found = 215.2216 and doubly charged ion $[M+2H]^{2+}$ = 108.1157, found = 108.1175.

Tetradeuterio hexahydropyrimidine derivative of spermine

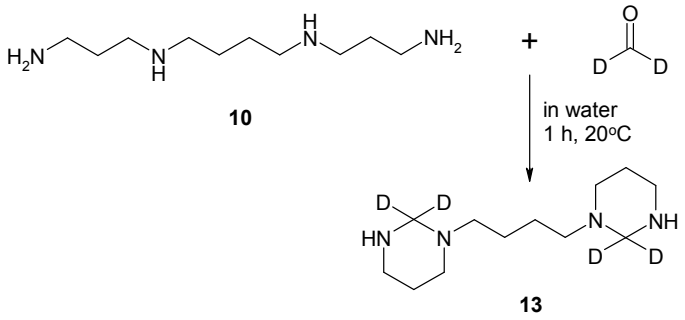

Spermine (**10**) 0.09 g (0.445 mmol), was dissolved in distilled water (25 mL) and the solution cooled to 5°C under N_2. An aqueous solution of dideuteriated formaldehyde 0.1 mL (2 equiv.) was added dropwise then the solution was stirred for 1 h at 20°C. The aqueous layer was saturated with solid NaCl and extracted four times with $CHCl_3$. The combined $CHCl_3$ extracts were dried ($MgSO_4$) and concentrated to dryness, giving the di-hexahydropyrimidine ring derivative of spermine, 1,4-(dihexahydropyrimidine-2,2,2′,2′-tetradeuterio) butane (**13**).

1,4-(Dihexahydropyrimidine-2,2,2′,2′-tetradeuterio) butane ($C_{12}H_{22}N_4D_4$, M.W. = 230.2408,) HR-ESI-MS expected m/z $[M+H]^+$ ion = 231.2486, found = 231.2472 and doubly charged ion of $[M+2H]^{2+}$ = 116.1282, found = 116.1258.

Dideuterio of hexahydropyrimidine derivative of thermospermine

Thermospermine (**6**) 0.09 g (0.445 mmol), was dissolved in distilled water (25 mL) and the solution cooled to 5°C under N_2. Aqueous solution of dideuteriated formaldehyde 0.1 mL (2 equiv.) was added dropwise then the solution was stirred for 1 h at 20°C. The aqueous layer was saturated with solid NaCl and extracted four times with $CHCl_3$. The combined $CHCl_3$ extracts were dried ($MgSO_4$) filtered and concentrated to dryness, giving the hexahydropyrimidine ring derivative of thermospermine, 8-(1-hexahydropyrimidine-2,2-dideuterio)-4-aza-aminooctane (**14**).

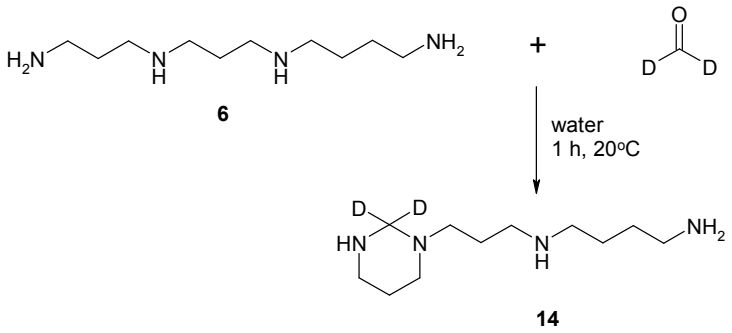

8-(1-Hexahydropyrimidine-2,2-dideuterio)-4-aza-aminooctane ($C_{11}H_{24}N_4D_2$, M.W. = 216.2283) HR-ESI-MS expected m/z $[M+H]^+$ ion = 217.2361, found = 217.2348, doubly charged ion $[M+2H]^{2+}$ = 109.1219, found = 109.1201

Reaction of formaldehyde:dideuteriated formaldehyde (1:1) to spermine

This experiment was repeated using an approximate 50:50 (v/v) mixture of formaldehyde and dideuteriated formaldehyde react with spermine.

1,4-(Dihexahydropyridine)butane(**11**) ($C_{12}H_{26}N_4$, M.W. = 226.2157) HR-ESI-MS expected m/z $[M+H]^+$ ion = 227.2236, found = 227.2223. 1-(hexahydropyrimidine)-5-aza-aminooctane ($C_{12}H_{24}N_4D_2$, M.W. = 228.2283) HR-ESI-MS expected m/z $[M+H]^+$ ion = 229.2361, found = 229.2343. 1,4-(Dihexahydropyrimidine tetradeuterio)butane ($C_{12}H_{22}N_4D_4$, M.W. = 230.2408) HR-ESI-MS expected m/z $[M+H]^+$ ion = 231.2486, found = 231.2480.

Reaction of formaldehyde:dideuteriated formaldehyde (1:1) to thermospermine

This experiment was repeated using an approximate 50:50 (v/v) mixture of formaldehyde and dideuteriated formaldehyde react with thermospermine.

1-(Hexahydropyrimidine)-4-aza-aminooctane (**12**) ($C_{11}H_{26}N_4$, M.W. = 214.2157) HR-ESI-MS expected m/z $[M+H]^+$ ion = 215.2236, found = 215.2225. 1-(Hexahydropyrimidine dideuterio)-4-aza-aminooctane ($C_{11}H_{24}N_4D_2$, M.W. = 216.2283,) expected m/z $[M+H]^+$ ion = 217.2361, found = 217.2355.

CHAPTER 3: SELECTIVE POLYAMINE DERIVATIZATIONS

3.1 Primary amine-*o*-phthalaldehyde/mercaptoethanol (OPA/MCE) derivatization

ortho-Phthalaldehyde (OPA) is selective reagent reacting only with primary amines in the presence of alkylthiols to form fluorescent isoindole derivatives. This reaction was introduced by Roth (1971) to investigate amino acids and the method has become widely used for the determination of amino acids (Patchett, 1988), peptides (Mendez, 1985), aminoglycoside antibiotics (Essers, 1984; Tawa, 1998), biogenic amines, polyamines and other primary amino group-containing compounds.

In Roth's original studies, 2-mercaptoethanol (MCE) was the thiol used (Roth, 1971) though later workers have explored a variety of thiols (Simons and Johnson, 1978). The main advantage of the derivatization by OPA/MCE is that the reaction is easy to perform at pH 10 in aqueous solution (usually borate buffer) under ambient temperature, with a short reaction of few minutes, yielding 1-alkylthio-2-alkylisoindole derivatives (Simons and Johnson, 1976, 1977) which are highly fluorescent (Figure 3.1). However, it has been reported that secondary amino groups do not form isoindoles (Lee, 1979; Roth, 1973).

1-Alkylthio-2-alkylisoindoles exhibit several excitation maxima. Usually the maximum wavelength at 340 nm is used, but wavelength 230 nm which gives higher fluorescence intensity could be used in order to improve the excitation of fluorescence (Schuster, 1988).

The isoindoles are unstable, and decompose via an intramolecular rearrangement to non-fluorescent 2,3-dihydro-1*H*-isoindole-1-one (Figure 3.2) (Simons and Johnson, 1978). The degree of instability depends somewhat on the thiol and the amines (Lindroth, 1979; Stobaugh, 1983).

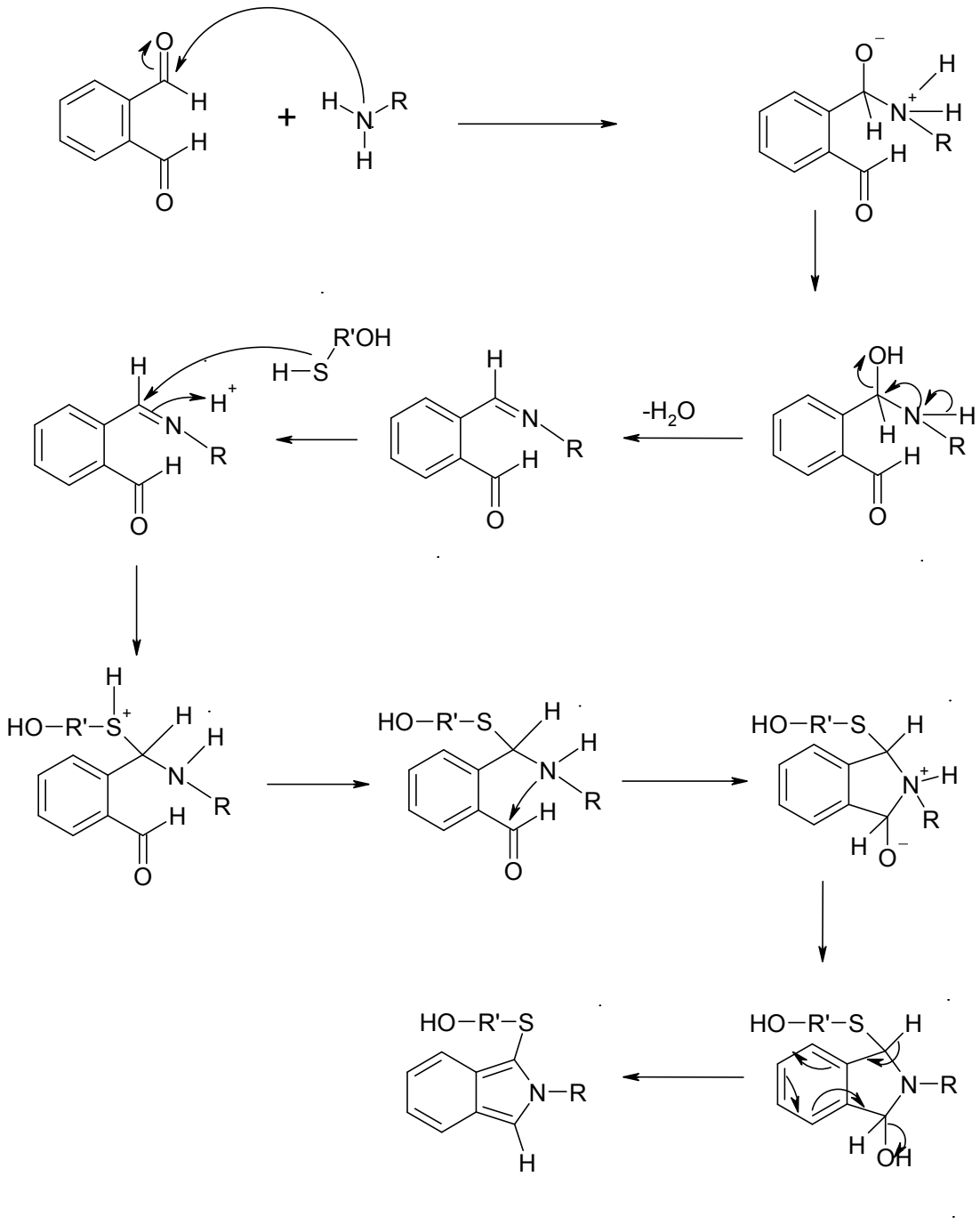

Figure 3.1 Formation of a 1-alkylthio-2-alkylisoindoles by reaction the OPA, a thiol and a primary amine.

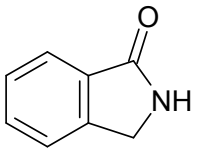

Figure 3.2 2,3-Dihydro-1*H*-isoindole-1-one.

In aqueous medium, OPA undergoes hydration quite extensively to form a mixture of *cis*-, *trans*-cyclic-1,3-phthalandiols (Figure 3.3). The 1,3-phthalandiols also absorb light at the same wavelength as the amine-OPA derivatives so the peak of this molecules always shows up in the chromatograms where UV absorbance detection is used.

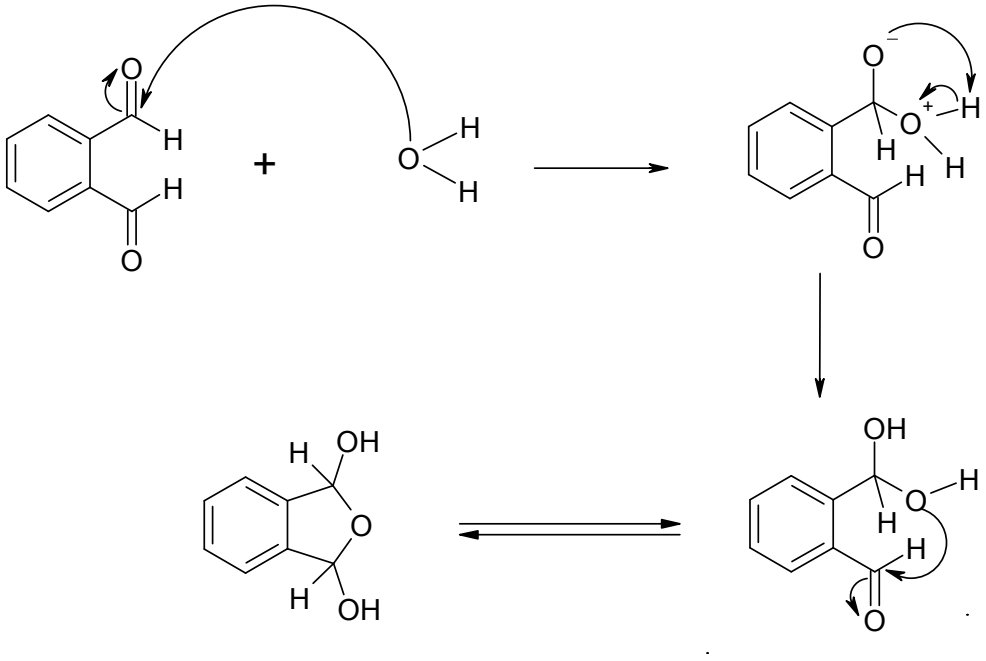

Figure 3.3 Hydration of OPA in basic medium.

The optimization of amine-OPA/MCE derivatization was by:

1. Optimisation the pH of borate buffer
2. Optimisation of the molar ratio of OPA/MCE reagent to sample solution.
3. Optimization of the mole ratio of MCE (mM) to 1 mM of OPA.
4. Optimisation of the reaction time.
5. Optimisation of the condition for maximum stability of the derivatives of amine-OPA/MCE.
6. Optimization the mobile phase for HPLC.

Optimization the pH of borate buffer

The reactions of OPA/MCE at various pHs with ethylamine as a model primary amine were performed to optimize the pH. The result (Figure 3.4) shows the range of pH from 8.3 to 10.5 gave the highest derivative yields while acidic and neutral pH gave lower yields. Calibration curves were constructed at pHs 8.3, 9.3 and 10.5 (Figure 3.5 and Table 3.1).

Calibration curves of the reactions at the 3 pHs examined (8.3, 9.3, 10.5) showed approximately the same slopes. However, the chromatogram of the reaction at pH 10.5 showed the best resolution and fewer by-products. Borate buffer pH 10.5 was used to determine the optimum reaction time by varying the reaction time of amines and OPA/MCE. The results were obtained with ethylamine (Figure 3.6) and also 1-butylamine (Figure 3.7). The best reaction time is 1 min, as longer reaction times gave smaller peak areas due to the instability of the reaction products.

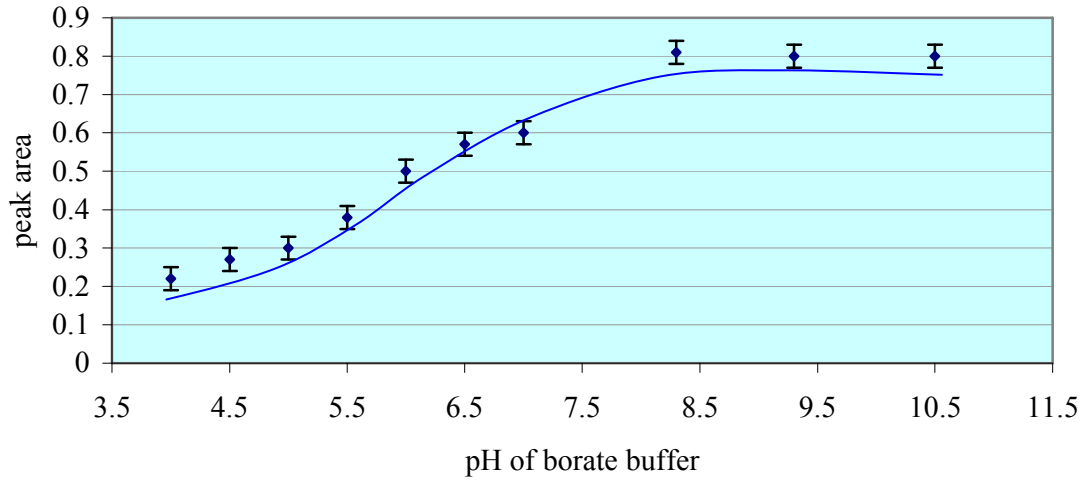

Figure 3.4 Effect of various borate buffer pHs on the ethylamine-OPA/MCE derivatives yield (n = 5). Peak areas were calculated by height x 0.5 width of peak, and peak areas are reported in cm^2.

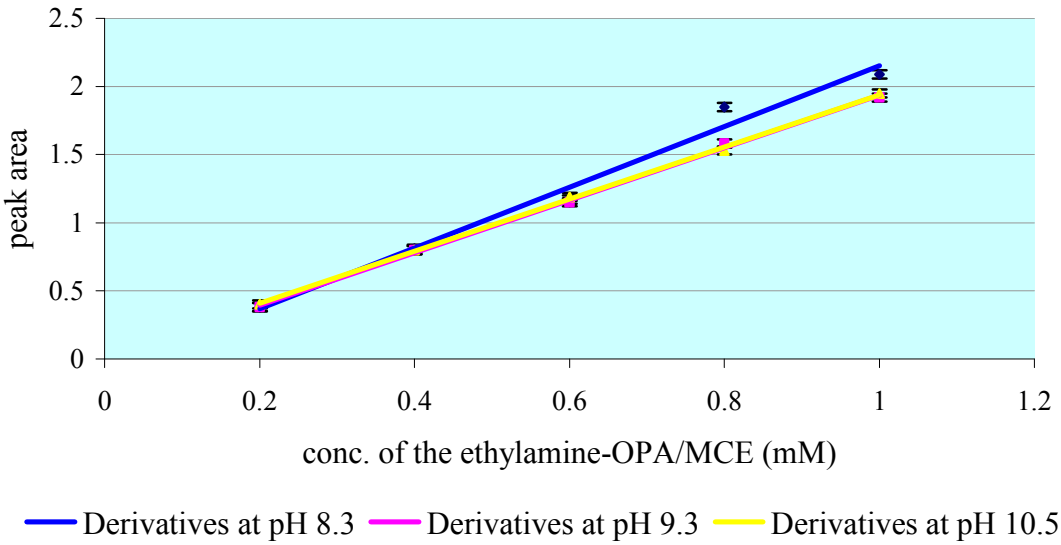

Figure 3.5 Calibration curve of ethylamine-OPA/MCE derivatives at various pHs (n = 5). Peak areas were calculated by height x 0.5 width of peak, and peak areas are reported in cm^2.

Table 3.1 The calibration curves' equations of ethylamine-OPA/MCE derivatives at various pHs.

Ethylamine-OPA/MCE derivatives at various pH	Calibration curve	R^2 (n = 5)
pH 8.3	y = 2.23x – 0.078	0.984
pH 9.3	y = 1.93x – 0.008	0.999
pH 10.5	y = 1.915x + 0.025	0.999

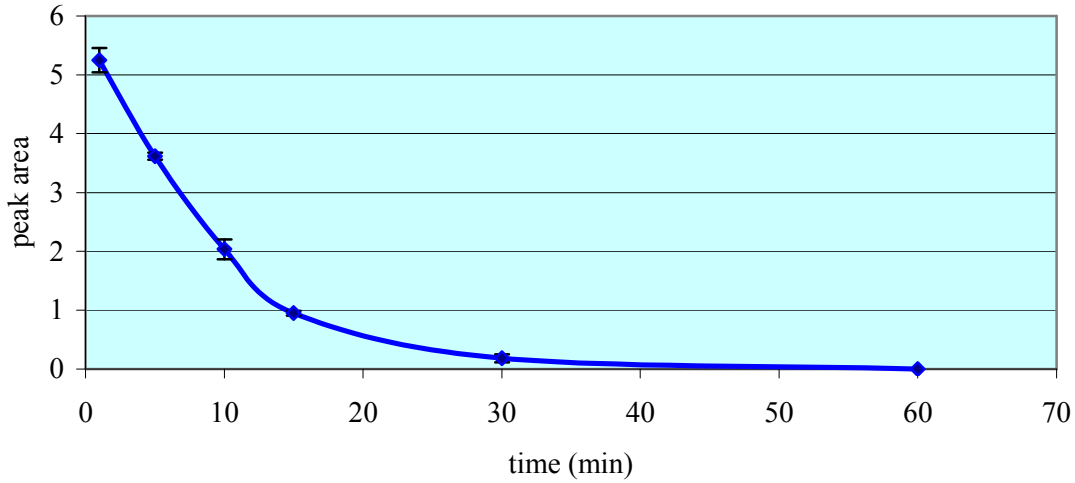

Figure 3.6 Reaction of 1 mL 1mM ethylamine with 1 mL of OPA/MCE at various reaction times (n = 5). Peak areas were calculated by height x 0.5 width of peak, and peak areas are reported in cm^2.

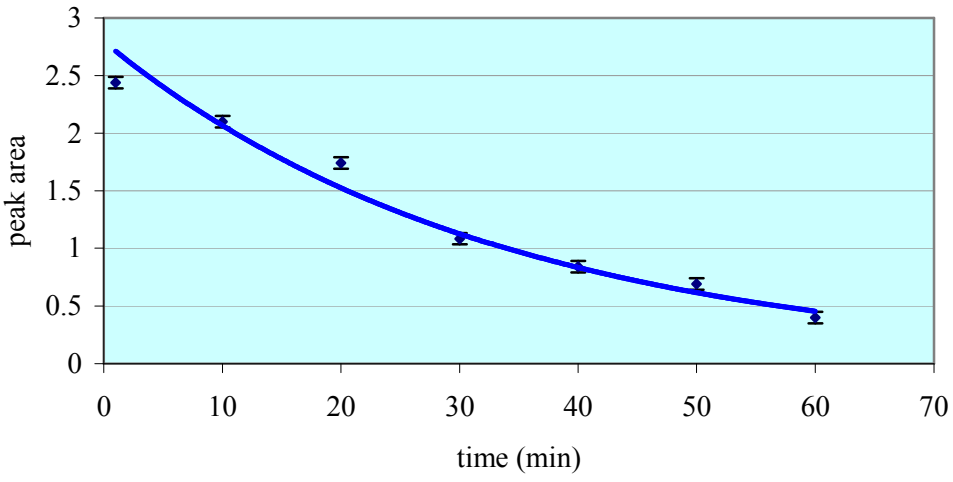

Figure 3.7 Reaction of 100 µl 5mM 1-butylamine with 100 µl of OPA/MCE at various reaction times (n = 5). Peak areas were calculated by height x 0.5 width of peak, and peak areas are reported in cm^2.

Optimizing the mole ratio of reagent composition

Mole ratios of MCE to OPA in the OPA reagent were altered from 1:1 to 17:1. Thus, the behaviour of 1-butylamine has been compared with variation in the OPA/MCE mole ratio (Figure 3.8). Further increasing the concentration of MCE in the reagent might result in increasing the rate of reaction as well as increasing of peak area. In this study, it was found that there is insignificant increase in the peak area, the observed rate suppression at high thiol concentration is probably due to one or more OPA-thiol adducts which decrease the free OPA concentration (Figure 3.9) (Wong, Sternson and Schowen, 1985). Thus the ratio of MCE: OPA = 10:1 was used for the next and subsequent studies.

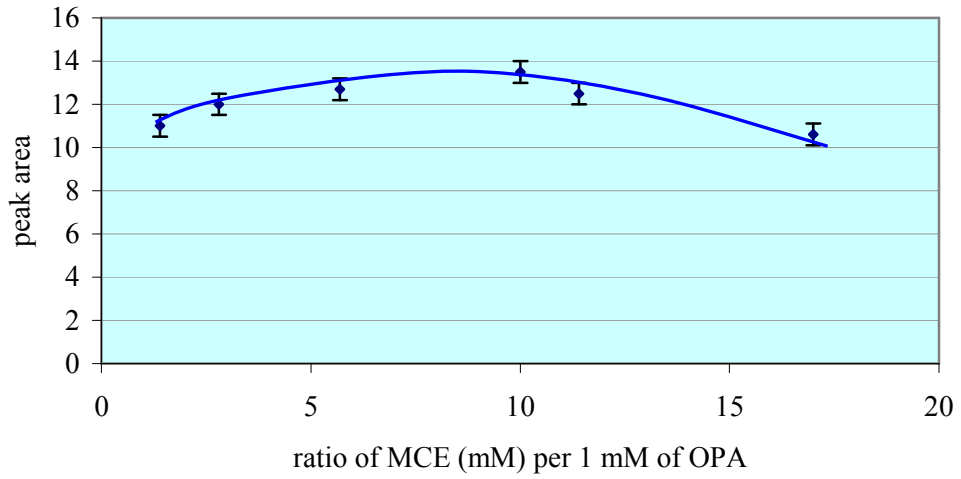

Figure 3.8 Reaction of 1 µL 5mM 1-butylamine with 1 µL of OPA/MCE at various ratio of MCE (mM) per 1 mM of OPA (n = 5). Peak areas were calculated by height x 0.5 width of peak, and peak areas are reported in cm^2.

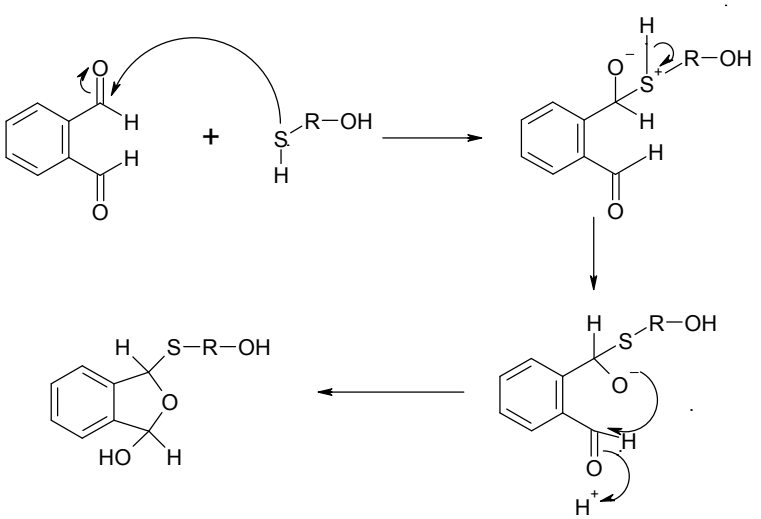

Figure 3.9 Reaction of thiol and OPA.

The derivatization method has been used to determine glucosamine (eluted by acetonitrile in Milli-Q-water (40:60), Rt = 2.0 min) which showed that the derivative is also unstable (Figure 3.10).

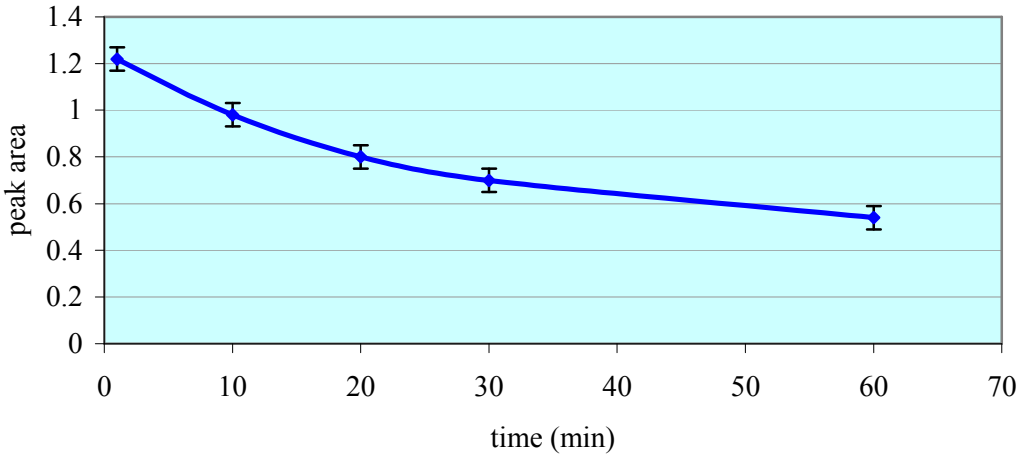

Figure 3.10 Glucosamine-OPA/MCE derivatives at various reaction times (n = 5). Peak areas were calculated by height x 0.5 width of peak, and peak areas are reported in cm^2.

Optimizing the mole ratio of OPA/MCE to amines

1-Butylamine (1 mM) was reacted with various mole ratios of OPA/MCE [1:10] at 0.2, 1, 2, 4, 8, 16 fold. Figure 3.11 shows that the completed yield was obtained from 1:1 mole ratio.

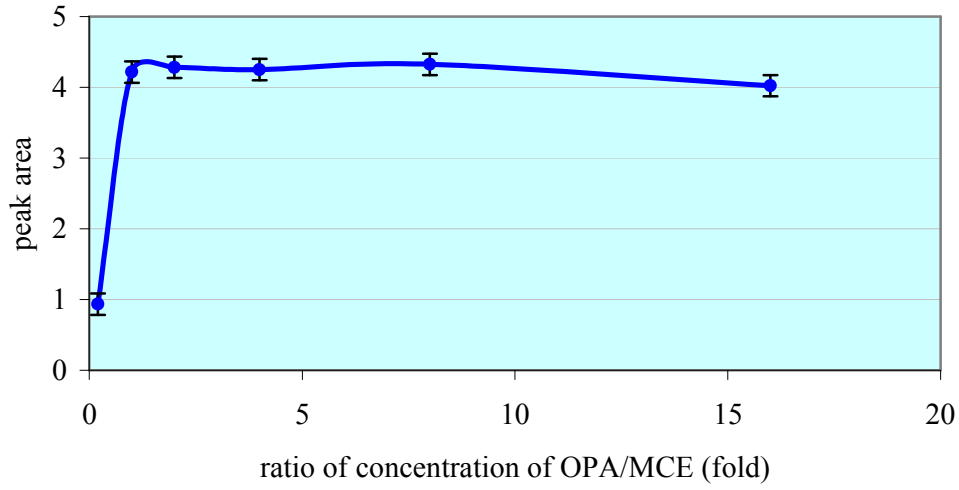

Figure 3.11 Ratio of concentration of OPA/MCE to 1-butylamine (by fold of mole, n = 5). Peak areas were calculated by height x 0.5 width of peak, and peak areas are reported in cm^2.

After the optimization reactions for amine-OPA/MCE, these optimization conditions were then applied to: 1,4-diaminobutane, 1,5-diaminopentane and 1,7-diaminoheptane. The conditions used were: 1 mL, 40 mM of OPA/MCE in borate buffer pH 10.5 and the reaction time was 1 min. The OPA-MCE-polyamines derivatives were formed rapidly, but the products were unstable (Figure 3.12 and Table 3.2).

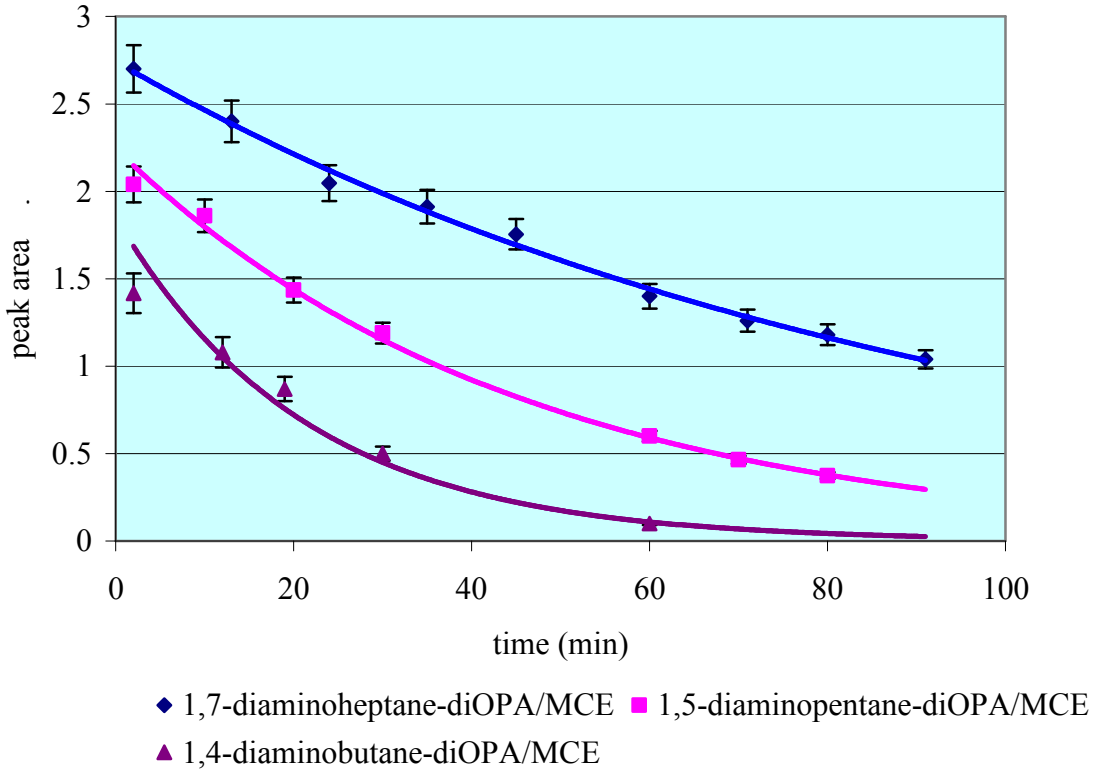

Figure 3.12 Polyamine-OPA/MCE derivatives at various reaction times (n = 5). Peak areas were calculated by height x 0.5 width of peak, and peak areas are reported in cm^2.

Table 3.2 Time for 50% decrease in peak area of amine-OPA/MCE derivatives.

Amine-OPA/MCE derivative	Time (min) for peak area to decrease by 50%
Ethylamine-monoOPA/MCE	9
1-Butylamine-monoOPA/MCE	25
1,4-Diaminobutane-diOPA/MCE	28
1,5-Diaminopentane-diOPA/MCE	38
1,7-Diaminoheptane-diOPA/MCE	45

The stability of the derivatives prepared under the same conditions, proved to be associated with the aliphatic chain length of the amine as the longer the chain length the slower the decomposition of the total of derivatives formed. This also proved that particular optimization of the reaction needs to be done for particular amines. The stability of the derivatives of OPA/MEC could be improved by putting the vial in an ice bath after 1 min reaction time; results are shown in Figure 3.13.

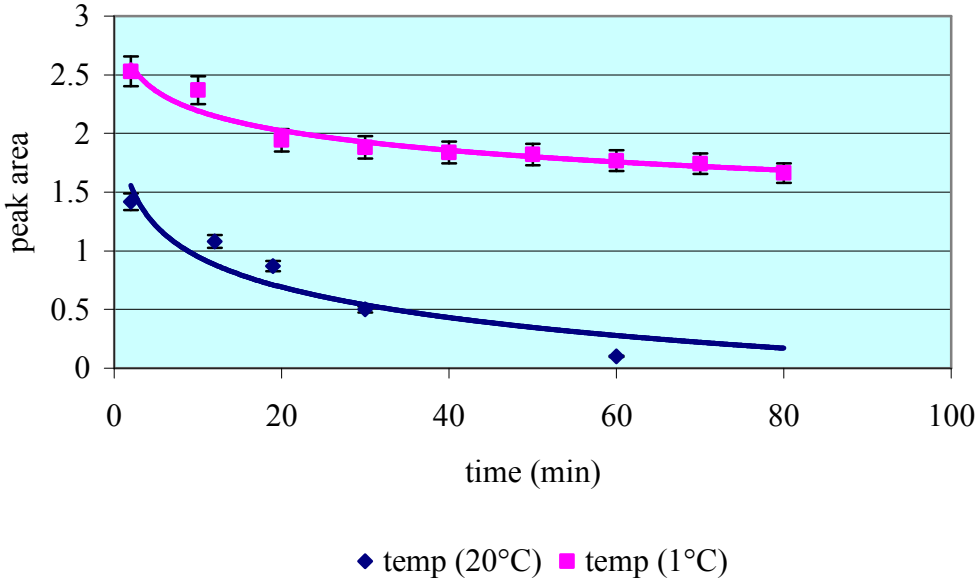

Figure 3.13 1,4-Diaminobutane-diOPA/MCE derivatives at various storage times at two different temperatures (20°C and 1°C, n = 5). Peak areas were calculated by height x 0.5 width of peak, and peak areas are reported in cm^2.

Polyamine-OPA/MCE derivatives

Using the optimized conditions, derivatizations were carried out with 1-butylamine, 1,4-diaminobutane, 1,5-diaminopentane, 1,7-diaminoheptane, 1,9-diaminononane, spermidine, and spermine. For the mono- and di-amines, the chromatograms showed good resolution and peak symmetry (Figure 3.14). The peak of 1,7-diaminoheptane-diOPA/MCE derivative was collected and the structure confirmed by HR-ESI-MS (Figure 3.15). By adjusting the mobile phase, the retention time of some amine-OPA/MCE derivatives is shorter and they also show improved (more symmetrical) peak shape (Table 3.3).

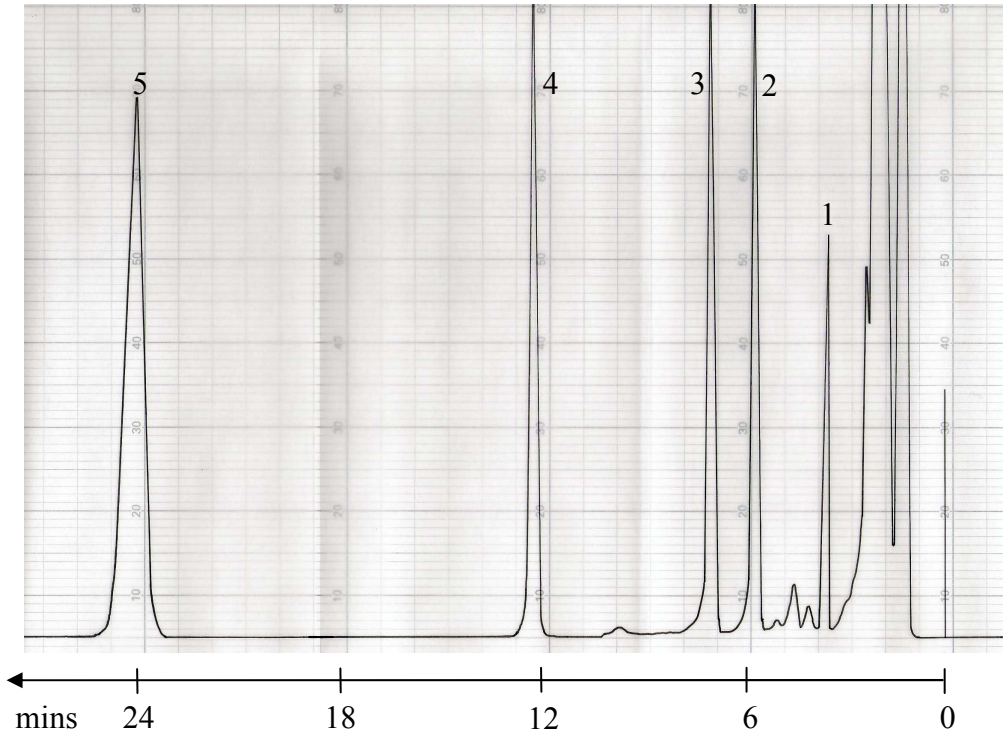

Figure 3.14 HPLC chromatogram of amines-OPA/MCE derivatives, HPLC conditions: column: Phenomenex hypersil C18 5µ 150 x 4.60 mm, mobile phase is acetonitrile: Milli-Q-water (70:30) with flow rate 1 mL/min, fluorescence detection at λ_{ex} = 340 nm, λ_{em} = 450 nm. The chromatogram shows the solvent front at Rt = 1.3 min, peak 1 = 1-butylamine-monoOPA/MCE at Rt = 3.4 min, peak 2 = 1,4-diaminobutane-diOPA/MCE at Rt = 5.6 min, peak 3 = 1,5-diaminopentane-diOPA/MCE at Rt = 7.0 min, peak 4 = 1,7-diaminoheptane-diOPA/MCE at Rt = 12.2 min, peak 5 = 1,9-diaminononane-diOPA/MCE at Rt = 24.0 min.

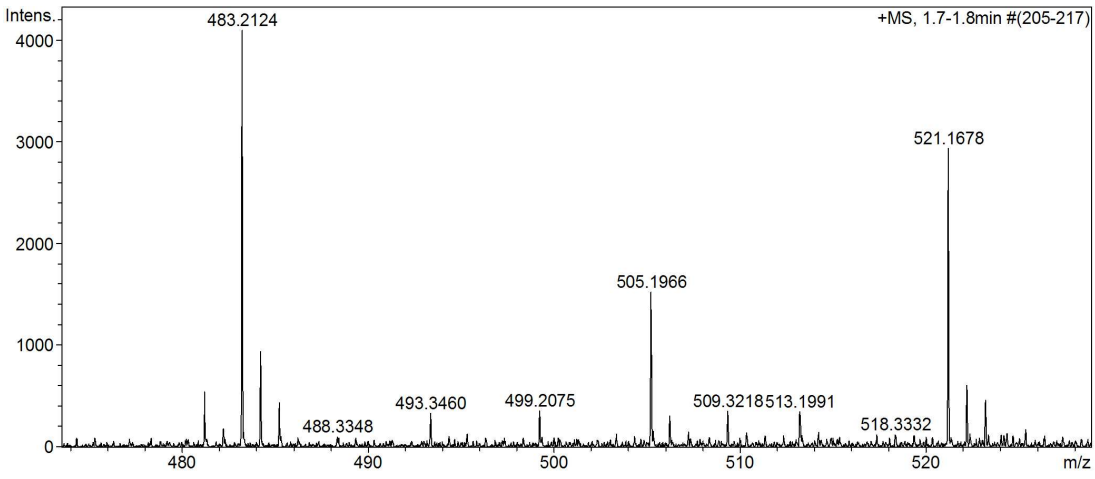

Figure 3.15 HR-ESI-MS spectra of 1,7-diaminoheptane di-OPA/MCE derivative, (M.W. = 482.2062, $C_{27}H_{34}N_2O_2S_2$) expected m/z $[M+H]^+$ ion = 483.2140 (found = 483.2124) and $[M+Na]^+$ ion m/z = 505.1959 (found = 505.1966).

Table 3.3 The retention time (Rt) of various amine-OPA/MCE derivatives with different mobile phases.

Amine-OPA/MCE derivatives	Rt (min) eluted by 70% MeCN	Rt (min) eluted by 80% MeCN	Rt (min) eluted by 90% MeCN
1,4-Diaminobutane-diOPA/MCE	5.6	4.0	-
1,5-Diaminopentane-diOPA/MCE	7.0	4.7	-
1,7-Diaminoheptane-diOPA/MCE	12.2	7.5	-
1,8-Diaminooctane-diOPA/MCE	21.3	-	3.0
1,12-Diaminododecane-diOPA/MCE	73.0	-	6.2

By varying the concentration of the amines, linearity of derivatization was calculated for each amine and the coefficient of regression ranged from 0.984 to 0.997 as shown in Table 3.4 and in Figure 3.16 for the calibration curves obtained from fluorescence detector and in Figure 3.17 from ultraviolet detector. These results mean that mono- and di-amines can be determined quantitatively by this method. The calibration curve equations have high intercepts especially 1,7-diaminoheptane-diOPA/MCE derivative which might be due to high fluorescence background.

Table 3.4 The calibration curve equations of various amine-OPA/MCE derivatives was detected by fluorescence.

Amine-OPA/MCE derivatives	Calibration curve equations	R^2
1-Butylamine-monoOPA/MCE	y = 82.64x + 0.24	0.989
1,4-Diaminobutane-diOPA/MCE	y = 31.69x + 0.72	0.989
1,5-Diaminopentane-diOPA/MCE	y = 23.79x + 0.47	0.984
1,7-Diaminoheptane-diOPA/MCE	y = 20.57x + 1.48	0.997

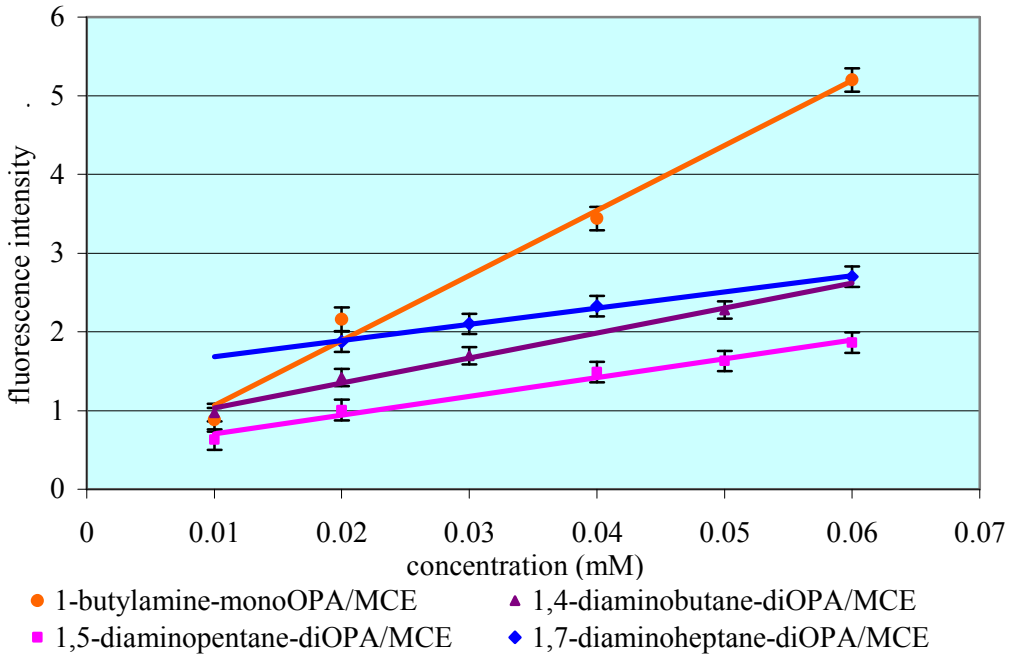

Figure 3.16 Calibration curves of amine-OPA/MCE derivatives by fluorescence detection (n = 5). Peak areas were calculated by height x 0.5 width of peak, and peak areas are reported in cm^2.

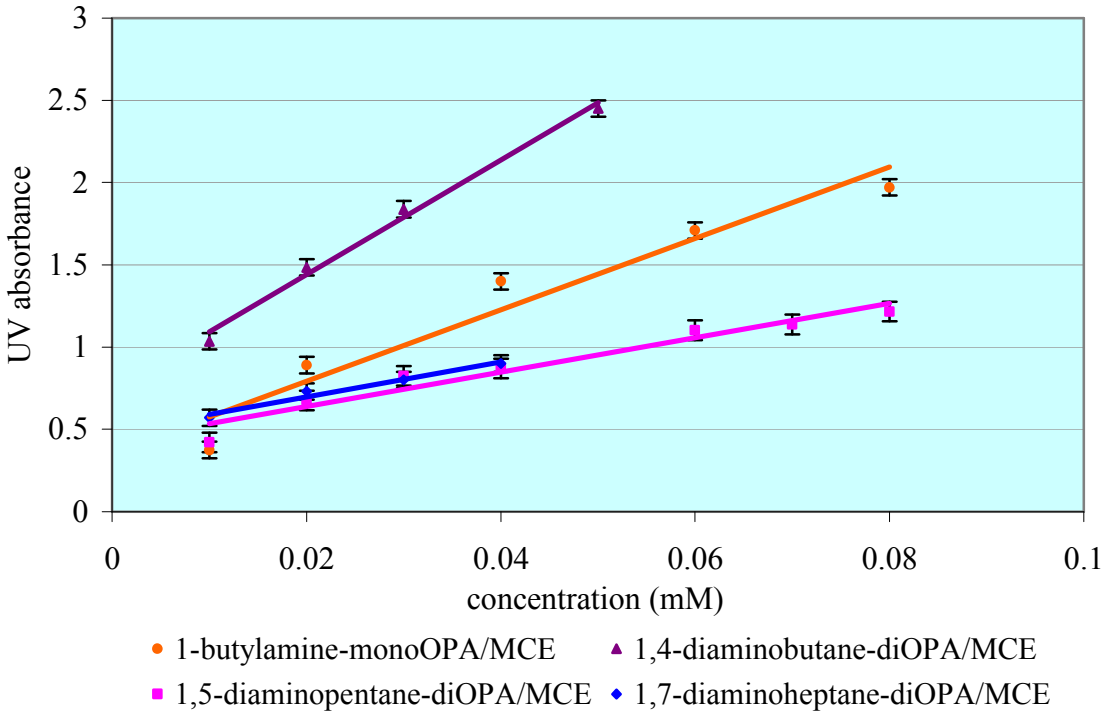

Figure 3.17 Calibration curve of amine-OPA/MCE derivatives by UV detection (n = 5). Peak areas were calculated by height x 0.5 width of peak, and peak areas are reported in cm^2.

Spermidine and spermine-OPA/MCE derivatization

Spermidine and spermine, have two terminal primary amine groups while in the middle of the molecule are one and two secondary amine groups for spermidine and spermine respectively. Thus, the derivatization reaction between OPA/MCE and spermidine, and spermine leads to the formation of di-isoindol-derivatives (Figures 3.18 and 3.19).

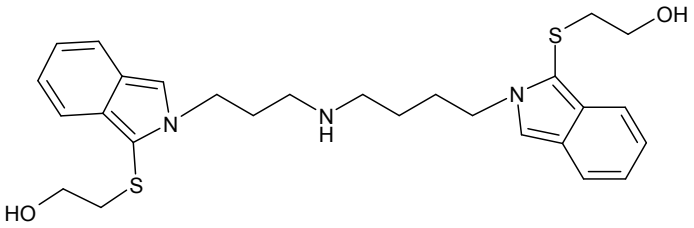

Figure 3.18 Spermidine-diOPA/MCE derivative.

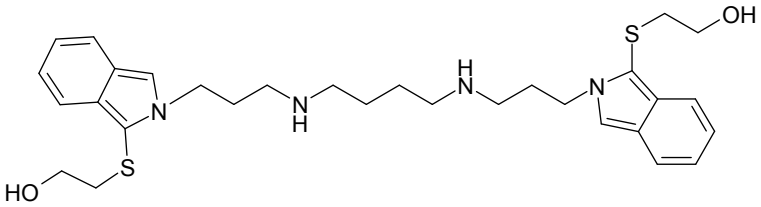

Figure 3.19 Spermine-diOPA/MCE derivative.

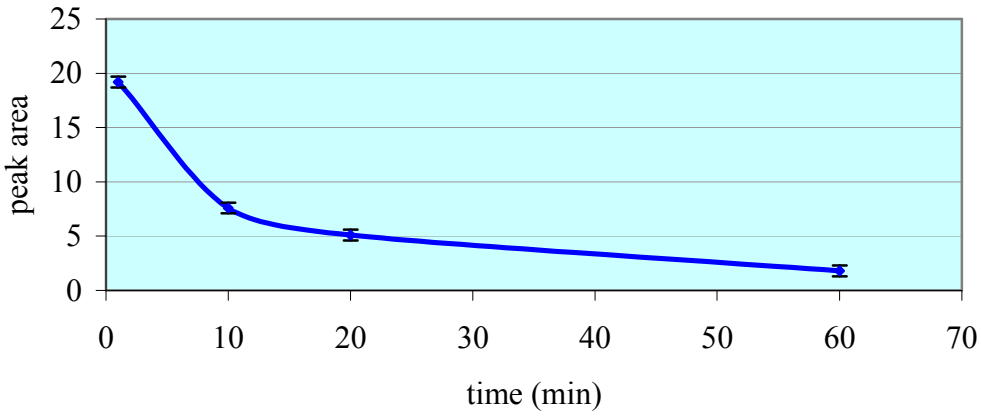

Figure 3.20 Spermidine-OPA/MCE reaction after various times (n = 5). Peak areas were calculated by height x 0.5 width of peak, and peak areas are reported in cm^2.

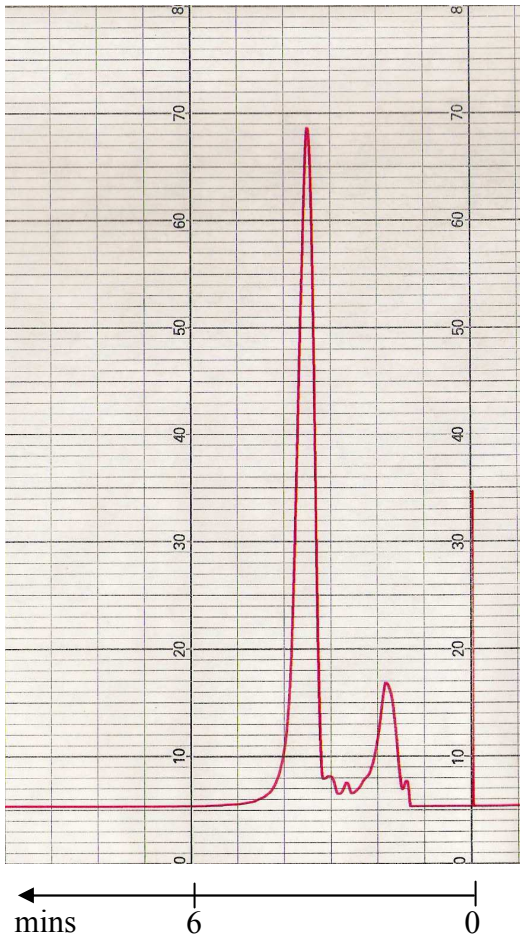

Figure 3.21 HPLC chromatogram of spermidine-diOPA/MCE (10 mM), HPLC conditions: column: Phenomenex luna C18 5µ 150 x 4.60 mm, mobile phase: acetonitrile: Milli-Q-water (90:10), flow rate 1 mL/min, fluorescence detection at λ_{ex} = 340 nm, λ_{em} = 450 nm. The chromatogram shows the solvent front at Rt = 1.5 min and spermidine-diOPA/MCE derivative at Rt = 3.7 min.

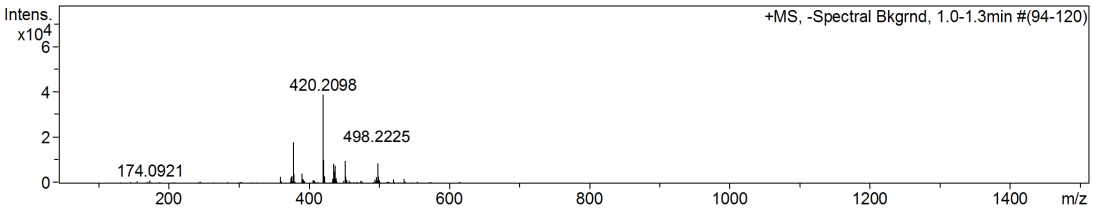

Figure 3.22 HR-ESI-MS spectra of spermidine-diOPA/MCE derivative, (M.W. = 497.2171, $C_{27}H_{35}N_3O_2S_2$) expected m/z $[M+H]^+$ ion = 498.2249 (found = 498.2225) and $[M+ Na]^+$ ion m/z = 520.2068 (found = 520.2068).

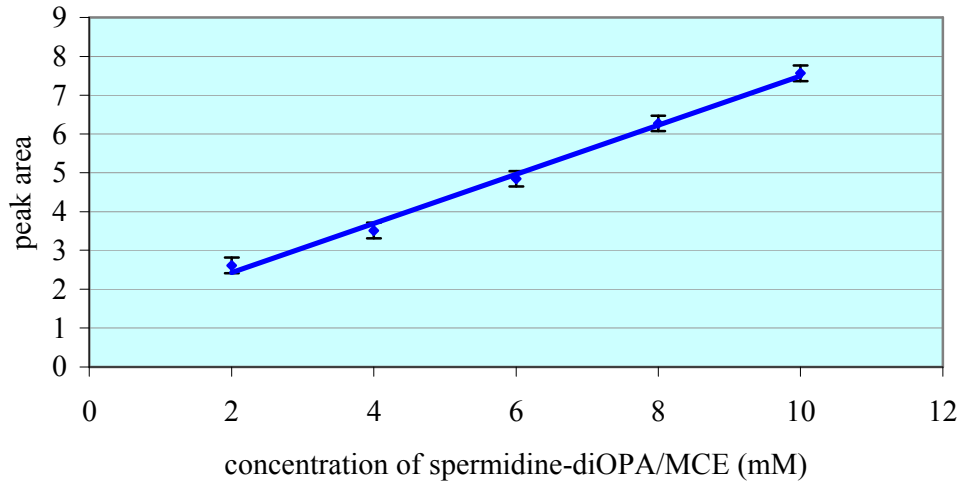

Figure 3.23 Calibration curve of spermidine-OPA/MCE derivatives by fluorescence detection. Calibration curve equation: $y = 0.6333x + 1.1615$, $R^2 = 0.995$, ($n = 5$). Peak areas were calculated by height x 0.5 width of peak, and peak areas are reported in cm^2.

For both spermidine and spermine a graph of yield against reaction time (Figure 3.20) showed a rapid degradation of the product. The HPLC chromatogram of the spermidine-diOPA/MCE derivative was symmetrical and sharp when eluted by 90% acetonitrile in Milli-Q-water at Rt = 3.7 min (Figure 3.21). HR-ESI-MS (Figure 3.22) showed a peak corresponding to the expected value, but the major peak at m/z 420.2098 could not be identified. By varying the concentration of the spermidine, linearity of derivatization was calculated and the coefficient of regression is 0.995 for fluorescence detection and 0.991 for UV detection. Figure 3.23 shows the calibration curve obtained from the fluorescence detector and in Figure 3.24 from the UV detector. For spermine-diOPA/MCE derivative, the peak was broad and also decreased rapidly in just 10 min of reaction and nearly disappeared after 30 min (Figure 3.25).

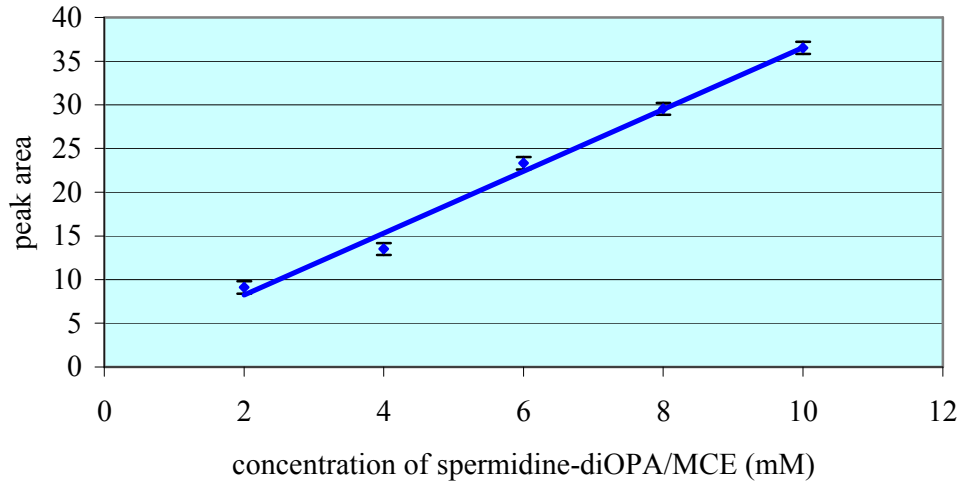

Figure 3.24 Calibration curve of spermidine-OPA/MCE derivatives by UV detection. Calibration curve equation: $y = 3.5453x + 1.1215$, $R^2 = 0.991$, (n = 5). Peak areas were calculated by height x 0.5 width of peak, and peak areas are reported in cm^2.

Although the stability of both spermidine-diOPA/MCE derivatives and spermine-diOPA/MCE derivative were low, the spermidine-diOPA/MCE derivative was more stable, perhaps due to the lower number of secondary amine groups in the molecule.

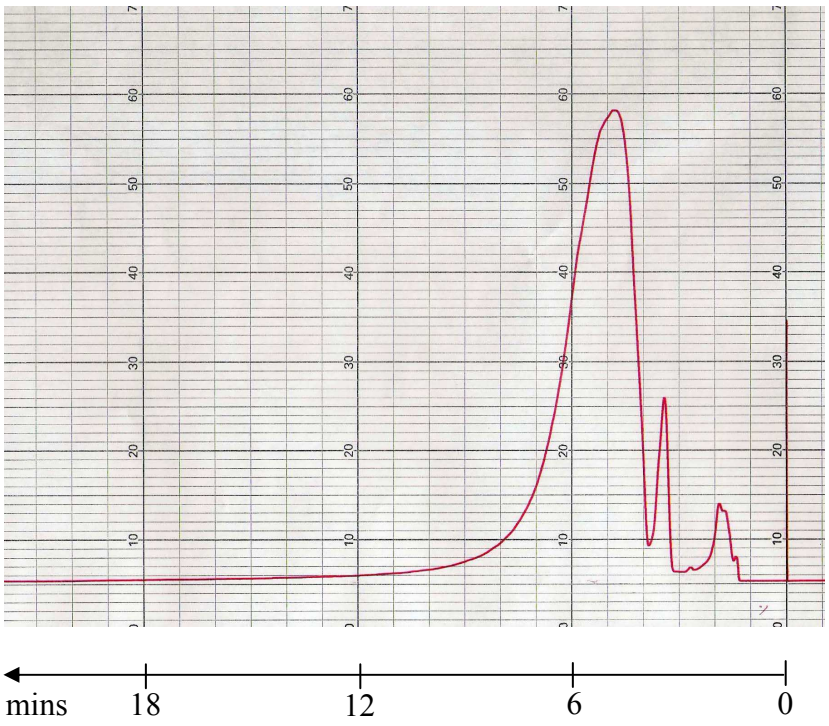

(A)

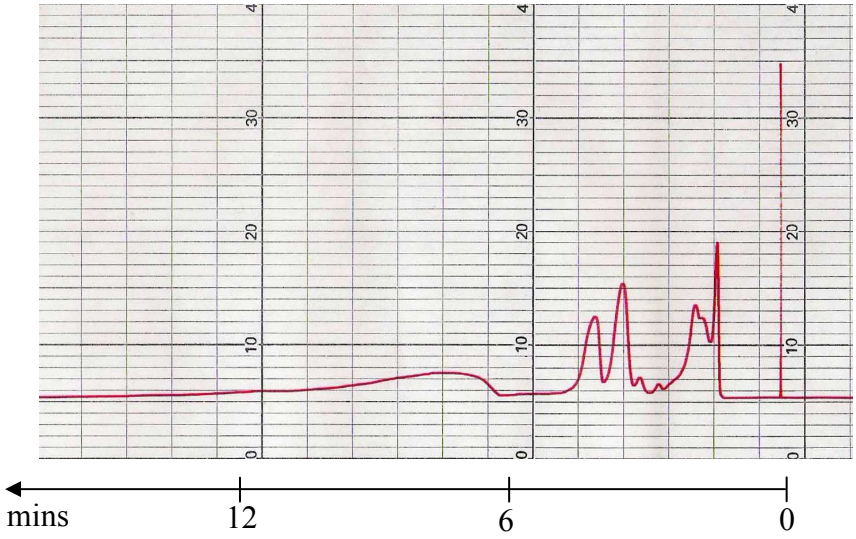

(B)

Figure 3.25 HPLC chromatogram of spermine-diOPA/MCE (10 mM), HPLC conditions: column: Phenomenex luna C18 5µ 150 x 4.60 mm, mobile phase: acetonitrile: Milli-Q-water (90:10) flow rate 1 mL/min, fluorescence detection at λ_{ex} = 340 nm, λ_{em} = 450 nm. The chromatogram shows the solvent front at Rt = 1.5 min and spermine-diOPA/MCE derivative as the broad peak start at Rt = 4.9 min. (A) reaction time 1 min (B) reaction time 15 min.

Relative quantum yield of amines-OPA/MCE derivatives

A comparison of fluorescence yields of the model series was obtained by comparison between the peak area of fluorescence intensity and peak area of UV absorbance rather than by collected the elution product from HPLC and separate measurement by UV/VIS spectrophotometer and fluorescence spectrometer due to the low stability of the amines-OPA/MCE derivatives. A plot of fluorescence intensity against absorbance (Figure 3.26) and the FI/UV equation (Table 3.5) were obtained.

Table 3.5 The FI/UV equation of amine-OPA/MCE derivatives.

Amine-OPA/MCE derivatives	FI/UV equation
1-Butylamine	y = 3.22x – 0.56
1,4-Diaminobutane	y = 0.91x – 0.04
1,5-Diaminopentane	y = 1.79x – 0.72
1,7-Diaminoheptane	y = 3.49x – 0.75

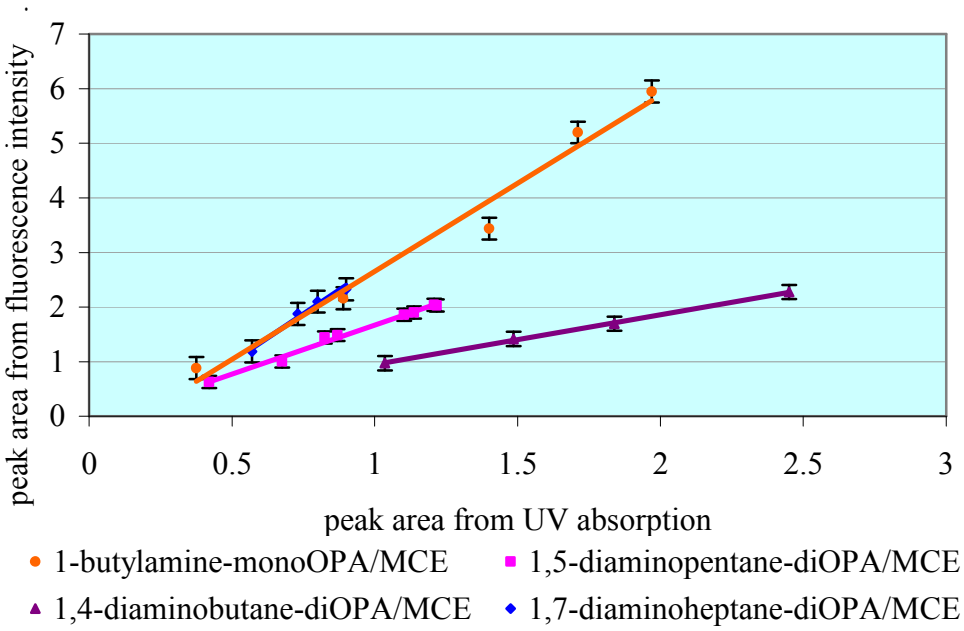

Figure 3.26 Plots of fluorescence intensity against absorbance at λ_{ex} of amine-OPA/MCE derivatives (n = 5). Peak areas were calculated by height x 0.5 width of peak, and peak areas are reported in cm^2.

From the results, it is concluded that fluorescence yield is reduced when the two fluorophores are tethered in close proximity, but that the seven carbon chain of 1,7-diaminoheptane allows sufficient flexibility for this not to occur.

OPA/MCE derivatives of a series of non-viral gene therapy (NVGT) vectors

The OPA/MCE derivatization method was applied to investigate two synthetic fatty acyl amides of spermine, N^4,N^9-didecanoyl spermine (Figure 3.27) and N^4,N^9-dilinoleoyl spermine (Figure 3.29). These C10 and C14 conjugates are experimental non-viral vectors for DNA condensation with potential in gene delivery and therefore in non-viral gene therapy (NVGT). The OPA/MCE labelling method was applied to these molecules and HPLC chromatograms of derivatives of N^4,N^9-didecanoyl spermine and N^4,N^9-dibutadecanoyl spermine (Figure 3.30) were obtained. The HR-ESI-MS of N^4,N^9-didecanoyl spermine (Figure 3.28) and N^4,N^9-dibutadecanoyl spermine (Figure 3.31) showed the mass expected for bis-isoindole derivatives.

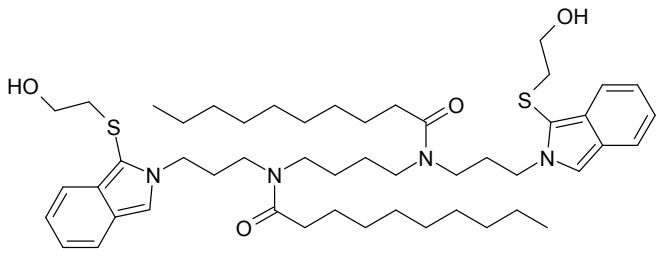

Figure 3.27 N^4,N^9-Didecanoyl spermine-diOPA/MCE derivative.

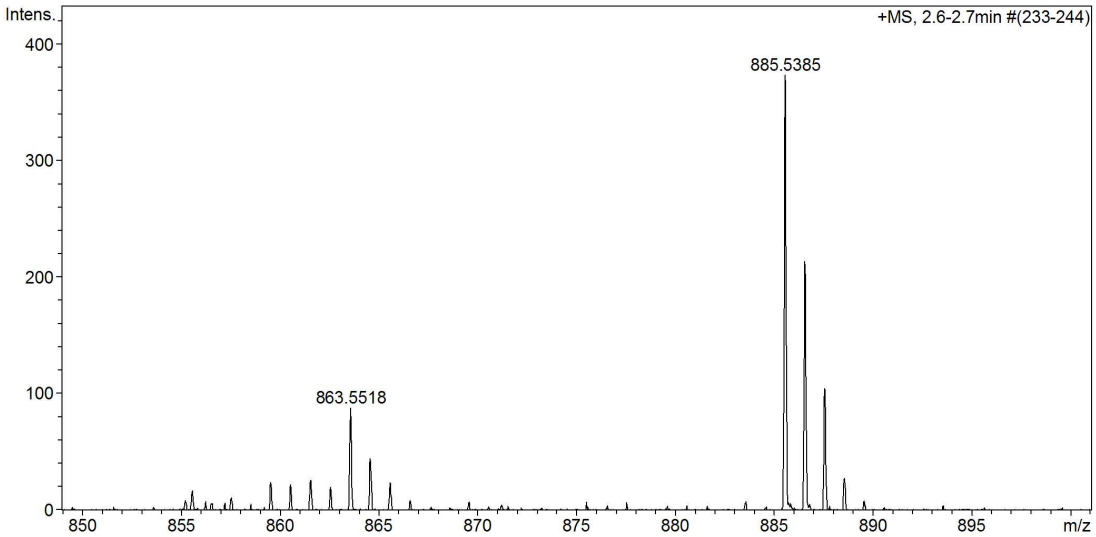

Figure 3.28 HR-ESI-MS spectra of N^4,N^9-didecanoyl spermine-diOPA/MCE derivative, (M.W. = 862.5465, $C_{50}H_{78}N_4O_4S_2$) expected m/z $[M+H]^+$ ion = 863.5543 (found = 863.5518) and $[M+ Na]^+$ ion m/z = 885.5362 (found = 885.5385).

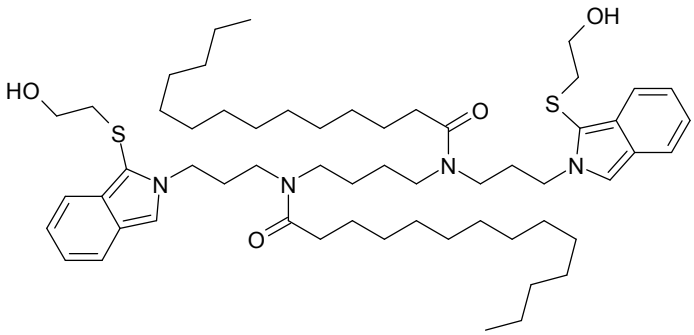

Figure 3.29 N^4,N^9-Dibutadecanoylspermine-diOPA/MCE derivative.

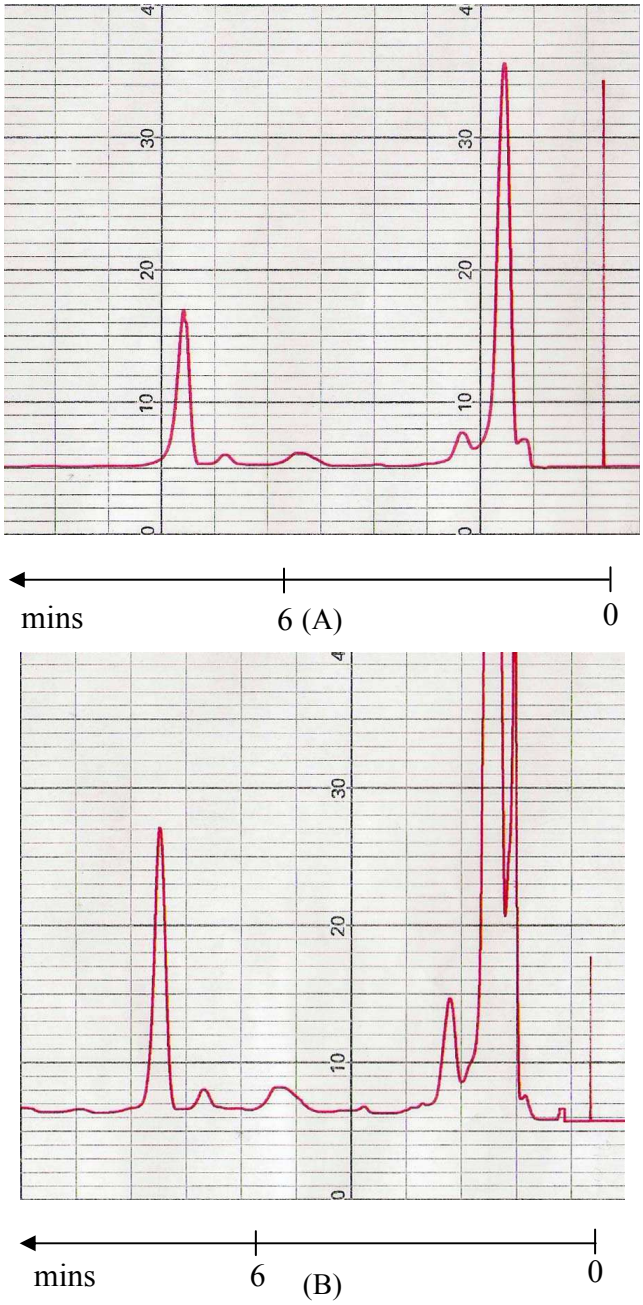

Figure 3.30 HPLC chromatogram of N^4,N^9-dibutadecanoylspermine-diOPA/MCE derivative. (10 mM), HPLC conditions: column: Phenomenex luna C18 5µ 150 x 4.60 mm, mobile phase is acetonitrile: Milli-Q-water (90:10) with flow rate 1 mL/min. The chromatogram shows the solvent front at Rt = 1.5 min and N^4,N^9-Dibutadecanoylspermine-diOPA/MCE derivative as the broad peak starting at Rt = 7.9 min, (A) from fluorescence detector x10 sensitivity at λ_{ex} = 340 nm, λ_{em} = 450 nm, (B) from UV detector 0.16 range at λ_{max} = 340 nm.

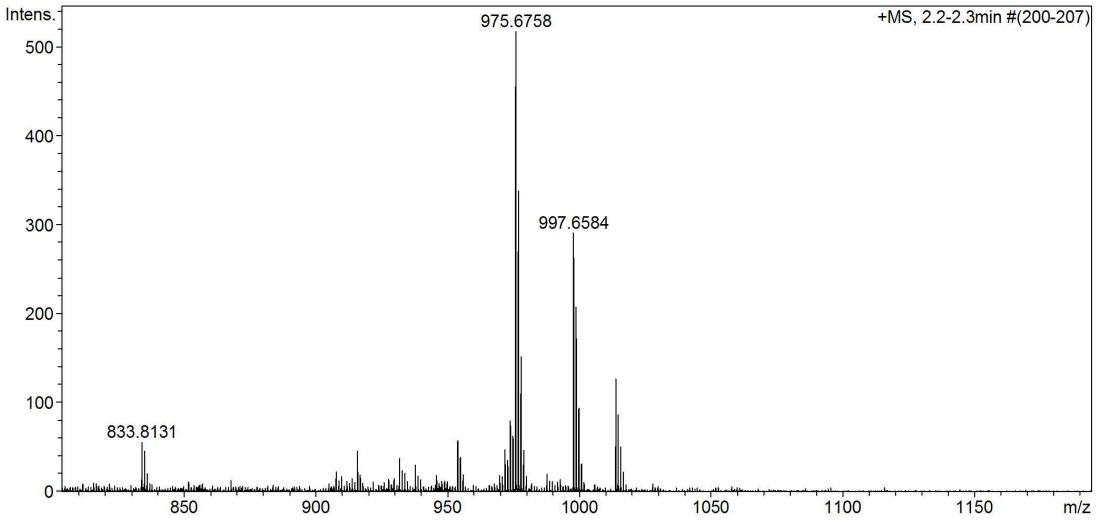

Figure 3.31 HR-ESI-MS spectra of N^4,N^9-Dibutadecanoylspermine-OPA/MCE derivative, (M.W. = 974.6717, $C_{58}H_{94}N_4O_4S_2$) expected m/z $[M+H]^+$ ion = 975.6795 (found = 975.6758), $[M+ Na]^+$ ion m/z = 997.6614 (found = 997.6584) and $[M+K]^+$ ion m/z = 1013.7700.

OPA/MCE derivatives of aminoglycosides

Aminoglycoside antibiotics present a problem of detection by spectroscopic methods. One approach to this problem is to derivatize the antibiotic with a UV or fluorescent chromophore for HPLC analysis.

Kanamycins (Figure 3.32) are aminoglycoside antibiotics, which are synthesized by *Streptomyces kanamyceticus*. Kanamycin A is the main component (>95%) kanamycin B is minor component (<5%) so kanamycin A is usually chosen as the detected target compound. The official British Pharmacopoeia method for the detection of kanamycin A is a microbiological method. However, this method is time consuming and has a low sensitivity which can hardly provide reliable results. There are also other analytical methods for determination of kanamycin A such as nuclear magnetic resonance (NMR) (Fourmy *et al.*, 1998), mass spectrometry (MS) (Oertel *et al.*, 2004) and high performance liquid chromatography (HPLC) (David *et al.*, 2001). Compared to NMR and MS methods, HPLC is a simple procedure for detecting aminoglycosides, relatively easy to develop, and is well suited for the analysis of small compounds. Simple chromatographic methods are not applicable due to lack of chromophores and strong hydrophilicity of aminoglycosides.

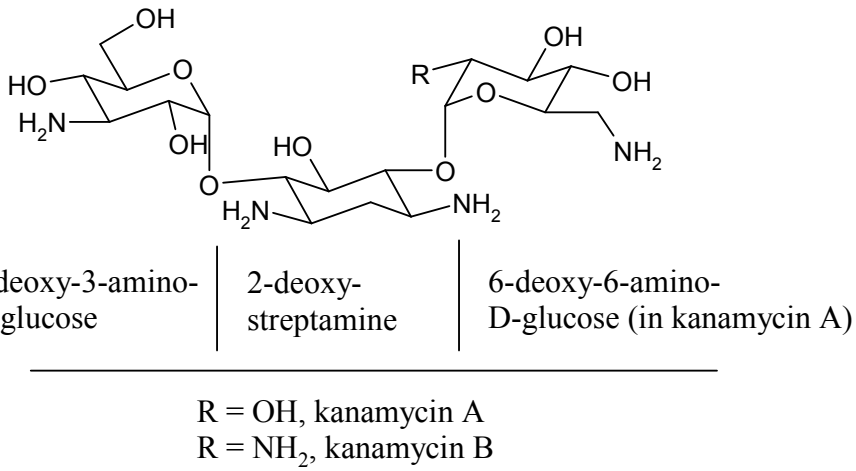

Figure 3.32 Kanamycin.

The OPA/MCE derivatization method was applied to the polyamine glycoside antibiotics, kanamycin and neomycin. The time of derivatization and the amount of derivative reagent were studied to optimize the derivatization conditions for kanamycin-OPA/MCE. For the optimization of reaction time, kanamycin was derivatized at 1, 10, 30, 45 min. The maximum peak area was reached at 10 min (Figure 3.33). The amount of OPA/MCE to kanamycin was also investigated from 1- to 24-fold. The results from the HPLC chromatogram show that the reaction was not complete with 2-fold mole ratio of OPA/MCE reagent (Figure 3.34), but appeared to be complete when a 10-fold mole ratio excess of reagent was used (Figure 3.35). The retention time of kanamycin-OPA/MCE is 9.7 min (mobile phase: 40% acetonitrile in Milli-Q-water). The graph of mole ratio of OPA/MCE vs. kanamycin (Figure 3.36) and the calibration curve were obtained (Figure 3.37).

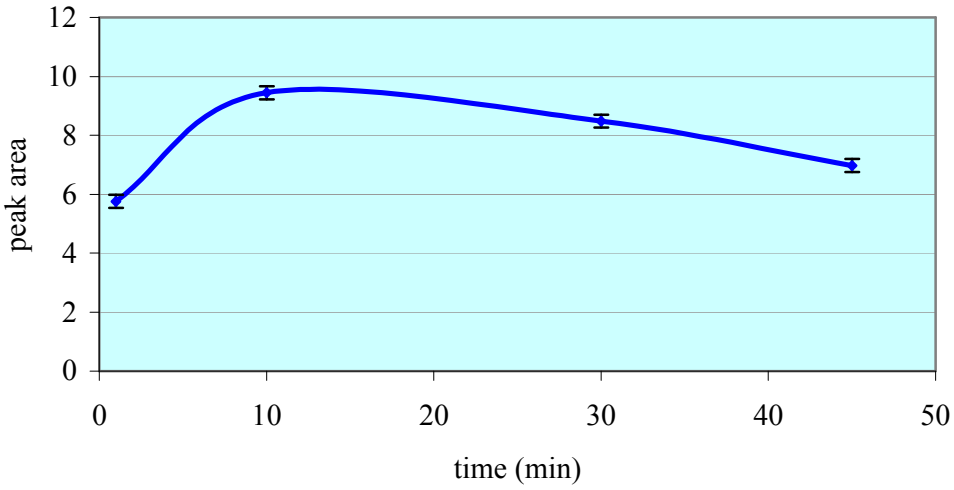

Figure 3.33 Reaction of 100 μL 1mM kanamycin with 100 μL of OPA/MCE at various reaction times (n = 5). Peak areas were calculated by height x 0.5 width of peak, and peak areas are reported in cm^2.

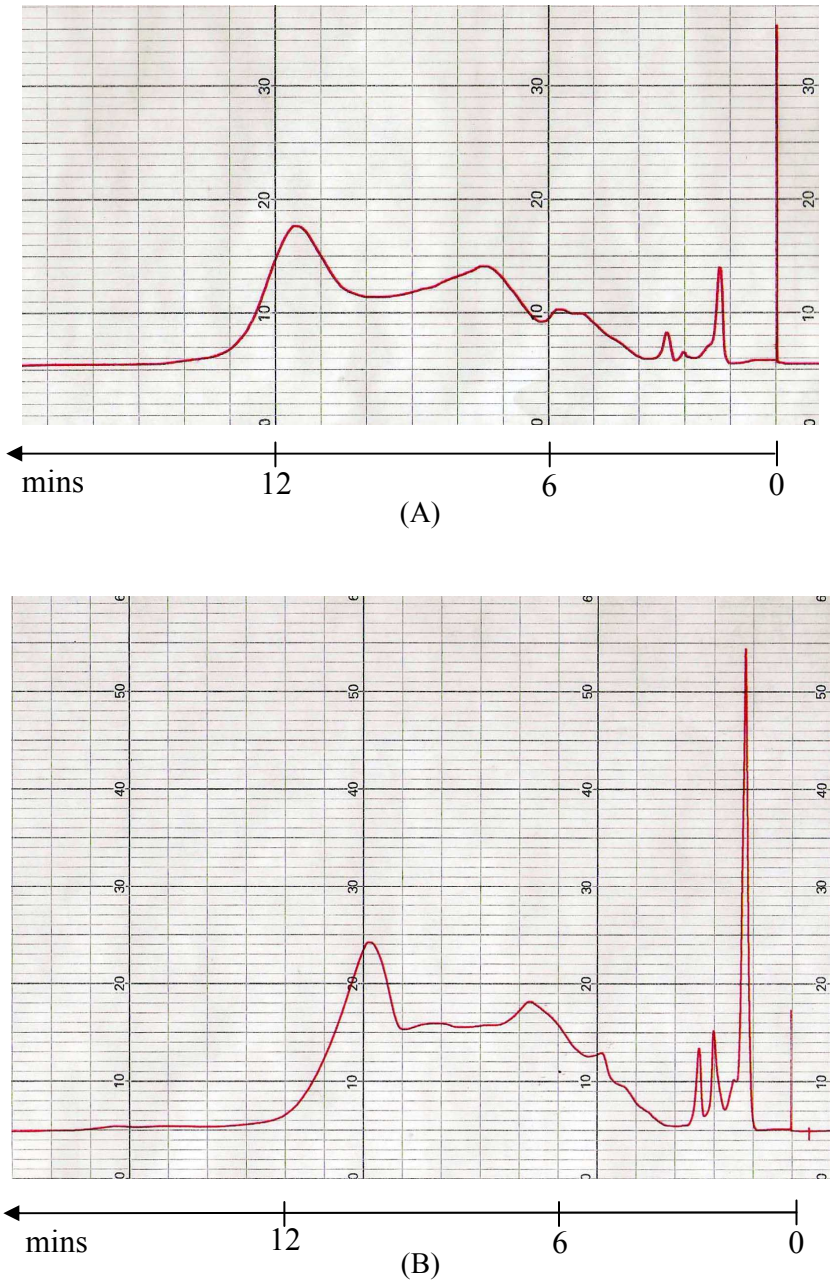

Figure 3.34 HPLC chromatogram of kanamycin-OPA/MCE (10 mM), HPLC conditions: column: Phenomenex luna C18 5µ 150 x 4.60 mm, mobile phase is acetonitrile: Milli-Q-water (40:60) with flow rate 1 mL/min, (A) from fluorescence detection at λ_{ex} = 340 nm, λ_{em} = 450 nm. (B) from UV detector at λ_{max} = 340 nm. The chromatogram shows the solvent front at Rt = 1.0 min and kanamycin-OPA/MCE derivative as the broad multiple peak starting at Rt = 3.0 min.

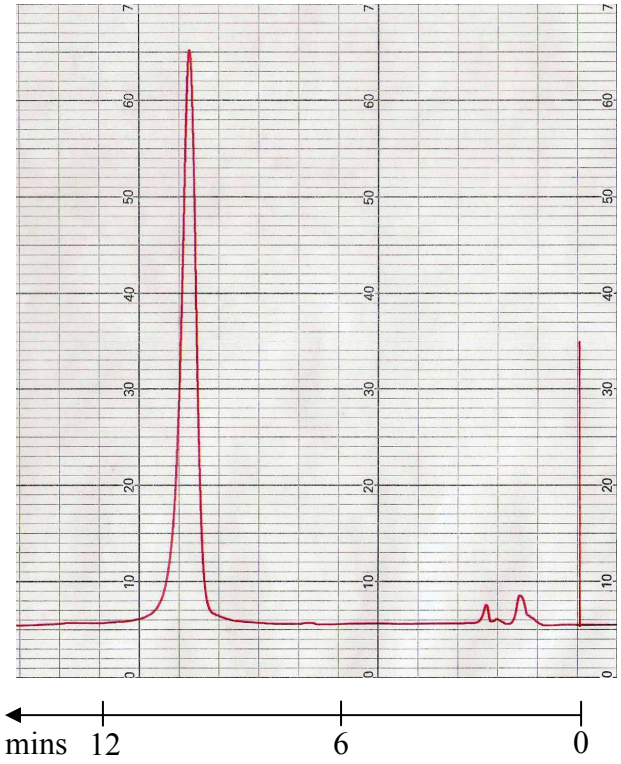

(A)

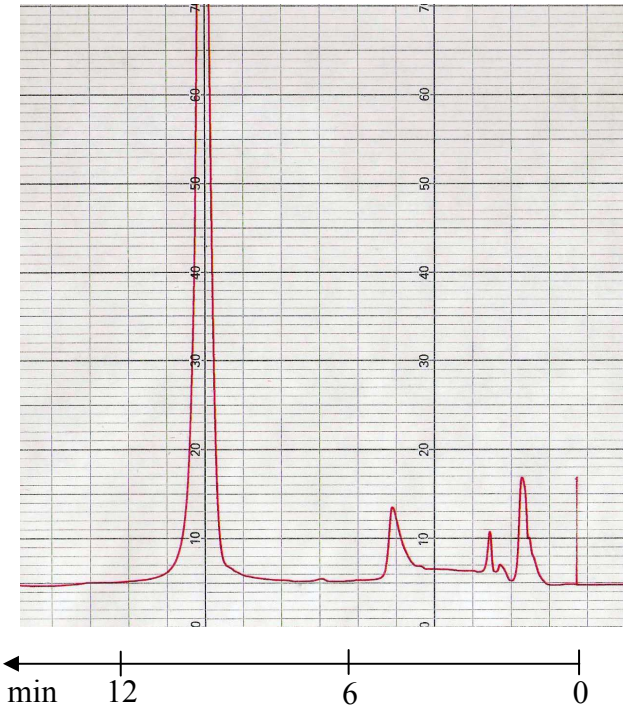

(B)

Figure 3.35 HPLC chromatogram of kanamycin-triOPA/MCE (10 mM), HPLC conditions: column: Phenomenex luna C18 5µ 150 x 4.60 mm, mobile phase: acetonitrile: Milli-Q-water (40:60), flow rate 1 mL/min, (A) fluorescence detection at λ_{ex} = 340 nm, λ_{em} = 450 nm. The chromatogram shows the solvent front at Rt = 1.0 min and kanamycin-triOPA/MCE derivative at Rt = 9.7 min (B) from UV detector at λ_{max} = 340 nm.

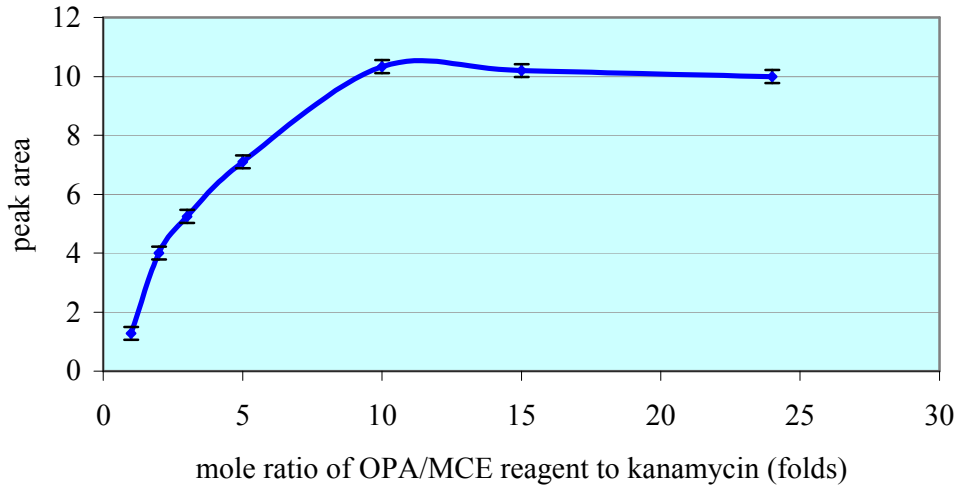

Figure 3.36 Reaction of 100 µL 1mM kanamycin with 100 µL of OPA/MCE at various mole ratio (n = 5). Peak areas were calculated by height x 0.5 width of peak, and peak areas are reported in cm^2.

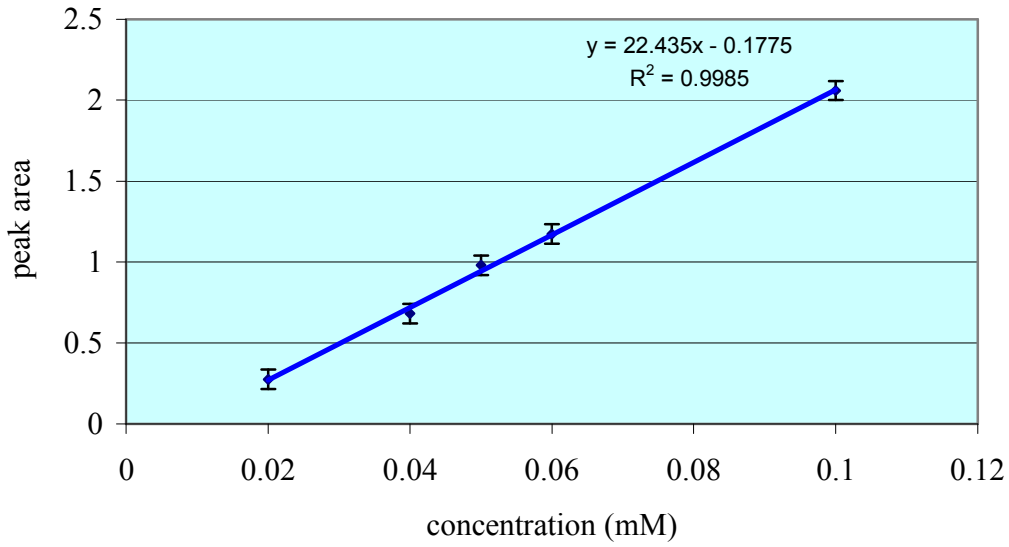

Figure 3.37 Calibration curve of kanamycin-OPA/MCE derivatives (n = 5). Peak areas were calculated by height x 0.5 width of peak, and peak areas are reported in cm^2.

However, the HR-ESI-MS suggested that this product was kanamycin-triOPA/MCE (Figure 3.38) instead of the expected tetra-OPA/MCE (Figure 3.39). This might due to the steric effect of the two amine groups on the same 2-deoxy streptamine ring allowing only one molecule of OPA/MCE to react at one of the amine positions of this ring. HR-ESI-MS from the broad peak of the incomplete reaction in Figure 3.34 showed the m/z kanamycin-diOPA/MCE derivatives (Figure 3.40), for which several different structures are possible.

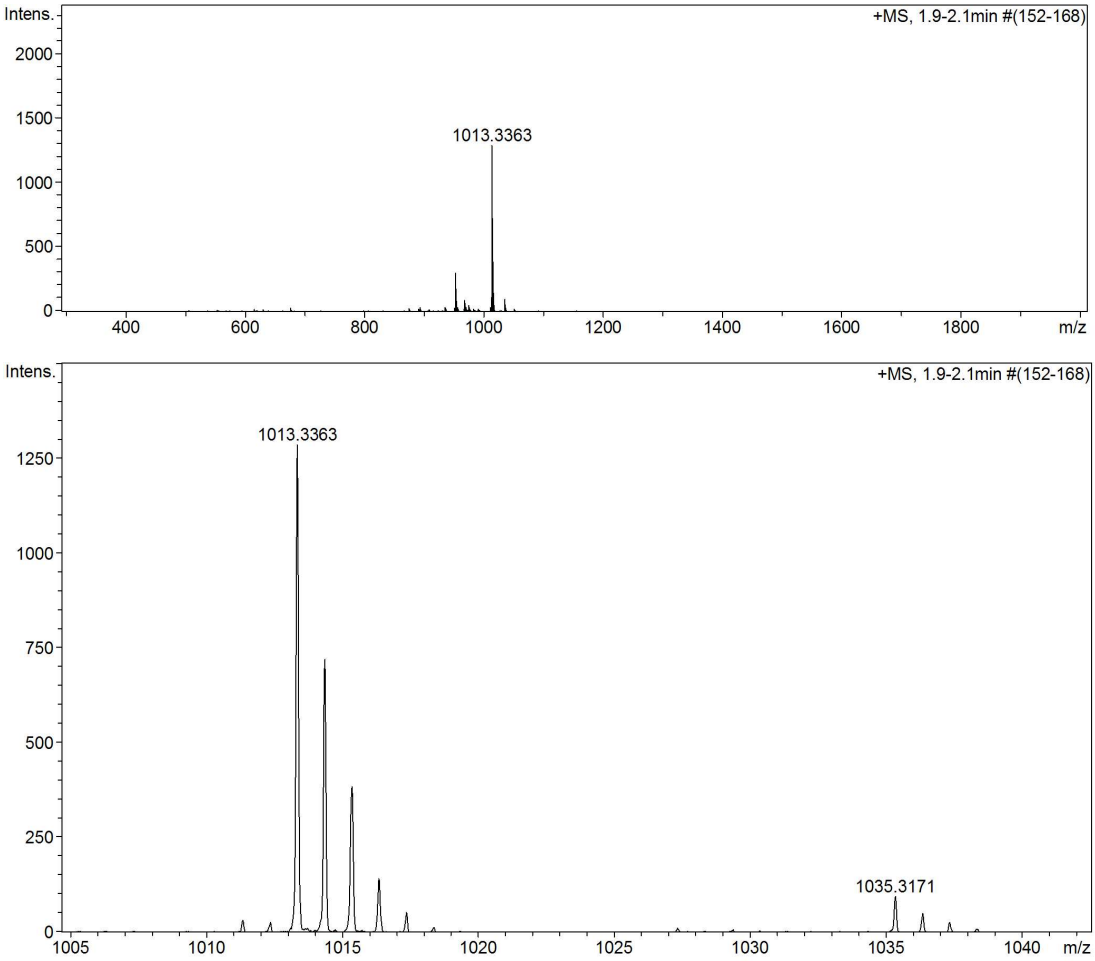

Figure 3.38 HR-ESI-MS spectra of kanamycin-triOPA/MCE derivative, (M.W. = 1012.3268, $C_{48}H_{60}N_4O_{14}S_3$) expected m/z $[M+H]^+$ ion = 1013.3346 (found = 1013.3363) and $[M+ Na]^+$ ion m/z = 1035.3166 (found = 1035.3171).

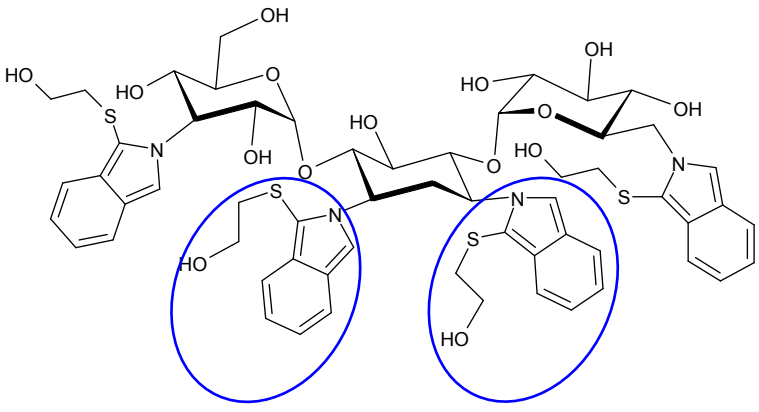

Figure 3.39 Kanamycin-tetraOPA/MCE derivative.

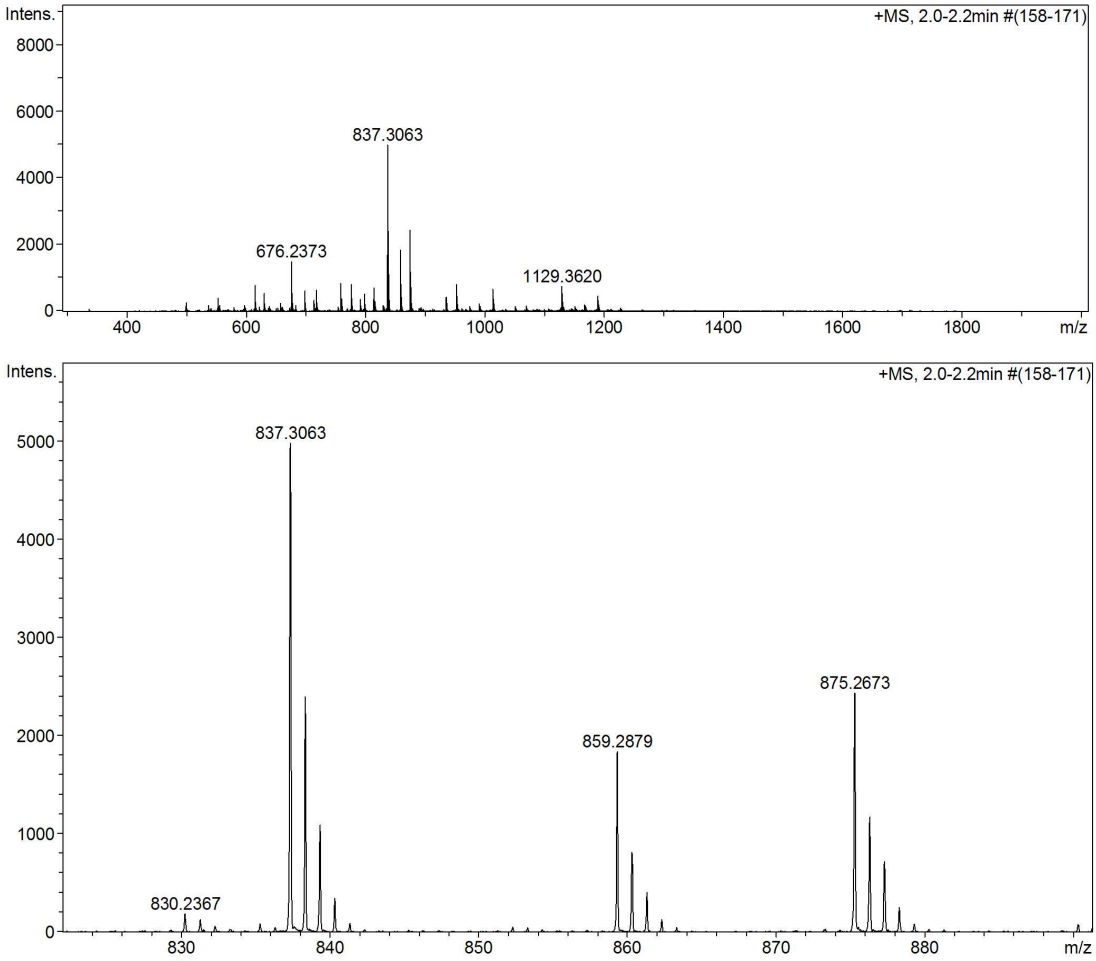

Figure 3.40 HR-ESI-MS spectra of kanamycin-diOPA/MCE derivative, (M.W. = 836.2972, $C_{38}H_{52}N_4O_{13}S_2$) expected m/z $[M+H]^+$ ion = 837.3050 (found = 837.3063), $[M+ Na]^+$ ion m/z = 859.2869 (found = 859.2879) and $[M+K]^+$ ion m/z = 875.3955 (found = 875.2673).

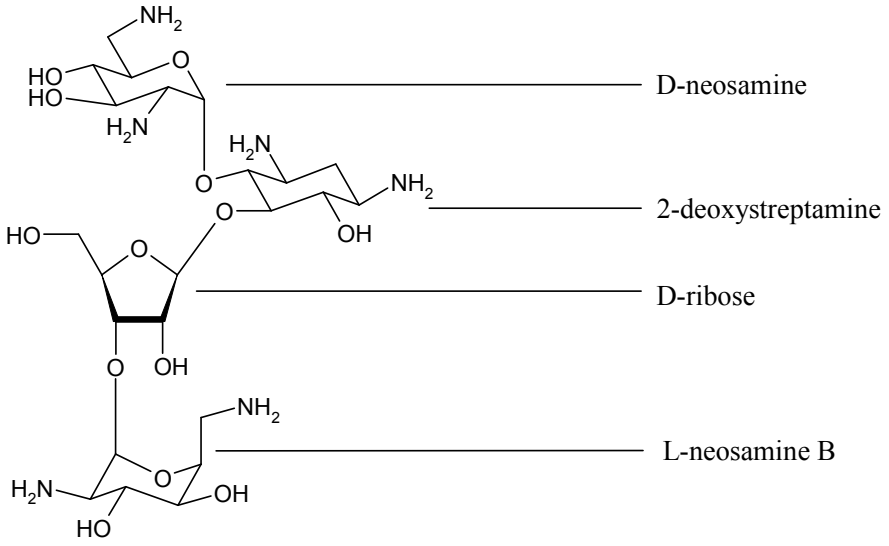

Figure 3.41 Neomycin B.

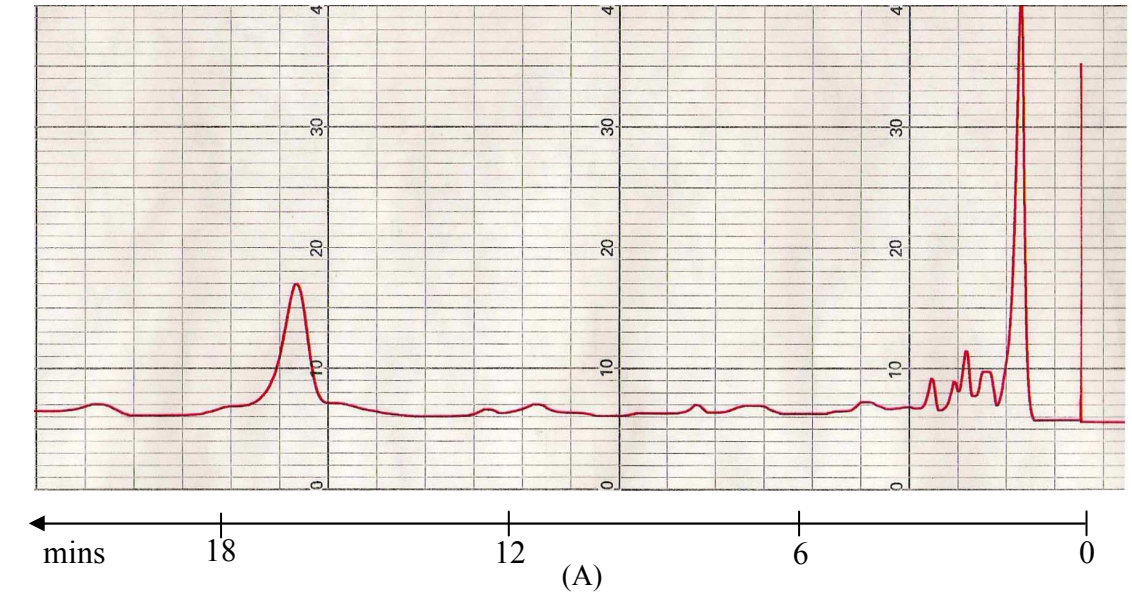

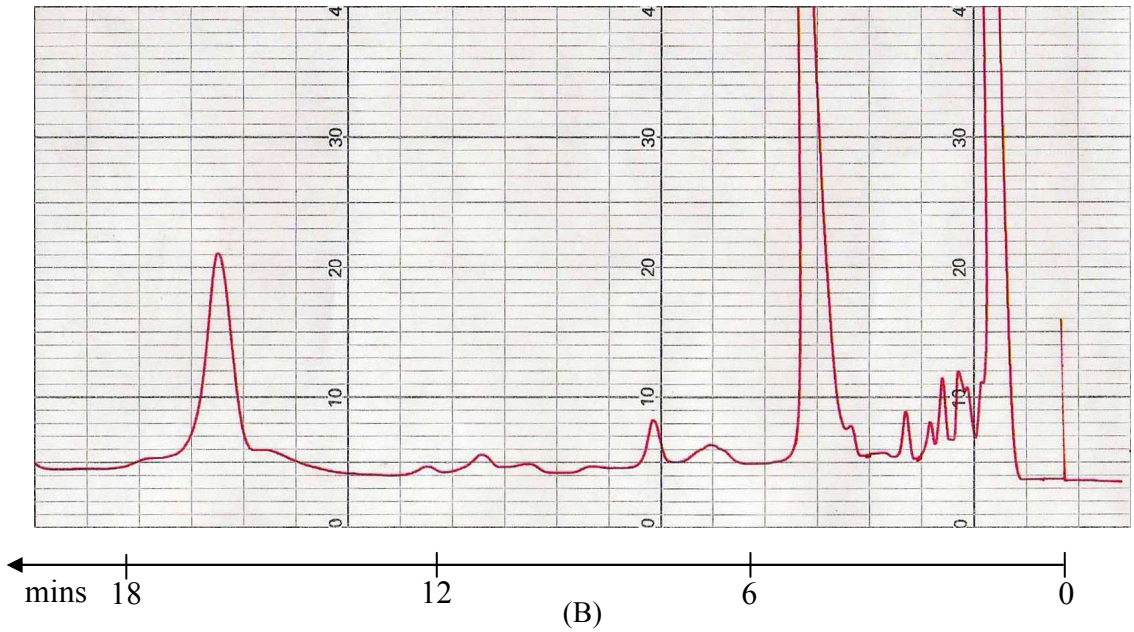

Figure 3.42 HPLC chromatogram of neomycin-pentaOPA/MCE (10 mM), HPLC conditions: column: Phenomenex luna C18 5µ 150 x 4.60 mm, mobile phase is acetonitrile: Milli-Q-water (40:60) flow rate 1 mL/min, (A) fluorescence detection at λ_{ex} = 340 nm, λ_{em} = 450 nm. (B) UV detection at λ_{max} = 340 nm. The chromatogram shows the solvent front at Rt = 1.0 min and neomycin-pentaOPA/MCE derivative at Rt = 16.7 min.

The method for derivatization of kanamycin with OPA/MCE was also used to investigate neomycin. Neomycin (Figure 3.41) is mainly composed of a mixture of neomycin B and its stereoisomer neomycin C (3-15% of the mixture) (Dutcher *et al.*, 1951). It is produced by cultures of *Streptomyces fradiae* (Waksman, 1949). The structure contains three sugar residues linked to 2-deoxystreptamine. One of these is the common sugar D-ribose.

Neomycin has very good activity against Gram-positive and Gram-negative bacteria, but it has a narrow therapeutic range and is ototoxic For neomycin, ratios of OPA/MCE to neomycin up to 15-fold were required to achieve a symmetrical peak at 16.7 min (Figure 3.42) eluted with mobile phase 40% acetonitrile in Milli-Q-water. HR-ESI-MS analysis of the derivative peak showed neomycin-pentaOPA/MCE (Figure 3.43). Instead of the expected hexaOPA/MCE as with kanamycin-triOPA/MCE, this may be due to the steric effect of the two amine groups on the same 2-deoxy streptamine ring. The two amine groups on the D-neosamine and L-neosamine of neomycin are unlikely to show such a steric effect due to the rigidity of the ring which holds the amine groups at positions two and six well apart.

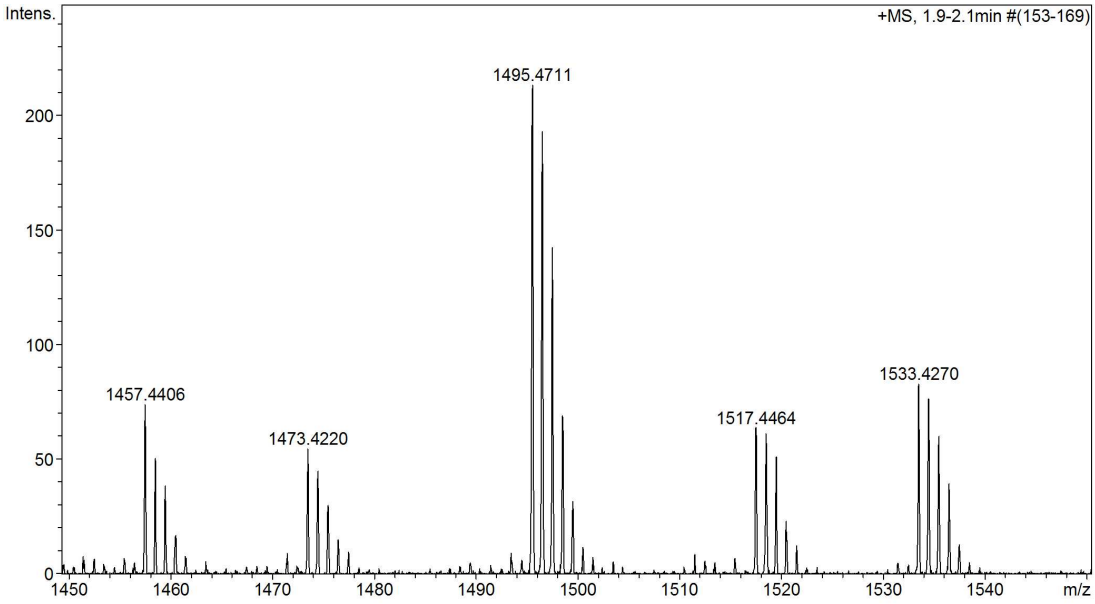

Figure 3.43 HR-ESI-MS spectra of neomycin-pentaOPA/MCE derivative, (M.W. = 1494.4602, $C_{73}H_{86}N_6O_{18}S_5$) expected m/z $[M+H]^+$ ion = 1495.4680 (found = 1495.4711), $[M+ Na]^+$ ion m/z = 1517.4499 (found = 1517.4464) and $[M+K]^+$ ion m/z = 1533.5585 (found = 1533.4270).

This OPA/MCE method for aminoglycosides is easy and simple to perform, the time of reaction (10 min) is also practical, and no process of extraction is needed. The derivatives of aminoglycosides-OPA/MCE are more stable than the aliphatic amines. RP-HPLC with C-18 column and isocratic mobile phase of acetonitrile and Milli-Q-water were used to separate aminoglycosides. By this method, we could use either UV or fluorescence detection to examine the aminoglycosides-OPA/MCE derivatives. Thus it is possible to introduce HPLC in official monographs to replace a microbiological assay (Adams *et al.*, 1998).

The two step derivatization of OPA/MCE/FMOC

The method of derivatization by OPA/MCE did not give stable peaks for spermidine and spermine-OPA/MCE derivatives in the HPLC chromatogram. Derivatives for molecules such as spermidine and spermine may be unstable due to their secondary amine groups which do not form OPA/MCE derivatives, but which may lead to rapid breakdown of the primary amine derivatives. A two-step derivatization process, by applying OPA/MCE followed by FMOC reagent was explored. By this method, spermidine and spermine should be fully labelled, at their primary amines with OPA/MCE and at their secondary amines with FMOC. This process resulted in more stable derivatives, detected by both fluorescence and UV absorption of both chromophores and gave reproducible responses. The derivatization product of spermidine-diOPA/MCE-monoFMOC (Figure 3.44) and spermine-diOPA/MCE-diFMOC (Figure 3.47) gave symmetrical HPLC peaks (Figures 3.45 and 3.49, respectively) in terms of increased fluorescent responses and better reproducibility. Table 3.6 shows the retention times of spermidine-diOPA/MCE-monoFMOC and spermine-diOPA/MCE-diFMOC derivative using hypersil C-18 column when the mobile phase was changed. Spermidine-diOPA/MCE-monoFMOC derivative and spermine-diOPA/MCE-diFMOC derivatives show the expected m/z by HR-ESI-MS (Figures 3.46 and 3.48 respectively).

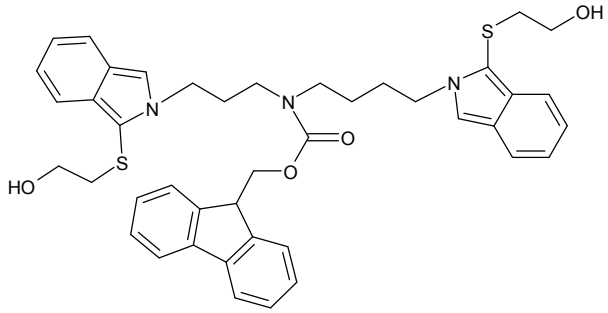

Figure 3.44 Spermidine-diOPA/MCE-monoFMOC.

Table 3.6 Retention time of spermidine-diOPA/MCE-mono derivative and spermine-diOPA/MCE-diFMOC derivative.

Mobile phase	Rt (min)	
	Spermidine	Spermine
65% Acetonitrile : 35% Milli-Q-Water	25.7	-
70% Acetonitrile : 30% Milli-Q-Water	22.0	49.5
80% Acetonitrile : 20% Milli-Q-Water	6.5	18.0
85% Acetonitrile : 15% Milli-Q-Water	5.3	9.0

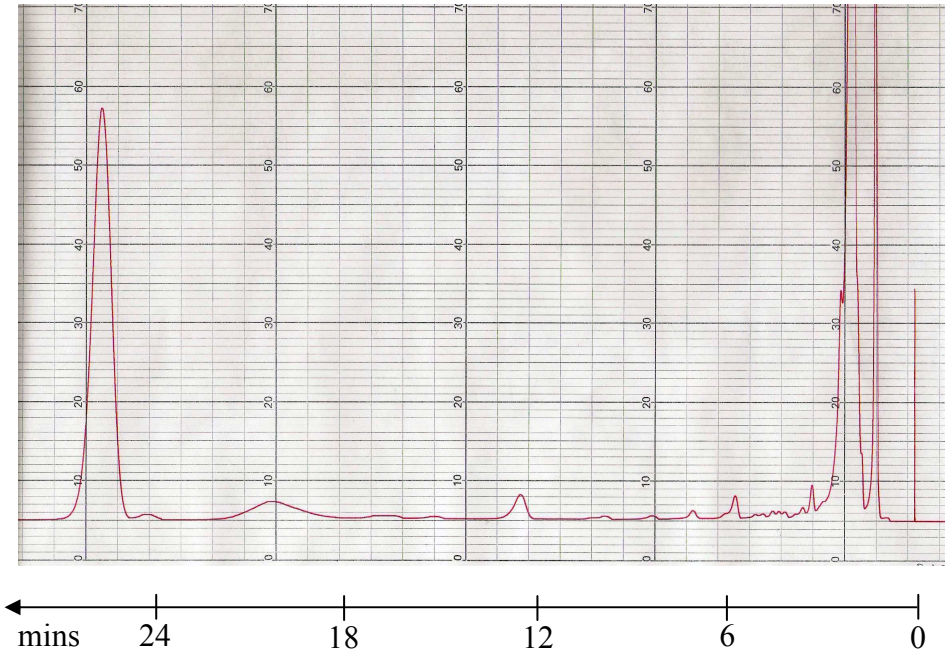

Figure 3.45 HPLC chromatogram of spermidine-diOPA/MCE-monoFMOC derivative, HPLC conditions: column: Phenomenex hypersil C18 5µ 150 x 4.60 mm, mobile phase is acetonitrile: Milli-Q-water (65:35) with flow rate 1 mL/min, fluorescence detection at λ_{ex} = 340 nm, λ_{em} = 450 nm. The chromatogram shows the solvent front at Rt = 1.0 min and spermidine-diOPA/MCE-monoFMOC derivative at Rt = 25.7 min.

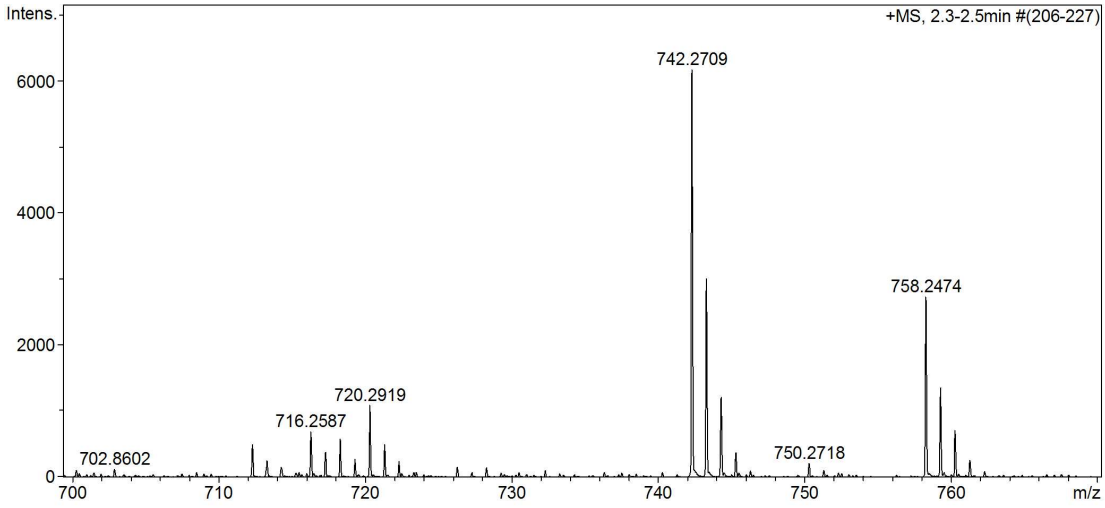

Figure 3.46 HR-ESI-MS spectrum of spermidine-diOPA/MCE-monoFMOC derivative, (M.W. = 719.2852, $C_{42}H_{45}N_3O_4S_2$) expected m/z $[M+H]^+$ ion = 720.2929 (found = 720.2919), $[M+ Na]^+$ ion m/z = 742.2749 (found = 742.2709) and $[M+K]^+$ ion m/z = 758.3835 (found = 758.2474).

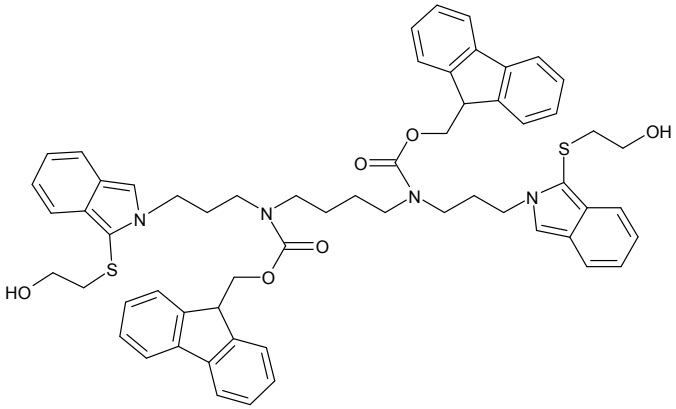

Figure 3.47 Spermine-diOPA/MCE-diFMOC.

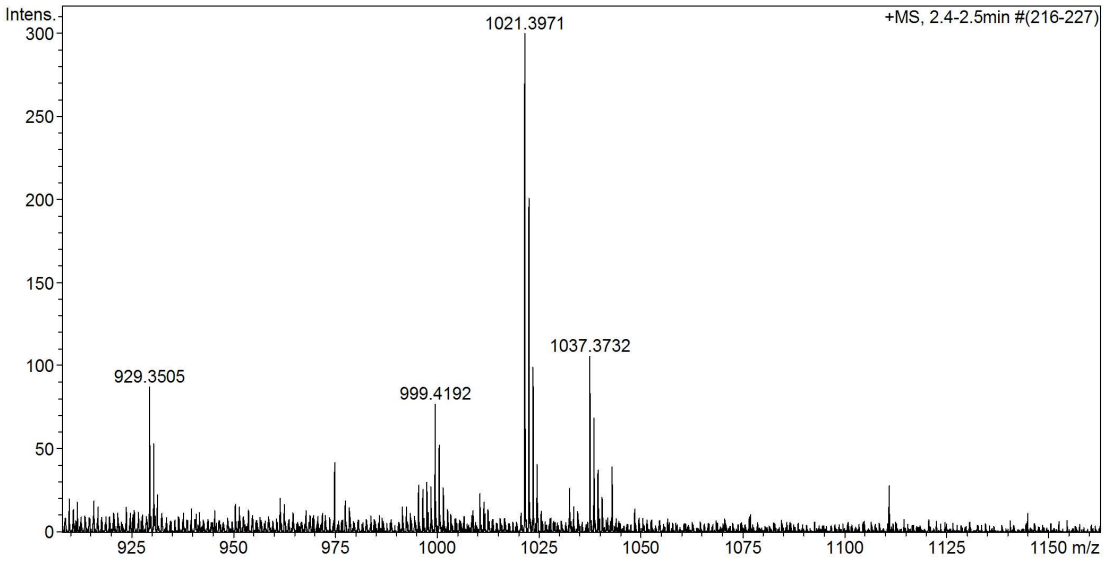

Figure 3.48 HR-ESI-MS spectra of spermine-diOPA/MCE-diFMOC derivative, (M.W. = 998.4111, $C_{60}H_{62}N_4O_6S_2$) expected m/z $[M+H]^+$ ion = 999.4189 (found = 999.4192), $[M+Na]^+$ ion m/z = 1021.4009 (found = 1021.3971) and $[M+K]^+$ ion m/z = 1037.5093 (found = 1037.3732).

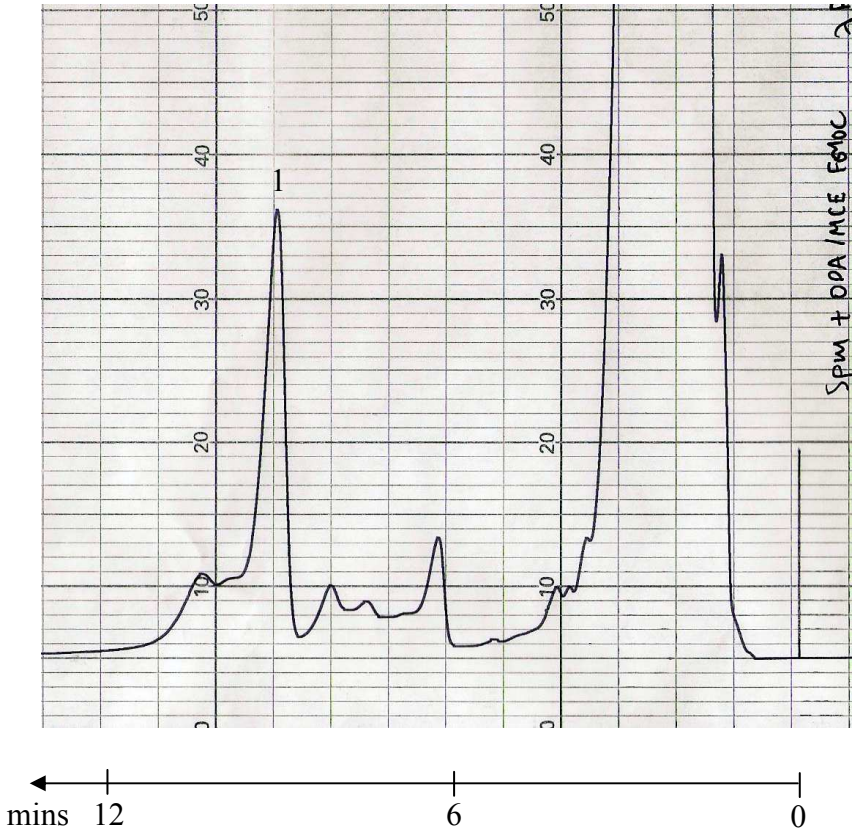

(A)

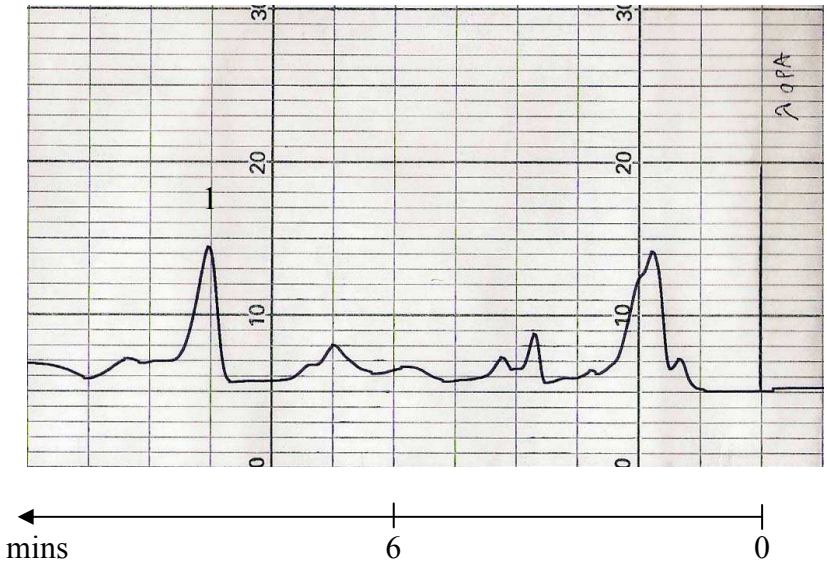

(B)

Figure 3.49 HPLC chromatogram of spermine-diOPA/MCE-diFMOC derivative, HPLC conditions: column: Phenomenex hypersil C18 5µ 150 x 4.60 mm, mobile phase is acetonitrile: Milli-Q-water (85:15) with flow rate 1 mL/min, fluorescence detection at (A) FMOC wavelength λ_{ex} = 264 nm, λ_{em} = 310 nm (B) OPA wavelength λ_{ex} = 340 nm, λ_{em} = 450 nm. The chromatogram shows the solvent front at Rt = 1.0 min and peak 1 = spermine-diOPA/MCE-diFMOC derivative at Rt = 9 min.

3.2 Primary amine-fluorescamine derivatives

Fluorescamine, (4-phenylspiro [furan-2(3H),1-phthalan]-3,3-dione) a heterocyclic dione, is a selective fluorophore which reacts with primary amines to form a highly fluorescent product. Udenfriend first described that phenylacetaldehyde, which is formed by oxidative decarboxylation of phenylalanine by ninhydrin, reacts with an excess of ninhydrin and with a primary amino group to give a 5-(2-carboxyphenyl)-5-hydroxy-3-phenyl-2-pyrroline-4-one derivative with highly fluorescent yield (λ_{ex} = 275, 390 nm, λ_{em} = 480 nm) (Udenfriend *et al.*, 1972). This main fluorescent product was characterized as a pyrrolinone which led to the synthesis of fluorescamine (Debernar *et al.*, 1974). Ammonia also reacts with fluorescamine, but the product has little fluorescence. The scheme of amine-fluorescamine reaction is shown in Figure 3.50.

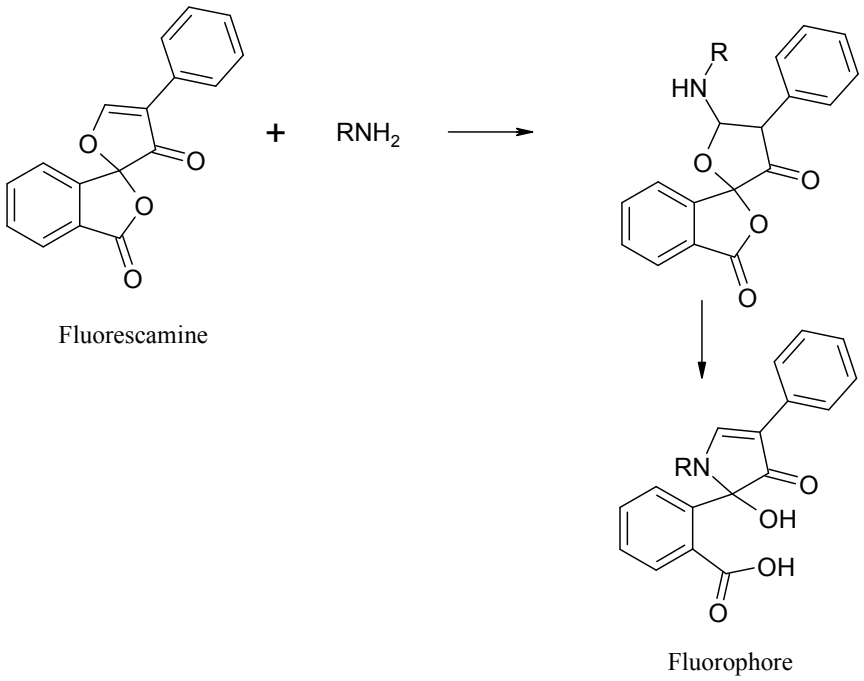

Fluorescamine

Fluorophore

Figure 3.50 Amine-fluorescamine reaction.

Fluorescamine is a non-fluorescent compound that reacts with primary amines at room temperature to yield a highly fluorescent product. The excess of reagent is destroyed by water to form a non-fluorescent hydrolysis product (Stein *et al.*, 1974). The reaction of fluorescamine with primary amines is strongly pH dependent and also the fluorescence is developed only in alkaline media (pH of 8.0-9.5) and disappears completely in acidic media. The derivatives of amines-fluorescamine are formed immediately and are stable for at least 1 day so they are more stable than OPA derivatives. The method of preparation of the amines-fluorescamine was tested (HPLC chromatogram shown in Figure 3.51, retention time shown in Table 3.7) and the calibration curves obtained were linear (Table 3.8, Figure 3.52). The

good linearity of the calibration curves is clearly evident by the values of the correlation coefficients. Derivatization of spermidine and spermine was attempted, but no stable products were observed by HPLC.

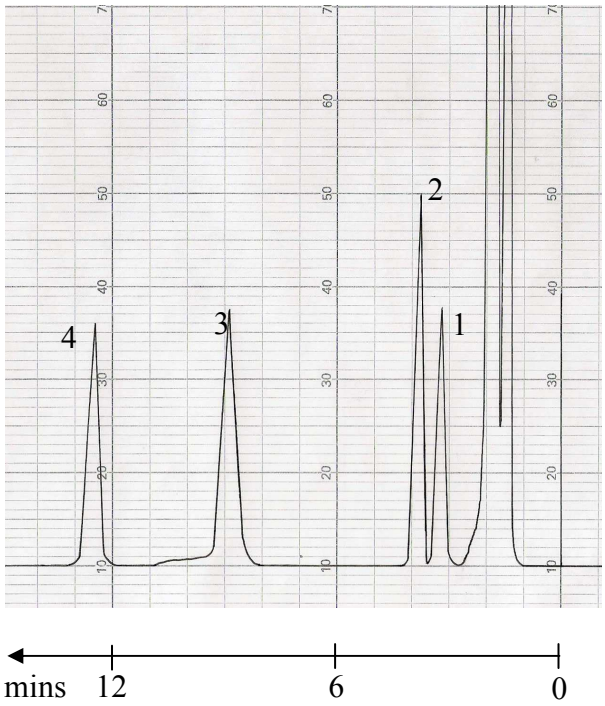

Figure 3.51 HPLC chromatogram of various amine-fluorescamine derivatives, HPLC conditions: column: Phenomenex hypersil C18 5µ 150 x 4.60 mm, mobile phase is methanol: Milli-Q-water (40:60), flow rate 1 mL/min, fluorescamine fluorescence detection at λ_{ex} = 400 nm, λ_{em} = 475 nm. The chromatogram shows the solvent front at Rt = 1.3 min, peak 1 = 1-Butylamine-monofluorescamine at Rt = 3.2 min, peak 2 = 1,4-diaminobutane-monofluorescamine at Rt = 3.8, peak 3 = 1,5-diaminopentane-monofluorescamine at Rt = 8.8 min, peak 4 = 1,7-diaminoheptane-monofluorescamine at Rt = 12.8 min.

Table 3.7 Retention time of various amine-fluorescamine derivatives.

Amine-fluorescamine derivatives	Rt (min) eluted by 40% MeOH	Rt (min) eluted by 50% MeOH	Rt (min) eluted by 70% MeCN
1-Butylamine-monofluorescamine	3.2	2.30	1.5
1,4-Diaminobutane-monofluorescamine	3.8	-	-
1,5-Diaminopentane-monofluorescamine	8.8	-	-
1,7-Diaminoheptane-monofluorescamine	12.8	8.30	1.8

Table 3.8 The calibration curves' equations for various amine-fluorescamine derivatives.

Amine-fluorescamine derivatives	Calibration curve equation	R^2
1-Butylamine-monofluorescamine	y = 1.245x +0.08	0.997
1,4-Diaminobutane-monofluorescamine	y = 1.501x + 0.16	0.994
1,5-Diaminopentane-monofluorescamine	y = 2.223x + 0.19	0.995
1,7-Diaminoheptane-monofluorescamine	y = 2.349x - 0.04	0.991

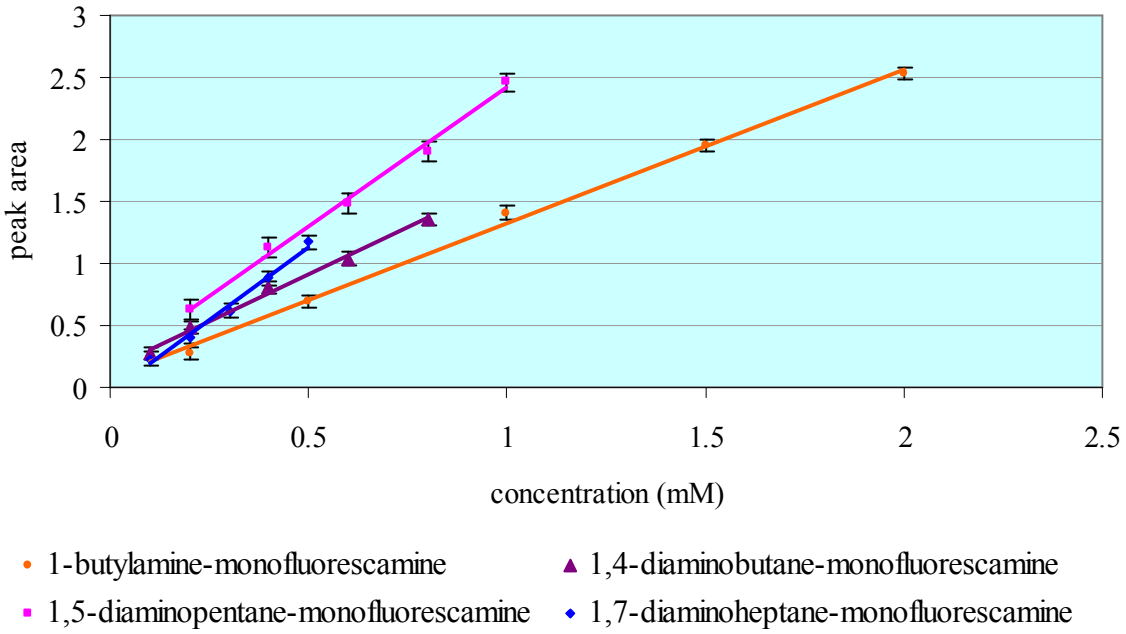

Figure 3.52 Calibration curves of amine-fluorescamine derivatives (n = 5). Peak areas were calculated by height x 0.5 width of peak, and peak areas are reported in cm^2.

HR-ESI-MS

The HR-ESI-MS for fluorescamine derivatives was investigated to confirm the structures of the derivatives as 1-butylamine gave the expected mono-fluorescamine derivative (Figure 3.53). 1,4-Diaminobutane (putrescine) could potentially form both mono- and di-fluorescent derivatives, but from the HPLC and MS results only the mono-derivative of fluorescamine was observed (Figure 3.54). The di-fluorescamine moiety attached to putrescine is expected to give m/z $[M+H]^+$ ion = 645.2237 (M.W = 644.2159, $C_{38}H_{32}N_2O_8$) which was not observed. This may be due to some steric hindrance in forming the second derivative of monofluorescamine-1,4-diaminobutane.

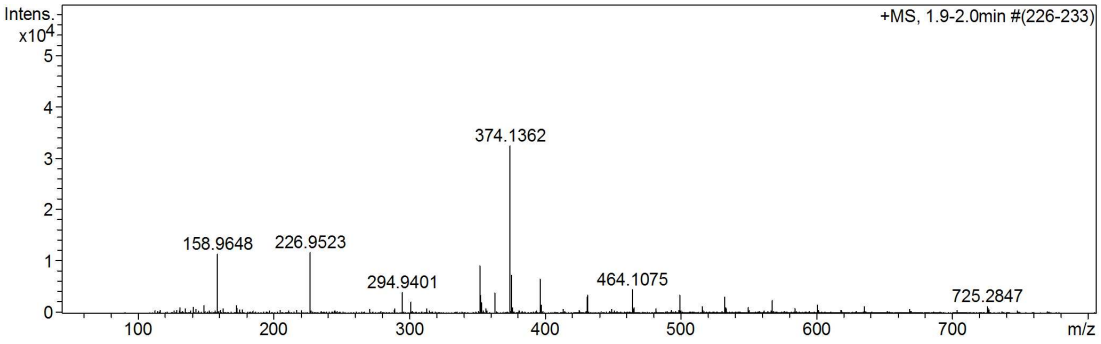

Figure 3.53 HR-ESI-MS spectra of 1-butylamine-monofluorescamine derivative, (M.W. = 351.1471, $C_{21}H_{21}NO_4$) expected m/z $[M+H]^+$ ion = 352.1549 and $[M+ Na]^+$ ion m/z = 374.1368 (found = 374.1362).

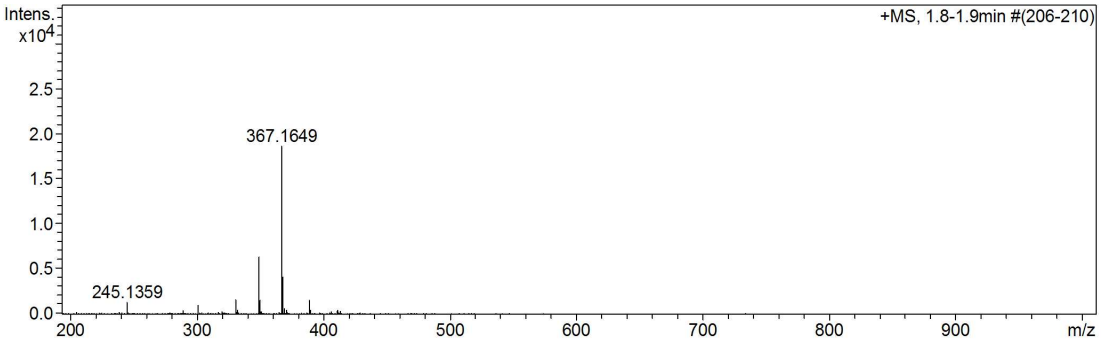

Figure 3.54 HR-ESI-MS of 1,4-diaminobutane (putrescine)-monofluorescamine derivative, M.W. = 366.1579, $C_{21}H_{22}N_2O_4$, the expected m/z $[M+H]^+$ ion = 367.1658 (found = 367.1649).

For 1,5-diaminopentane (cadaverine) the monofluorescamine derivative was the major product with a trace of the di-fluorescamine derivative as shown in Figures 3.55 and 3.56.

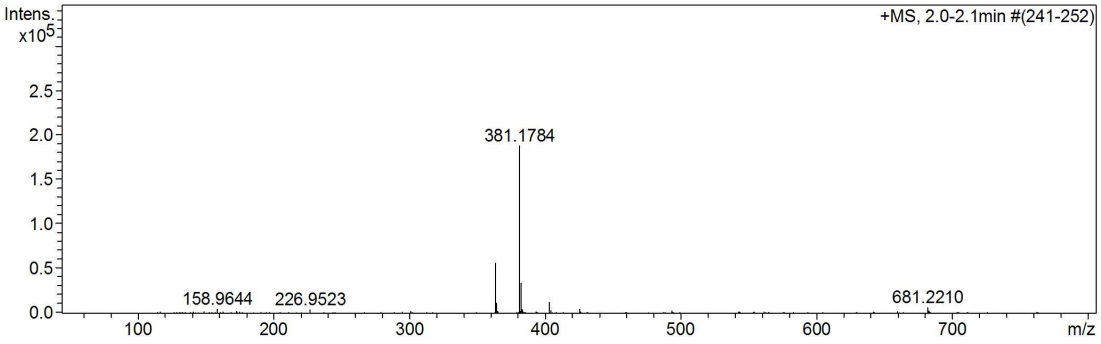

Figure 3.55 HR-ESI-MS of 1,5-diaminopentane (cadaverine)-monofluorescamine derivative M.W. = 380.1736, $C_{22}H_{24}N_2O_4$, the expected m/z $[M+H]^+$ ion = 381.1814 (found = 381.1784).

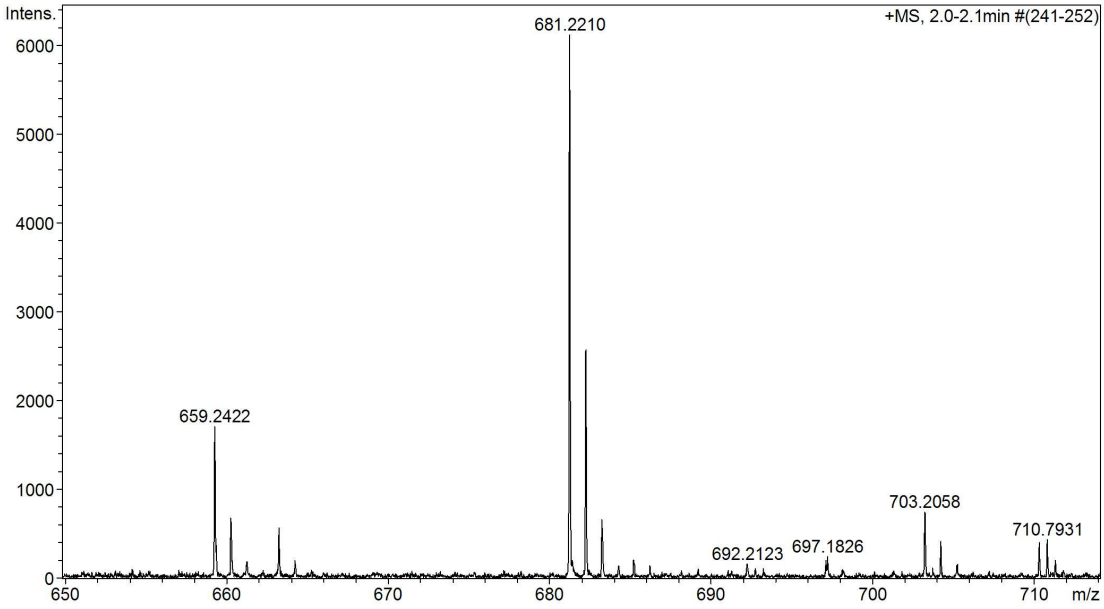

Figure 3.56 HR-ESI-MS of 1,5-diaminopentane (cadaverine)-difluorescamine derivative ($C_{39}H_{34}N_2O_8$, M.W. = 658.2315) is expected at m/z $[M+H]^+$ ion = 659.2393 (found = 659.2422) and $[M+ Na]^+$ ion as $C_{39}H_{34}N_2NaO_8$ m/z = 681.2213 (found = 681.2210).

For 1,7-diaminoheptane-monofluorescamine derivative, M.W. = 408.2049 $C_{24}H_{28}N_2O_4$, the expected m/z $[M+H]^+$ ion = 409.2127. Also, the 1,7-diaminoheptane-difluorescamine moiety is expected at m/z $[M+H]^+$ ion = 687.2706 (M.W. = 686.2628, $C_{41}H_{38}N_2O_8$) (Figure 3.57).

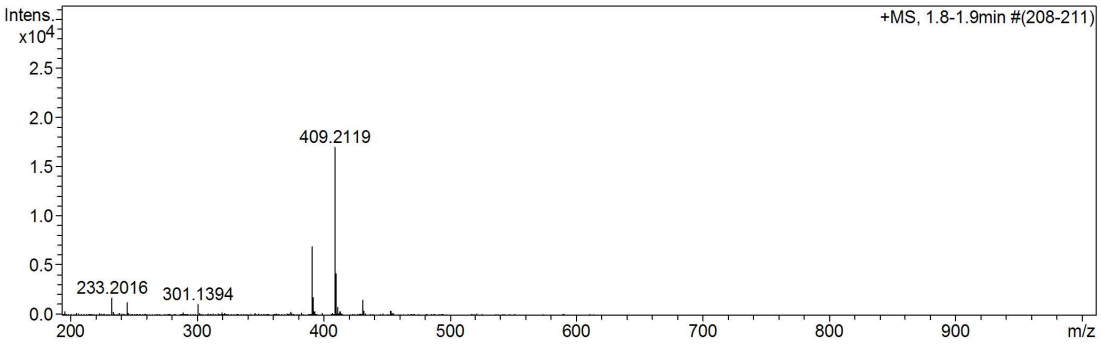

Figure 3.57 HR-ESI-MS of 1,7-diaminoheptane-monofluorescamine derivative, M.W. = 408.2049, $C_{24}H_{28}N_2O_4$, the expected m/z $[M+H]^+$ ion = 409.2127.

The derivatives of fluorescamine were stable in neutral and mildly alkaline media. In acidic solutions the fluorescence rapidly deteriorated.

Relative quantum yield of amine-fluorescamine derivatives

A comparison of fluorescence yields of the model amine series was obtained by comparison between the fluorescence intensity and UV absorption by collected the elution products from HPLC and separate measurement by fluorescence spectrometer and UV/VIS spectrophotometer. A plot of fluorescence intensity against UV absorbance (Figure 3.58) and the FI/UV equation (Table 3.9) were obtained. The results show that fluorescence yield is equal when one fluorophore is derivatized to each amine molecule.

Table 3.9 The FI/UV equation of amine-fluorescamine derivatives.

Amine-Fluorescamine derivatives	FI/UV equation	R^2
1-Butylamine-monofluorescamine	y = 5661.3x – 24.91	0.993
1,4-Diaminobutane-monofluorescamine	y = 5410.3x – 17.83	0.999
1,5-Diaminopentane-monofluorscamine	y = 5437.1x – 22.64	0.998
1,7-Diaminoheptane-monofluorescamine	y = 5441.6x – 12.60	1.000

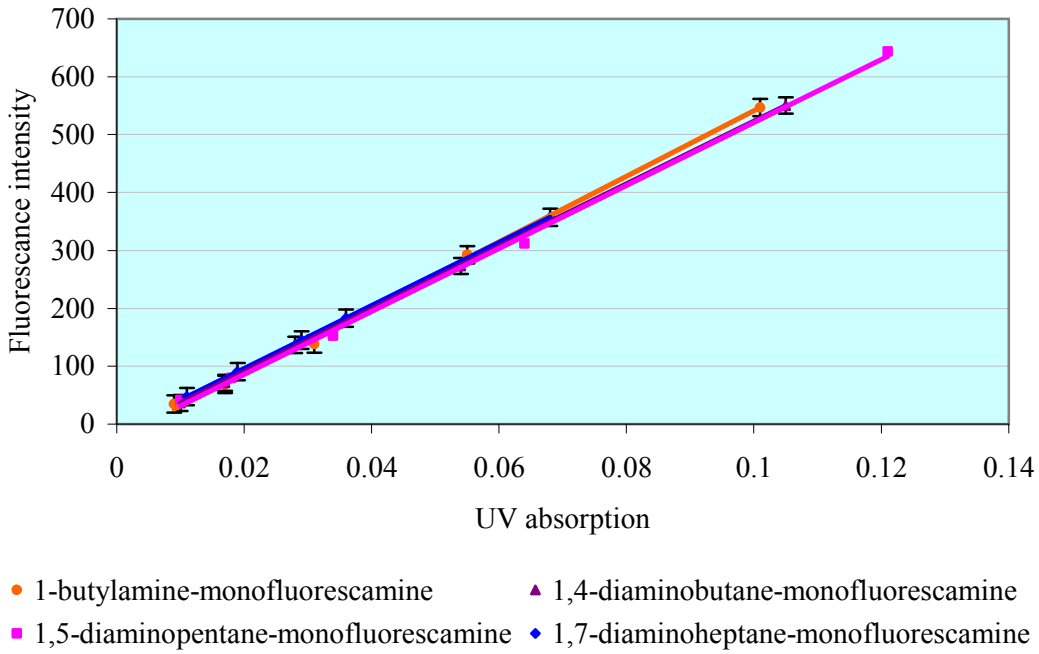

Figure 3.58 Plots of fluorescence intensity against absorbance at λ_{ex} of amine-monofluorescamine derivatives (n = 5).

Fluorescamine derivative of glucosamine

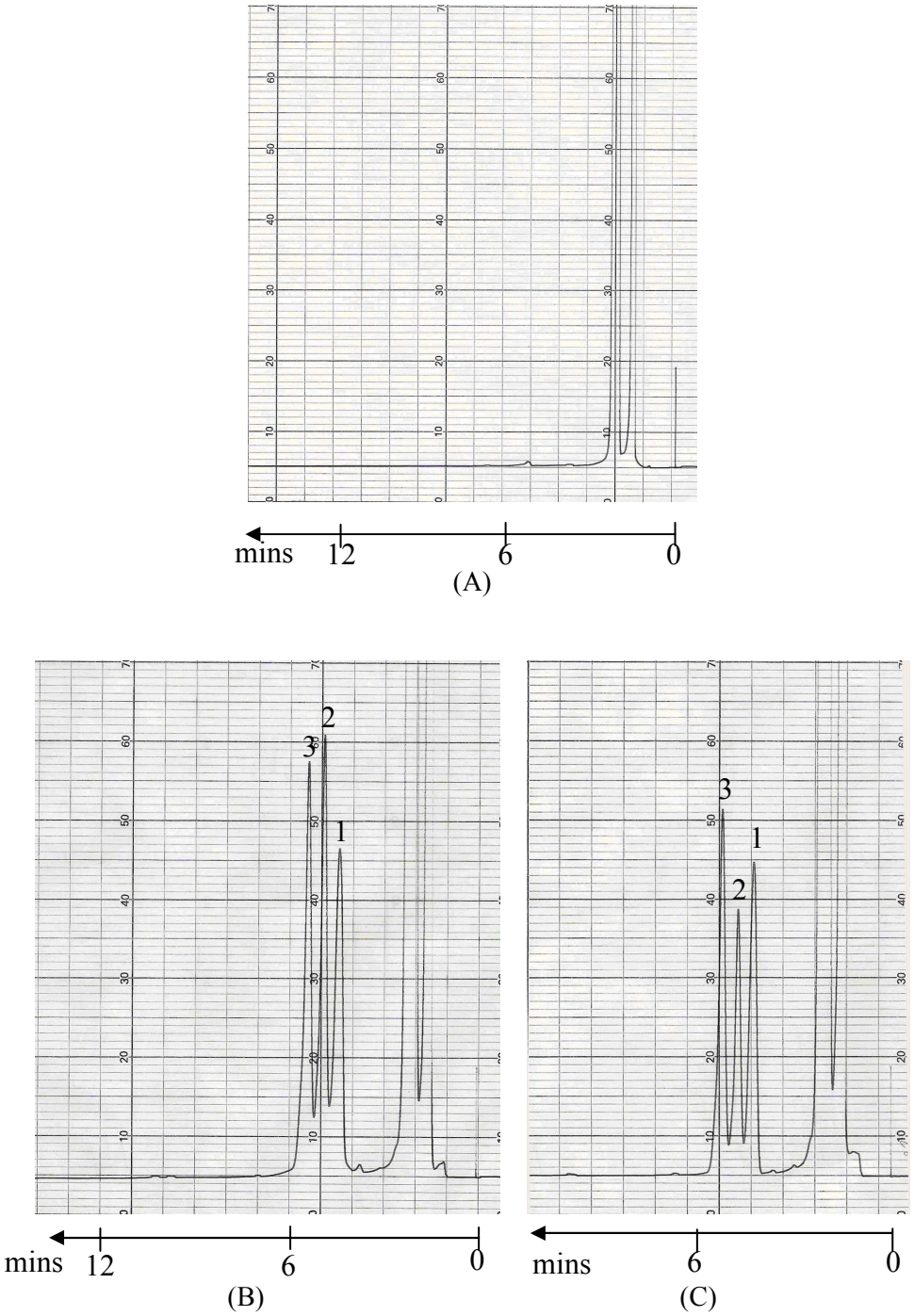

Figure 3.59 HPLC chromatogram of glucosamine-fluorescamine derivatives (50 mM). HPLC conditions: column: Phenomenex luna C18 5µ 150 x 4.60 mm, mobile phase is acetonitrile: Milli-Q-water (30:70) with flow rate 1 mL/min, UV detector at λ_{max} = 330 nm. Glucosamine-fluorescamine derivatives Rt = 4.5, 5.0, 5.4 min. (A) Blank (B) injection 1 (C) injection 2.

Prior to investigation of the aminoglycoside derivatization by fluorescamine, glucosamine (with only 1 amine group) was tested as a simple model. The HPLC chromatogram of glucosamine-fluorescamine derivative showed three peaks as in Figure 3.59, probably due to the formation of several diastereoisomeric products. The peak area and peak height of each peak were not stable possibly due to derivatization influencing the proportions of the two anomers of glucosamine. However, at least the stereoisomers of glucosamine-fluorescamine derivatives were separated on the reversed phase C18 column under the chromatographic conditions described.

HR-ESI-MS of peak 1 (Figure 3.60), peak 2 (Figure 3.61) and peak 3 (Figure 3.62) all showed similar MS profiles with the expected m/z $[M+H]^+$ ion = 458.1451 (glucosamine-monofluorescamine derivative, $C_{23}H_{23}NO_9$, M.W. = 457.1373) and m/z $[M+Na]^+$ ion ($C_{23}H_{23}NNaO_9$) = 480 and a probable $[M+H-H_2O]^+$ at m/z = 440.1345.

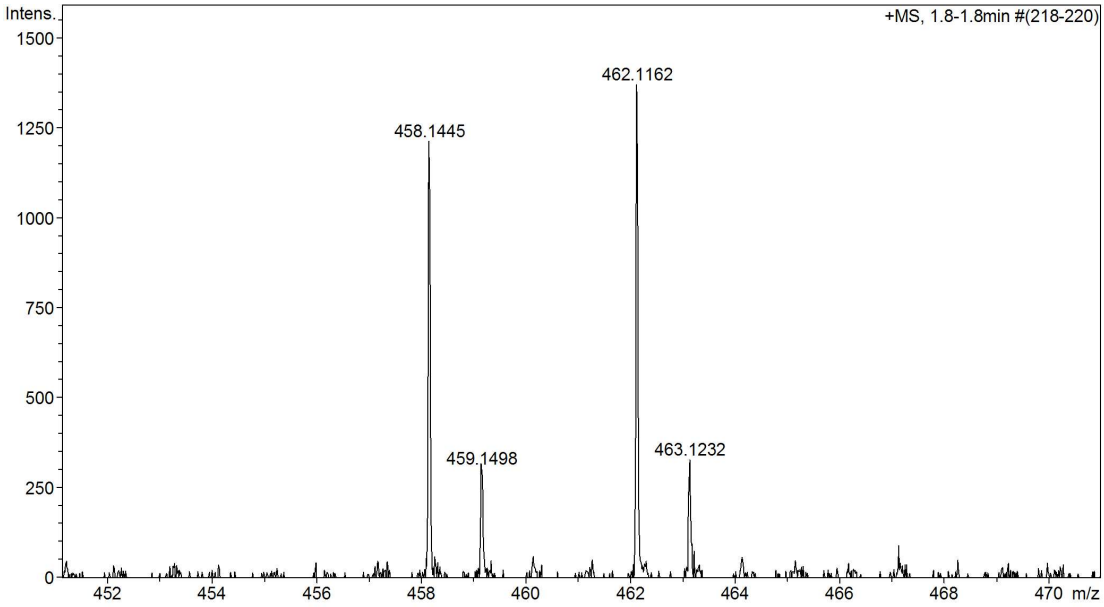

Figure 3.60 HR-ESI-MS of glucosamine-fluorescamine derivative ($C_{23}H_{23}NO_9$, M.W. = 457.1373) from peak 1 expected at m/z $[M+H]^+$ ion = 458.1451 (found = 458.1445), m/z $[M+Na]^+$ ion ($C_{23}H_{23}NNaO_9$) = 480.1249 and $[M+H-H_2O]^+$ at m/z = 440.1345.

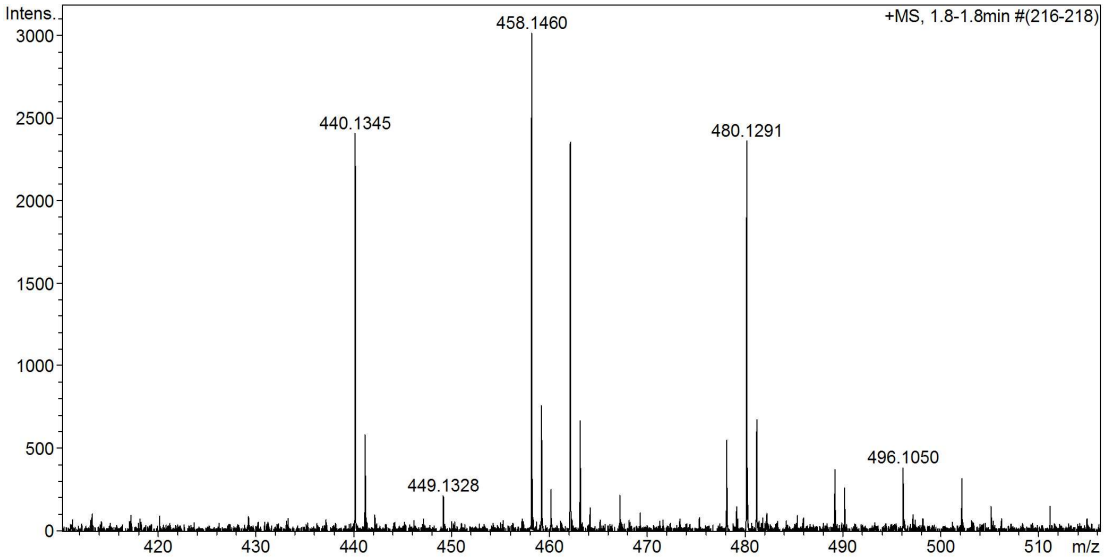

Figure 3.61 HR-ESI-MS of glucosamine-fluorescamine derivative ($C_{23}H_{23}NO_9$, M.W. = 457.1373) from peak 2 expected at m/z $[M+H]^+$ ion = 458.1451 (found = 458.1460), m/z $[M+Na]^+$ ion ($C_{23}H_{23}NNaO_9$) = 480.1249 (found = 480.1291) and $[M+H-H_2O]^+$ at m/z = 440.1345 (found = 440.1345).

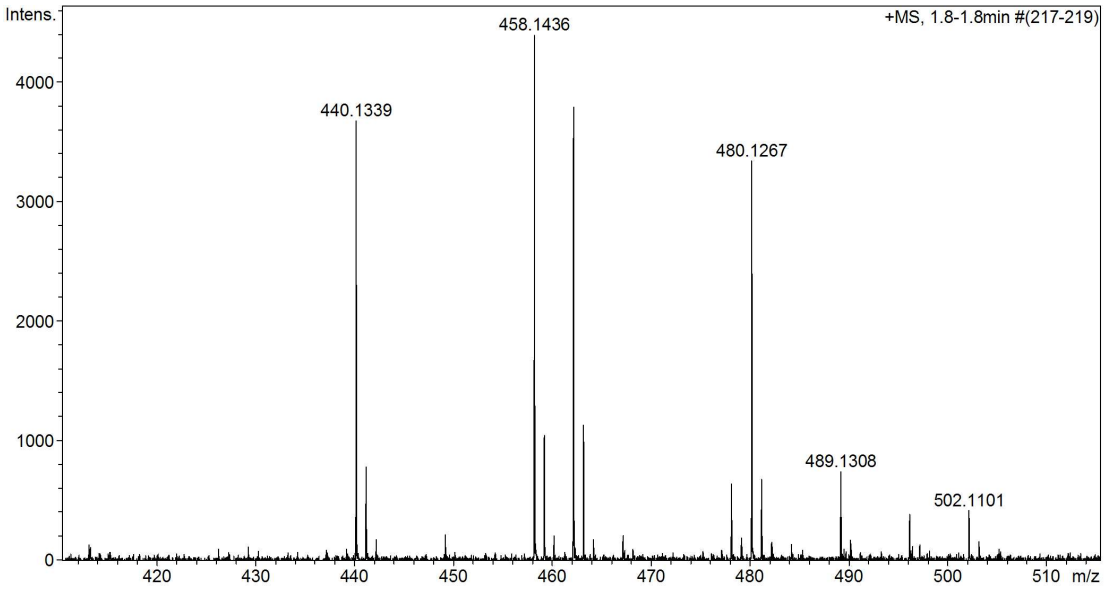

Figure 3.62 HR-ESI-MS of glucosamine-fluorescamine derivative ($C_{23}H_{23}NO_9$, M.W. = 457.1373) from peak 3 expected at m/z $[M+H]^+$ ion = 458.1451 (found = 458.1436), m/z $[M+Na]^+$ ion ($C_{23}H_{23}NNaO_9$) = 480.1249 (found = 480.1267) and $[M+H-H_2O]^+$ at m/z = 440.1345 (found = 440.1339).

Reaction of chiral non-fluorescent fluorescamine with a chiral amine begins by nucleophilic addition of the amine nitrogen to the C=C double bond of fluorescamine resulting in the breakage of a C-O bond and loss of fluorescamine's chiral centre (to yield the diketone). Closing the 5-membered ring by a second nucleophilic attack of the amine nitrogen on the benzoyl ketone forms a fluorescent product with two chiral centres (Figure 3.63).

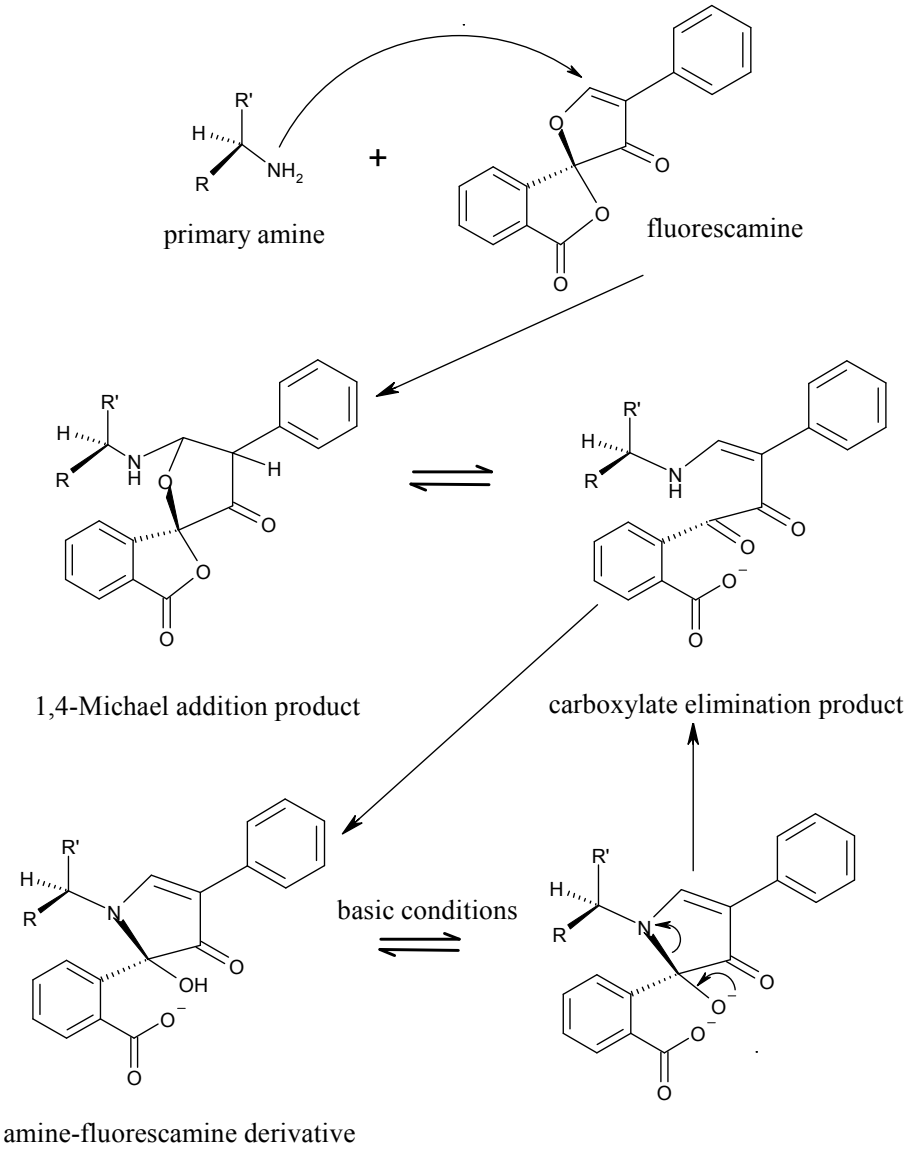

Figure 3.63 The reaction mechanism of the fluorescamine derivatization for amines.

As from Figure 3.63, fluorescamine itself is a chiral molecule so when it reacts with a non-chiral amine it will give rise to a pair of enantiomers. Glucosamine (Figure 3.64) is an example of a chiral molecule which when it reacts with fluorescamine generates two diastereoisomers. The existence of two anomeric forms of glucosamine will lead to the

formation of four diastereoisomeric products (Figure 3.65). From the HPLC chromatogram (Figure 3.59), the four diastereoisomeric products of glucosamine-monofluorescamine derivatives show just three peaks, where in one peak might be the combination of two diastereoisomers and these three peaks are not reproducible in the heights which is probably due to the changeable ratios of the four anomers.

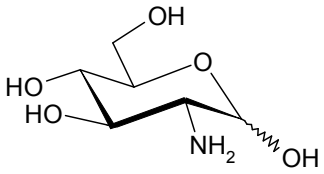

Figure 3.64 D-Glucosamine, $C_6H_{13}NO_5$.

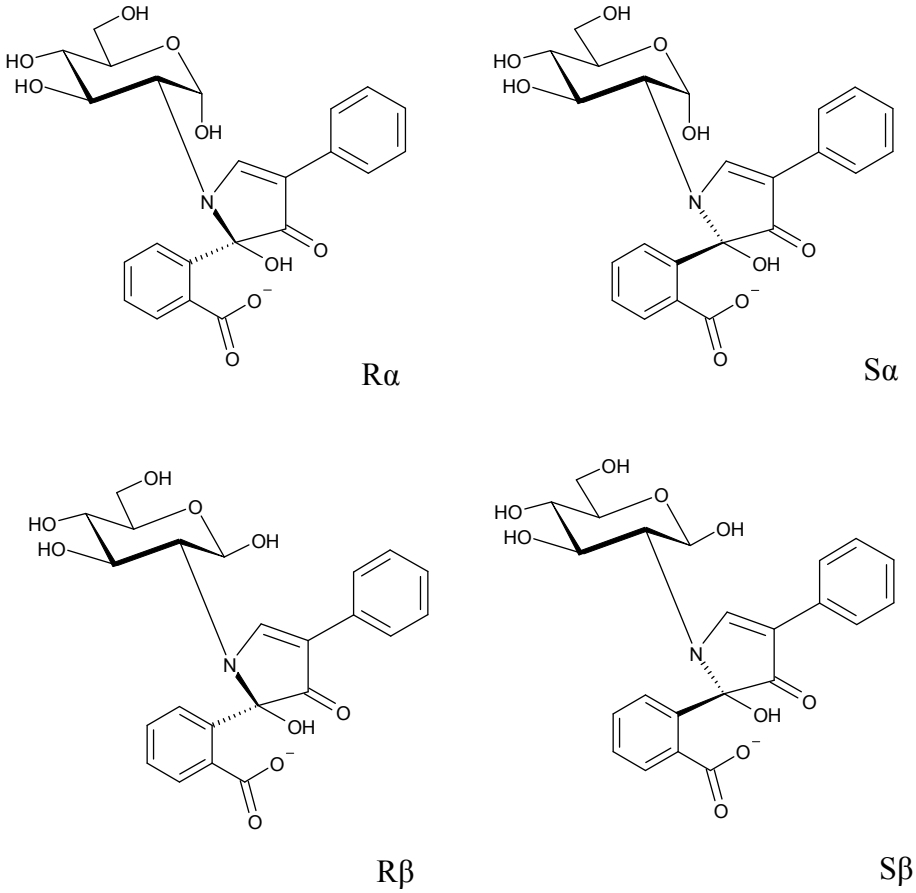

Figure 3.65 Structure of four fluorescent stereoisomers formed by the reaction of fluorescamine with glucosamine, where R and S relate to the chiral centre of fluorescamine, α and β relate to the anomeric centre of glucosamine.

Thus, the derivatization of the polyamine aminoglycoside with fluorescamine was not pursued due to the likelihood of highly complex stereochemical mixtures being produced.

Conclusions of *o*-phthalaldehyde-mercaptoethanol (OPA/MCE) derivatization

The reaction of *o*-phthalaldehyde (OPA) and 2-mercaptoethanol (MCE) selectively with primary amine gives a 1-alkylthio-2-alkylisoindole as the fluorogenic product. Investigating the derivatization of amines as amine-OPA/MCE, the reaction occurred in alkaline media (pH 8.3–10.5) and the optimized pH which gave fewer by-products was 10.5. By varying the composition of the OPA reagent in the reaction, it was demonstrated that the higher the concentration of MCE (SH-group additive), the lower the amount of the transformed product. Varying the mole ratios of the OPA/MCE from 1:1 to 1:17, it was shown that the optimum ratio of OPA/MCE was 1:10. At this ratio, when compared to other ratios at a strict reaction time, it gave the highest derivative product. However, at higher ratio than 1:10, the rate suppression was observed at high thiol concentration. This implied that the free OPA concentration favoured the transformation of the initially formed isoindole if the concentration of MCE is too much it might cause OPA-thiol adducts which decrease the free OPA concentration. Stability of derivatives prepared under the same conditions, proved to be associated with the chain length of the aliphatic amines: the longer the chain length the slower the decomposition of the total of derivatives formed. It is important in choosing optimum reaction times for the amine in question. In cases of aliphatic amines with number of C from 4 to 12, the optimum reaction time is 1 min, but for larger molecule with many amine groups such as aminoglycosides a reaction time required at 10 min. Thus, this suggested that the optimum reaction time need to be considered depend on the compound to be derivatized to obtain the maximum responses. The advantage of amine-OPA/MCE derivatization is the simplicity of derivatization method with rapid reaction, short analysis time, and no process of extraction. However, the drawback of OPA/MCE derivatization is the instability of the derivative.

Conclusions of fluorescamine derivatization

Fluorescamine is highly reactive with primary amines to produce fluorescent products, also fluorescamine and its hydrolysis products are non-fluorescent. This property makes a clean chromatographic separation. The results showed just one moiety of fluorescamine reacted with a diamine. Therefore, steric hindrance of the bulky fluorescamine molecule made difficulty to complete the reaction of fluorescamine with all the amine positions even in small aliphatic diamines. Also to be considered when using fluorescamine as the labelling reagent is that fluorescamine, itself is a chiral molecule, thus when it reacts with another chiral molecule, there is a greater chance of obtaining many peaks from one sample which will complicate its quantification.

CHAPTER 4: DERIVATIZATION OF PRIMARY AND SECONDARY AMINES WITH 9-FLUORENYLMETHYL-CHLOROFORMATE (FMOC Cl)

9-Fluorenylmethyl chloroformate (FMOC Cl) reacts with primary and secondary amines (Carpino and Han, 1970, 1972; Koole *et al.*, 1989) under alkaline conditions to form derivatives (Figure 4.1). FMOC Cl forms derivatives with amines in a short reaction time in buffered aqueous solution at room temperature to yield stable derivatives, so it is useful for analytical purposes (Moye and Boning, 1979). The FMOC Cl was originally introduced into analytical practice (Einarsson *et al.*, 1983) as a fluorescent label in amino acid analysis. Unfortunately, when a portion of the derivatization mixture was injected directly after the reaction, many interference peaks resulted. This was expected, because FMOC Cl reagent remained after the reaction and its hydrolytic by-products (Figure 4.2) have almost identical excitation and emission spectra (Lopez, 1996; Varady *et al.*, 2000).

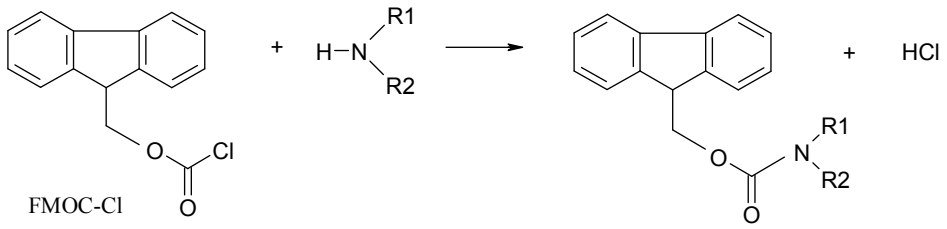

Figure 4.1 Reaction of FMOC Cl with an amine.

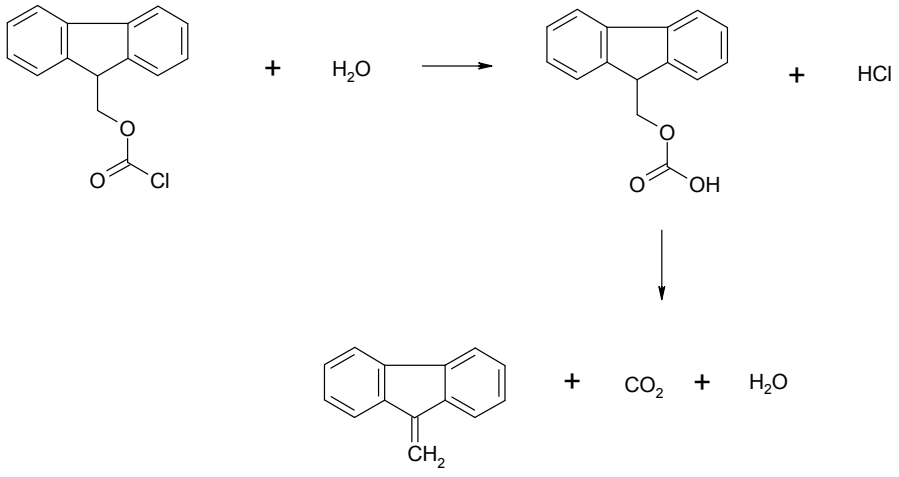

Figure 4.2 Hydrolysis reaction of FMOC Cl.

FMOC Cl, its derivatives and its cleavage products are strong chromophores absorbing at λ_{max} = 264 nm which allow spectrophotometric analysis. FMOC Cl is one of the few

protecting groups for amines that is not cleaved under acidic conditions, but it is readily cleaved under mildly basic conditions *e.g.* using piperidine (Figure 4.3) (Bayermann *et al.*, 1990; Carpino *et al.*, 1990; Greene and Wuts, 1991). In a subsequent slower step, elimination generates dibenzofulvene, an unstable species that rapidly adds nucleophiles, and a carbamate residue, which then decomposes with loss of carbon dioxide to release the free amine. However, this deprotection method employs a large excess of secondary amine (in this case, piperidine) in dimethylformamide (DMF). Use of piperidine/DMF is better suited to FMOC deprotections on solid-phase than in solution (Sheppeck II *et al.*, 2000).

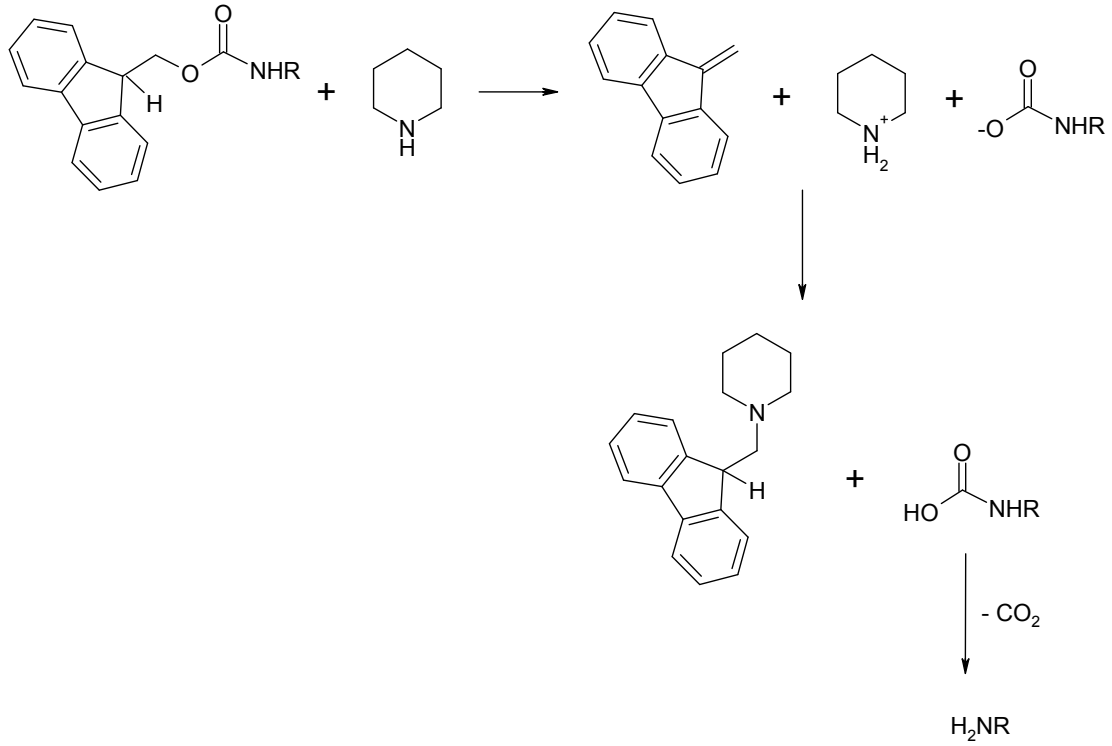

Figure 4.3 Deprotection of amine-FMOC by piperidine.

The derivatization reaction of FMOC Cl was optimized by using 1-butylamine and 1,5-diaminopentane solutions (1 mM in water) as the models for monoamine and diamine for various factors such as: the reaction time, FMOC Cl concentration, pH of the buffer and fluorescence spectrum. The HPLC chromatograms of blank-FMOC and 1-butylamine-monoFMOC (Figure 4.4) both show a peak of hydrolysis product of FMOC Cl reagent at Rt = 3.6 min. The HR-ESI-MS of 1-butylamine-monoFMOC (Figure 4.5) proved that the peak labelled 2 (Figure 4.4 (B)) is the desired molecule.

It has been reported that a reaction time of 1 min is sufficient for complete derivatization of amino acids with FMOC-C1 (Einarsson *et al.*, 1983) and other authors (Gustavsson and

Betner, 1990) reported that most amino acids were fully derivatized after 30 s. In this study, the reaction time was examined by allowing the derivatization to proceed for various times ranging from 1 to 60 min. The amine-FMOC derivative was formed within 1 min, but the optimum yield was obtained at 5 min after which the yields slightly decreased (Figure 4.6). The hydrolysis reaction of FMOC Cl also occurred which was observed as a small amount of precipitate and gave undesirable chromatographic peaks. These undesirable chromatographic peaks were observed when the reaction time was greater than 10 min and when a high concentration of FMOC Cl reagent was used.

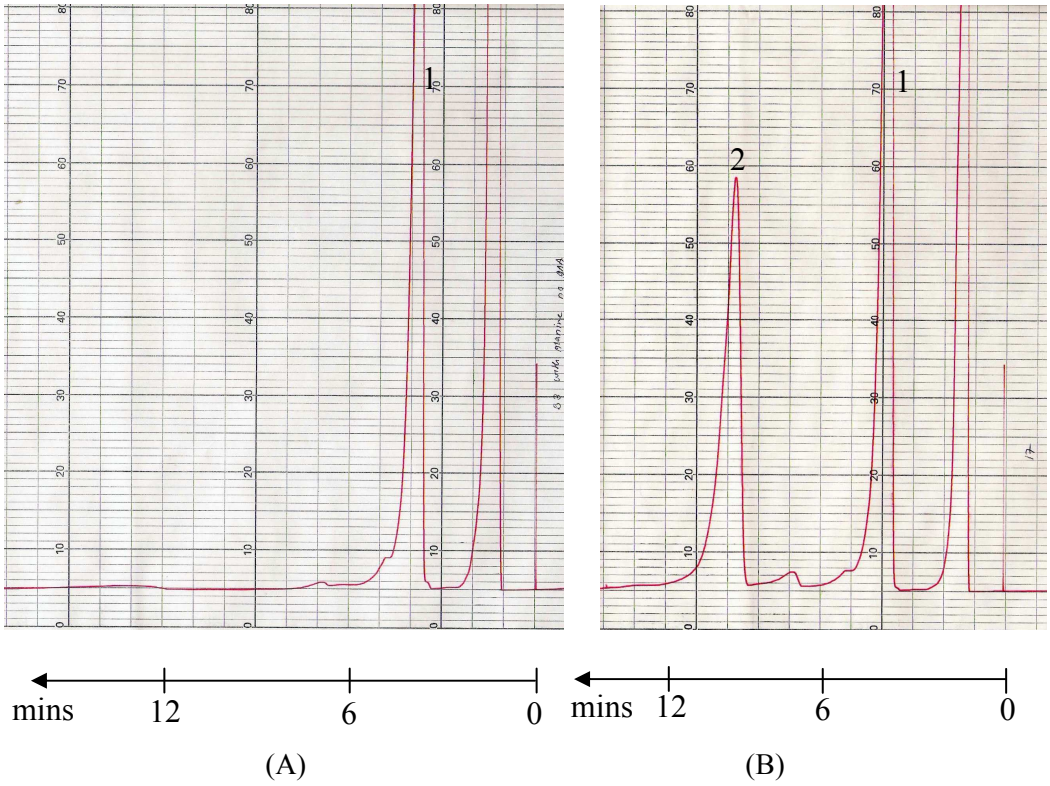

Figure 4.4 HPLC chromatogram of amine-FMOC derivatives, HPLC conditions: column: Phenomenex hypersil C18 5µ 150 x 4.60 mm, mobile phase is acetonitrile: Milli-Q-water (65:35) flow rate 1 mL/min, fluorescence detection at λ_{ex} = 264 nm, λ_{em} = 390 nm.
(A) Chromatogram of blank-FMOC shows the solvent front at Rt = 1.1 min, peak 1 = hydrolysis product of FMOC Cl reagent at Rt = 3.6 min.
(B) Chromatogram of 1-butylamine-monoFMOC shows the solvent front at Rt = 1.1 min, peak 1 = hydrolysis product of FMOC Cl reagent at Rt = 3.6 min, peak 2 = 1-butylamine-monoFMOC derivative at Rt = 8.9 min.

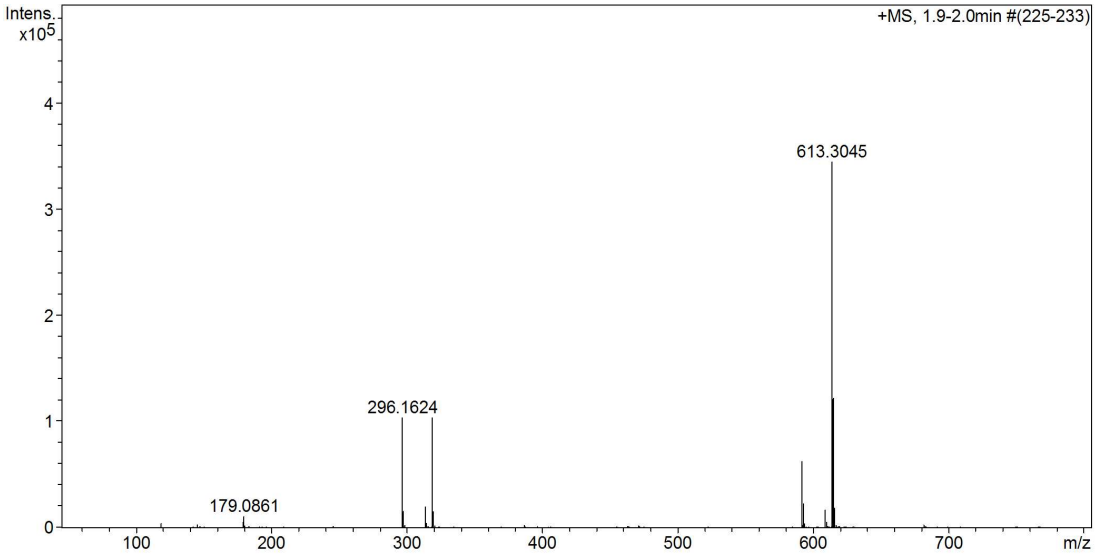

Figure 4.5 HR-ESI-MS spectra of 1-butylamine-monoFMOC derivative, (M.W. = 295.1572, $C_{19}H_{21}NO_2$) expected m/z $[M+H]^+$ ion = 296.1650 (found = 296.1624), [M+Na]+ ion m/z = 318.1469 and $[2M+Na]^+$ ion m/z = 613.3042 (found = 613.3045).

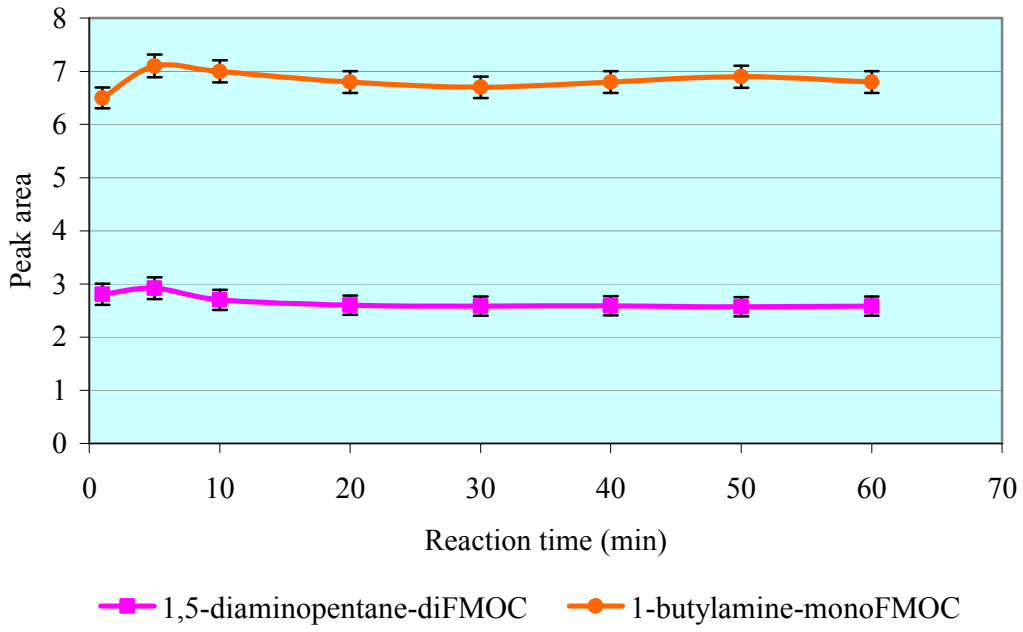

Figure 4.6 Effect of reaction time of 1-butylamine-mono FMOC derivative and 1,5-diaminopentane-di FMOC derivative. Both derivatives show the maximum yield at 5.0 min (n = 5). Peak areas were calculated by height x 0.5 width of peak, and peak areas are reported in cm^2.

Optimization of the concentration of FMOC Cl reagent

The influence of concentration of FMOC Cl reagent on the reaction yield was examined in the range of 1-10 mM by reacting with 1 mM of mono- and diamine samples. The optimum condition for 1, 5-diaminopentane-diFMOC derivative was gained when 4 mM FMOC Cl reagent reacted with 1 mM 1,5-diaminopentane. For 1 mM 1-butylamine, a stable peak area was observed from 2 mM FMOC Cl reagent (Figure 4.7). It was concluded that a 2-fold excess of FMOC is required to achieve complete reaction.

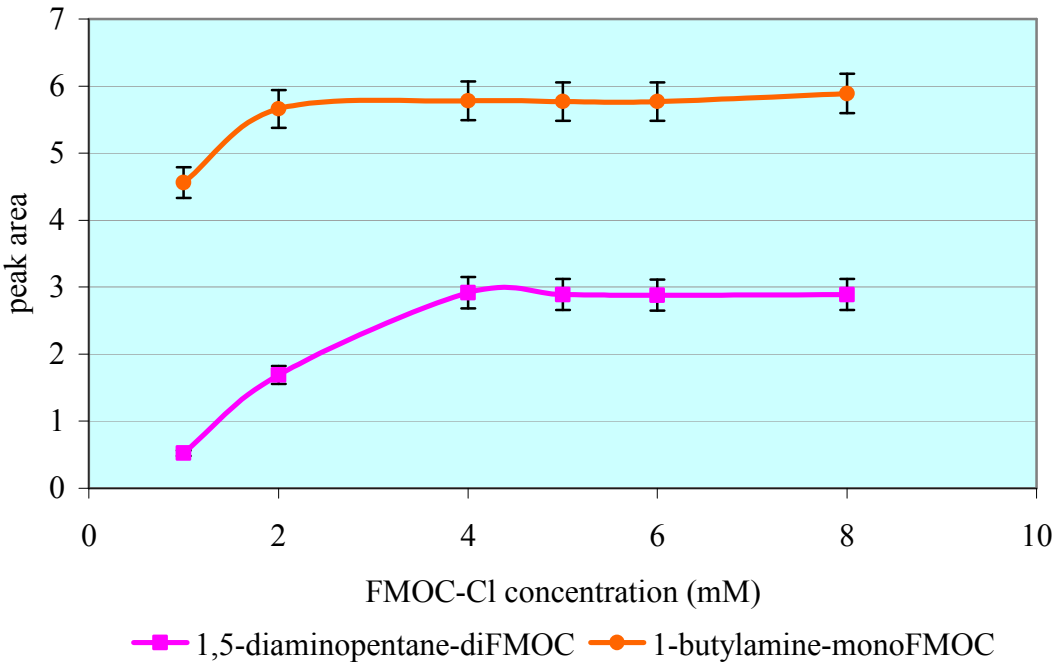

Figure 4.7 Effect of FMOC Cl reagent concentration (n = 5). Using 1 mM 1-butylamine, and 1 mM of 1,5-diaminopentane reacted with various concentration of FMOC Cl reagent. Peak areas were calculated by height x 0.5 width of peak, and peak areas are reported in cm^2.

Optimization for the effect of pH of the borate buffer

Since the reaction of FMOC Cl with amines is reported to occur better under alkaline condition (Price *et al.*, 1987; Gao *et al.*,1990; Tonin *et al.*, 1991) the optimization of the pH of the borate buffer was investigated. 1-Butylamine was used as the model compound for this study, using 200 mM borate buffer range of pH 4.0–10.5 for the reaction (Figure 4.8). The optimum reaction occurred at pH 9.0-10.5. In addition to the higher yield of 1-butylamine-monoFMOC derivative at higher pH there was also a reduction of multiple by-product peaks, most probably due to the hydrolysis of FMOC Cl reagent. The optimum pH of borate buffer at 9.5 was used for FMOC derivatization.

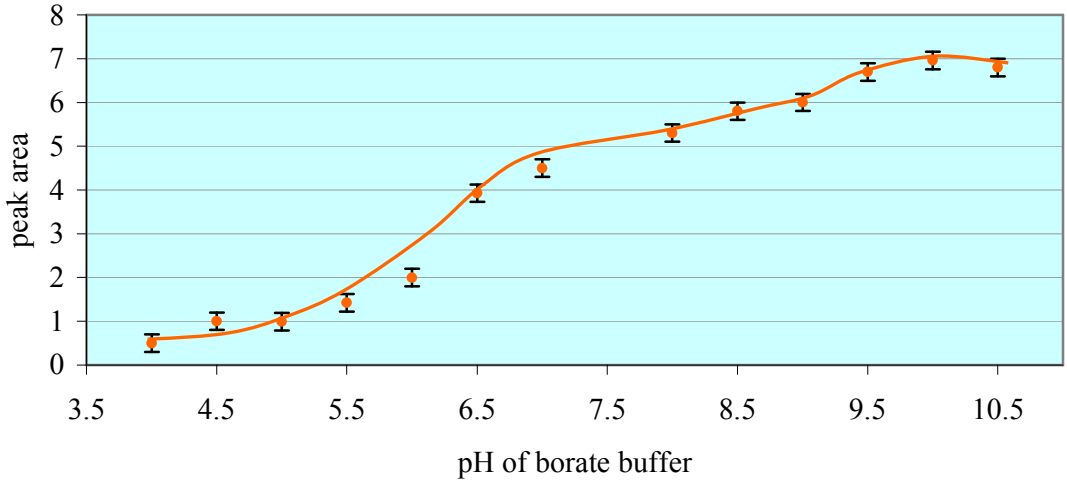

Figure 4.8 Effect of various pH of borate buffer on the 1-butylamine-monoFMOC derivative yield (n = 5). Peak areas were calculated by height x 0.5 width of peak, and peak areas are reported in cm^2.

Methods to terminate the reaction of FMOC Cl

The excess of FMOC Cl reagent reacts with water to form FMOC OH, which is also fluorescent and which may cause interference in the chromatogram. To overcome this problem, a modification of the pre-column derivatization with FMOC described by Price *et al.* (1987) was developed, based on the addition of aspartic acid to the reaction mixture. In their study, after the derivatization of polyamines, the excess of FMOC was reacted with aspartic acid to form an aspartic-FMOC derivative. This derivative distributed into the aqueous phase, while the hydrophobic FMOC-polyamines were extracted with pentane. The addition of aspartic acid did not affect the reaction yield and minimized the formation of FMOC-alcohol and reaction by-products. The reactions with different amines were examined by the other research groups using adamantanyl amine (Gustavsson and Betner, 1990), heptylamine (Kirschbaum and Lukkas, 1994), glycine (Stead and Richards, 1996).

In this study, three main methods of termination of the reaction and removal of the excess of FMOC Cl were investigated. In method 1, the excess of FMOC was removed by the reaction with alanine 100 mM, method 2 removes the excess of FMOC Cl by extraction of amine-FMOC derivatives with pentane after derivatization, and method 3 uses glacial acetic acid to stop the reaction at the desired time (Lopez *et al.*, 1996). In a series of experiments, these methods were evaluated alone and in combination against controls as shown in Table 4.1.

Table 4.1 Termination of FMOC Cl reaction experiments.

Experiment No.	Termination method		
	Addition of alanine	pH reduction with Glacial acetic acid	Extraction with pentane
1			
2	√		
3		√	
4	√	√	
5			√
6	√		√
7		√	√
8	√	√	√

Experiments 1 to 4 were done without extraction with pentane while experiments 5 to 8 used pentane for separation of the amine-FMOC derivatives as the last step. Experiment 1, 5 mM 1-butylamine reacts with FMOC Cl in alkaline environment without removal of the excess of FMOC reagent (Figure 4.9). In experiment 2, after 5 min of reaction time, the excess of FMOC reagent was removed by using alanine (Figure 4.9). In experiment 3, the reaction was stopped by the addition of glacial acetic acid. In experiment 4, alanine followed by glacial acetic acid was used to stop the reaction. Experiments 5, 6, 7 and 8 involved the extraction with pentane at the end of the reaction. Experiment 5 is equal to experiment 1, experiment 6 = experiment 2, experiment 7 = experiment 3 and experiment 8 = experiment 4, but with the extraction step as the last step before dilution of the sample and injection onto HPLC.

The HPLC chromatograms from each experiment above were obtained (Figures 4.9 and 4.10) and the peak areas of the desired product (n = 5) were compared as histograms (Figure 4.13). The identities of the hydrolysis product of FMOC peak at Rt = 5.3 min and the alanine-monoFMOC derivative peak at Rt = 1.2 min were confirmed by HR-ESI-MS (Figures 4.11 and 4.12).

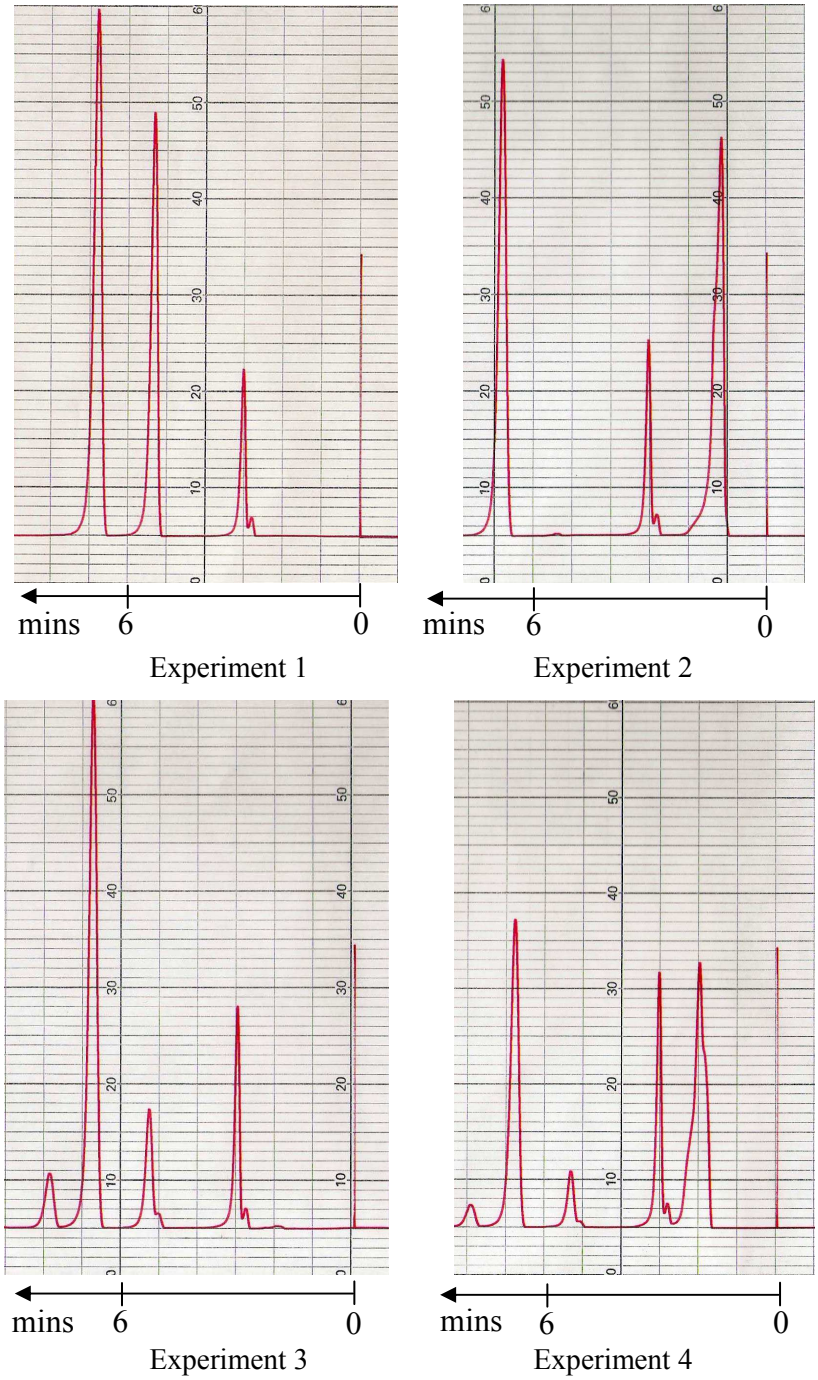

Figure 4.9 HPLC chromatogram of 1-butylamine-monoFMOC derivatives by different methods of stopping the reaction, HPLC conditions: column: Phenomenex hypersil C18 5µ 150 x 4.60 mm, mobile phase is acetonitrile: Milli-Q-water (70:30) with flow rate 1 mL/min, fluorescence detector x10 sensitivity at λ_{ex} = 264 nm, λ_{em} = 390 nm. Retention time of 1-butylamine-monoFMOC is 6.8 min. Experiment 1, the chromatogram shows the peaks at Rt = 3.0, 5.3, 6.8 min. Experiment 2, the chromatogram shows the peaks at Rt = 1.2, 3.0, 6.8 min. Experiment 3, the chromatogram shows the peaks at Rt = 3.0, 5.3, 6.8, 7.9 min. Experiment 4, the chromatogram shows the peaks at Rt = 2.0, 3.0, 5.3, 6.8 min.

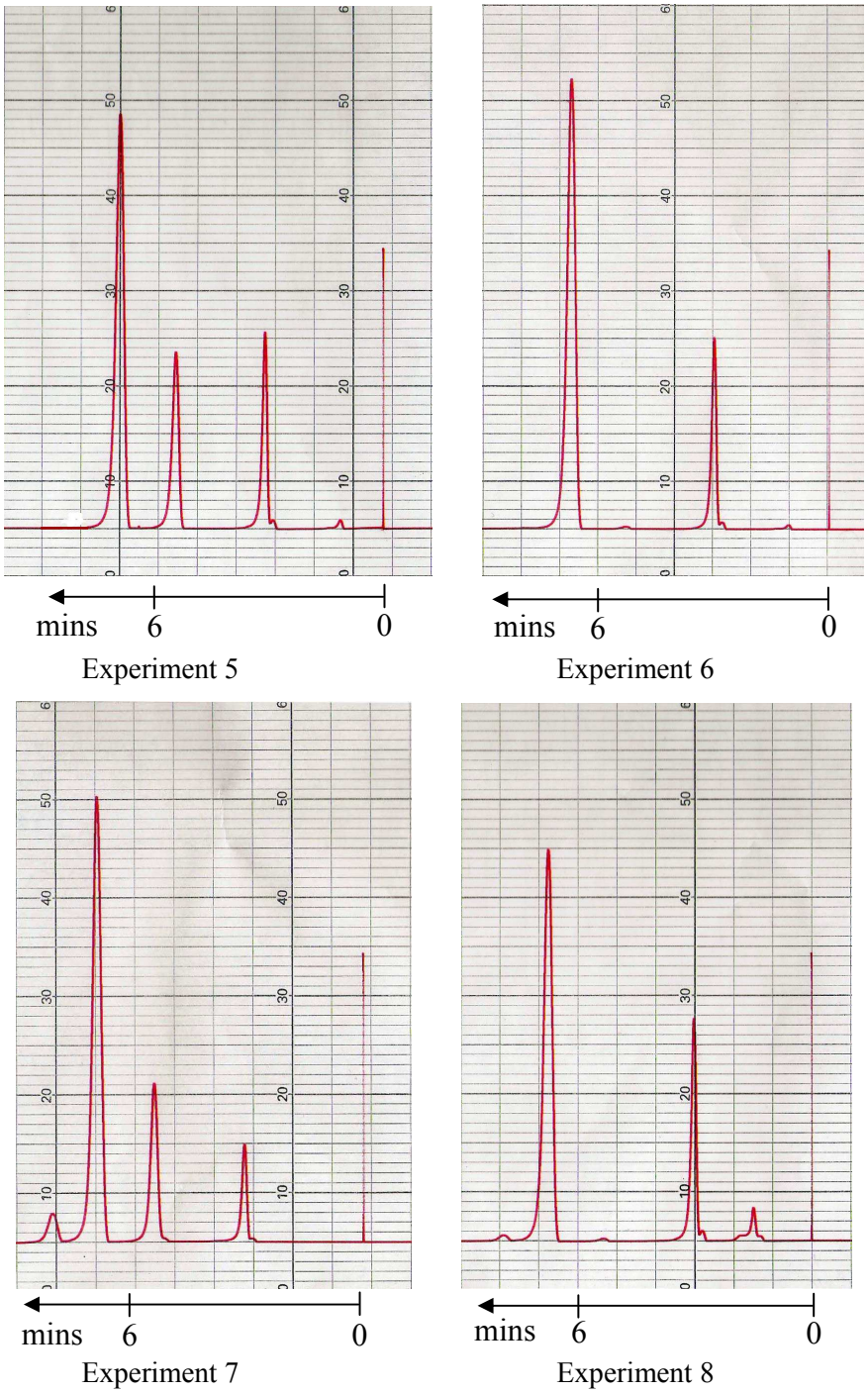

Figure 4.10 HPLC chromatogram of 1-butylamine-monoFMOC derivatives with different methods of stopping the reaction, HPLC conditions: column: Phenomenex hypersil C18 5µ 150 x 4.60 mm, mobile phase is acetonitrile: Milli-Q-water (70:30) with flow rate 1 mL/min, fluorescence detector x10 sensitivity at λ_{ex} = 264 nm, λ_{em} = 390 nm. Retention time of 1-butylamine-monoFMOC is 6.8 min. Experiment 5, the chromatogram shows the peaks at Rt = 3.0, 5.3, 6.8, 7.9 min. Experiment 6, the chromatogram shows the peaks at Rt = 1.2, 3.0, 6.8 min. Experiment 7, the chromatogram shows the peaks at Rt = 3.0, 5.3, 6.8, 7.9 min. Experiment 8, the chromatogram shows the peaks at Rt = 2.0, 3.0, 5.3, 6.8 min.

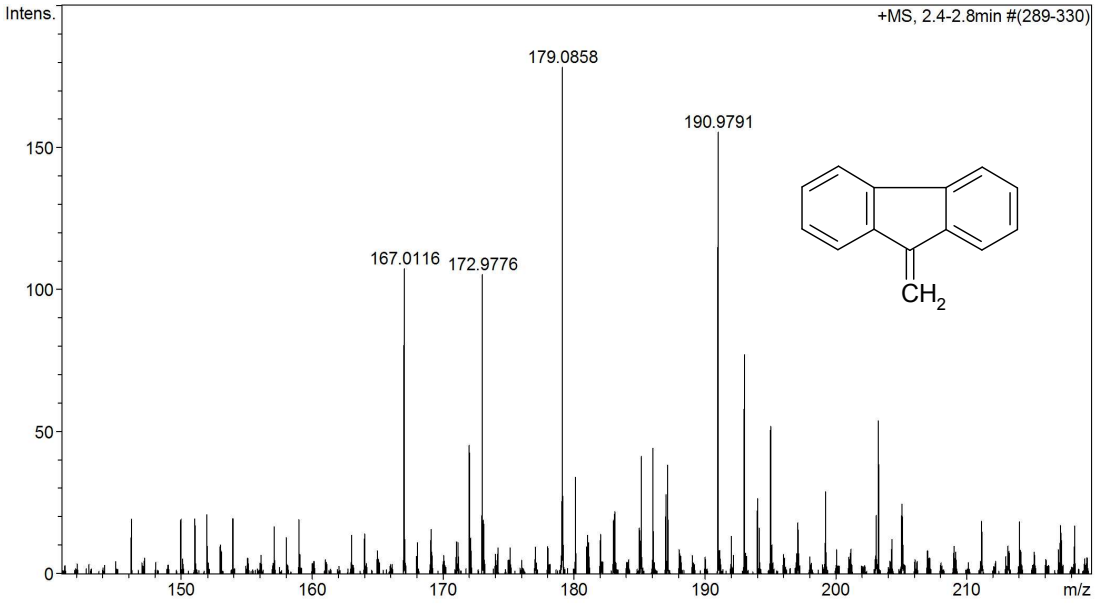

Figure 4.11 HR-ESI-MS spectrum of hydrolysis product of FMOC reagent, (M.W. = 178.0783, $C_{14}H_{10}$) expected m/z $[M+H]^+$ ion = 179.0861 (found = 179.0858).

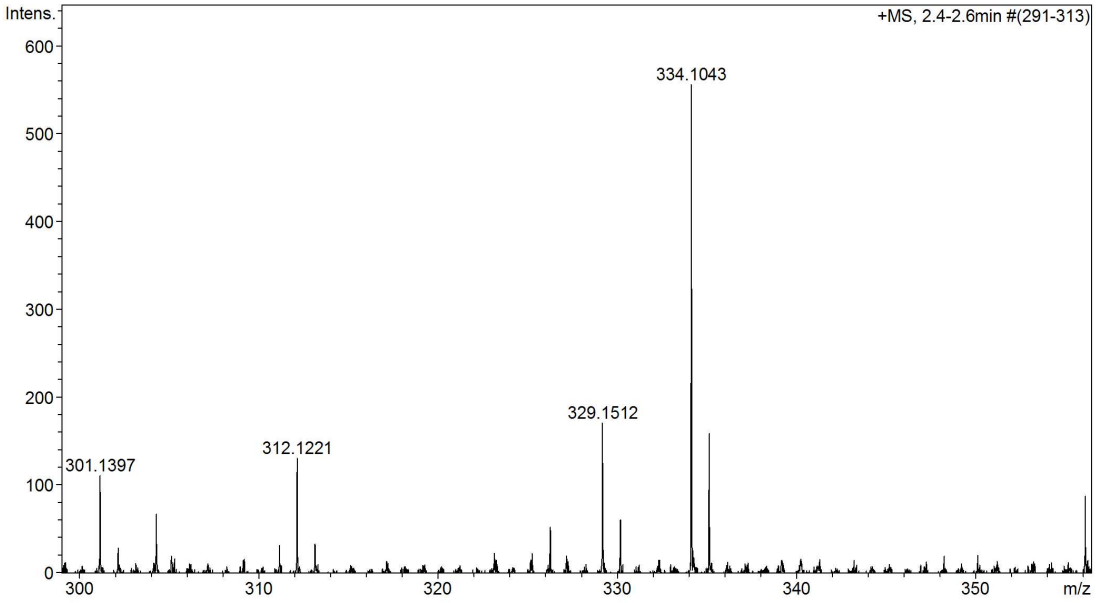

Figure 4.12 HR-ESI-MS spectrum of alanine-monoFMOC derivative, (M.W. = 311.1158, $C_{18}H_{17}NO_4$) expected m/z $[M+H]^+$ ion = 312.1236 (found = 312.1221) and $[M+ Na]^+$ ion m/z = 334.1055 (found = 334.1043).

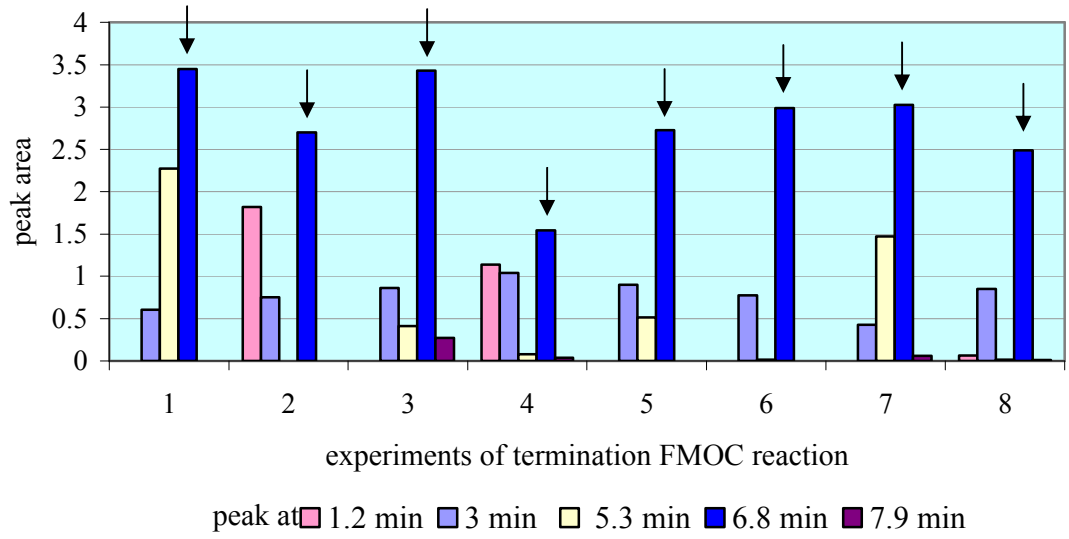

Figure 4.13 Comparison of 1-butylamine-monoFMOC derivatives' peak area obtained by different methods of terminating the reaction. The 1-butylamine-monoFMOC derivative is at Rt = 6.8 min (blue column). Peak areas were calculated by height x 0.5 width of peak, and peak areas are reported in cm^2.

The histogram (Figure 4.13) shows 1-butylamine-monoFMOC derivatives (bars marked with arrows). The chromatogram obtained from the direct injection after the derivatization (without the extraction) from Experiment 1 gave the highest peak area, but also showed a large peak area of hydrolysis product of FMOC Cl (Rt = 5.3 min). Experiment 2 gave a good chromatogram without the hydrolysis peak, but it showed the peak for alanine-monoFMOC derivative (Rt = 1.2 min). Using glacial acetic acid to stop the reaction, created one more interfering peak at Rt = 7.9 min. When both alanine and glacial acetic acid were used the 1-butylamine-monoFMOC derivative peak was decreased. The peak areas that were obtained from the extraction method seemed to be less than the non-extraction methods which might be due to incomplete extraction of amine-FMOC derivative. Experiment 6 gave the best chromatogram in terms of less interfering peaks and showed that the alanine-monoFMOC derivative was left in the aqueous phase after extraction with pentane. Thus, the method in which the reaction was terminated by alanine and the amine derivatives extracted with pentane was chosen for derivatization of various amines.

The amine-FMOC derivatives were separated by HPLC and the results from 5 replicates are shown in Table 4.2 using isocratic mobile phase of 70% acetonitrile: Milli-Q-water (Figure 4.14).

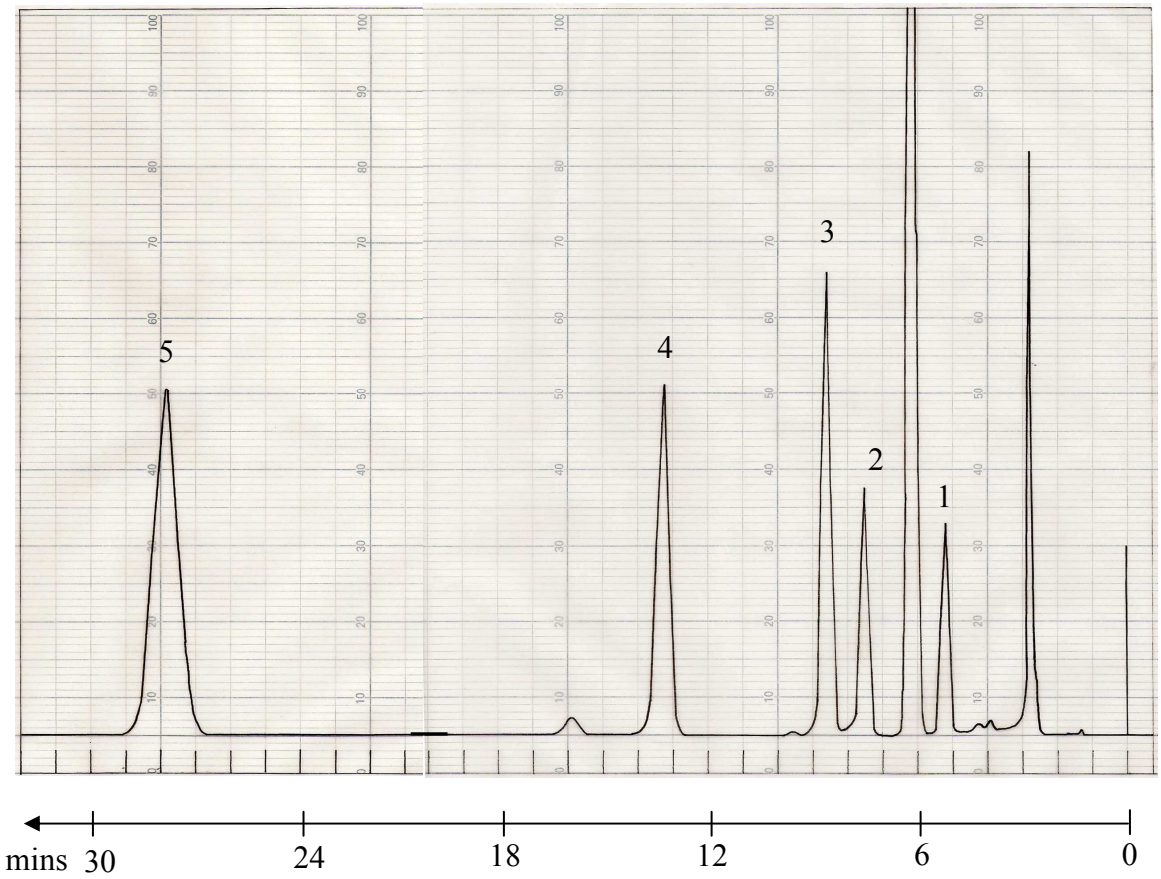

Figure 4.14 HPLC chromatogram of amines-FMOC derivatives, HPLC conditions: column: Phenomenex hypersil C18 5µ 150 x 4.60 mm, mobile phase is acetonitrile: Milli-Q-water (70:30) with flow rate 1 mL/min, fluorescence detector x10 sensitivity at λ_{ex} = 264 nm, λ_{em} = 390 nm. HPLC chromatogram of mixed amines-FMOC derivatives, 1 = 1-butylamine-monoFMOC, 2 = 1,4-diaminobutane-diFMOC, 3 = 1,5-diaminopentane-diFMOC, 4 = 1,7-diaminoheptane-diFMOC, 5 = spermidine-triFMOC.

Table 4.2 The calibration curves of various amine-FMOC derivatives.

Amine-FMOC derivatives	Rt (min)	Calibration curve equation	R^2
1-Butylamine-monoFMOC	5.3	y = 0.091x +0.34	0.986
Piperidine-monoFMOC	7.4	y = 0.019x – 0.01	0.990
Piperazine-diFMOC	13.5	y = 0.023x - 0.16	0.999
1,4-Diaminobutane-diFMOC	7.5	y = 0.054x + 0.41	0.995
1,5-Diaminopentane-diFMOC	8.6	y = 0.113x - 1.51	0.998
1,7-Diaminoheptane-diFMOC	13.0	y = 0.062x + 0.97	0.999
Spermidine-triFMOC	27.7	y = 0.109x – 0.66	0.998

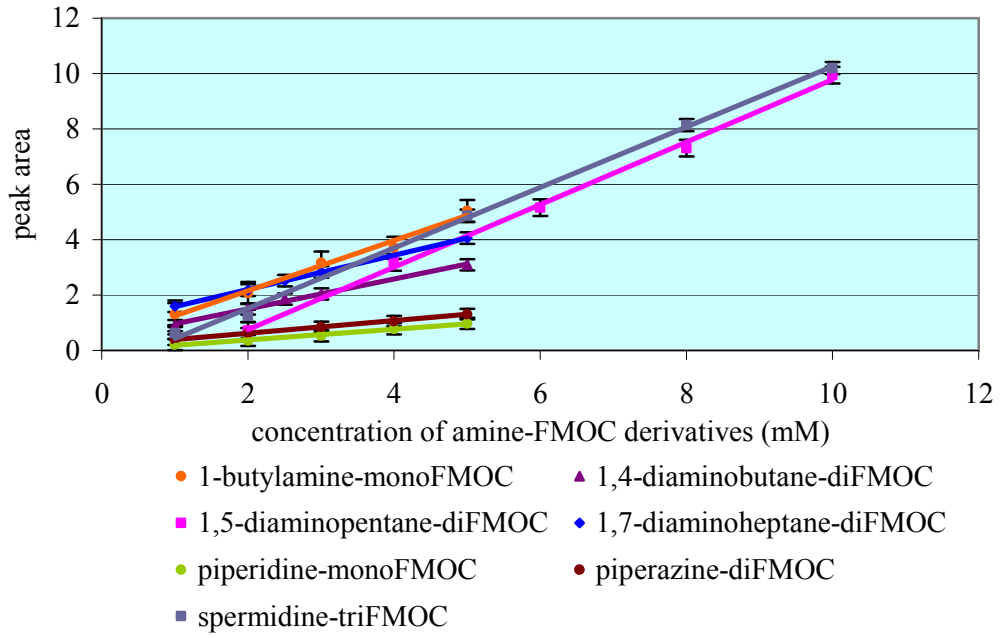

Figure 4.15 Calibration curves of amine-FMOC derivatives (n = 5). HPLC condition: column: Phenomenex hypersil C18 5µ 150 x 4.60 mm, mobile phase: acetonitrile: Milli-Q-water (70:30) flow rate 1 mL/min, fluorescence detection at λ_{ex} = 264 nm, λ_{em} = 390 nm. Peak areas were calculated by height x 0.5 width of peak, and peak areas are reported in cm^2.

The calibration curves of amine-FMOC derivatives showed linearity with correlation coefficients higher than 0.99 (Figure 4.15, Table 4.2).

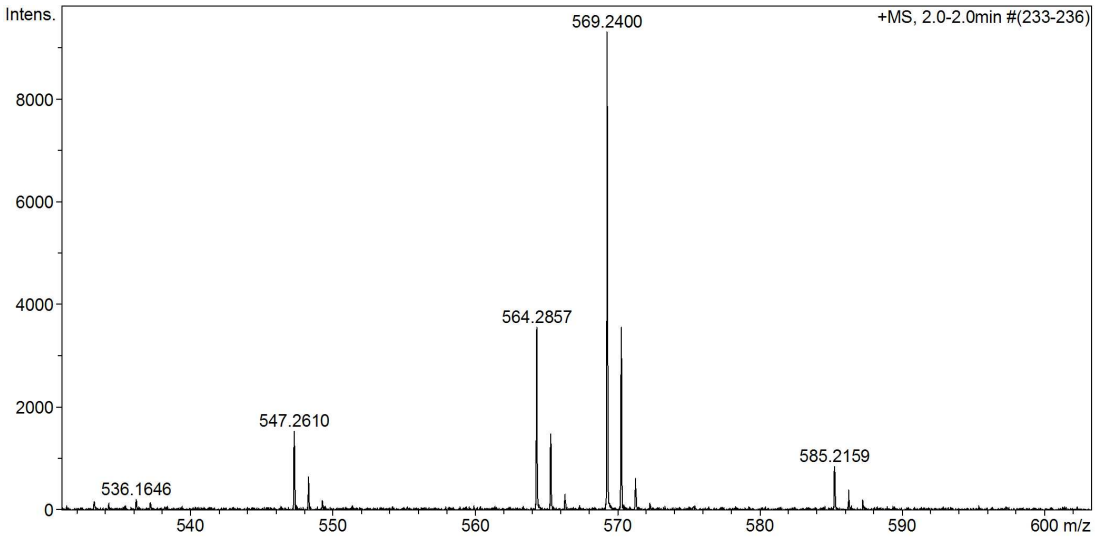

Figure 4.16 HR-ESI-MS spectrum of 1,5-diaminopentane-diFMOC derivative, (M.W. = 546.2519, $C_{35}H_{34}N_2O_4$) expected m/z $[M+H]^+$ ion = 547.2597 (found = 547.2610), $[M+ Na]^+$ ion m/z = 569.2416 (found = 569.2400) and $[M+K]^+$ ion m/z = 585.3502 (found 585.2159).

Peaks collected from the HPLC chromatogram were confirmed by HR-ESI-MS as the expected molecular mass for 1,5-diaminopentane-diFMOC derivative (Figure 4.16), 1,7-diaminoheptane-diFMOC derivative (Figure 4.17), piperidine-monoFMOC (Figure 4.18) and piperazine-diFMOC (Figure 4.19).

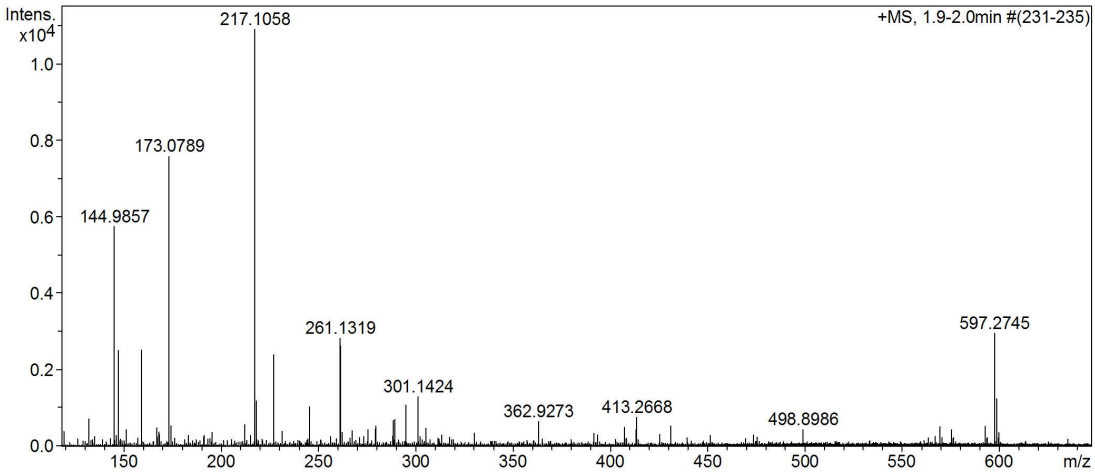

Figure 4.17 HR-ESI-MS spectrum of 1,7-diaminopentane-diFMOC derivative, (M.W. = 574.2832, $C_{37}H_{38}N_2O_4$) expected m/z $[M+H]^+$ ion = 575.2909 and $[M+ Na]^+$ ion m/z = 597.2729 (found = 597.2745).

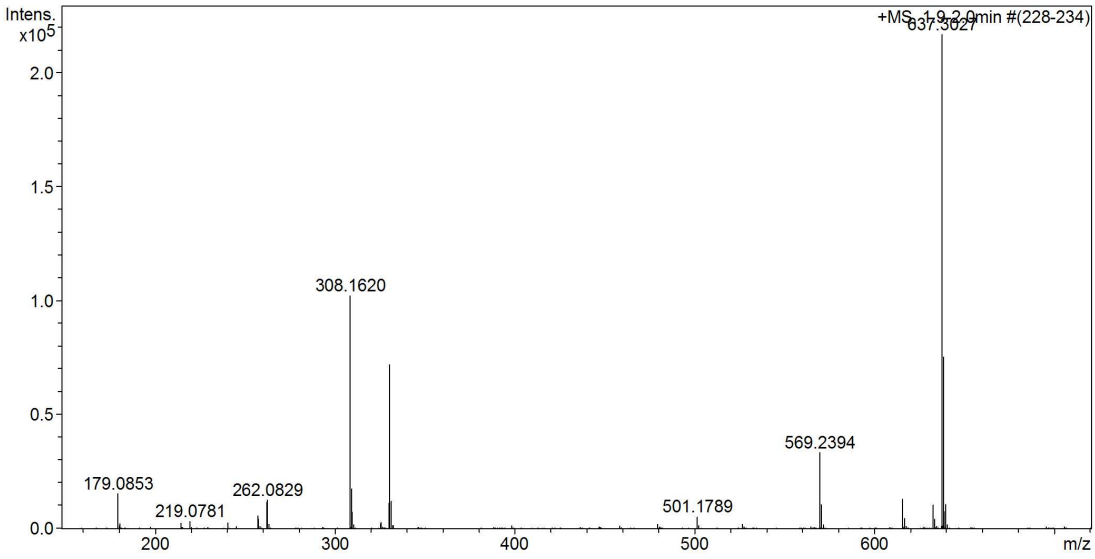

Figure 4.18 HR-ESI-MS spectrum of piperidine-monoFMOC derivative, (M.W. = 307.1572, $C_{20}H_{21}NO_2$) expected m/z $[M+H]^+$ ion = 308.1651 (found = 308.1620) $[M+ Na]^+$ ion m/z = 330.1470 and $[2M+Na]^+$ ion m/z = 637.3042 (found = 637.3027).

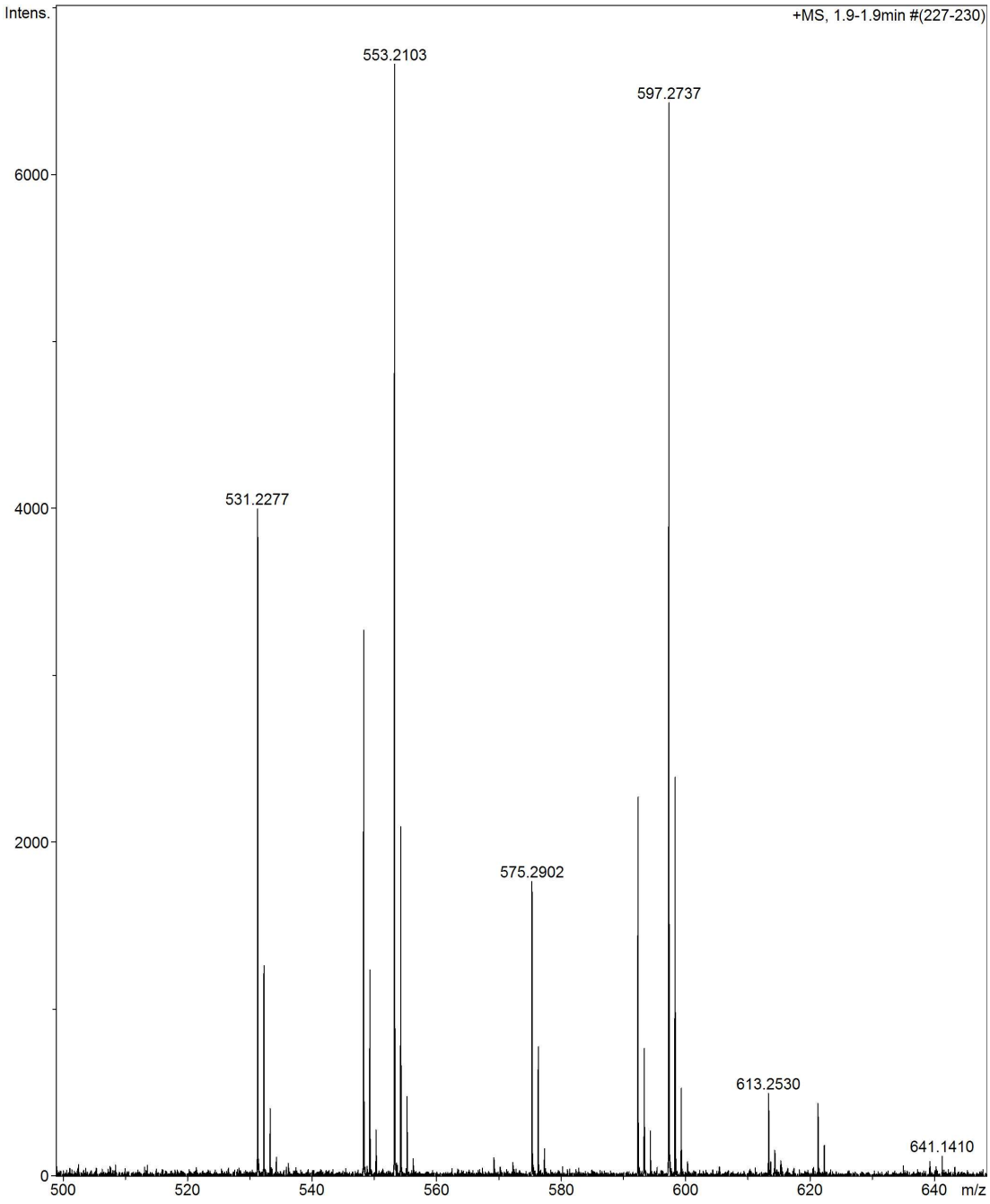

Figure 4.19 HR-ESI-MS spectrum of piperazine-diFMOC derivative, (M.W. = 530.2206, $C_{34}H_{30}N_2O_4$) expected m/z $[M+H]^+$ ion = 531.2284 (found = 531.2277) and $[M+ Na]^+$ ion m/z = 553.2103 (found = 553.2103).

The relative quantum yield of amine-FMOC derivatives was studied. A comparative analysis of fluorescence yields of the model series was obtained by collecting the elution product from HPLC and separate measurement by fluorescence spectrometer and UV/vis spectrophotometer. A plot of fluorescence intensity against absorbance (Figure 4.20) and the FI/UV equation (Table 4.3) was obtained.

Table 4.3 The FI/UV equation of amine-FMOC derivatives.

Amine-FMOC derivatives	FI/UV equation	R^2
Piperidine-monoFMOC	y = 43929x – 65.31	0.993
Piperazine-diFMOC	y = 20302x - 36.39	0.998
1,5-Diaminopentane-diFMOC	y = 34174x – 89.53	0.999
1,7-Diaminoheptane-diFMOC	y = 32370x + 29.09	0.995
Spermidine-triFMOC	y = 14246x – 91.96	0.997

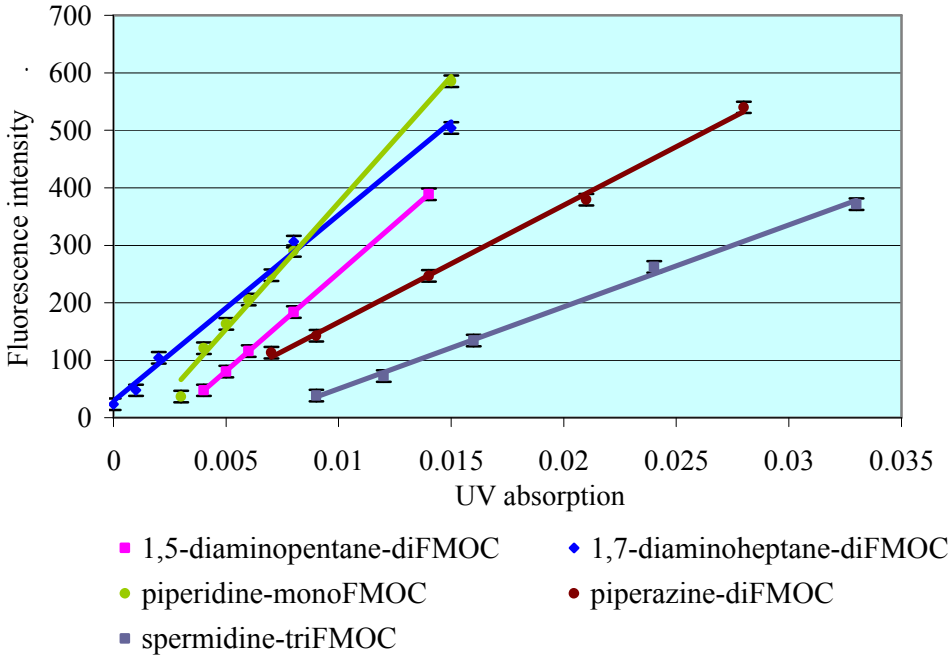

Figure 4.20 Fluorescence intensity against UV absorbance of amine-FMOC derivatives (n = 5). Peak areas were calculated by height x 0.5 width of peak, and peak areas are reported in cm^2.

The stability of the amine-FMOC derivatives was examined by using 1 mM of 1-butylamine as the model amine reacted with 4 mM FMOC Cl reagent for 5 min in the presence of borate buffer pH 9.5. The reaction was terminated by the addition of alanine and then extracted with pentane. The stability of the sample was monitored over the period 5 min after the reaction to 70 min. The peak area of the derivative remained constant for more than 70 min after the derivatization reaction had been stopped. Over a longer time scale, the 1-butylamine-monoFMOC derivative was stable for at least 5 days (the sample was kept at 20^{o}C, and could be stable for longer periods if the sample is stored in a fridge) then the peak area gradually decreased to 75% after 2 weeks (Figure 4.21).

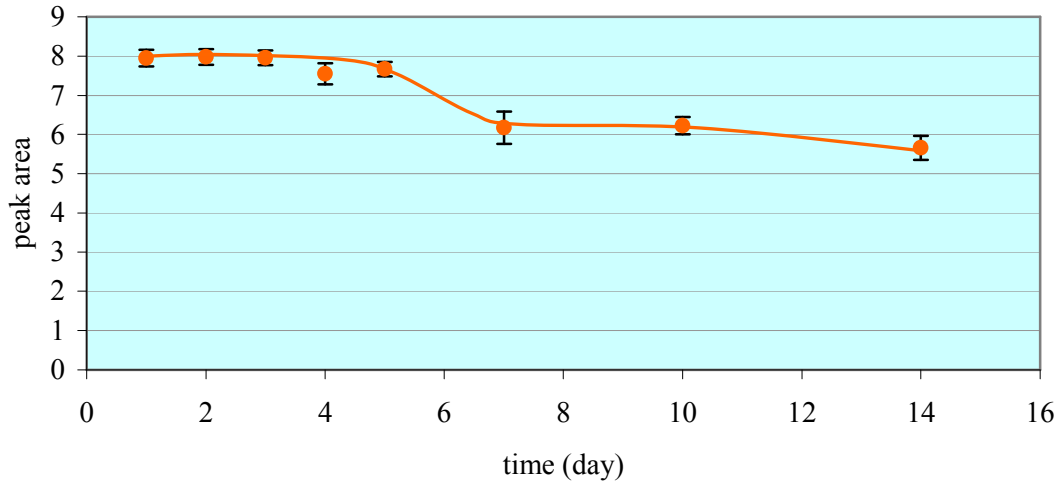

Figure 4.21 Stability of 1-butylamine-monoFMOC (n = 5). Peak areas were calculated by height x 0.5 width of peak, and peak areas are reported in cm^2.

Spermidine and spermine-FMOC derivatives

For biological polyamines spermidine and spermine, their derivatization requires larger quantities of reagent because of the presence the secondary amines. Moreover, in 70% acetonitrile: Milli-Q-water the retention time of spermidine-triFMOC derivative was 27.7 min and that of spermine-tetraFMOC derivative was likely to be even longer. With a mobile phase of acetonitrile: methanol: Milli-Q-water = 85:10:5, the retention time of 1,7-diaminoheptane-diFMOC derivative was 3.5 min and the retention times of spermidine-triFMOC derivative and spermine-tetraFMOC derivative were also shorter (Table 4.4). Calibration curves of both biological amines were obtained (Figure 4.22). HR-ESI-MS of spermidine-triFMOC derivative and spermine-tetraFMOC derivative were confirmed (Figures 4.23 and 4.24).

Table 4.4 Calibration curve equations of biological polyamine-FMOC derivatives, the condition of HPLC: column: Phenomenex hypersil C18 5µ 150 x 4.60 mm, mobile phase is acetonitrile: methanol: Milli-Q-water (85:10:5) with flow rate 1 mL/min, fluorescence detection at λ_{ex} = 264 nm, λ_{em} = 390 nm.

Amine-FMOC derivatives	Retention time	Calibration curve	R^2 (n = 5)
Spermidine	4.6 min	y = 17.85x – 0.088	0.999
Spermine	7.8 min	y = 23.43x - 0.125	0.999

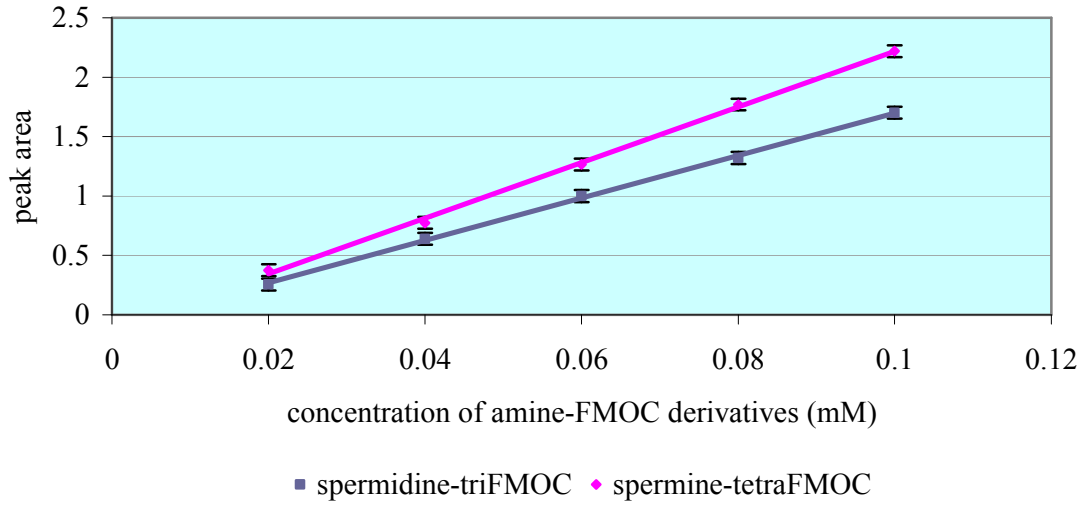

Figure 4.22 The calibration curve of polyamine-FMOC derivatives (n = 5). The HPLC conditions: column: Phenomenex hypersil C18 5µ 150 x 4.60 mm, mobile phase is acetonitrile: methanol: Milli-Q-water (85:10:5) flow rate 1 mL/min, fluorescence detection at λ_{ex} = 264 nm, λ_{em} = 390 nm. Peak areas were calculated by height x 0.5 width of peak, and peak areas are reported in cm^2.

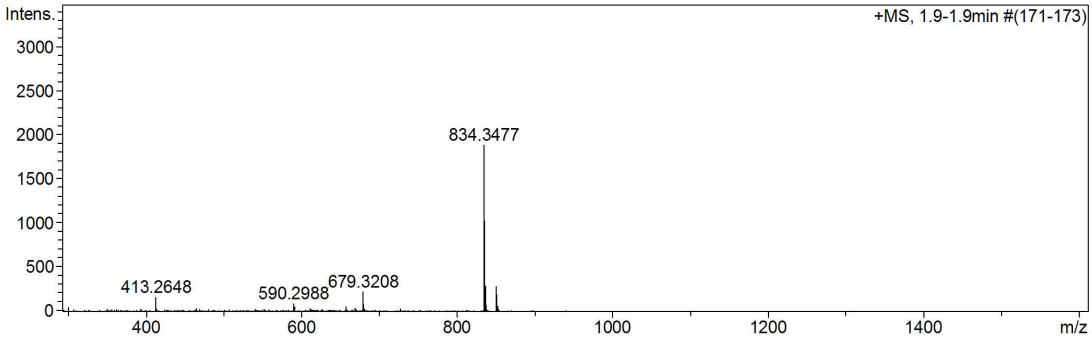

Figure 4.23 HR-ESI-MS spectrum of spermidine-triFMOC derivative, (M.W. = 811.3621, $C_{52}H_{49}N_3O_6$) expected m/z $[M+H]^+$ ion = 812.3699 and $[M+ Na]^+$ ion m/z = 834.3519 (found = 834.3477).

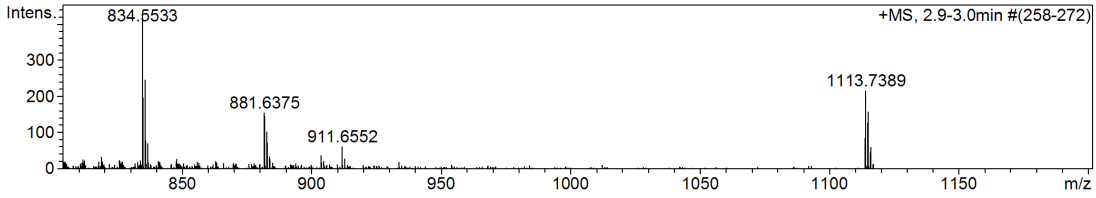

Figure 4.24 HR-ESI-MS spectra of spermine-tetraFMOC derivative, (M.W. = 1090.4881, $C_{70}H_{66}N_4O_8$) expected m/z $[M+H]^+$ ion = 1091.4959 and $[M+ Na]^+$ ion m/z = 1113.4778 (found = 1113.7389).

Analysis of spermidine and spermine as their hexahydropyrimidine derivatives.

Spermidine and spermine were converted into their respective hexahydropyrimidine ring derivatives by reaction with formaldehyde (Figures 4.25 and 4.26) then labelled with FMOC. As FMOC does not react with tertiary amines these amines were detectable with shorter retention time when compared with the authentic molecules (spermidine and spermine) due to smaller molecular weight after labelling with two moieties of FMOC (Figure 4.27).

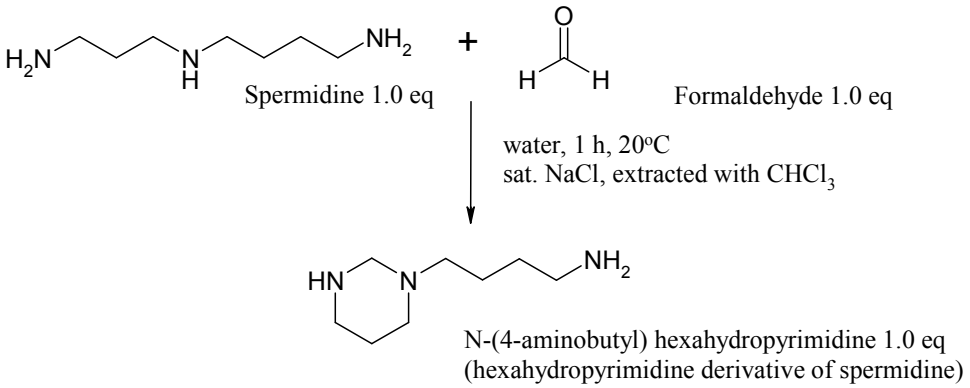

Figure 4.25 Reaction of spermidine with formaldehyde.

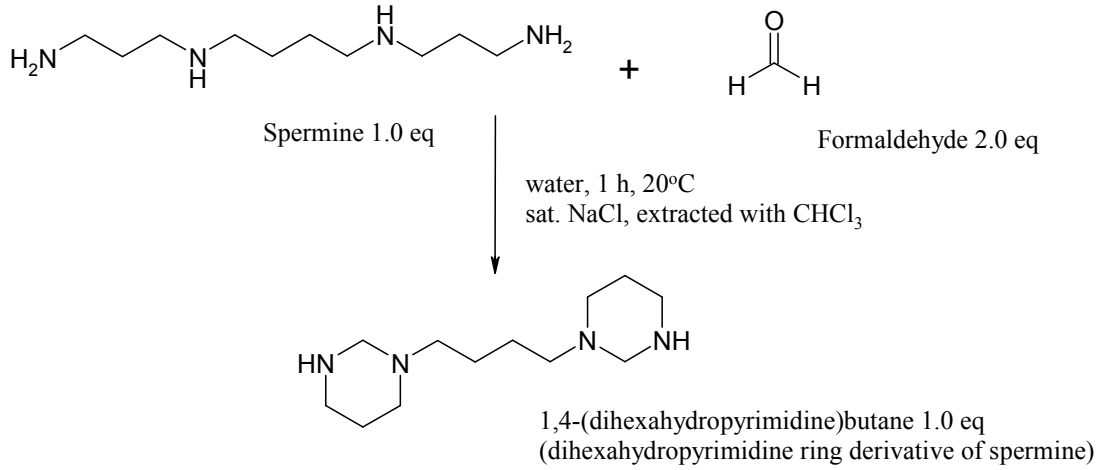

Figure 4.26 Reaction of spermine with formaldehyde.

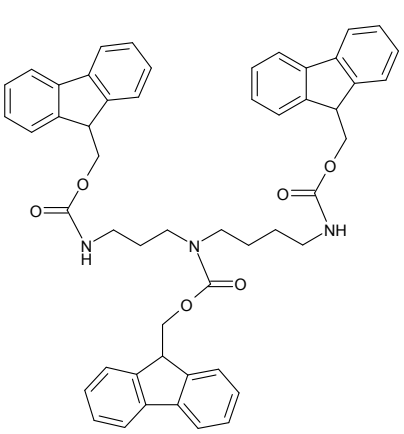

spermidine-triFMOC

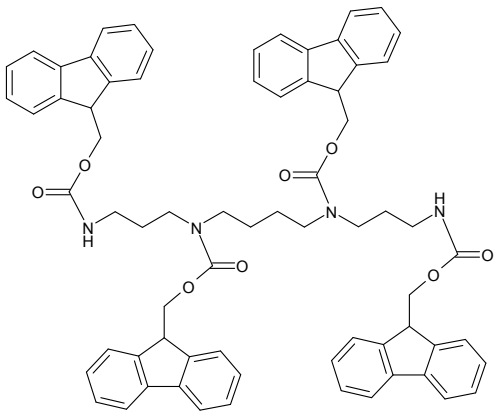

spermine-tetraFMOC

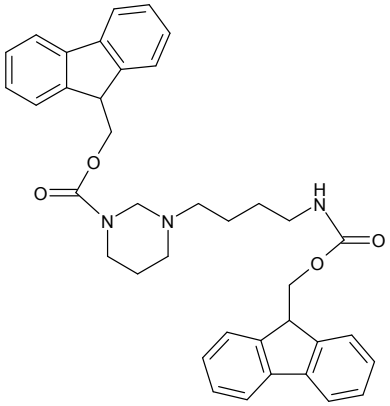

N-(4-Aminobutyl) hexahydropyrimidine-diFMOC

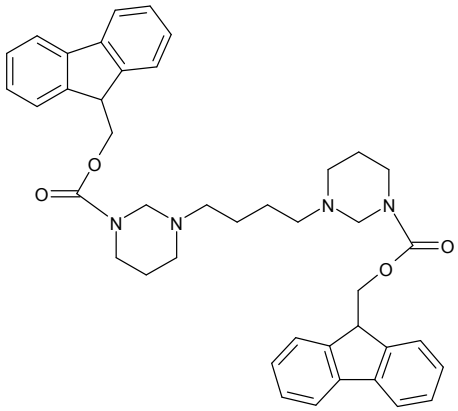

1,4-(Dihexahydropyrimidine)butane-diFMOC

Figure 4.27 Comparison of the FMOC derivatization products of spermidine, spermine, *N*-(4-Aminobutyl) hexahydropyrimidine and 1,4-(Dihexahydropyrimidine)butane.

Table 4.5 Retention time of biological polyamine-FMOC derivatives. HPLC conditions: column: Phenomenex hypersil C18 5µ 150 x 4.60 mm, mobile phase: acetonitrile: Milli-Q-water (70:30) flow rate 1 mL/min, fluorescence detection at λ_{ex} = 264 nm, λ_{em} = 390 nm.

Amine-FMOC derivatives	Retention time (min)
Spermidine-triFMOC	27.7
N-(4-Aminobutyl) hexahydropyrimidine-diFMOC	13.2
Spermine-tetraFMOC	59.0
1,4-(Dihexahydropyrimidine)butane-diFMOC	27.1

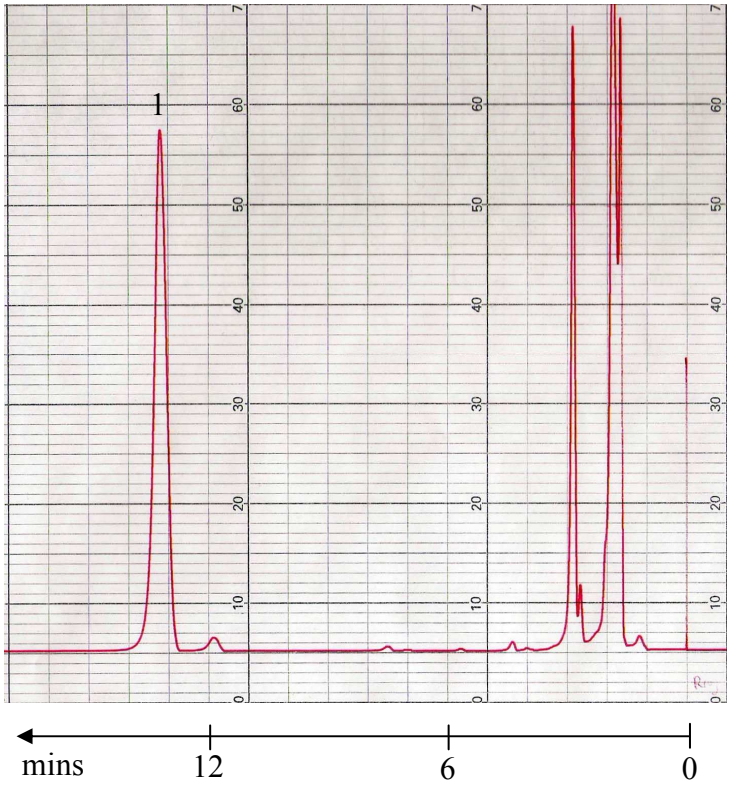

Figure 4.28 Chromatogram of *N*-(4-aminobutyl) hexahydropyrimidine-diFMOC derivative, HPLC conditions: column: Phenomenex hypersil C18 5µ 150 x 4.60 mm, mobile phase is acetonitrile: Milli-Q-water (70:30) flow rate 1 mL/min, fluorescence detection at λ_{ex} = 264 nm, λ_{em} = 390 nm, peak 1 = *N*-(4-aminobutyl) hexahydropyrimidine -diFMOC at Rt = 13.2 min.

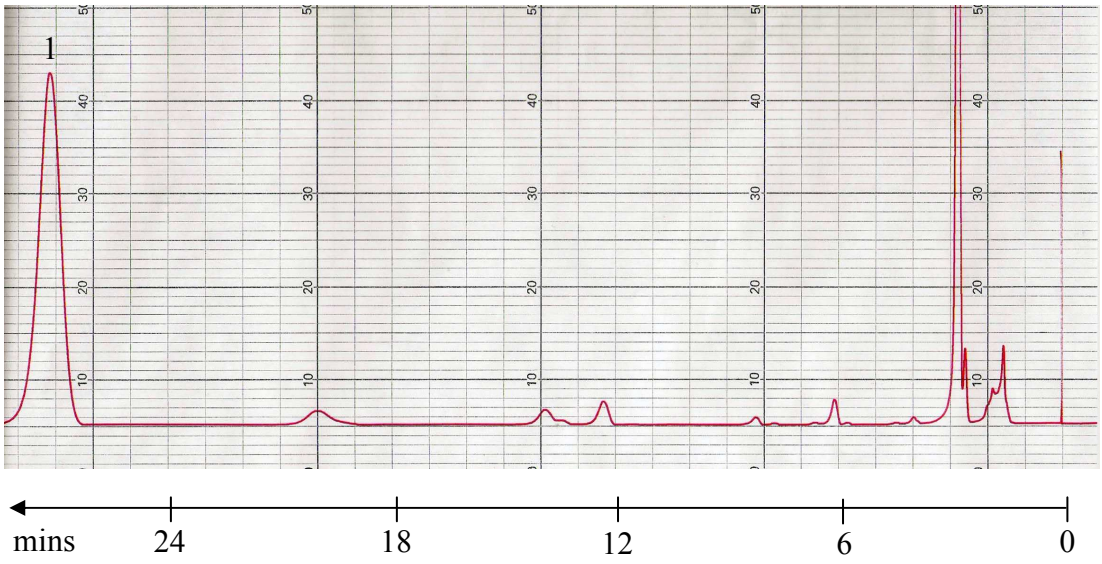

Figure 4.29 HPLC chromatogram of 1,4-(dihexahydropyrimidine)butane-diFMOC derivative, HPLC conditions: column: Phenomenex hypersil C18 5µ 150 x 4.60 mm, mobile phase is acetonitrile: Milli-Q-water (70:30) flow rate 1 mL/min, fluorescence detection at λ_{ex} = 264 nm, λ_{em} = 390 nm, peak 1 = 1,4-(dihexahydropyrimidine)butane-diFMOC at Rt = 27.1 min.

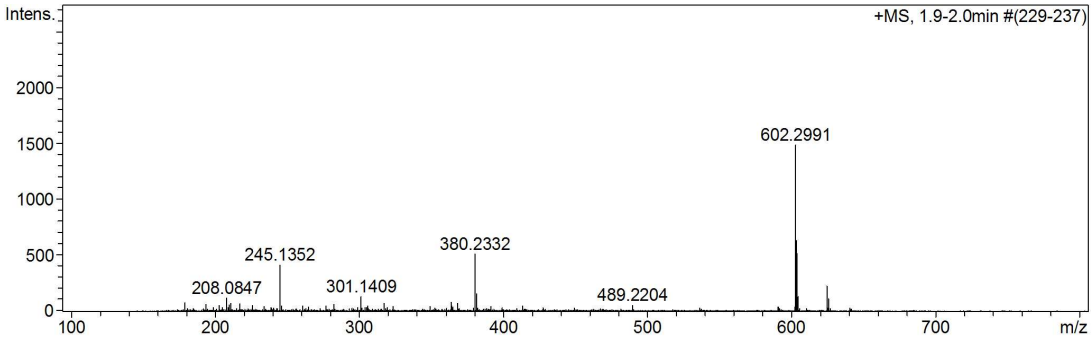

Figure 4.30 HR-ESI-MS spectrum of *N*-(4-aminobutyl) hexahydropyrimidine-diFMOC derivative, (M.W. = 601.2940, $C_{38}H_{39}N_3O_4$) expected m/z $[M+H]^+$ ion = 602.3019 (found = 602.2991) and $[M+ Na]^+$ ion m/z = 624.2838.

FMOC derivatives of spermidine, hexahydropyrimidine of spermidine, spermine and 1,4-(Dihexahydropyrimidine)butane were examined using a mobile phase of acetonitrile: Milli-Q-water (70:30) (Table 4.5, Figure 4.28, Figure 4.29). Molecular weight of *N*-(4-aminobutyl) hexahydropyrimidine-diFMOC was confirmed by HR-ESI-MS (Figure 4.30).

FMOC derivatives of non-viral gene therapy (NVGT) vectors

The FMOC derivatization method was applied to investigate three synthetic fatty acyl amides of spermine and confirmed the structures by HR-ESI-MS: 1,12-diphthalimido-4,9-diazadodecane (Figure 4.31, HPLC chromatograms is Figures 4.32 and HR-ESI-MS is Figure 4.33), N^4,N^9-didecanoyl spermine (Figures 4.34 and 4.35) and N^4,N^9-didodecanoyl spermine (Figures 4.36 and 4.37). These C10 and C12 conjugates are experimental non-viral vectors for DNA condensation with potential in gene delivery and therefore in non-viral gene therapy (NVGT).

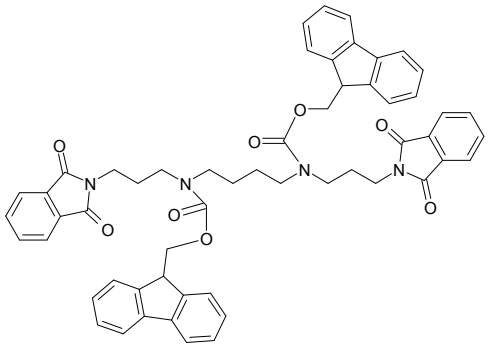

Figure 4.31 1,12-Diphthalimido-4,9-diazadodecane-diFMOC derivative.

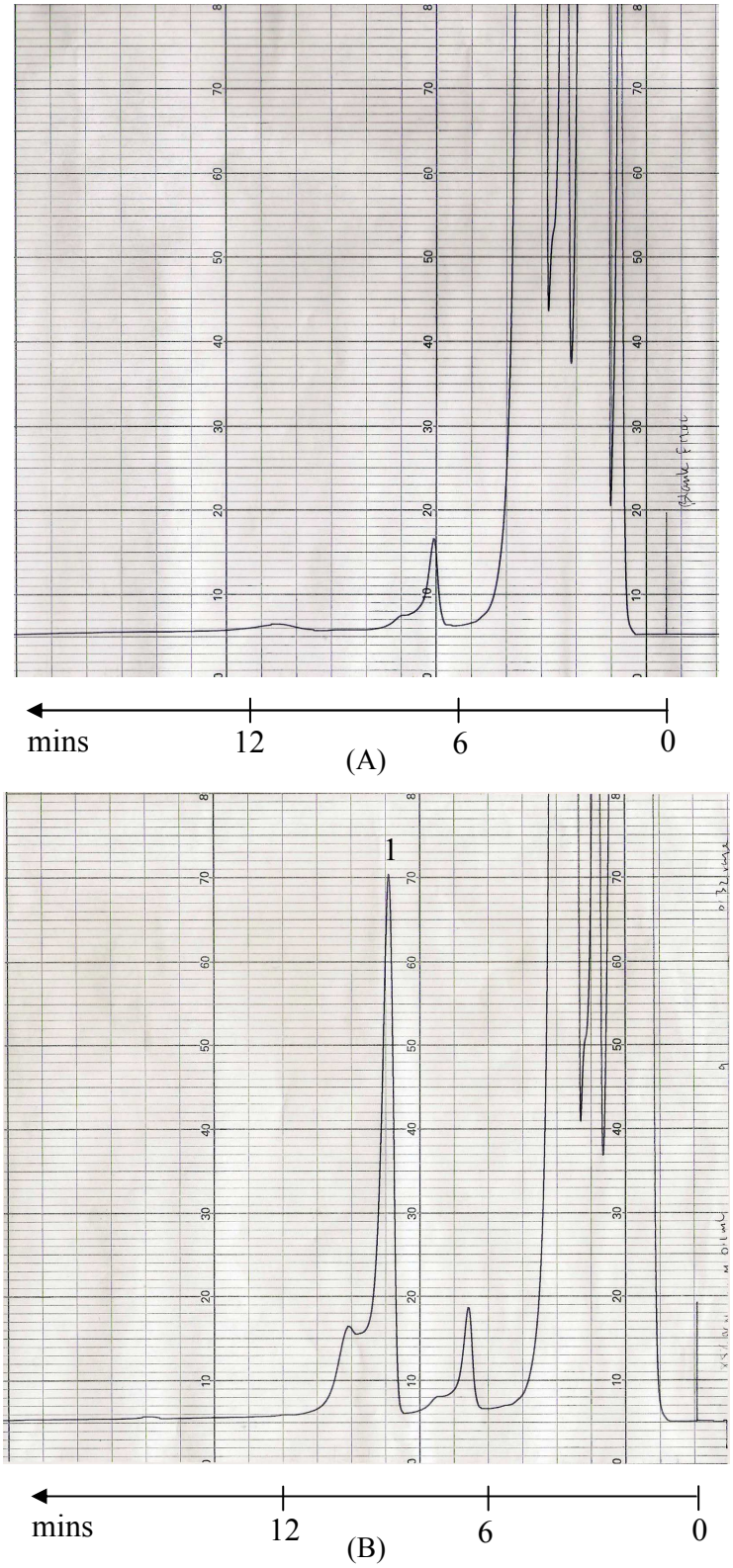

Figure 4.32 HPLC chromatogram of 1,12-diphthalimido-4,9-diazadodecane-diFMOC derivative, HPLC conditions: column: Phenomenex hypersil C18 5µ 150 x 4.60 mm, mobile phase is acetonitrile: Milli-Q-water (85:15) flow rate 1 mL/min, fluorescence detector x10 sensitivity at λ_{ex} = 264 nm, λ_{em} = 390 nm, (A) blank chromatogram (B) peak 1 = 1,12-diphthalimido-4,9-diazadodecane-diFMOC derivative at Rt = 9.1 min.

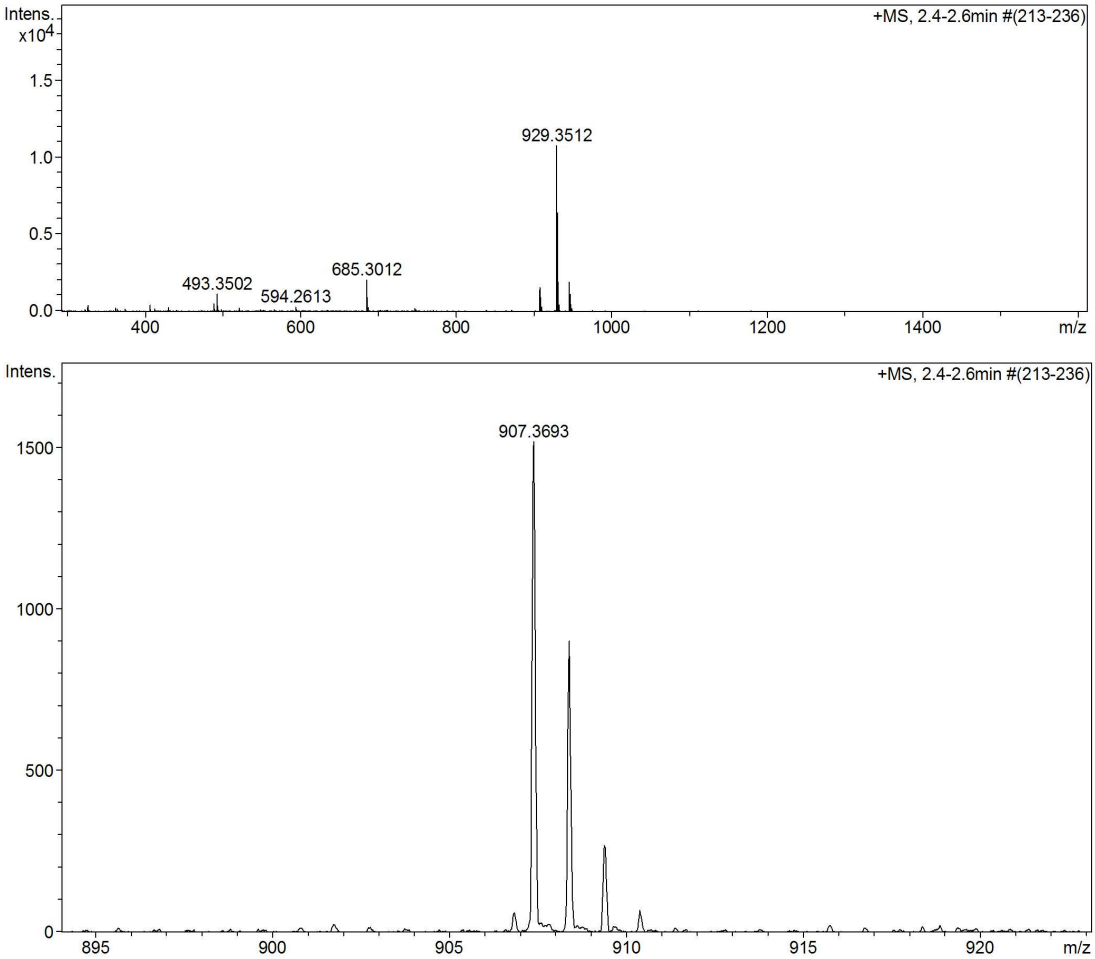

Figure 4.33 HR-ESI-MS spectra of 1,12-diphthalimido-4,9-diazadodecane-diFMOC derivative, (M.W. = 906.3629, $C_{56}H_{50}N_4O_8$) expected m/z $[M+H]^+$ ion = 907.3707 (found = 907.3693) and $[M+ Na]^+$ ion m/z = 929.3526 (found = 929.3512).

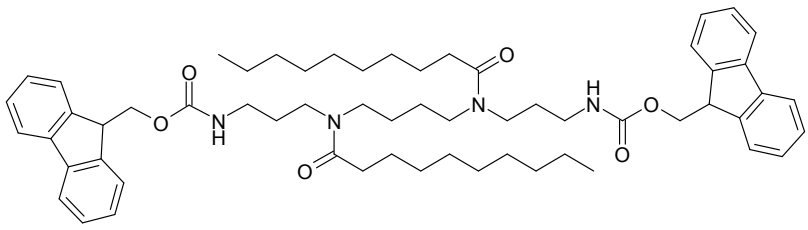

Figure 4.34 N^4,N^9-Didecanoyl spermine-diFMOC derivative.

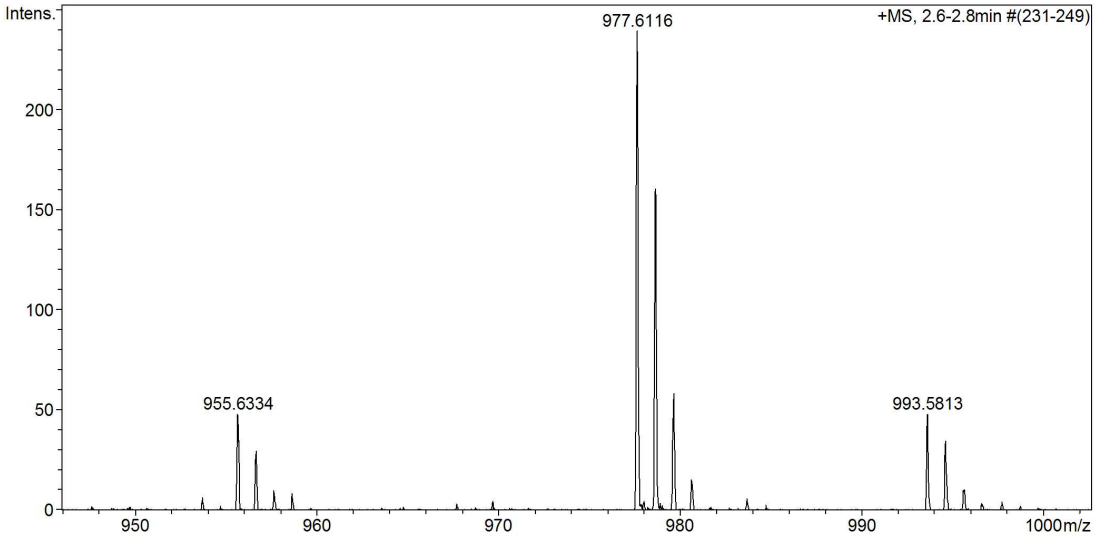

Figure 4.35 HR-ESI-MS spectrum of N^4,N^9-didecanoyl spermine-diFMOC derivative, (M.W. = 954.6234, $C_{60}H_{82}N_4O_6$) expected m/z $[M+H]^+$ ion = 955.6312 (found = 955.6334) and $[M+ Na]^+$ ion m/z = 977.6132 (found = 977.6116).

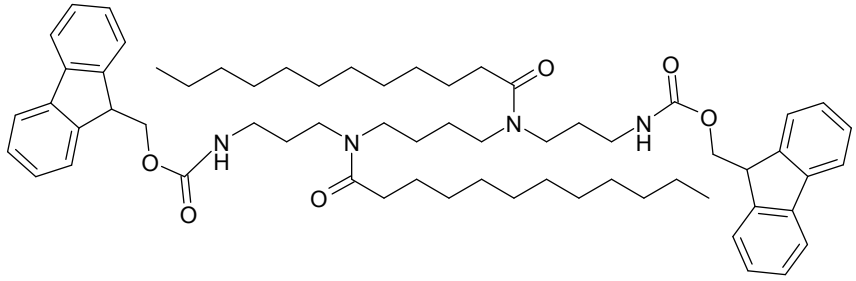

Figure 4.36 N^4,N^9-Didodecanoyl spermine-diFMOC derivative.

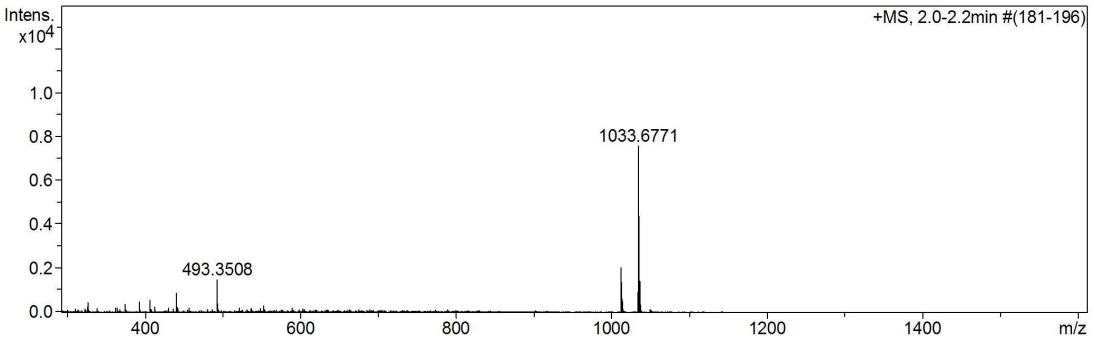

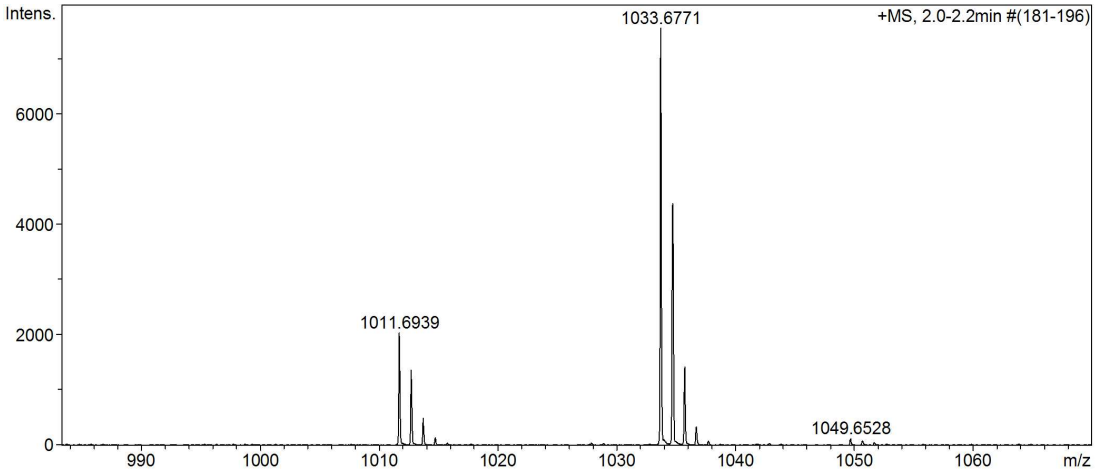

Figure 4.37 HR-ESI-MS spectra of N^4,N^9-didodecanoyl spermine-diFMOC derivative, (M.W. = 1010.6860, $C_{64}H_{90}N_4O_6$) expected m/z $[M+H]^+$ ion = 1011.6938 (found = 1011.6939) and $[M+ Na]^+$ ion m/z = 1033.6758 (found = 1033.6771).

FMOC derivatization of aminoglycosides

The FMOC derivatization was carried out at alkaline pH (in borate buffer) in order to prevent extensive hydrolysis by reaction with phenols or alcohols (Figure 4.38). In this alkaline environment, the reaction of hydroxyl groups on aminoglycosides such as kanamycin (Figure 4.39) is prevented. Kanamycin reacts with 4 moieties of FMOC only at the amine functional groups.

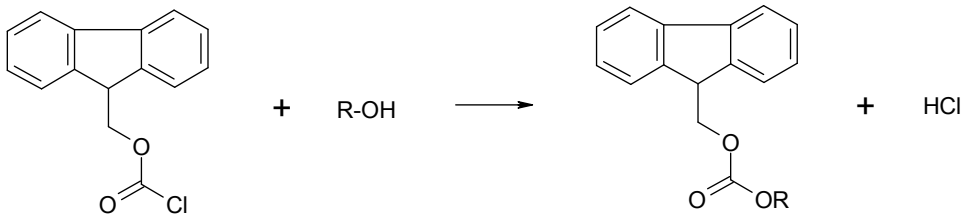

Figure 4.38 The reaction of an aliphatic alcohol with FMOC Cl reagent.

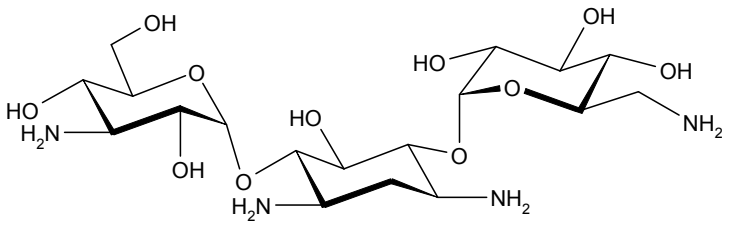

Figure 4.39 Kanamycin has four primary amino groups.

We have proved that kanamycin reacts with four molecules of FMOC Cl to yield kanamycin-tetraFMOC derivative which gave the symmetrical peak of HPLC chromatogram at peak at Rt = 8.30 min (Figure 4.40). The elution of kanamycin-FMOC derivative was confirmed as tetra-substituted by HR-ESI-MS (Figure 4.41). The expected formula is $C_{78}H_{76}N_4O_{19}$ m/z = 1372.5104, $[M+H]^+$ = 1373.518, $[M+Na]^+$ = 1395.4998, found = 1395.5003. Paramomycin is another aminoglycoside that was also examined, the HPLC chromatogram of the FMOC derivative has Rt = 12.2 min (Figure 4.42).

The amine-FMOC derivatives gave predominantly $[M+Na]^+$ ions in addition to monovalent ions $(M+H)^+$ as the summary Table shows in Table 4.6.

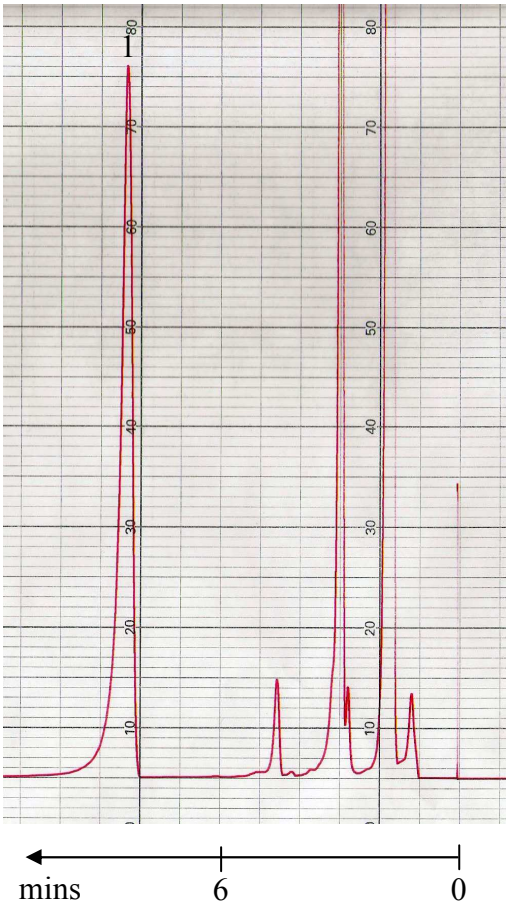

Figure 4.40 HPLC chromatogram of kanamycin-tetraFMOC derivative, HPLC conditions: column: Phenomenex hypersil C18 5µ 150 x 4.60 mm, mobile phase is acetonitrile: Milli-Q-water (60:40) with flow rate 1 mL/min, fluorescence detector at λ_{ex} = 264 nm, λ_{em} = 390 nm, peak 1 = kanamycin-tetraFMOC at Rt = 8.2 min.

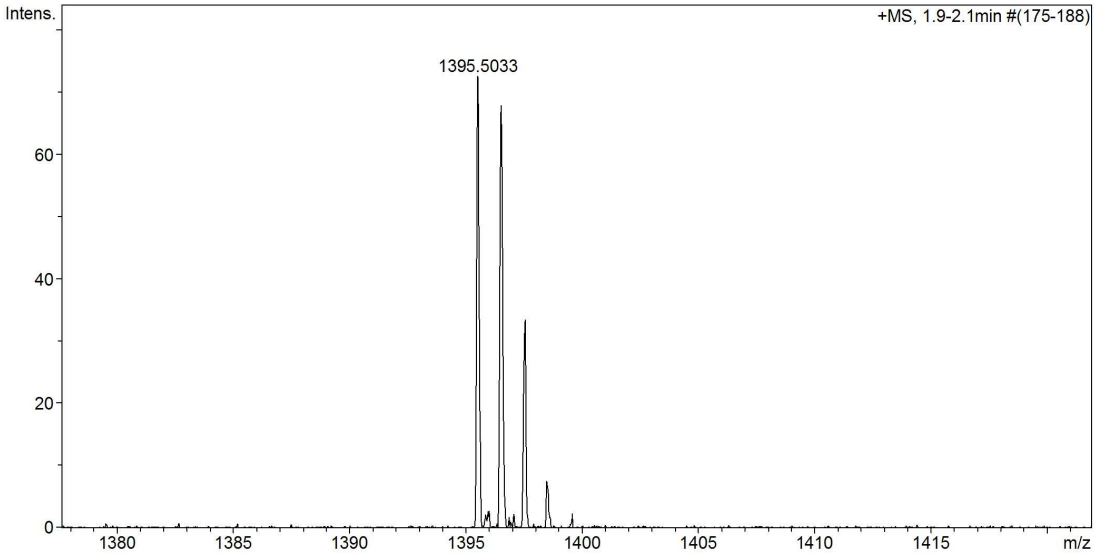

Figure 4.41 HR-ESI-MS spectrum of kanamycin-tetraFMOC derivatives, expected m/z $[M+Na]^+$ = 1395.4998, found = 1395.5003.

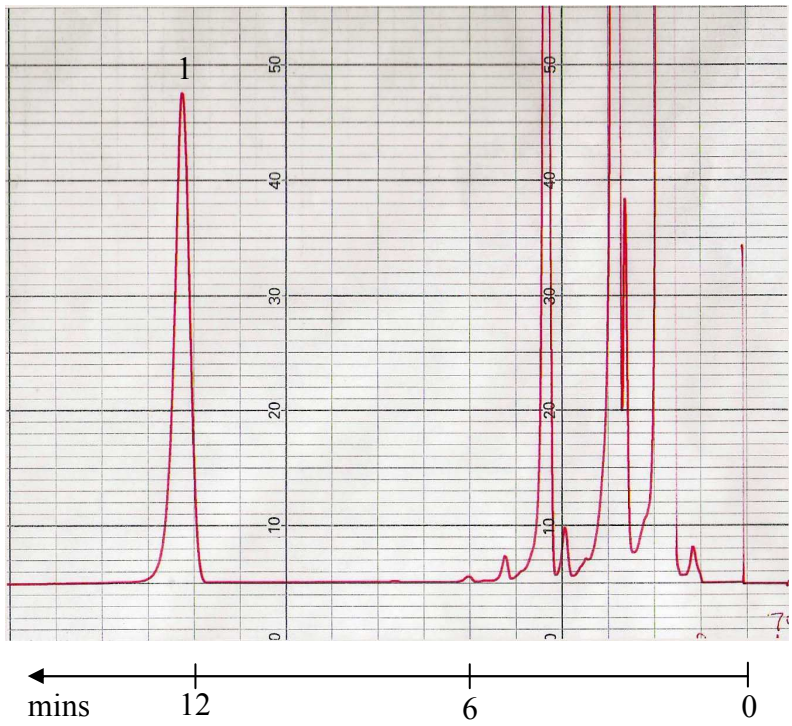

Figure 4.42 HPLC chromatogram of paramomycin-pentaFMOC derivative, HPLC conditions: column: Phenomenex hypersil C18 5µ 150 x 4.60 mm, mobile phase is acetonitrile: Milli-Q-water (60:40) flow rate 1 mL/min, fluorescence detector x10 sensitivity at λ_{ex} = 264 nm, λ_{em} = 390 nm, peak 1 = paramomycin-pentaFMOC at Rt = 12.2 min.

Table 4.6 Summary of HR-ESI-MS data of FMOC derivatives.

FMOC derivatives	Molecular Formula	HR-ESI-MS calculated	HR-ESI-MS found
Alanine-monoFMOC $C_{18}H_{17}NO_4$	$C_{18}H_{18}NO_4$ $[M+H]^+$	312.1236	312.1230
	$C_{18}H_{17}NNaO_4$ $[M+Na]^+$	334.1055	334.1050
1-Butylamine-monoFMOC $C_{19}H_{21}NO_2$	$C_{19}H_{22}NO_2$ $[M+H]^+$	296.1651	296.1645
Piperidine-monoFMOC $C_{20}H_{21}NO_2$	$C_{20}H_{22}NO_2$ $[M+H]^+$	308.1651	308.1620
	$C_{20}H_{21}NNaO_2$ $[M+Na]^+$	330.1469	330.1542
Piperazine-diFMOC $C_{34}H_{30}N_2O_4$	$C_{34}H_{31}N_2O_4$ $[M+H]^+$	531.2284	531.2277
	$C_{34}H_{30}N_2NaO_4$ $[M+Na]^+$	553.2103	553.2103
1,5-Diaminopentane-diFMOC $C_{35}H_{34}N_2O_4$	$C_{35}H_{35}N_2O_4$ $[M+H]^+$	547.2597	547.2591
1,7-Diaminoheptane-diFMOC $C_{37}H_{38}N_2O_4$	$C_{37}H_{38}N_2NaO_4$ $[M+Na]^+$	597.2729	597.2724
Spermidine-triFMOC $C_{52}H_{49}N_3O_6$	$C_{52}H_{49}N_3NaO_6$ $[M+Na]^+$	834.3519	834.3514
Spermine-tetraFMOC $C_{70}H_{66}N_4O_8$	$C_{70}H_{66}N_4NaO_8$ $[M+Na]^+$	1113.4778	1113.7389
1,12-Diphthalimido-4,9-diazadodecane-diFMOC $C_{56}H_{50}N_4O_8$	$C_{56}H_{51}N_4O_8$ $[M+H]^+$	907.3707	907.3693
	$C_{56}H_{50}N_4NaO_8$ $[M+Na]^+$	929.3526	929.3512
N^4,N^9-Didecanoyl spermine-diFMOC $C_{60}H_{82}N_4O_6$	$C_{60}H_{83}N_4O_6$ $[M+H]^+$	955.6307	955.6334
	$C_{60}H_{82}N_4NaO_6$ $[M+Na]^+$	977.6132	977.6153
N^4,N^9-Didodecanoyl spermine-diFMOC $C_{64}H_{90}N_4O_6$	$C_{64}H_{91}N_4O_6$ $[M+H]^+$	1011.6938	1011.6913
	$C_{64}H_{90}N_4NaO_6$ $[M+Na]^+$	1033.6758	1033.6740
Kanamycin-tetraFMOC $C_{78}H_{76}N_4O_{19}$	$C_{78}H_{76}N_4NaO_{19}$ $[M+Na]^+$	1395.5001	1395.5033

Conclusions of FMOC Cl derivatization

The reaction of FMOC is carried out at alkaline pH, in borate buffer, in order to prevent extensive reaction with phenolic or alcoholic hydroxyls. In this way, the polyols of *e.g.* aminoglycosides will not react with FMOC, only the amines will react with FMOC. The amine derivatization reaction is fast, but it also depends upon the structure of the molecule *e.g.* with short chain 1-butylamine, the reaction was complete in under 60 s, but for kanamycin up to 5 min was required to complete the reaction.

We proved that the amount of reaction volume can be restricted to 300 µl (from 1-2 ml) and on this scale it was not necessary to extract the derivative, rather the whole reaction mixture can be directly injected into the HPLC. This is a convenient analytical method. However, when the reaction was extracted with pentane, the HPLC chromatogram obtained had fewer interfering peaks which is better for applying the method for mixed amine samples or biological samples so we can separate biological amines in the organic phase and amino acid derivatives in the aqueous phase prior to chromatographic separation. FMOC (fluorescent) derivatives of amines are stable at 20^{o}C and in daylight for at least five days.

A disadvantage of FMOC Cl is its reactivity toward water. After hydrolysis and decarboxylation, the resulting fluorescent alcohol elutes in the middle of the chromatogram.

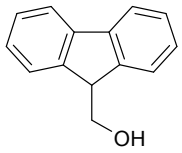

Hydrolysis product of FMOC Cl

At high concentrations, this hydrolysis peak overlaps with the other analytes in the chromatogram which complicates the quantification of the analyses. Also, FMOC Cl is fluorescent, therefore the excess of reagent should be removed before chromatography. Comparisons of three methods to terminate the excess of FMOC Cl reagent were made using: alanine, glacial acetic acid, and pentane extraction. With the pentane extraction, the majority of the hydrolysis product of FMOC Cl (the alcohol) is removed, thus minimizing interference in the chromatograms.

CHAPTER 5: DERIVATIZATION OF PRIMARY AND SECONDARY AMINES WITH DANSYL CHLORIDE

Background to amine dansyl derivatization

In 1952, 5-dimethylaminonaphthalene-1-sulfonyl chloride (dansyl chloride, DNS Cl) was introduced by Weber as the reagent for the preparation of fluorescent conjugates of proteins (Weber, 1952) and in 1956, the dansylation procedure was first applied to the identification of biogenic amines (Seiler and Wiechmann, 1965). They also published the first method for the quantitative estimation of DNS amine derivatives (Seiler and Wiechmann, 1966). Currently, dansylation is widely used to prepare fluorescent derivatives which are then separated by HPLC and detected by UV as well as by fluorescence.

Dansylation mechanism

DNS Cl reacts with both primary and secondary amino groups even at slightly alkaline pH (Figure 5.1) to yield stable fluorescent derivatives (Seiler, 1970).

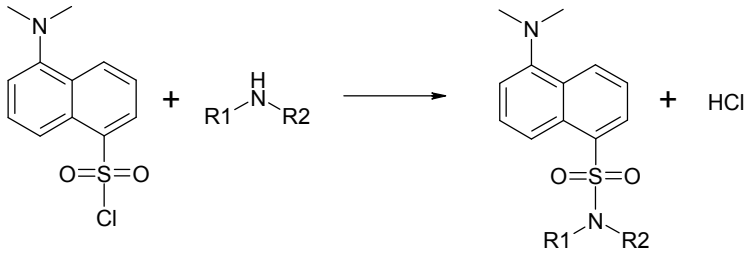

Figure 5.1 DNS derivatization of amines.

The rate of dansylation increases with increasing pH, but is paralleled by an increased rate of hydrolysis of the DNS Cl. Optimal conditions should give the most effective reaction of reactive groups in a limited amount of reagent. Most amino acids and amines are optimized at pH 9.5-10.0 (at 20^{o}C). DNS Cl is slightly soluble in water, and so dansylation is mostly performed in a mixed solvent system of acetone/water which is homogeneous.

Properties of DNS-derivatives

The DNS derivatives are yellow crystalline solids, mostly readily soluble in organic solvents and only slightly soluble in water. The spectroscopic properties of DNS derivatives are

dependent on their structures, but are also changed by different solvents and pH (Chen, 1967; Schmidt-Glenewinkel, 1973; Schneider, 1973; Seiler *et al.*, 1973).

In addition to UV absorption, fluorimetry, quantitative MS and the application of radioactive DNS have been used to quantify DNS derivatives. The intense absorption bands of DNS derivatives are in the range of 250-255 and 335-350 nm (Seiler, 1970). UV absorption is less sensitive than fluorimetry in which DNS derivatives have excitation wavelengths between 340 and 395 nm and emission fluorescence between 500 and 530 nm. For amine derivatives, the fluorescence intensity is linearly related to the amount of DNS derivatives up to a concentration of 10 μM (Seiler, 1970) and even up to 2 mM in our studies (see below).

Stability of DNS Cl reagent

The chromatographic peak of standard DNS Cl was observed by dissolving DNS Cl in acetone from concentration 0.1-0.8 mM, then injecting the solution onto the HPLC column, HPLC conditions: mobile phase is acetonitrile: Milli-Q-water (70:30), C18-luna column, flow rate 1 mL/min using two detectors in series: fluorescence detector at λ_{ex} = 330 nm, λ_{em} = 510 and then UV detector at λ_{max} = 330 nm. Chromatograms obtained from the fluorescence detector showed the solvent front at retention time (Rt) = 1.0 min, but no other peaks were observed. However, with UV detection, the chromatogram showed at least three peaks which are: (1) the solvent front at Rt = 1.0 min, (2) unknown peak at Rt = 1.9 min, and (3) the DNS Cl peak at Rt = 9.0 min (Figure 5.3). Using UV detection, the DNS Cl peak gave a linear calibration curve (Figure 5.2). The stability of the DNS reagent was good within 2 weeks after preparation (stored at 4^{o}C) as the calibration curve of the reagent showed good linearity.

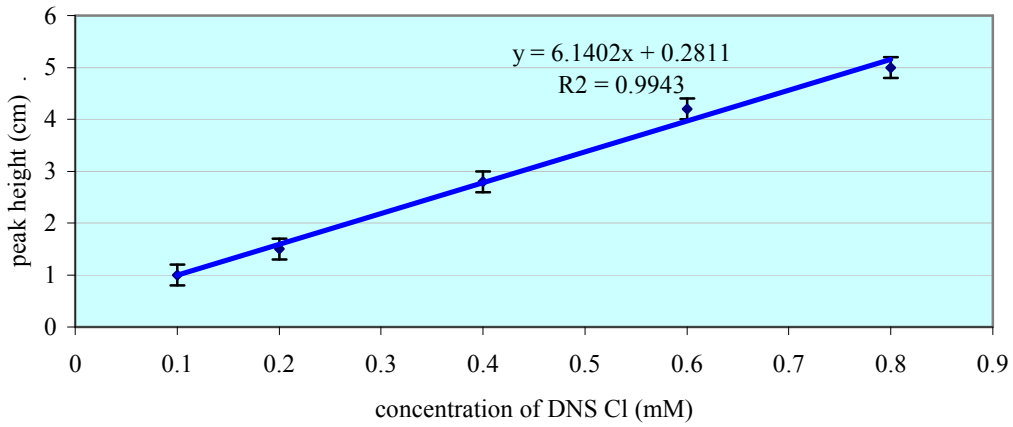

Figure 5.2 Calibration curve of DNS Cl (freshly prepared) detected by UV, (n = 5).

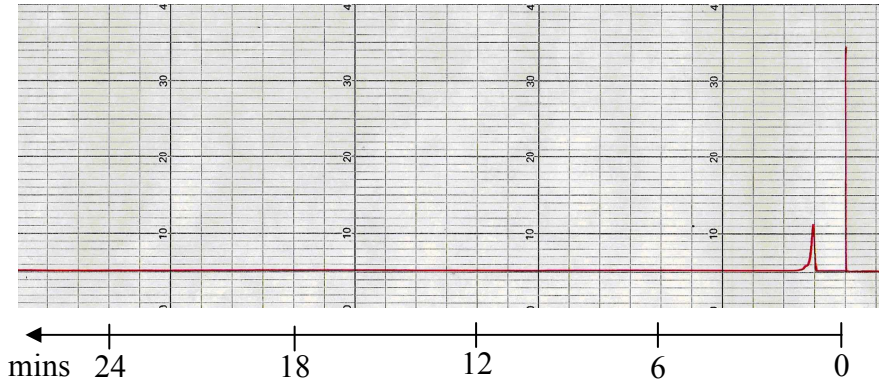

(A)

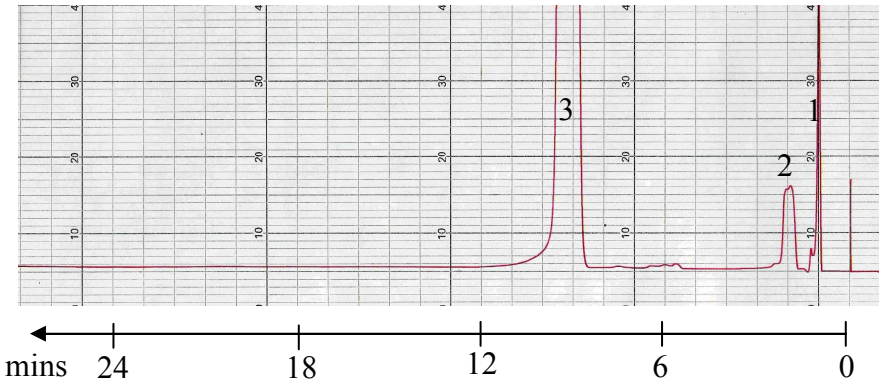

(B)

Figure 5.3 HPLC chromatogram of solution of DNS Cl in acetone (10 mM), HPLC conditions: mobile phase is acetonitrile: Milli-Q-water (70:30), C18-luna column, flow rate 1 mL/min, (A) from fluorescence detector at λ_{ex} = 330 nm, λ_{em} = 510 nm. The chromatogram shows only the solvent front at Rt = 1.0 min, (B) from UV detector at λ_{max} = 330 nm. The chromatogram shows peak 1 = the solvent front at Rt = 1.0 min, peak 2 unknown peak at Rt = 1.9 min, and peak 3 = DNS Cl at Rt = 9.0 min.

From the HPLC chromatogram above, unchanged DNS Cl would give no interfering peaks in fluorescence detection. The reaction of DNS Cl with amines was found to be pH-dependent. The DNS-derivatives will not form if the conditions are not alkaline enough (pH should be more than 8.5). The reaction can be explained in terms of three competing reactions (Fu et al., 1998):

$$R\text{-}NH_2 + DNS\text{-}Cl \longrightarrow R\text{-}NH\text{-}DNS + HCl \quad (1)$$

$$H_2O + DNS\ Cl \longrightarrow DNS\text{-}OH + HCl \quad (2)$$

$$R\text{-}NH\text{-}DNS + DNS\ Cl \longrightarrow DNS\text{-}NH_2 + \text{other products} \quad (3)$$

Where R-NH_2 represents polyamine, DNS-OH is dansylic acid and DNS-NH_2 is dansyl amide. Desirable reaction (1) is accelerated by alkaline pH from pH 8.5, but at high pH reaction (2) also occurred. Reaction (3) leads to decomposition of R-NH-DNS (polyamine-DNS derivative). This reaction (3) could happen in the presence of an excess of DNS Cl reagent (Neadle and Pollit, 1965). Thus, an optimum pH must be found and the concentration ratio of DNS Cl to the amines needed to be examined.

A "blank-DNS" reaction was performed where water was used instead of a solution of amine to react with DNS Cl reagent followed by removal of the excess of DNS Cl by using alanine solution. The elution of peaks that appeared in the HPLC chromatograms from the fluorescence detector and from the UV detector (Figure 5.4) were confirmed by HR-ESI-MS for dansylic acid (Figure 5.5), dansyl amide (Figure 5.6) and DNS Cl (Figure 5.7).

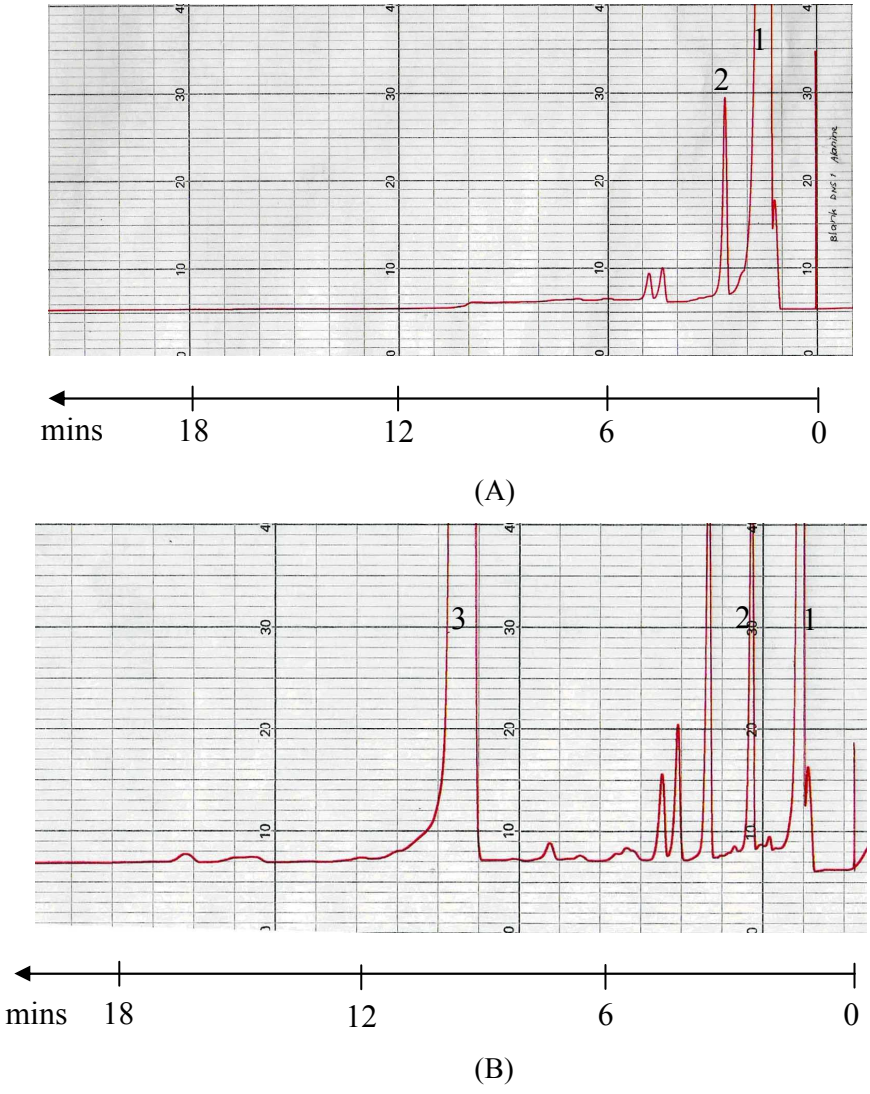

Figure 5.4 HPLC chromatogram of "Blank-DNS", HPLC conditions: mobile phase is acetonitrile: Milli-Q-water (70:30) C18-luna column, flow rate 1 mL/min, (A) from

fluorescence at λ_{ex} = 330 nm, λ_{em} = 510 nm. The chromatogram shows: peak 1 = dansylic acid at Rt = 1.2 min and peak 2 = dansyl amine at Rt = 2.6 min, (B) from UV detector at λ_{max} = 330 nm. The chromatogram shows peak 1 = dansylic acid, peak 2 = dansyl amide and peak 3 = DNS-Cl at Rt = 8.9 min.

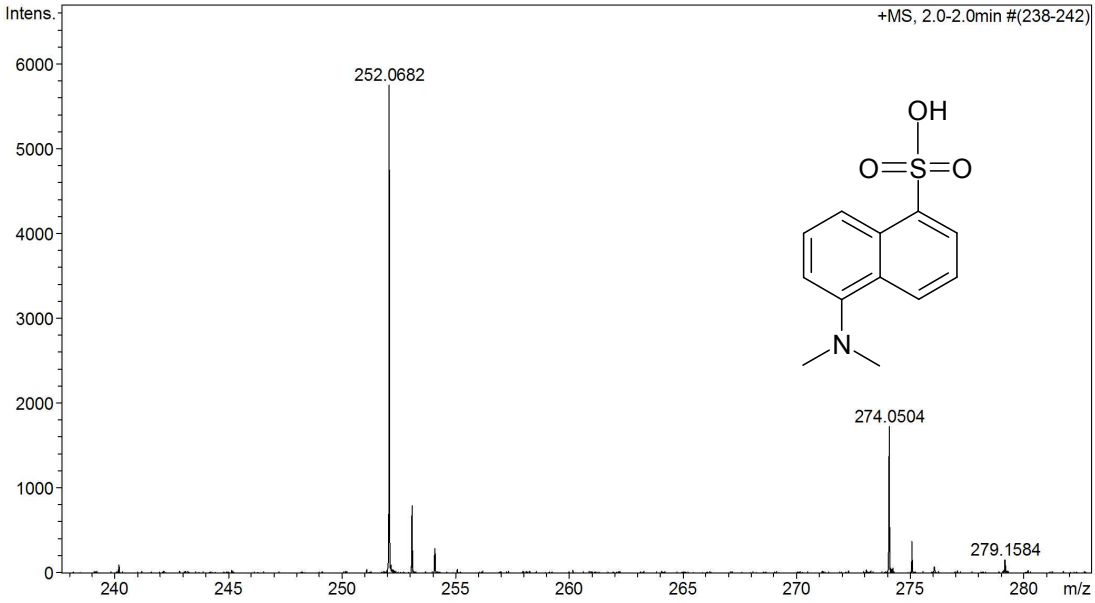

Figure 5.5 HR-ESI-MS spectrum of dansylic acid from peak 1, (M.W. = 251.0616 $C_{12}H_{13}NO_3S$) expected m/z $[M+H]^+$ ion = 252.0694 (found = 252.0682) and $[M+Na]^+$ ion = 274.0513 (found = 274.0504).

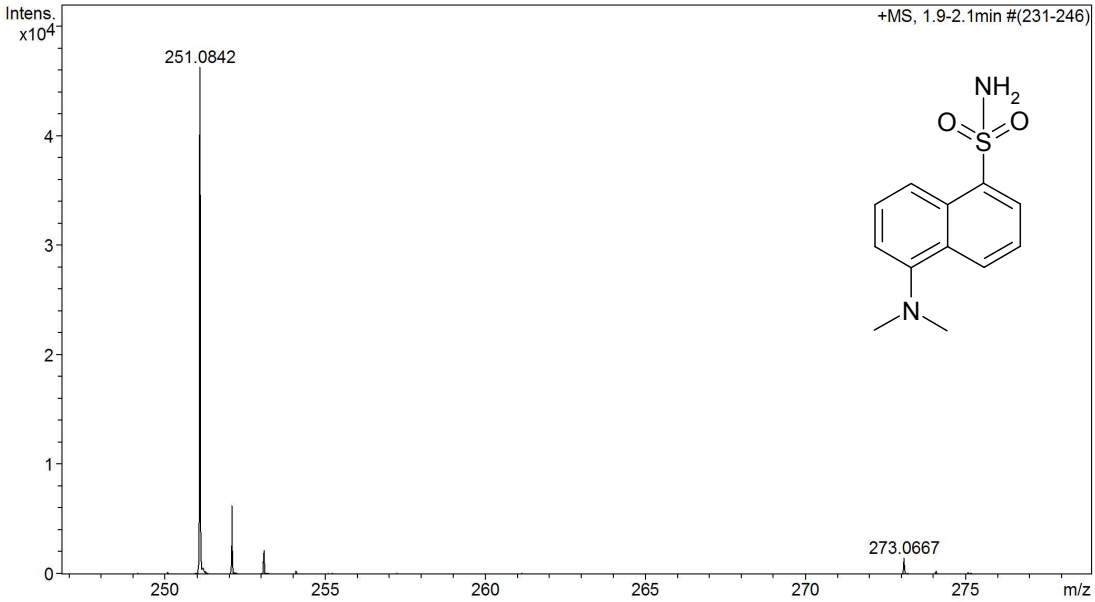

Figure 5.6 HR-ESI-MS spectrum of dansyl amide from peak 2, (M.W. = 250.0776 $C_{12}H_{14}N_2O_2S$) expected m/z $[M+H]^+$ ion = 251.0854 (found = 251.0842) and $[M+Na]^+$ ion = 273.0673 (found = 273.0667).

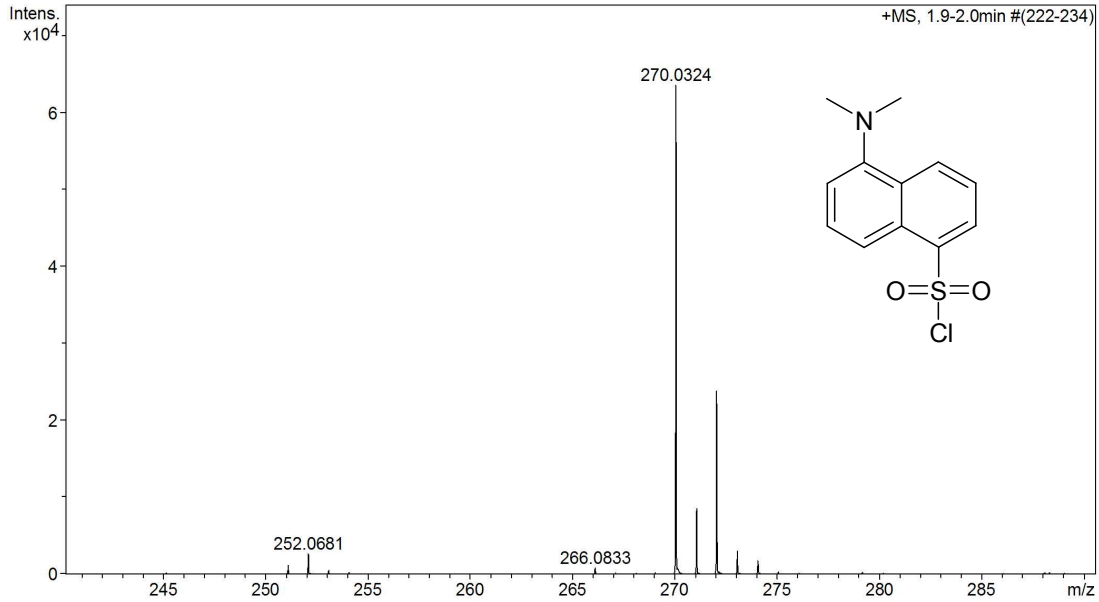

Figure 5.7 HR-ESI-MS spectrum of DNS Cl (M.W. = 269.0277, $C_{12}H_{12}ClNO_2S$) expected m/z $[M+H]^+$ from $C_{12}H_{13}{}^{35}ClNO_2S$ ion = 270.0355 (found = 270.0324) and expected m/z $[M+H]^+$ from $C_{12}H_{13}{}^{37}ClNO_2S$ ion = 272.0317.

HPLC mobile phase conditions

The peaks were separated by isocratic elution. In order to optimize the mobile phase for HPLC, the following mixtures were used:

Acetonitrile: Milli-Q-water (40:60)
Acetonitrile: Milli-Q-water (60:40)
Acetonitrile: 0.1 % formic acid in Milli-Q-water (60:40)
Acetonitrile: 2.5 % formic acid in Milli-Q-water (60:40)
Acetonitrile: Milli-Q-water (65:35)
Methanol: acetonitrile: Milli-Q-water (65:20:15)
Acetonitrile: Milli-Q-water (70:30)

Addition of formic acid to the mobile phase did not make any significant difference to the separation of analytes. Thus, mixtures of acetonitrile, methanol and water and adjustment of the ratio of these solvents were used in preparing suitable mobile phases. The peaks produced by hydrolysis of DNS Cl were completely separated from the analytes. The best separation of derivatives was obtained using the mobile phase of 70:30 acetonitrile: Milli-Q-water.

Two detectors, fluorescence and UV, were simultaneously employed to detect peaks after HPLC separation. Although amine-DNS derivatives could be monitored by both UV and fluorescence detection, the fluorescence detector was more sensitive than the UV under the conditions employed. Both the UV absorbance and fluorescence spectra of the different analyte amine derivatives were sufficiently similar to allow the same detection parameters to be used throughout.

Due to the differences between the two detection modes, regarding the sensitivity and selectivity of the detectors, there are cases where some peaks not detected by UV absorbance can be investigated by fluorescence and vice versa as shown in Figure 5.4. This enables the detection of possible non-fluorescent by-products and increases the reliability of the method. When detected by UV absorption, the chromatograms gave multiple peaks compared with fluorescence detection. Thus, the selectivity of the fluorescence detector is better (than using the UV detector) and from the size of the peaks, it is concluded that fluorescence detection is more sensitive than UV for dansylated amines. An advantage of using fluorescence detection is that the fluorescence detector is more selective as only the analyte with the appropriate λ_{ex} and λ_{em} will be observed while UV is not so selective and can give rise to additional peaks in the HPLC. The hydrolysis products produced by DNS Cl were observed as intense HPLC peaks in chromatograms which eluted rapidly and might not cause any interference with the analyte peaks. However, UV detection revealed that an excess of DNS Cl remained after the reaction. Thus, simultaneous detection minimizes the risk of missing trace amounts of an analyte, further increasing the reliability of this analytical method.

Selection of the excitation and emission wavelengths of amine-DNS derivatives

Fluorescence excitation and emission were recorded using a Hitachi F-2000 Fluorescence Spectrometer. Using model primary amines, e.g. 1-butylamine monoDNS derivative showed λ_{ex} = 328 nm, λ_{em} = 509 nm and 1,7-diaminoheptane monoDNS derivative showed λ_{ex} = 334 nm, λ_{em} = 525 nm. Also studied were primary amine diDNS derivatives e.g. 1,5-diaminopentane-diDNS derivative, λ_{ex} = 334 nm, λ_{em} = 519 nm, and a typical secondary amine (piperidine monoDNS derivative) λ_{ex} = 332 nm, λ_{em} = 510 nm for detection using an HPLC system (Table 5.1). Thus, the HPLC fluorescence detection was typically set at λ_{ex} = 330 nm and λ_{em} = 510 nm. It has recently been reported in the literature (during these studies) (Loukou and Zotou, 2003; Gaboriau et al., 2003; Geuns et al., 2006; Takao et al., 2008) that polyamine-dansyl derivatives are detected at λ_{ex} = 320 nm to 340 nm and λ_{em} = 500 nm to 550 nm when analyzed by HPLC with fluorescence detection.

Table 5.1 The excitation (λ_{ex}) and emission (λ_{em}) wavelengths of amine-DNS derivatives.

Amine-DNS derivatives	λ_{ex} (nm)	λ_{em} (nm)
1-Butylamine-mono DNS	328	509
1,5-Diaminopentane-diDNS	334	519
1,7-Diaminoheptane-monoDNS	334	524
1,7-Diaminoheptane-diDNS	333	525
1,8-Diaminooctane-diDNS	332	515
Piperidine-monoDNS	332	523
Piperazine-diDNS	336	529
Spermidine-triDNS derivative	336	522
Spermine-tetraDNS derivative	335	523

Dansylation methods

Method 1 Without termination of the excess of DNS Cl

1-Butylamine (1 mM) was used against various concentration of DNS Cl (5 mM to 40 mM). Results showed that excess DNS Cl peak appeared at Rt = 8.9 min when DNS Cl was used at 5-fold excess (UV detector, HPLC conditions: mobile phase is acetonitrile: Milli-Q-water (70:30) C18-luna column, flow rate 1 mL/min). However, the reaction was completed when DNS Cl was used at 10-fold excess. Without termination of the excess of DNS Cl, the final product separated into two phases. Small droplets of the excess of DNS Cl were observed, thus, this product was inhomogeneous. This product was stirred and injected onto HPLC, however, the results from 5 replicates were non-reproducible.

Method 2 Using alanine to remove the excess of DNS Cl

A solution of L-alanine was used to remove the excess of DNS Cl (Ala-DNS is held in the aqueous phase), followed by extraction of the desired amine-DNS derivative with toluene which was then evaporated and the residue was redissolved in mobile phase and analyzed by HPLC. With this elimination step, the chromatogram was improved as there were fewer interfering peaks, no peak from the excess (e.g. 70-fold or 10-fold) of DNS Cl and the peaks of the desired product were reproducible (n = 5).

Optimization of DNS Cl derivatization method

Published conditions for DNS derivatization are different from one research group to another. For example, the reaction temperature ranged from 20 to 90°C. Many conditions such as temperature, reaction time, pH of medium, concentration of DNS Cl have effects on the yield of DNS derivatization. The dansylation reaction was optimized for the following variables: the pH of buffer for amine and DNS Cl reaction, the ratio of volume of DNS Cl, the reaction time and the temperature.

Optimization of the pH of buffer for DNS Cl reaction with amines

Only the neutral form of an amine will react with DNS Cl (Seiler, 1975), and therefore, the optimum pH must be high enough to ensure that the amine is unionized. However, the pH is limited by an increase in side reactions, such as the formation of the sulfonic acid at high values (Gros and Labouesse, 1969). Moreover HCl is released during the dansylation reaction, so a buffer is always required. The effect of the pH of buffer was investigated by using borate buffer, pH range from 4.5 to 10.5 (Figure 5.8). The result showed that under acidic conditions, the reaction occurred to only a small extent when compared to the region from pH 8.5 to 10.5. The peak areas were stable and the yields of the derivatives were high. When borate buffer and saturated sodium carbonate which has the pH = 9.80 were compared, insignificant difference of the yields were obtained (Figure 5.9). Thus, saturated sodium carbonate was used routinely in the DNS Cl reaction because it was more convenient for preparation.

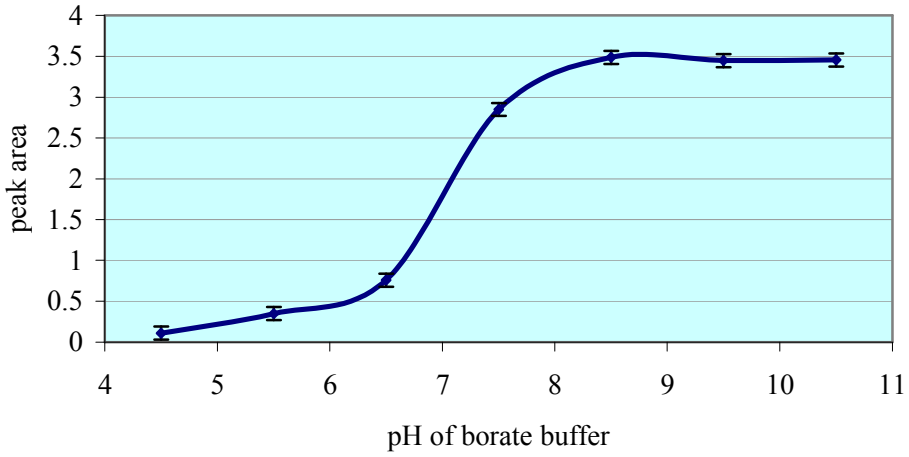

Figure 5.8 Optimization of pH of borate buffer in the reaction of 1-butylamine and DNS Cl (n = 5). Peak areas were calculated by height x 0.5 width of peak, and peak areas are reported in cm^2.

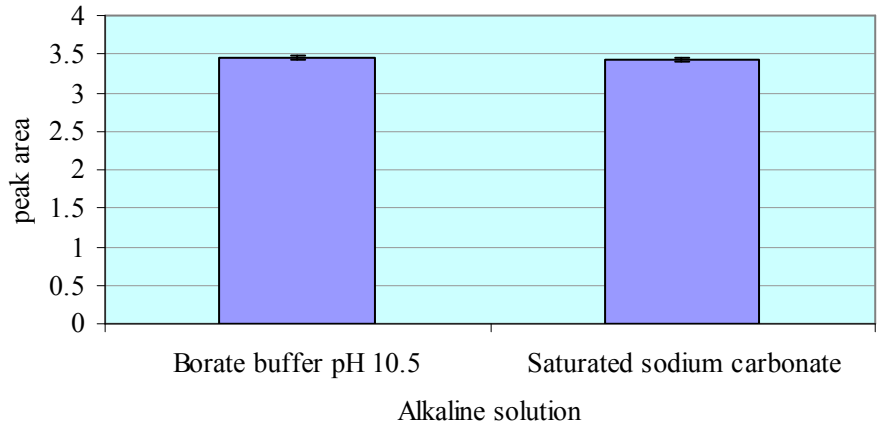

Figure 5.9 Comparison of the yields of 1-butylamine-monoDNS obtained using borate buffer pH 10.5 and saturated sodium carbonate for making the solution alkaline for dansylation.

Optimization of the reaction temperature of dansylation

Different temperatures were examined with the fixed reaction time of 15 min to determine the optimum conditions for derivatization of polyamine. A temperature series was run at 20, 40, 60, and 80°C with 1 mM of 1-butylamine while other solvents and reagent concentrations remained constant. The yields were evaluated by HPLC by measurement of the peak areas. Yields of derivatization increased with rising temperature (Figure 5.10). However, at temperatures greater than 60°C, rapid evaporation of acetone from the reaction led to solubility problems and bumping of the reaction mixture. Therefore 60°C was used for the remainder of the study.

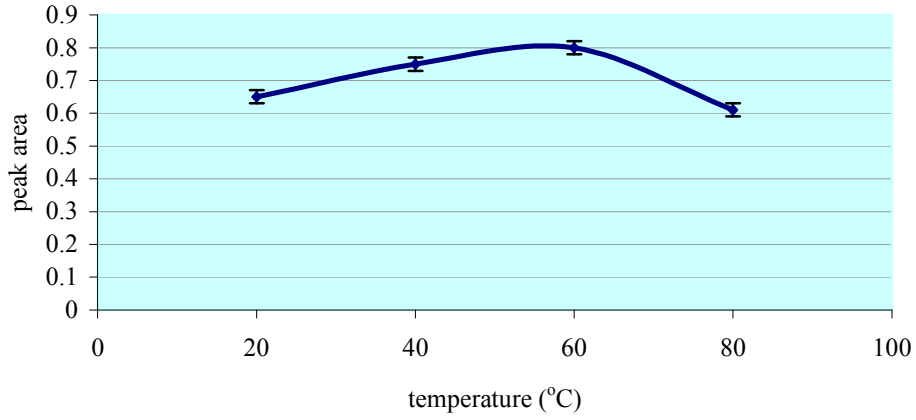

Figure 5.10 Optimization of temperature of dansylation (n = 5). Peak areas were calculated by height x 0.5 width of peak, and peak areas are reported in cm^2.

Optimization of the reaction time of dansylation

The time effect studies were carried out from 1 min to a maximum of 60 min (Figure 5.11). The reactions were run at 60°C with 1 mM of 1-butylamine. The optimum reaction time for 1-butylamine was about 15 min which was subsequently used routinely.

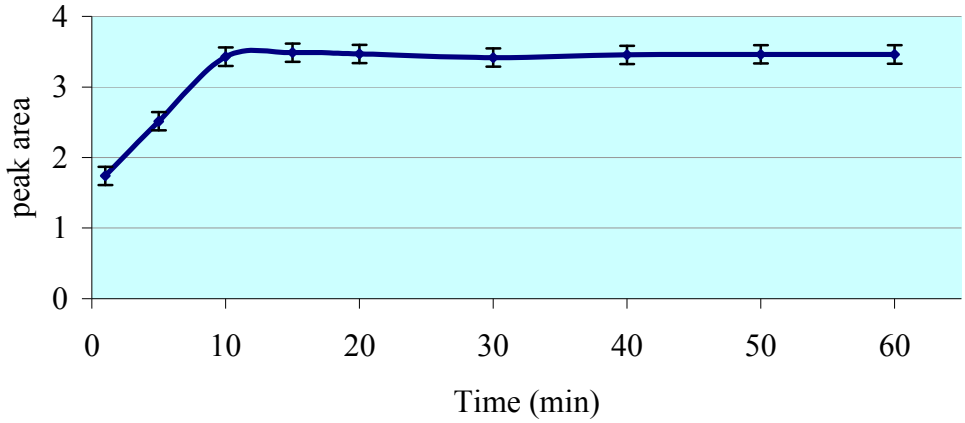

Figure 5.11 Influence of time on the dansylation reaction of 1 mM 1-butylamine (n = 5). Peak areas were calculated by height x 0.5 width of peak, and peak areas are reported in cm^2.

Optimization of the concentration ratio of DNS Cl

After optimizing the pH of the reaction, the reaction time, the reaction temperature, intense HPLC-peaks overlapping the derivatives were observed due to hydrolysis products generated by the reaction of DNS Cl with water. Cleaner chromatograms were obtained by using a minimum amount of DNS Cl.

For the optimization of DNS Cl concentration, 1 mM of model amines were reacted with DNS Cl concentration range from 1 to 100 mM. The desired amine-DNS derivatives increased with the increasing DNS solution concentration up to 10 mM then they were stable or increased indistinctively. For the pH optimization, the reaction required an alkaline pH of 9.5. For the ranges of pH examined, saturated sodium carbonate solution (pH 9.80) was selected to give an optimum pH. However, different amines required different amounts of DNS Cl to complete the reaction; for example to complete the reaction of piperidine and DNS Cl required a 5-fold excess of DNS Cl whereas 1-butylamine required 10-fold excess of DNS Cl (Figure 5.13). From Figure 5.13, the peak areas obtained for amine-DNS derivative increased by increasing the concentration of DNS Cl. An excess of DNS Cl was needed to achieve complete reaction. However, the excess of DNS Cl can also give competitive reactions with water and the amine-DNS derivative. So, the optimized

concentration of DNS Cl was chosen at 10 mM. The amine-DNS derivatives were examined with 10 mM DNS Cl and the retention times from 5 replicates are shown in Table 5.2. By varying the concentration of the amines, calibration curves were plotted as shown in Figure 5.14 and the equations were obtained as shown in Table 5.3. Derivatization conditions of DNS Cl, for the rest of the study used 10-fold excess of DNS Cl reagent to amines, at pH 9.8 saturated sodium carbonate solution for 15 min at 60^{o}C, the reaction was terminated and the excess of DNS Cl removed by adding 112 mM L-alanine. The desired products were extracted by toluene to leave the undesired by-products in the aqueous phase. After evaporation of the toluene, the residue was redissolved with mobile phase, filtered through 0.45 µm nylon filter before injection onto the HPLC. DNS derivatives are very stable as they gave the nearly same peak area after 10 days (stored in the fridge, 4^{o}C). Using a Phenomenex Hypersil C18 5µ 150 x 4.60 mm column, the optimized condition of mobile phase was 70:30 acetonitrile: Milli-Q-water. A good resolution was obtained of the amine-DNS derivative from the potential interference peaks, *e.g.* a chromatogram of 1-butylamine-monoDNS (Figure 5.12).

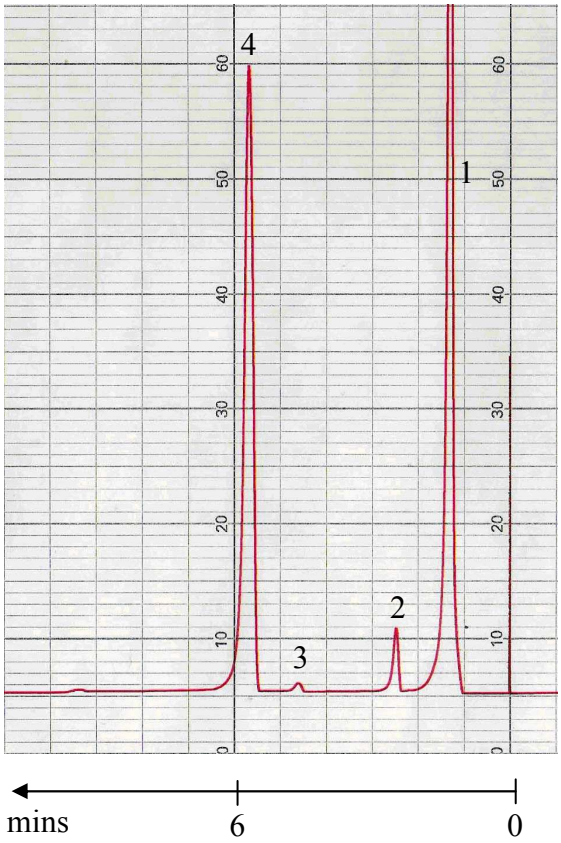

Figure 5.12 HPLC chromatogram of 1-butylamine-DNS derivative, HPLC conditions: column: Phenomenex Hypersil C18 5µ 150 x 4.60 mm, mobile phase is acetonitrile: Milli-Q-water (70:30) with flow rate 1 mL/min, fluorescence detector at λ_{ex} = 330 nm, λ_{em} = 510

nm, peak 1 = solvent front, peak 2 = dansylic acid, peak 3 = dansylamide and peak 4 = 1-butylamine-monoDNS derivative.

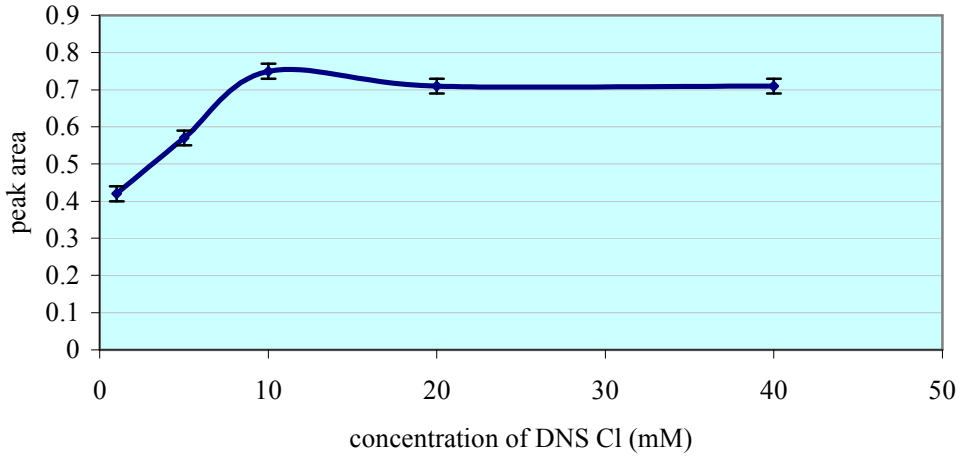

Figure 5.13 Optimization of conditions in the reaction between 1.0 mM 1-butylamine and various concentrations of DNS Cl (n = 5). Peak areas were calculated by height x 0.5 width of peak, and peak areas are reported in cm^2.

Table 5.2 The retention times of various amine-DNS derivatives. HPLC conditions: column: Phenomenex Hypersil C18 5µ 150 x 4.60 mm, mobile phase is acetonitrile: Milli-Q-water (60:40) with flow rate 1 mL/min

Amine-DNS derivatives	Type of amine	Retention time (min) ± range
Ethylamine	Primary monoamine	4.12 ± 0.17
1-Butylamine	Primary monoamine	7.15 ± 0.15
Phenylethylamine	Primary monoamine	8.10 ± 0.30
1,4-Diaminobutane	Primary diamine	9.20 ± 0.15
1,7-Diaminoheptane	Primary diamine	16.95 ± 0.35
Piperidine	Secondary monoamine	9.35 ± 0.25
Piperazine	Secondary diamine	19.60 ± 0.08

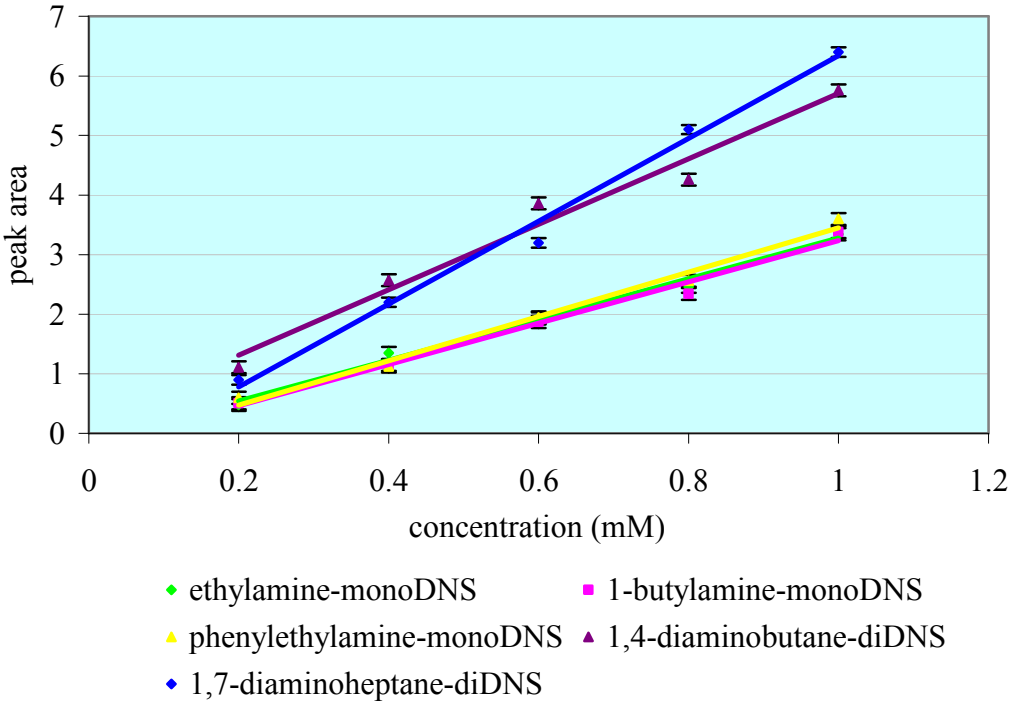

Figure 5.14 Calibration curves of amine-DNS derivatives (n = 5). Peak areas were calculated by height x 0.5 width of peak, and peak areas are reported in cm^2.

Table 5.3 The calibration curve equations of various amine-DNS derivatives

Amine-dansyl derivatives	Calibration curve	R^2 (n = 5)
Ethylamine	y = 3.42x-0.139	0.991
1-Butylamine	y = 3.65x-0.122	0.996
2-Phenylethylamine	y = 3.72x-0.265	0.988
1,4-Diaminobutane	y = 5.75x + 0.161	0.989
1,7-Diaminoheptane	y = 6.90x-0.612	0.992
Piperidine	y = 9.40x-0.300	0.999
Piperazine	y = 9.11x – 0.144	0.968

At concentrations from 0.2 mM to 1.0 mM, both 1,4-diaminobutane-DNS and 1,7-diaminoheptane-DNS derivatives show linear calibration curves (Figure 5.15), but from the concentration 2.0 mM up to 10 mM, the line of 1,4-diaminobutane-DNS was not linear whereas the line of 1,7-diaminoheptane-DNS is remained linear (Figure 5.16). This result might due to "self-quenching" of two DNS groups linked by the short hydrocarbon chain of butane compared to a heptane chain.

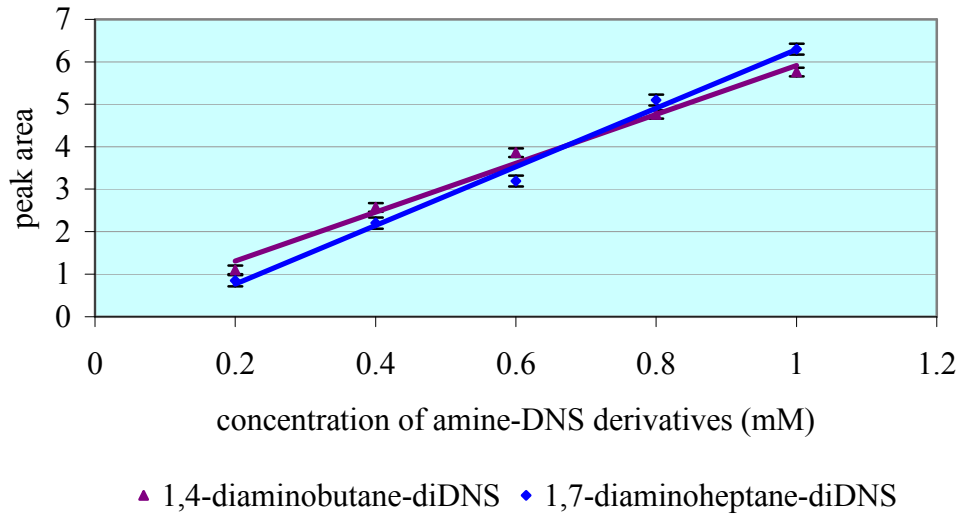

Figure 5.15 Calibration curves of 1,4-diaminobutane-diDNS derivative and 1,7-diaminoheptane-diDNS derivative which were both linear from concentration 0.2 to 1 mM (n = 5). Peak areas were calculated by height x 0.5 width of peak, and peak areas are reported in cm^2.

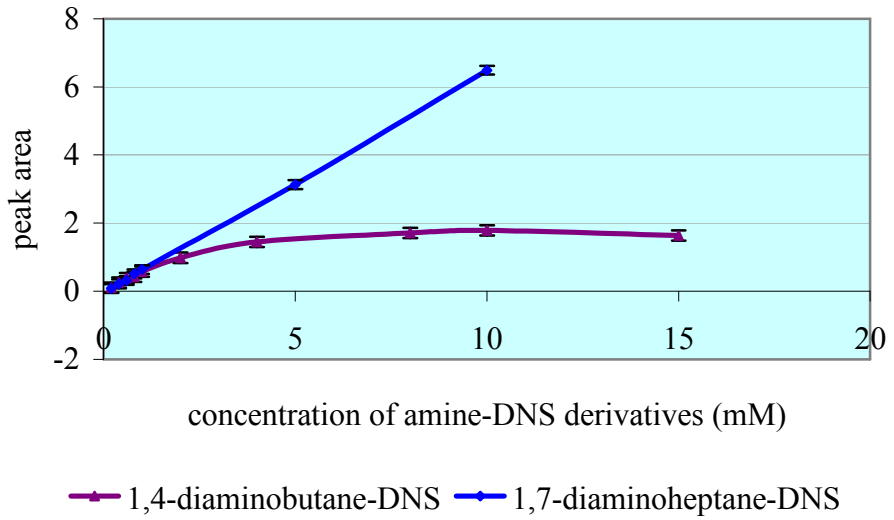

Figure 5.16 Calibration curves of 1,4-diaminobutane-diD NS derivative and 1,7-diaminoheptane-diDNS derivative (n = 5). This graph shows 1,4-diaminobutane-diDNS became non-linear at higher concentrations due to "self-quenching". Peak areas were calculated by height x 0.5 width of peak, and peak areas are reported in cm^2.

Spermine and Spermidine

The same procedure was applied to spermidine and spermine except the composition of mobile phase was changed from 60:40 acetonitrile: Milli-Q-water to 65 % methanol: 20 %

acetonitrile: 15 % Milli-Q-water due to the shorter retention time gained from 36 min to 6 min for spermidine and 39 min to 8 min for spermine. By varying the concentration of biological amines, calibration curves were obtained, the results are shown in Figure 5.17 and Table 5.4. Structure of spermidine-triDNS derivative and spermine-tetraDNS derivative (Figure 5.18) were confirmed the expected M.W. by HR-ESI-MS. (Figure 5.19 for spermidine-triDNS derivative and Figure 5.20 spermine-tetraDNS derivative).

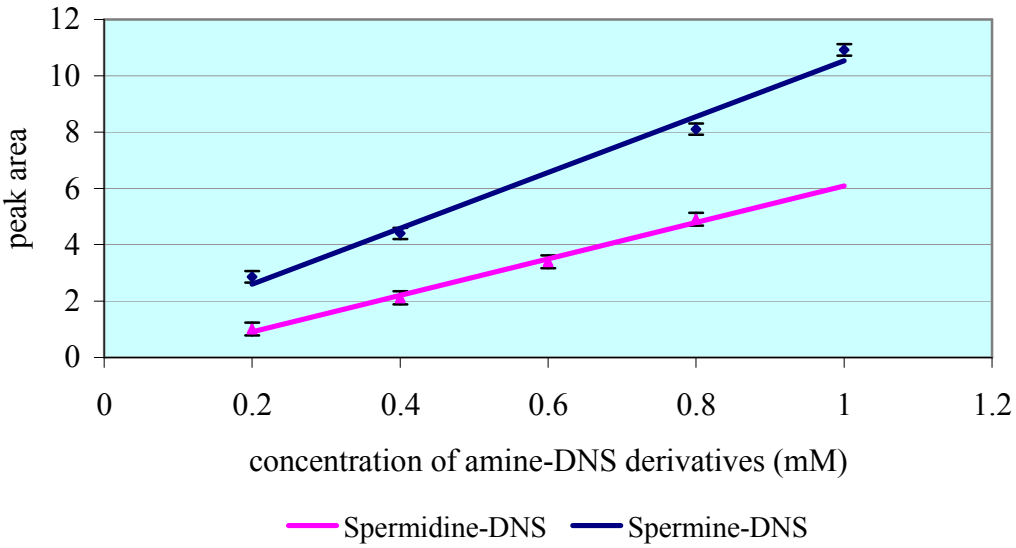

Figure 5.17 Calibration curves of natural amine-DNS derivatives (n = 5). Peak areas were calculated by height x 0.5 width of peak, and peak areas are reported in cm^2.

Table 5.4 Calibration curve equations of natural amine-DNS derivatives.

Amine-dansyl derivatives	Calibration curve	R^2 (n = 5)
Spermidine	y = 6.47x – 0.380	0.995
Spermine	y = 9.91x + 0.624	0.989

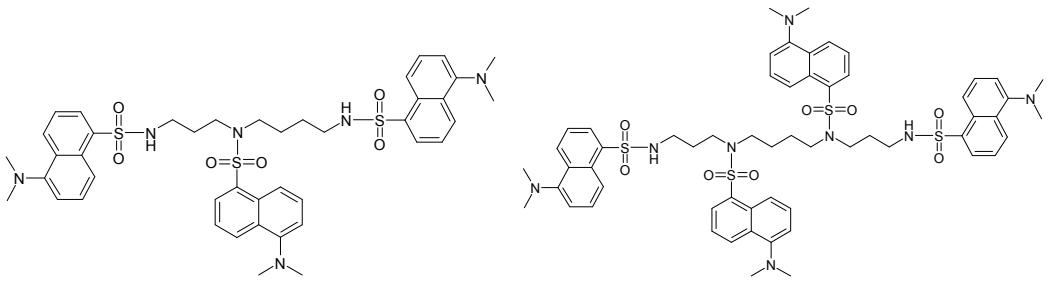

(A) Spermidine-triDNS derivative (B) Spermine-tetraDNS derivative

Figure 5.18 (A) Spermidine-triDNS derivative, (B) spermine-tetraDNS derivative.

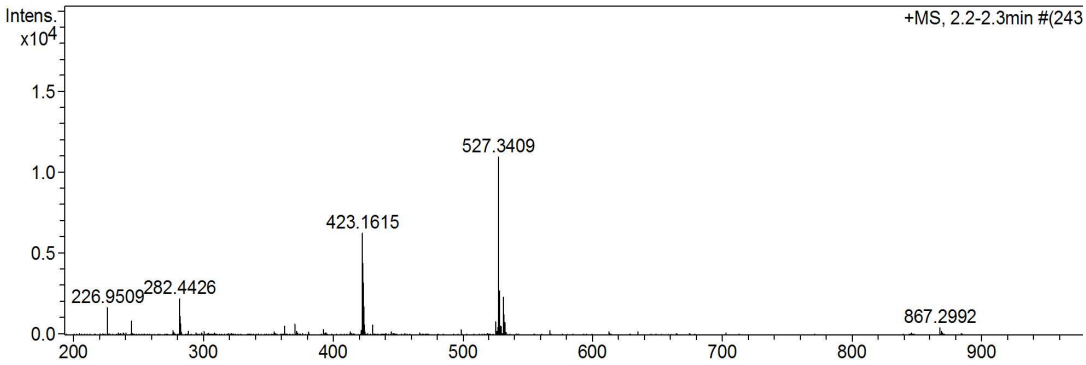

Figure 5.19 HR-ESI-MS spectra of spermidine triDNS derivative (M.W. = 844.3110, $C_{43}H_{52}N_6O_6S_3$) expected m/z $[M+H]^+$ ion = 845.3188, doubly charged $[M+2H]^{2+}$ ion = 423.1633 (found = 423.1615) and $[M+Na]^+$ ion = 867.3008 (found = 867.2992).

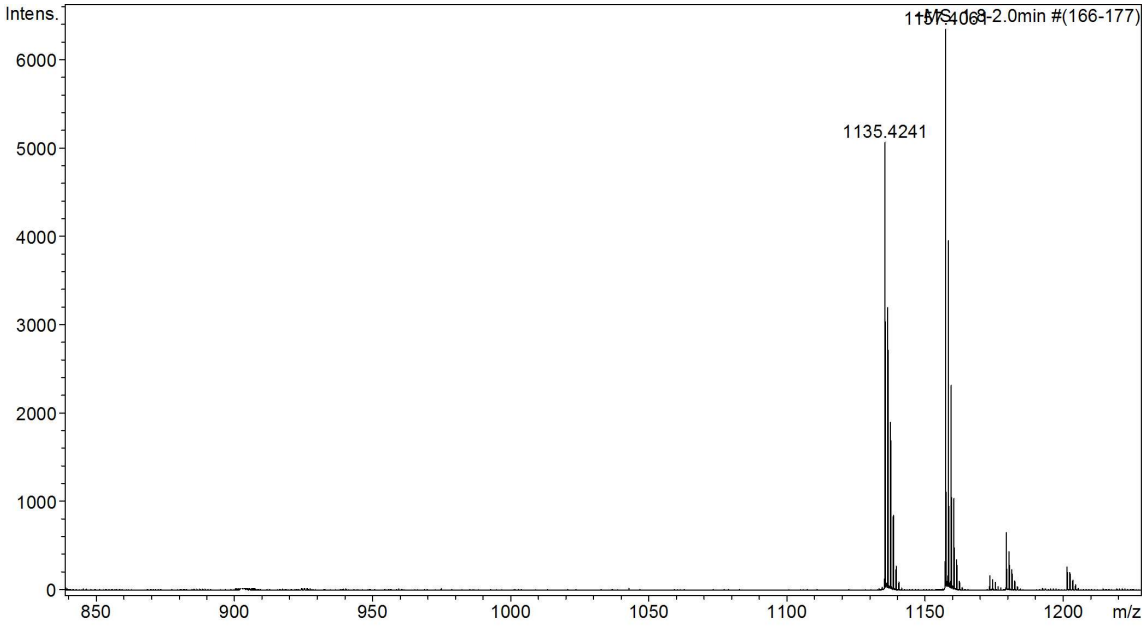

Figure 5.20 HR-ESI-MS spectra of spermine tetraDNS derivative (M.W. = 1134.4199, $C_{58}H_{70}N_8O_8S_4$) expected m/z $[M+H]^+$ ion = 1135.4277 (found = 1135.4241) and $[M+Na]^+$ ion = 1157.4097 (found = 1157.4061).

Relative quantum yield

The fluorescence intensity and UV absorbance of various polyamine-DNS derivatives were determined in order to compare the relative quantum yields. The derivatives of diamines-DNS were made in order to obtain both diamines-monoDNS and diamines-diDNS (the

chromatogram is shown in Figure 5.21). The peak of each amine-DNS was collected after separation on a semi-preparative HPLC column. As these derivatives eluted they were collected and the molecular mass of all these derivatives were confirmed using HR-ESI-MS: 1,4-diaminobutane-monoDNS derivative (Figure 5.22), 1,4-diaminobutane-diDNS derivative (Figure 5.23), 1,7-diaminoheptane-monoDNS derivative (Figure 5.24), 1,7-diaminoheptane-diDNS derivative (Figure 5.25).

A series of dilutions of each eluted peak of the model series was prepared and the UV absorbance and fluorescence intensity of each were measured. The HPLC was monitored by measurement of absorbance at the λ_{ex} using Unicam Helios UV-VIS spectrophotometer and measurement of fluorescence intensity on a Perkin Elmer Luminescence Spectrometer LS 50B. For each compound, a plot of fluorescence intensity against UV absorbance was made (Table 5.5, Figure 5.26). The fluorescence yield of each derivative is proportional to the gradient.

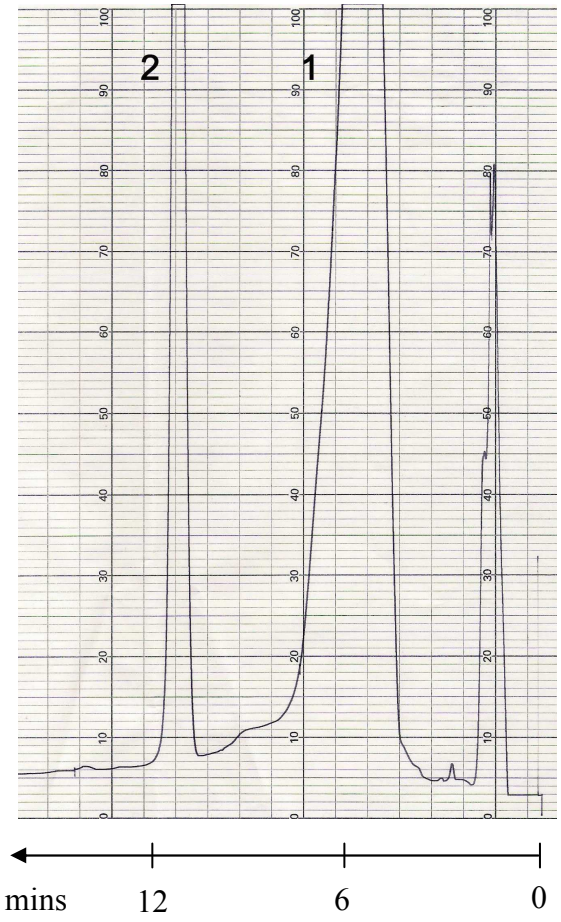

Figure 5.21 HPLC chromatogram of 1,7-diaminoheptane-DNS derivative amine-dansyl derivatives, HPLC conditions: semi-preparative column: Phenomenex Gemini 10 µ C18 110A 250 x 10 mm with guard column: Phenomenex Gemini 5 µ C18 10 x 10 mm. Mobile phase is acetonitrile: Milli-Q-water (70:30) with flow rate 5 mL/min, fluorescence detector at

λ_{ex} = 330 nm, λ_{em} = 510 nm, peak 1 = 1,7-diaminoheptane-monoDNS derivative, peak 2 = 1,7-diaminoheptane-diDNS derivative.

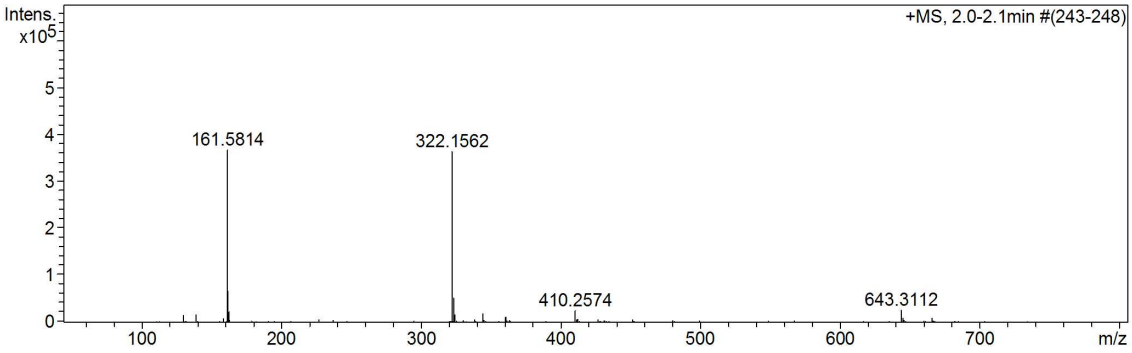

Figure 5.22 HR-ESI-MS spectrum of 1,4-diaminobutane monoDNS derivative (M.W. = 321.1511, $C_{16}H_{23}N_3O_2S$) expected m/z $[M+H]^+$ ion = 322.1589 (found = 322.1562) doubly charged ion $[M+2H]^{2+}$ = 161.5834 (found = 161.5814) and $[2M+H]^+$ ion = 643.3100 (found = 642.3112).

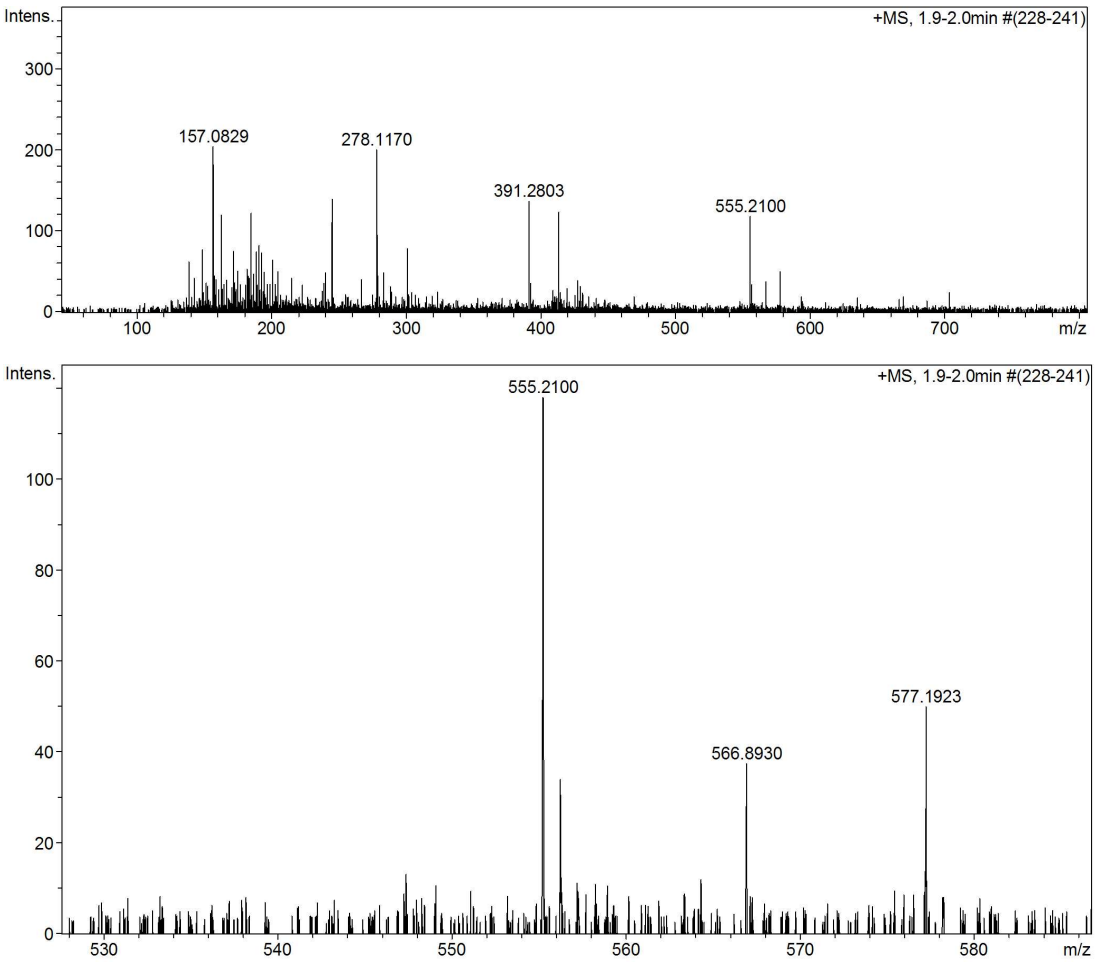

Figure 5.23 HR-ESI-MS spectra of 1,4-diaminobutane diDNS derivative (M.W. = 554.2375, $C_{28}H_{34}N_4O_4S_2$) expected m/z $[M+H]^+$ ion = 555.2099 (found = 555.2100) doubly

charged ion $[M+2H]^{2+}$ = 278.1089 (found = 278.1170) and $[M+Na]^{+}$ = 577.1919 (found = 577.1923).

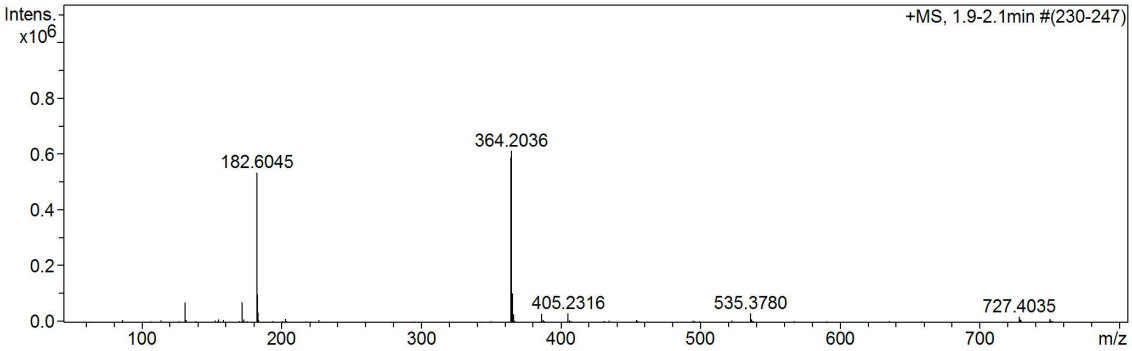

Figure 5.24 HR-ESI-MS spectrum of 1,7-diaminoheptane monoDNS derivative (M.W. = 363.1980, $C_{19}H_{29}N_3O_2S$) expected m/z $(M+H)^{+}$ ion = 364.2059 (found = 364.2036), doubly charged ion $[M+2H]^{2+}$ = 182.6068 (found = 182.6045), $[M+Na]^{+}$ = 386.1878 and $[2M+H]^{+}$ = 727.4038 (found = 727.4035).

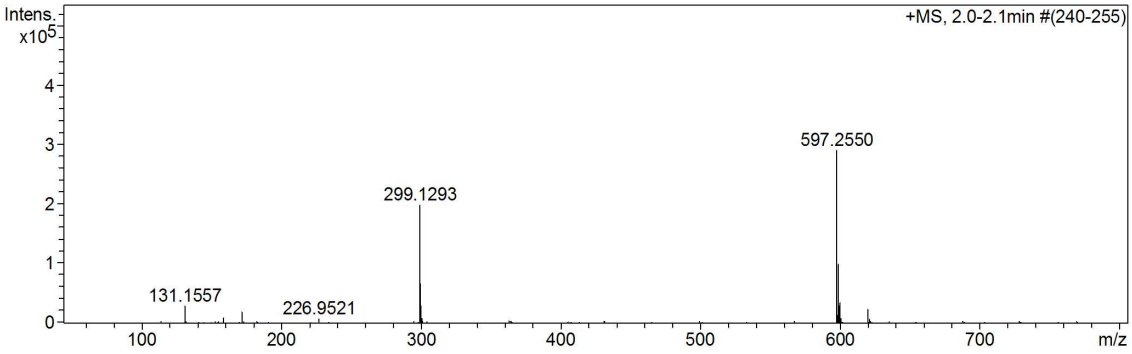

Figure 5.25 HR-ESI-MS spectrum of 1,7-diaminoheptane diDNS derivative (M.W. = 596.2491, $C_{31}H_{40}N_4O_4S_2$) expected m/z $[M+H]^{+}$ ion = 597.2569 (found = 597.2550) doubly charged ion $[M+2H]^{2+}$ = 299.1324 (found = 299.1293).

Table 5.5 Equation of F.I. and U.V. absorption of various amine-DNS derivatives.

Amines-DNS derivatives	Equation of F.I and UV absorption	R^2
1-Butyl-monoDNS	y = 2623.3x + 15.17	0.997
1,4-Diaminobutane-monoDNS	y = 2782.2x + 8.91	0.991
1,7-Diaminoheptane-monoDNS	y = 2662.8x + 9.42	0.999
1,4-Diaminobutane-diDNS	y = 2011.6x + 7.78	0.994
1,7-Diaminoheptane-diDNS	y = 2179.2x + 18.94	0.997
Spermidine-triDNS	y = 1834.3x + 38.89	0.999

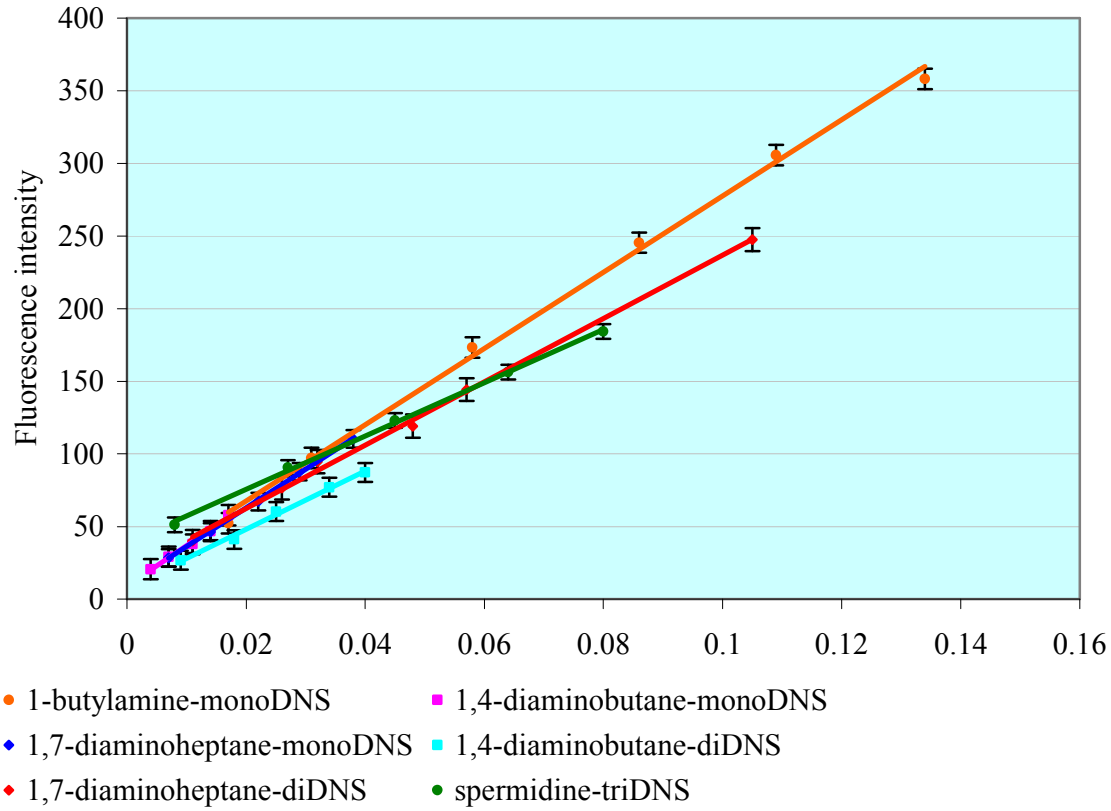

Figure 5.26 F.I. and U.V. absorption of various amine-DNS derivatives (n = 5).

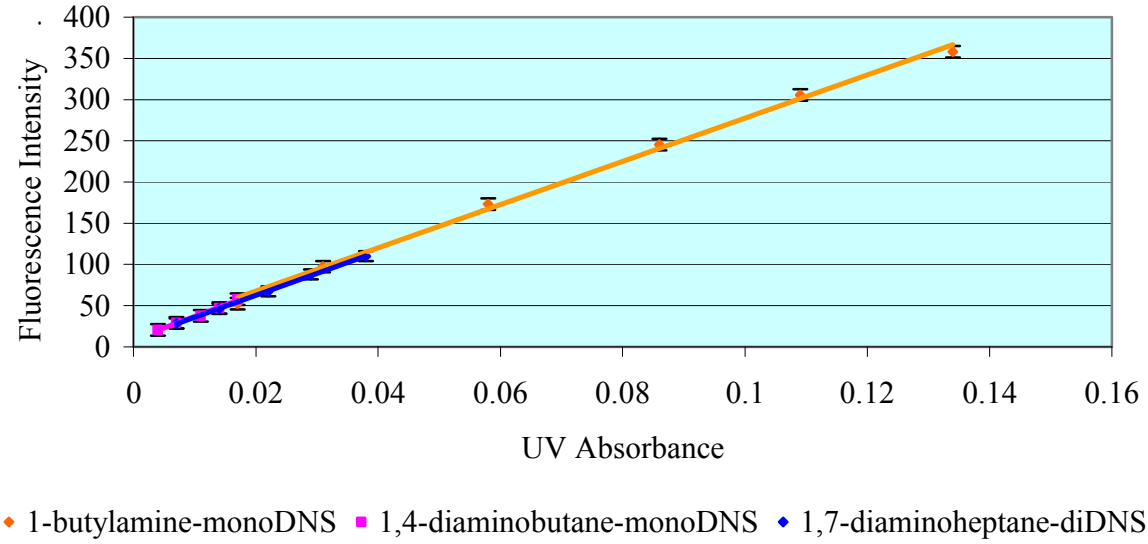

Figure 5.27 Linear plots for three amine-monoDNS derivatives (n = 5). The gradients of all three samples are similar in value.

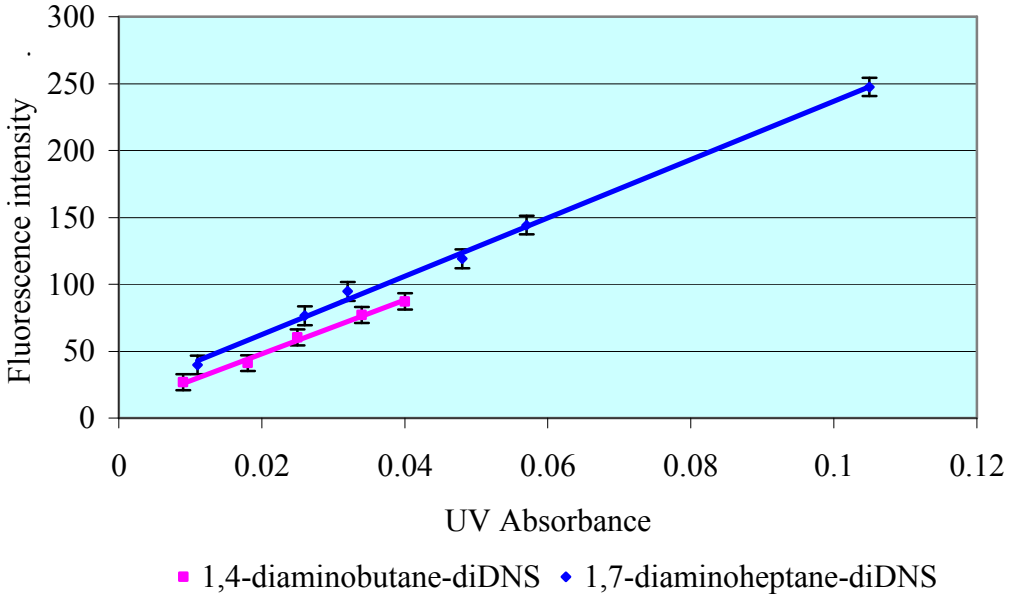

Figure 5.28 Linear plots for two amine-diDNS derivatives (n = 5). The gradients for both samples are similar in value.

The gradients of all amine-monoDNS are similar (Figure 5.27) as are the gradients from amine-diDNS (Figure 5.28), the latter values are smaller when compared with the former. The lowest gradient was obtained from amine-triDNS. From the results, it is concluded that the more DNS moieties that are bound to the polyamine molecule, the lower the gradients are. From theory, the gradient should be the same when the number of fluorophores is increased. However, from the experiment, the more fluorophores added, the lower the resultant gradient. A comparison of fluorescence yield showed those of the polyamine conjugates to be lower than those of monoamine conjugates. So, it is shown that two or more fluorophores tethered in close proximity interfere with the fluorescence process.

Piperidine- and piperazine-DNS derivatives

The relationship between the number of fluorophores and the intensity of fluorescence was examined to determine if the fluorescence intensity doubled when the DNS derivative has two fluorophores in its structure. The experiment initially used piperidine and piperazine as the amine models, both are heterocyclic secondary amines piperidine containing one nitrogen atom and piperidine containing two (1,4)-nitrogen atoms. The same concentration of piperidine and piperazine was used to react with the DNS Cl reagent. Piperazine contains two secondary amines groups so sufficient DNS Cl to derivatize both amine groups was used otherwise the combination of monoDNS derivative and diDNS derivative of this compound

would be obtained. Silica gel TLC was used to confirm and monitor the reaction of DNS-derivatization using dichloromethane: methanol (4:1) as the mobile phase. The results showed that the DNS Cl to piperidine 5: 1 (mole) was an efficient mole ratio to obtain the complete reaction. If the ratio of piperidine: DNS Cl was 1:1, only 60% product was obtained. Moreover, TLC showed that dansylic acid was still present in the organic phase after 3-fold extraction with toluene. Method 2 (see page 45 in Chapter 2) was used to prepare piperidine-monoDNS derivative and piperazine-diDNS derivative. The retention time of piperidine-monoDNS derivative was 8.6 min (Figure 5.29 (A)) and for piperazine-diDNS derivative was 15.1 min (Figure 5.29 (B)) when eluted with 65% acetonitrile: 35% Milli-Q-water.

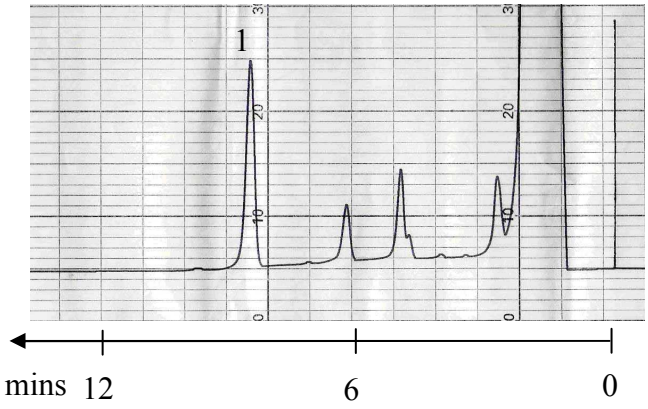

(A)

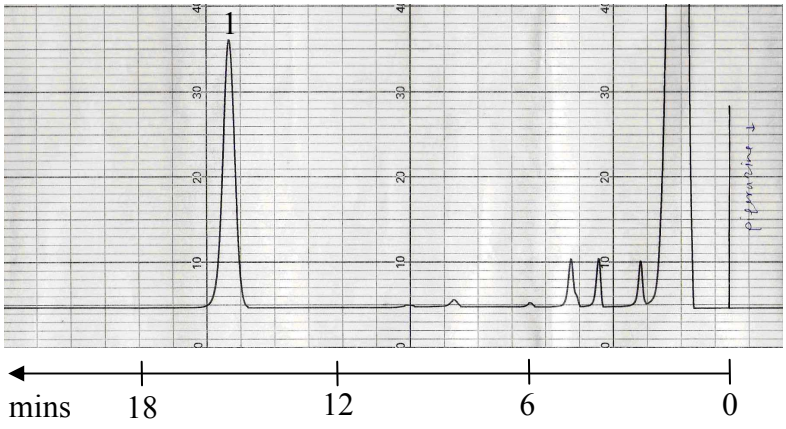

(B)

Figure 5.29 HPLC chromatogram of piperidine-monoDNS and piperazine-diDNS derivative, HPLC conditions: mobile phase is acetonitrile: Milli-Q-water (65:35) C18-hypersil column, flow rate 1 mL/min, fluorescence detector at λ_{ex} = 330 nm, λ_{ex} = 510 nm. (A) piperidine-monoDNS derivative. The chromatogram shows peak 1 = piperidine-monoDNS derivative at Rt = 8.6 min. (B) piperazine-diDNS derivative. The chromatogram shows peak 1 = piperazine-diDNS derivative at Rt = 15.1 min.

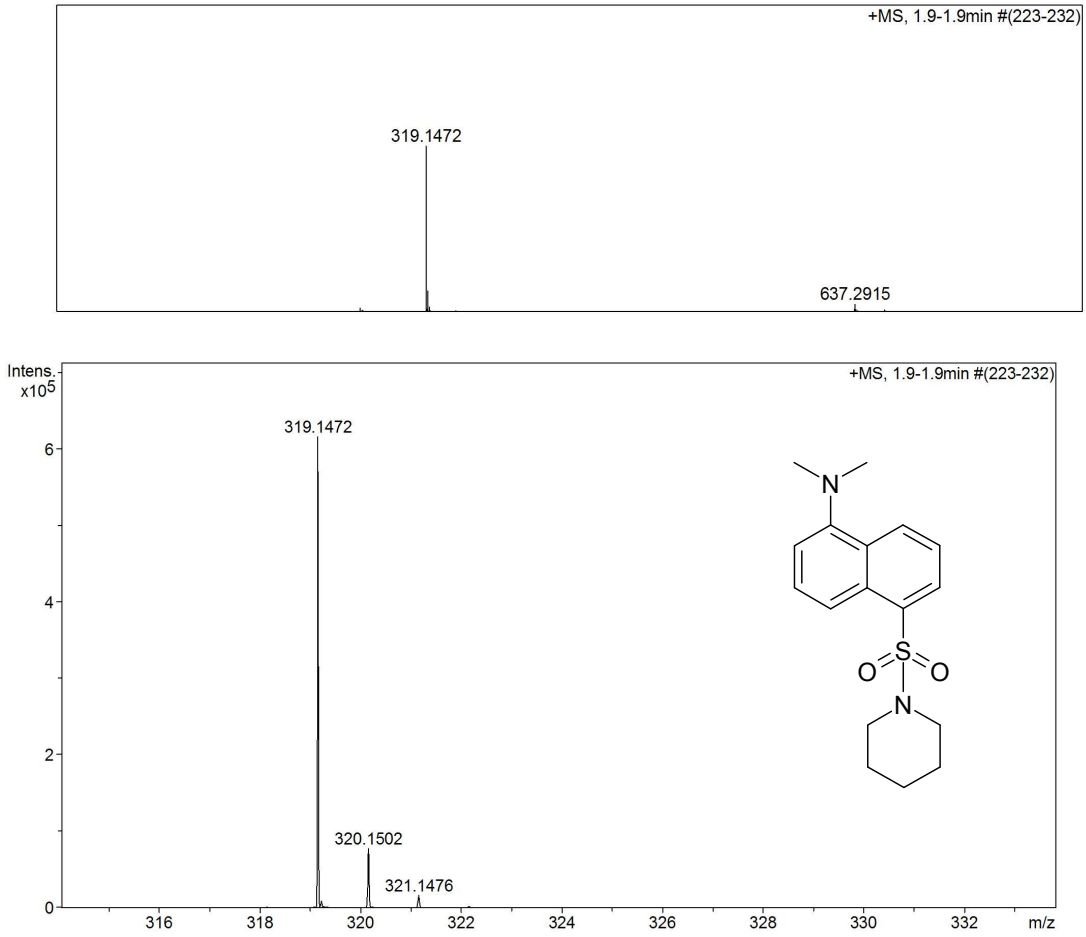

Figure 5.30 HR-ESI-MS spectra of piperidine-monoDNS derivative (M.W. = 318.1402, $C_{17}H_{22}N_2O_2S$) expected m/z $[M+H]^+$ ion = 319.1480 (found = 319.1472) and m/z $[2M+H]^+$ ion = 637.2882 (found = 637.2915).

These peaks were proved to be the expected DNS derivatives by HR-ESI-MS (Figure 5.30 for piperidine monoDNS derivative and Figure 5.31 for piperazine diDNS derivative). When the chromatographic peak area per millimole on column for a monoamine (piperidine) and diamine (piperazine) were compared, the peak area of piperazine was nearly twice that of the monoDNS compound. The slightly lower than expected values may be due to the differences in the chromatographic conditions.

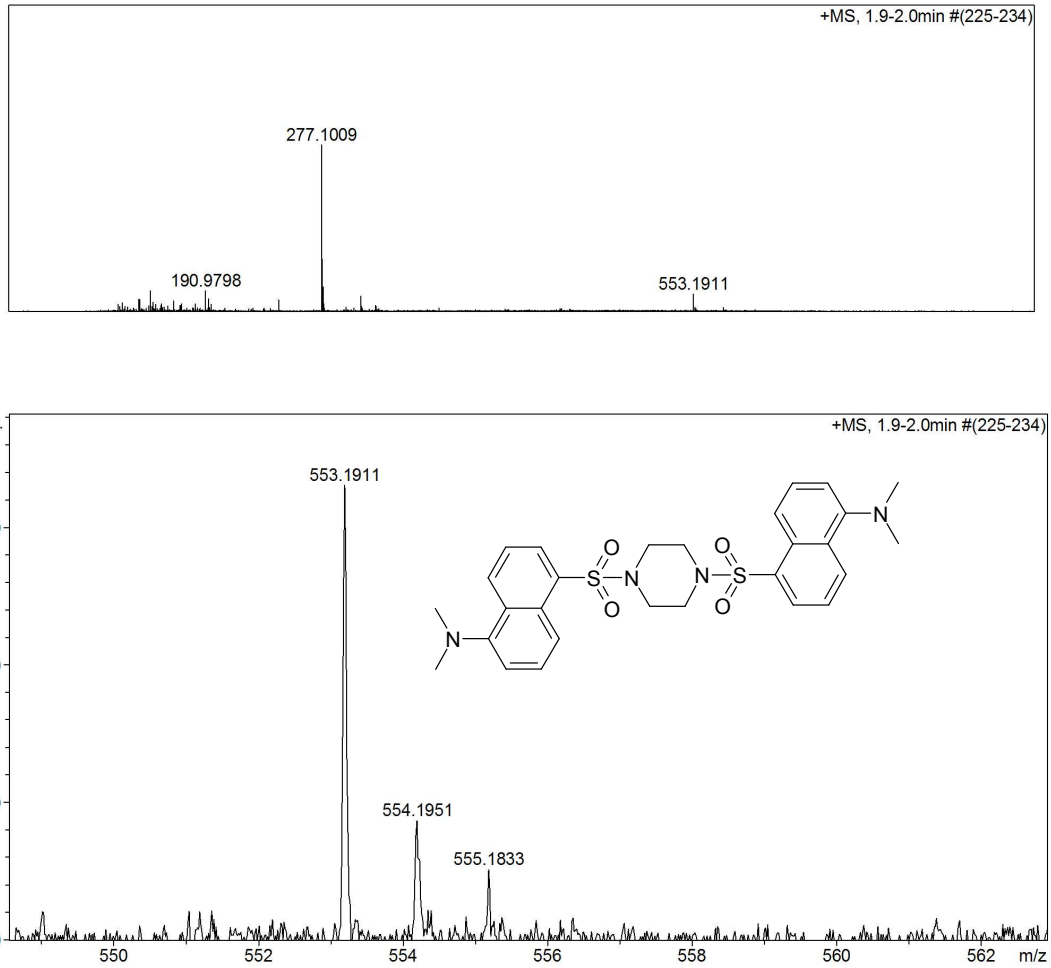

Figure 5.31 HR-ESI-MS spectra of piperazine-diDNS derivative (M.W. = 552.1865, $C_{28}H_{32}N_4O_4S_2$) expected m/z $[M+H]^+$ ion = 553.1943 (found = 553.1911). The spectrum is dominated by the doubly charged peak $[M+2H]^{2+}$ at m/z = 277.1011 (found = 277.1009).

For piperazine, no quenching effect of two fluorophores bound to piperazine was observed. Due to the rigid stereochemistry of (1,4-)piperazine-disulfonamide (diDNS), the two fluorophores are held apart from each other.

Characteristic of amine-DNS derivatives by HR-ESI-MS

One characteristic of amine-DNS derivatives is doubly charged ions which were observed by HR-ESI-MS *e.g.* spectra of 1,12-diaminododecane-diDNS derivative (Figure 5.32) and 1,5-diaminopentane-diDNS derivative (Figure 5.33) and the summary table of the doubly charged ions in Table 5.8.

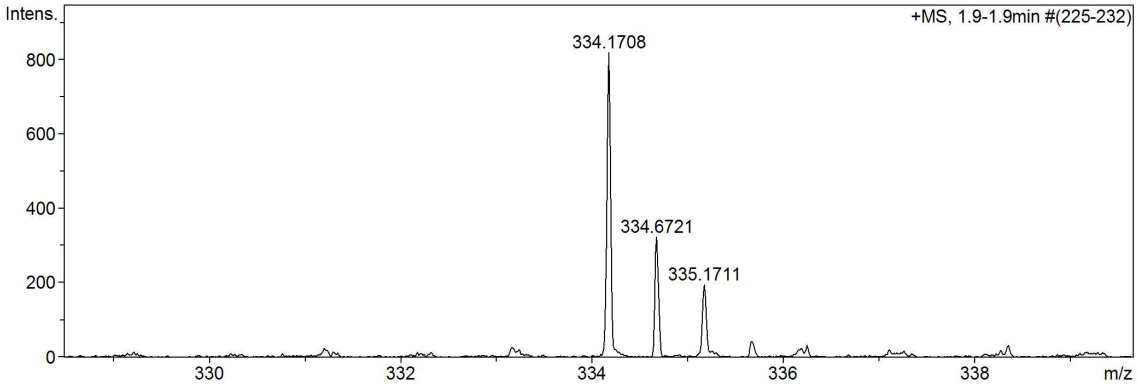

Figure 5.32 HR-ESI-MS spectrum of 1,12-diaminododecane-diDNS derivative (M.W. = 666.3273, $C_{36}H_{50}N_4O_4S_2$) expected m/z $[M+H]^+$ ion = 667.3352, doubly charged ion $[M+2H]^{2+}$ = 334.1715 (found = 334.1708).

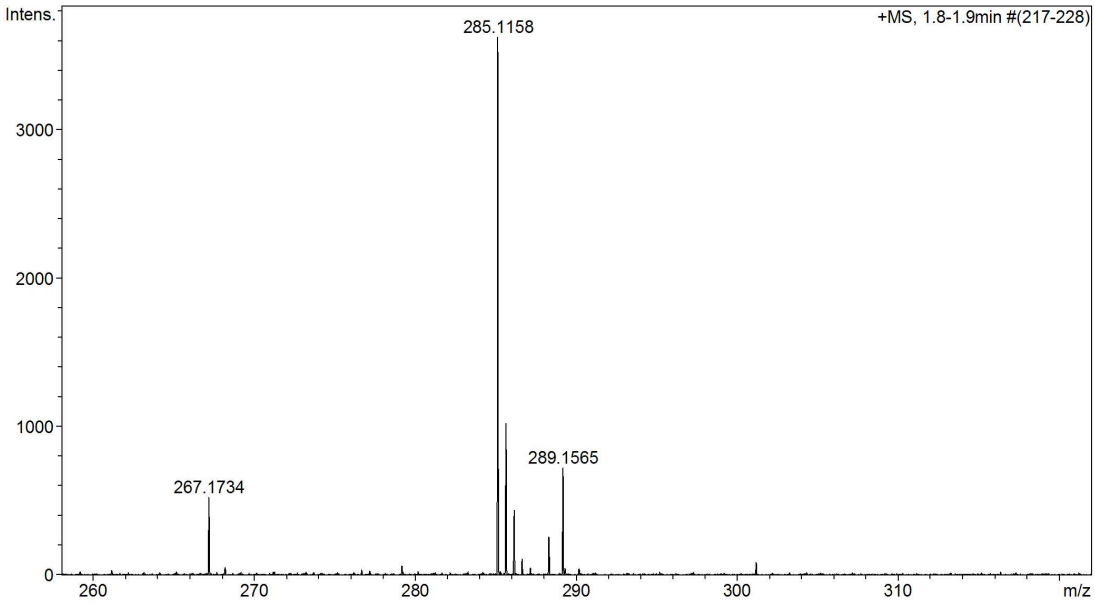

Figure 5.33 HR-ESI-MS spectrum of 1,5-diaminopentane-diDNS derivative (M.W. = 568.2178, $C_{29}H_{36}N_4O_4S_2$) expected m/z $[M+H]^+$ ion = 569.2256, doubly charged ion $[M+2H]^{2+}$ = 285.1167. (found = 285.1158).

DNS derivatives of a series of non-viral gene therapy (NVGT) vectors

The DNS derivatization method was applied to synthetic spermine fatty acyl amides, N^4,N^9-didecanoyl spermine-diDNS (Figure 5.34), N^4,N^9-dihexadecanoyl spermine-monoDNS (Figure 5.36), N^1,N^{12}-di-trifluoroacetyl-N^4,N^9-spermine-diDNS (Figure 5.38), N^1,N^4,N^9-tri-*t*-Boc-N^{12}-DNS spermine (Figure 5.40), N^4,N^9-digeranoyl spermine-monoDNS (Figure 5.42), N^1-DNS-N^4-decanoyl-N^9-cholesteryl carbamate spermine (Figure 5.44), N^4,N^9-oleoyl spermine monoDNS (Figure 5.46) and N^4,N^9-dioctadecanoyl spermine-monoDNS (Figure 5.48).

These conjugates are experimental non-viral vectors for DNA condensation with potential in gene delivery and therefore in non-viral gene therapy (NVGT). The DNS labelling method was applied to these molecules and HPLC chromatograms of these spermine derivatives were obtained, the data for retention time are shown in Table 5.6. The HR-ESI-MS of N^4,N^9-didecanoyl spermine-diDNS (Figure 5.35), N^4,N^9-dihexadecanoyl spermine-monoDNS (Figure 5.37), N^1,N^{12}-di-trifluoroacetyl-N^4,N^9-diDNS spermine (Figure 5.39), N^1,N^4,N^9-tri-*t*-Boc-N^{12}-DNS spermine (Figure 5.41), N^4,N^9-digeranoyl spermine-monoDNS (Figure 5.43), N^1-DNS-N^4-decanoyl-N^9-cholesteryl carbamate spermine (Figure 5.45), N^4,N^9-oleoyl spermine monoDNS (Figure 5.47) and N^4,N^9-dioctadecanoyl spermine-monoDNS (Figure 5.49) were all satisfactorily obtained.

Table 5.6 Retention time of non-viral gene therapy (NVGT) vectors-DNS derivative, HPLC conditions: mobile phase: acetonitrile: 1% formic acid in Milli-Q-water (90:10) C8-luna column, flow rate 1 mL/min, fluorescence detector at λ_{ex} = 330 nm, λ_{ex} = 510 nm.

NVGT vectors-DNS derivative	Retention time (min)
N^4,N^9-Didecanoyl spermine-diDNS	10
N^4,N^9-Digeranoyl spermine-monoDNS	19
N^4-Decanoyl-N^9-cholesteryl carbamate spermine-mono DNS	21
N^4,N^9-Oleoyl spermine monoDNS	13
N^4,N^9-Dioctadecanoyl spermine-monoDNS	24

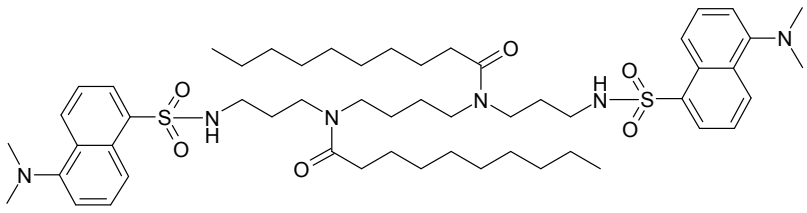

Figure 5.34 N^4,N^9-Didecanoyl spermine-diDNS.

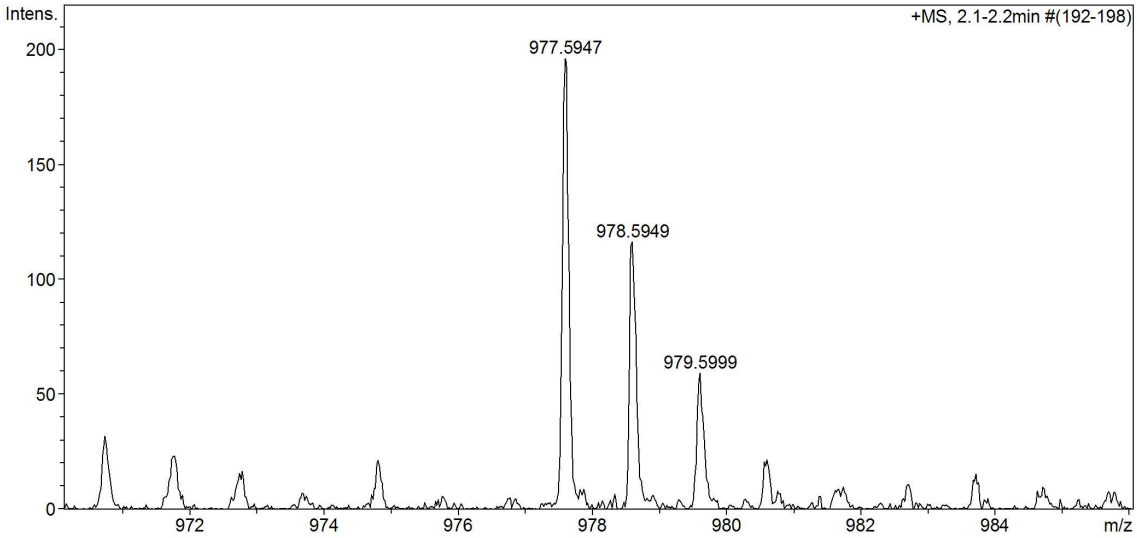

Figure 5.35 HR-ESI-MS spectrum of N^4,N^9-didecanoyl spermine-diDNS derivative (M.W. = 976.5894, $C_{54}H_{84}N_6O_6S_2$) expected m/z $[M+H]^+$ ion = 977.5972 (found = 977.5947) and $[M+Na]^+$ ion = 986.7472 (found = 986.7472).

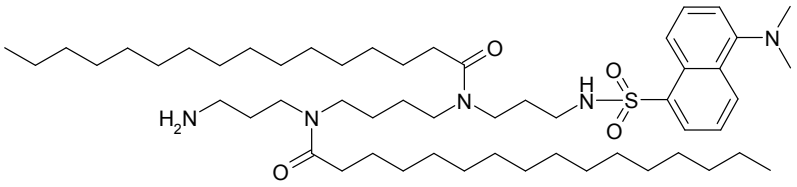

Figure 5.36 N^4,N^9-Dihexadecanoyl spermine-monoDNS.

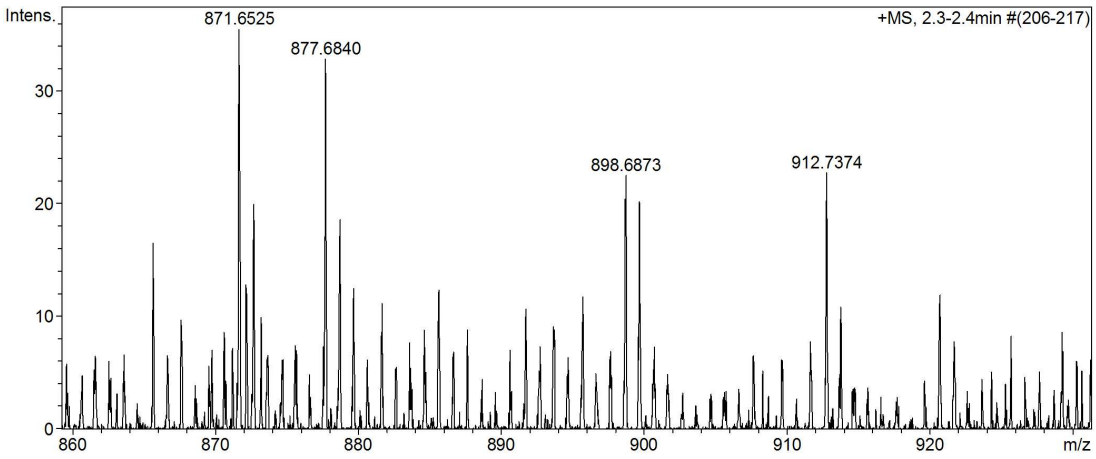

Figure 5.37 HR-ESI-MS spectrum of N^4,N^9-dihexadecanoyl spermine-monoDNS derivative (M.W. = 911.7261, $C_{54}H_{97}N_5O_4S$) expected m/z $[M+H]^+$ ion = 912.7339 (found = 912.7374).

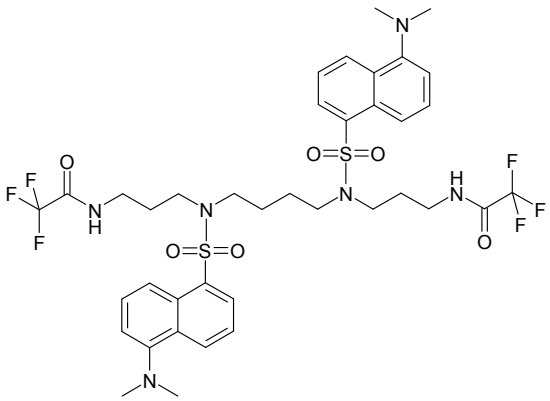

Figure 5.38 N^1,N^{12}-Di-trifluoroacetyl-N^4,N^9-diDNS spermine.

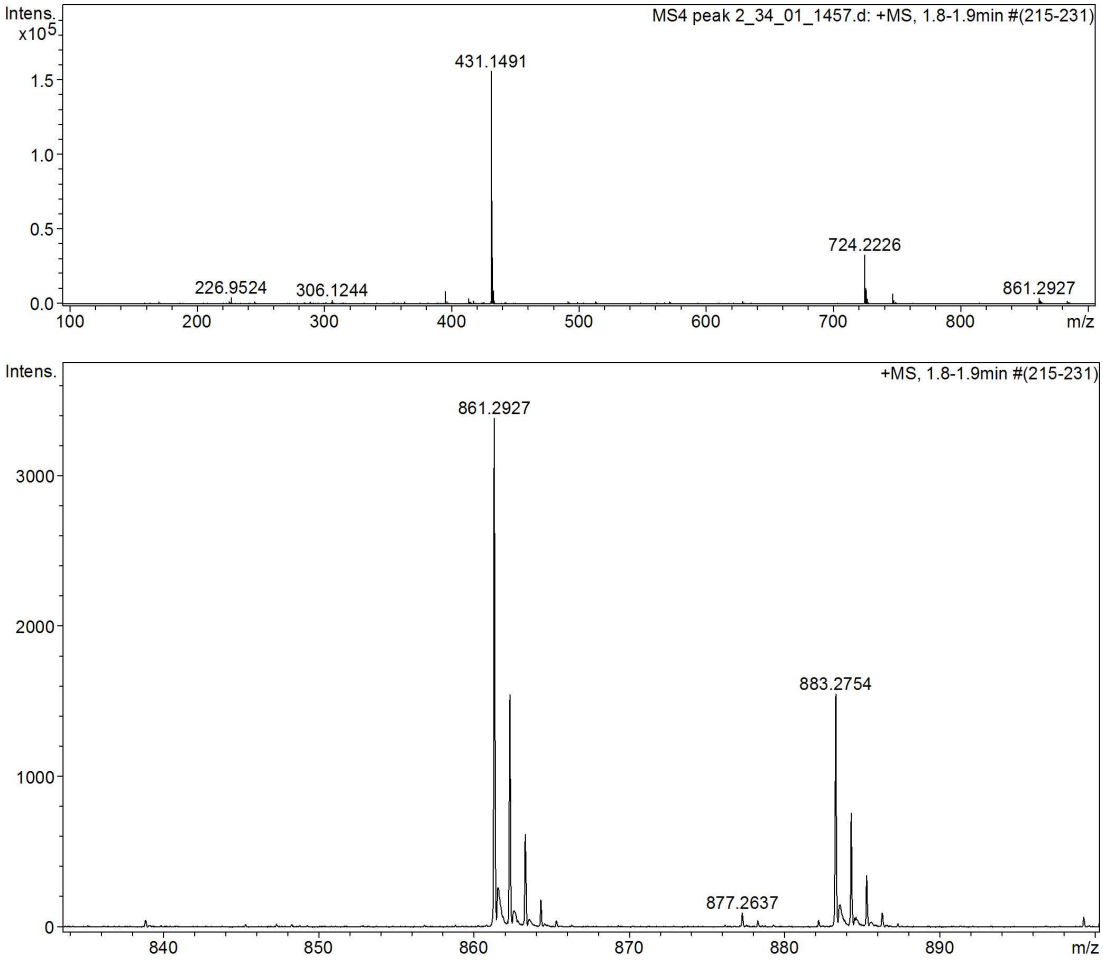

Figure 5.39 HR-ESI-MS spectra of N^1,N^{12}-di-trifluoroacetyl-N^4,N^9-diDNS spermine derivative (M.W. = 860.2824, $C_{38}H_{46}F_6N_6O_6S_2$) expected m/z $[M+H]^+$ ion = 861.2902 (found = 861.2927) doubly charged ion $[M+2H]^{2+}$ = 431.1490 (found = 431.1491) and $[M+Na]^+$ ion = 883.2722 (found = 883.2754).

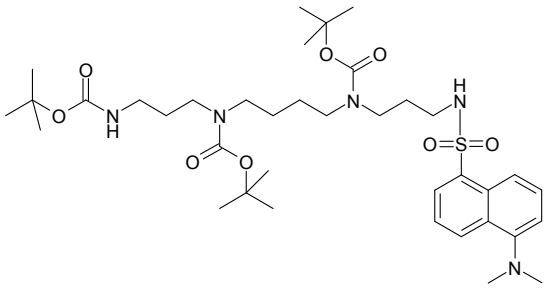

Figure 5.40 N^1,N^4,N^9-Tri-*t*-Boc-N^{12}-DNS spermine.

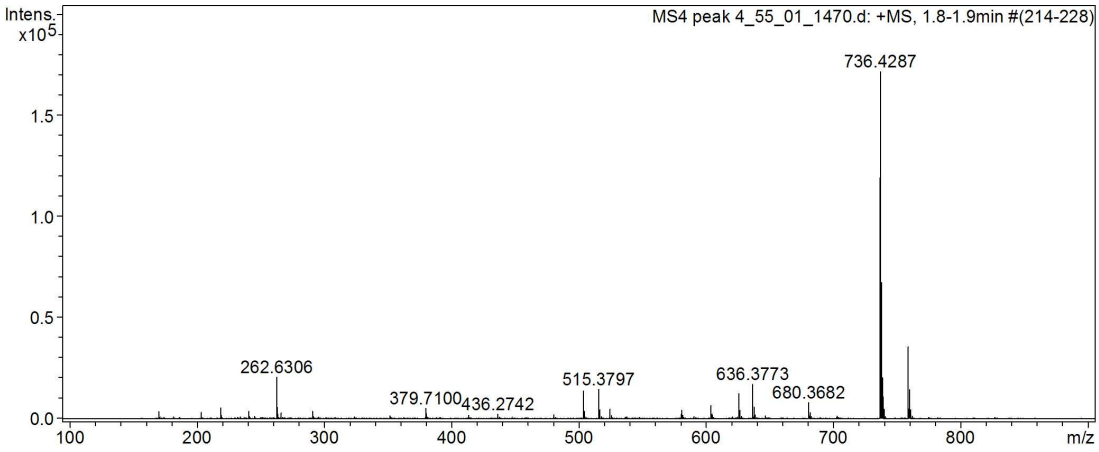

Figure 5.41 HR-ESI-MS spectrum of N^1,N^4,N^9-tri-*t*-Boc-N^{12}-DNS spermine derivative (M.W. = 735.4241, $C_{37}H_{61}N_5O_8S$) expected m/z $[M+H]^+$ ion = 736.4319 (found = 736.4287) and $[M+Na]^+$ ion = 758.4139.

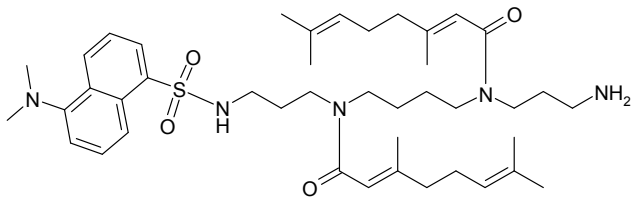

Figure 5.42 N^4,N^9-Digeranoyl spermine-monoDNS derivative.

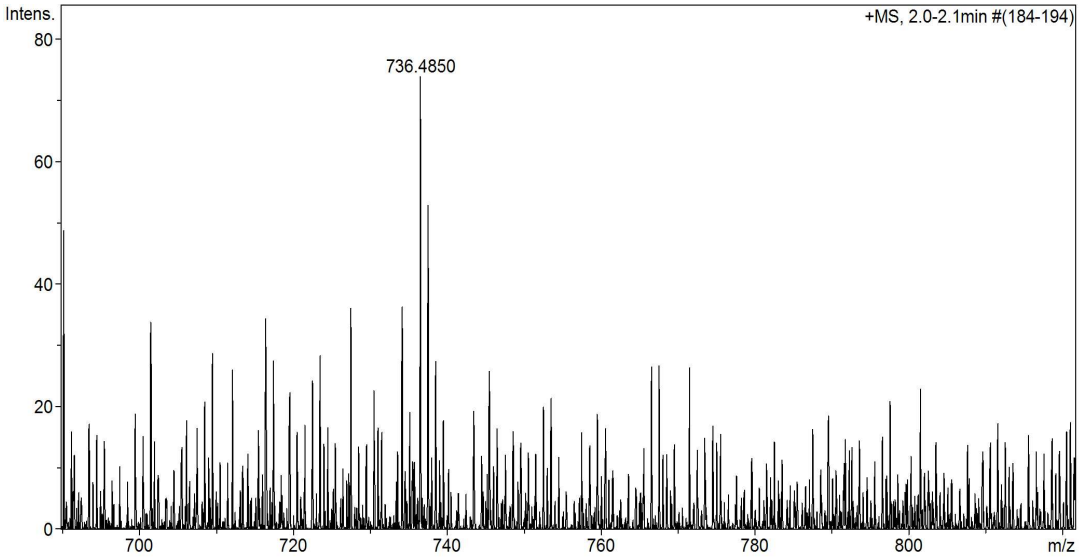

Figure 5.43 HR-ESI-MS spectrum of N^4,N^9-Digeranoyl spermine-monoDNS derivative (M.W. = 735.4757, $C_{42}H_{65}N_5O_4S$) expected m/z $[M+H]^+$ ion = 736.4835 (found = 736.4850).

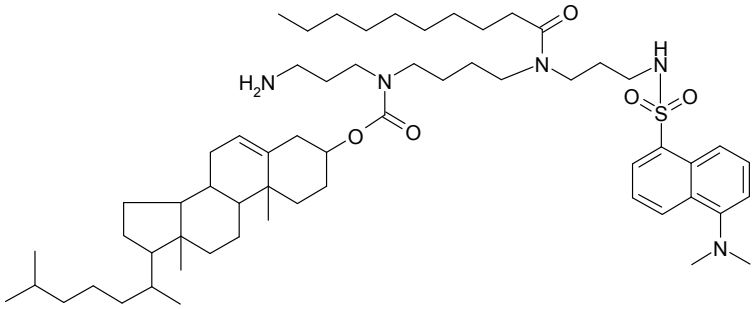

Figure 5.44 N^1-DNS-N^4-decanoyl-N^9-cholesteryl carbamate spermine $C_{60}H_{99}N_5O_5S$.

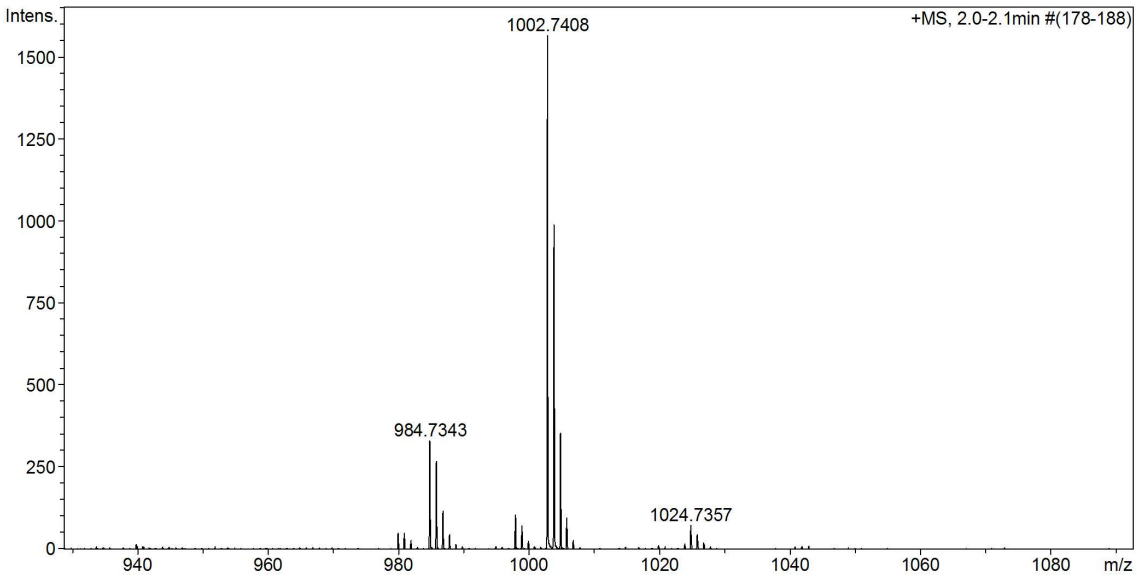

Figure 5.45 HR-ESI-MS spectrum of N^1-DNS-N^4-decanoyl-N^9-cholesteryl carbamate spermine derivative (M.W. = 1001.7367, $C_{60}H_{99}N_5O_5S$) expected m/z $[M+H]^+$ ion = 1002.7445. (found = 1002.7408) and $[M+Na]^+$ ion = 1024.7264 (found = 1024.7357).

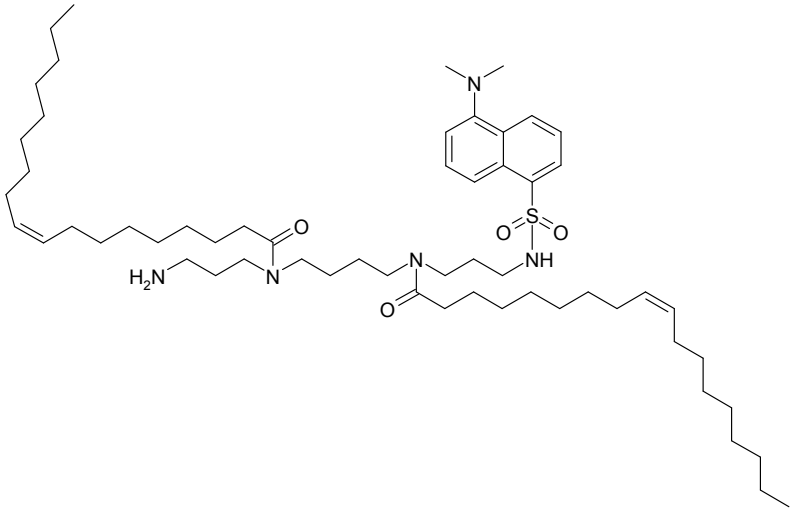

Figure 5.46 N^4,N^9-Oleoyl spermine monoDNS derivative.

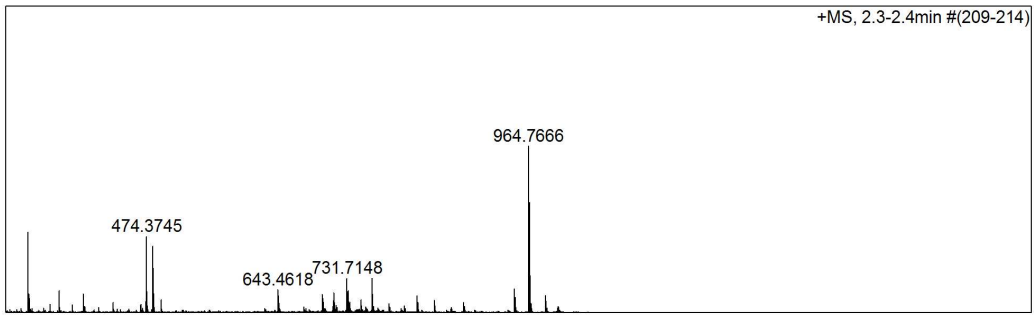

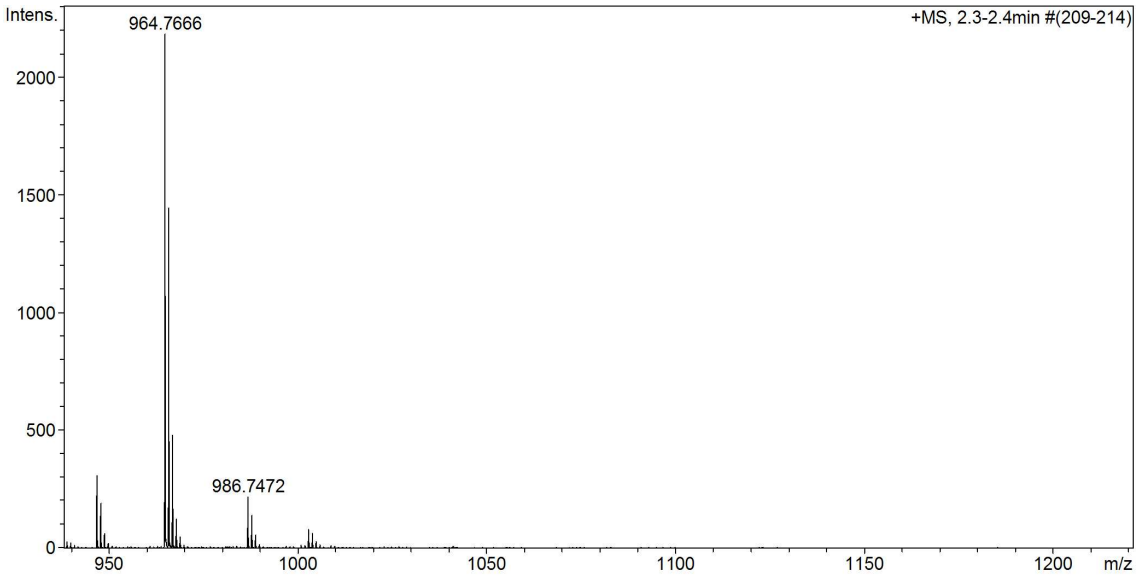

Figure 5.47 HR-ESI-MS spectra of N^4,N^9-Oleoyl spermine monoDNS derivative (M.W. = 963.7574, $C_{58}H_{101}N_5O_4S$) expected m/z $[M+H]^+$ ion = 964.7652. (found = 964.7666), doubly charged $[M+2H]^{2+}$ = 482.8865 and $[M+Na]^+$ ion = 986.7472 (found = 986.7472).

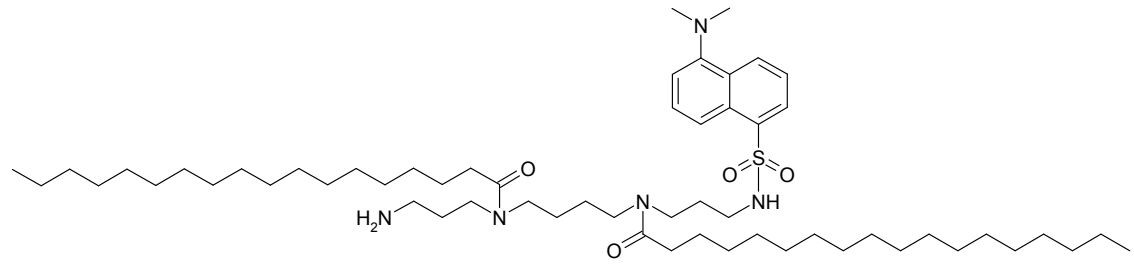

Figure 5.48 N^4,N^9-Dioctadecanoyl spermine-monoDNS derivative.

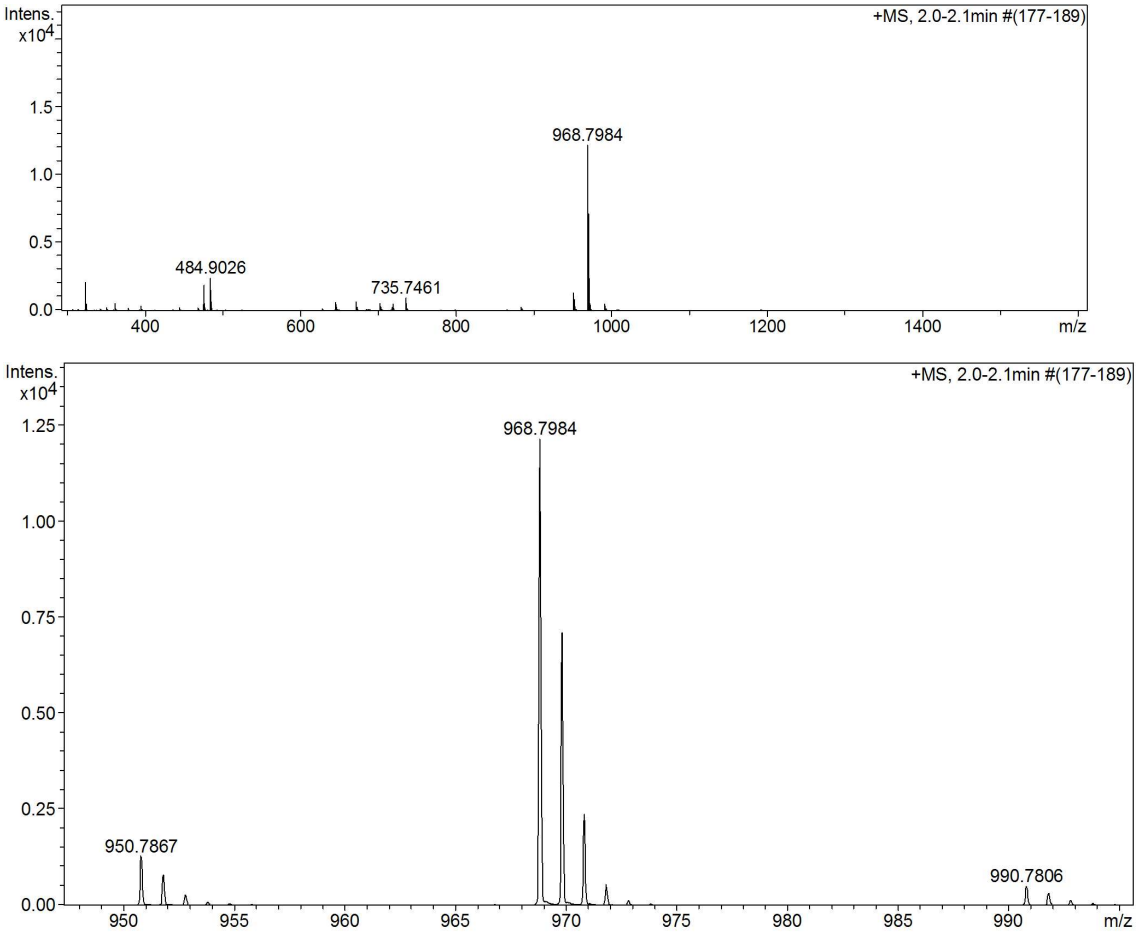

Figure 5.49 HR-ESI-MS spectra of N^4,N^9-Dioctadecanoyl spermine-monoDNS derivative (M.W. = 967.7887, $C_{58}H_{105}N_5O_4S$) expected m/z $[M+H]^+$ ion = 968.7965. (found = 968.7984), doubly charged ion $[M+2H]^{2+}$ = 484.9022 (found = 484.9026) and $[M+Na]^+$ ion = 990.7785 (found = 990.7806).

DNS derivatization of aminoglycosides

Glucosamine was examined by using method 2 for dansylation. The glucosamine-monoDNS derivative is a polar molecule which contains many OH groups so it can elute

rapidly under reversed-phase conditions (Figure 5.50). Glucosamine-monoDNS derivative was confirmed by HR-ESI-MS (Figure 5.51).

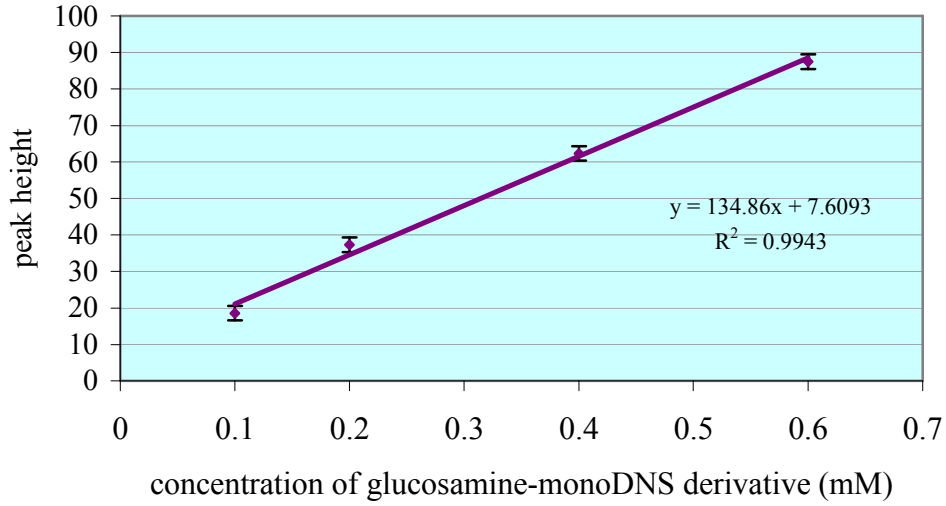

Figure 5.50 Calibration curve of glucosamine-DNS derivatives (n = 5).

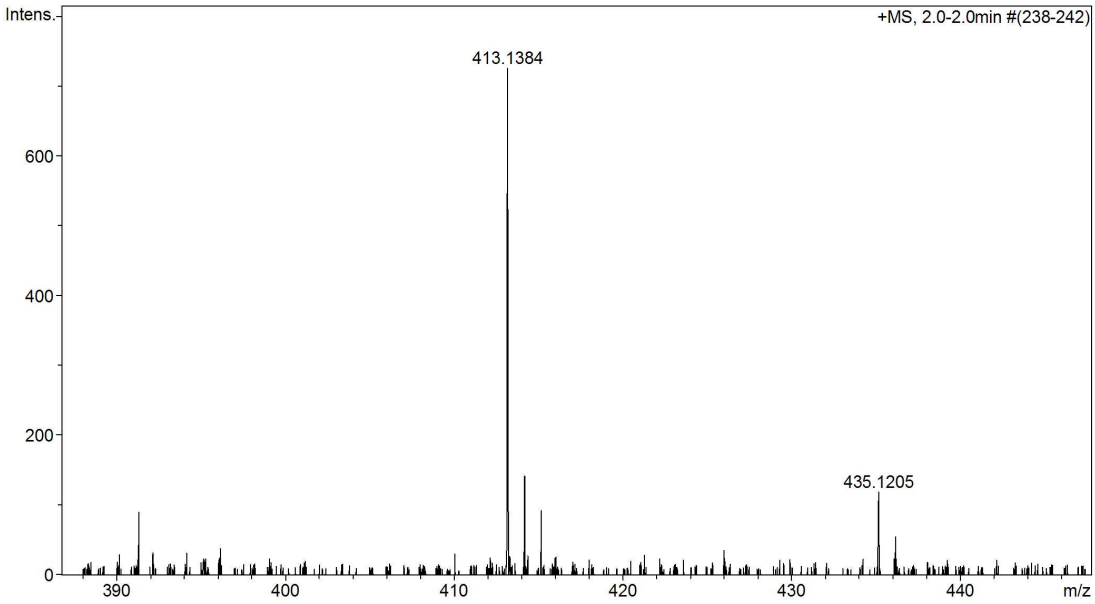

Figure 5.51 HR-ESI-MS spectra of glucosamine-monoDNS derivative (M.W. = 412.1304, $C_{18}H_{24}N_2O_7S$) expected m/z $[M+H]^+$ ion = 413.1383 (found = 413.1384) and $[M+Na]^+$ ion = 435.1202 (found= 435.1205).

Using method 1 to derivatize 0.1 mM glucosamine with DNS Cl reagent, the glucosamine-DNS derivative eluted at Rt = 1.60 min (HPLC conditions: mobile phase: acetonitrile: Milli-Q-water (40:60) C18-Hypersil column, flow rate 1 mL/min, fluorescence detector at λ_{ex} = 330 nm, λ_{ex} = 510 nm). The reaction was completed using a 4-fold excess of DNS Cl (Figure 5.52).

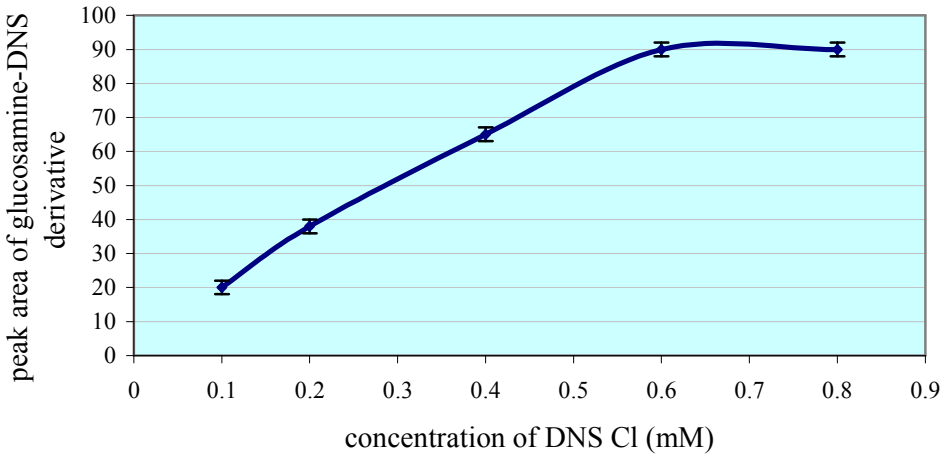

Figure 5.52 Peak area of glucosamine-DNS derivative versus the concentration of DNS Cl (n = 5), glucosamine (1 mL, 1 mM) against DNS Cl (1 mL of various concentrations). Peak areas were calculated by height x 0.5 width of peak, and peak areas are reported in cm^2.

Kanamycin-DNS derivatives

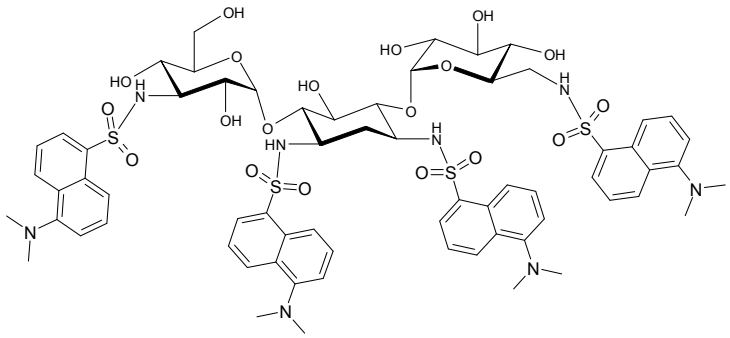

Figure 5.53 Kanamycin-tetraDNS derivative.

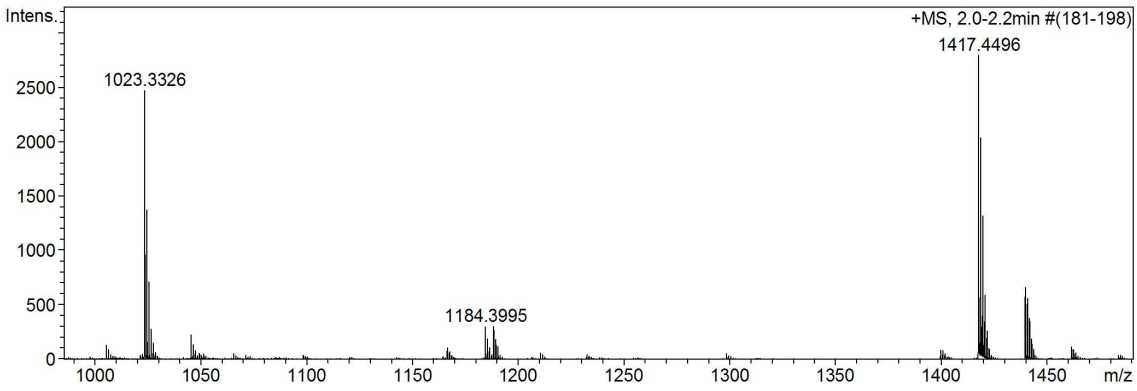

Figure 5.54 HR-ESI-MS spectra of kanamycin-tetraDNS derivative (M.W. = 1416.4422, $C_{66}H_{80}N_8O_{19}S_4$) expected m/z $[M+H]^+$ ion = 1417.4500 (found = 1417.4496) and $[M+Na]^+$ ion = 1439.4320.

Method 2 was used for dansylation to prepare kanamycin-tetraDNS derivative (Figure 5.53). The HPLC chromatogram was obtained (Figure 5.55), the desired peak collected and the product was confirmed as the tetrasubstituted derivative by HR-ESI-MS (Figure 5.54).

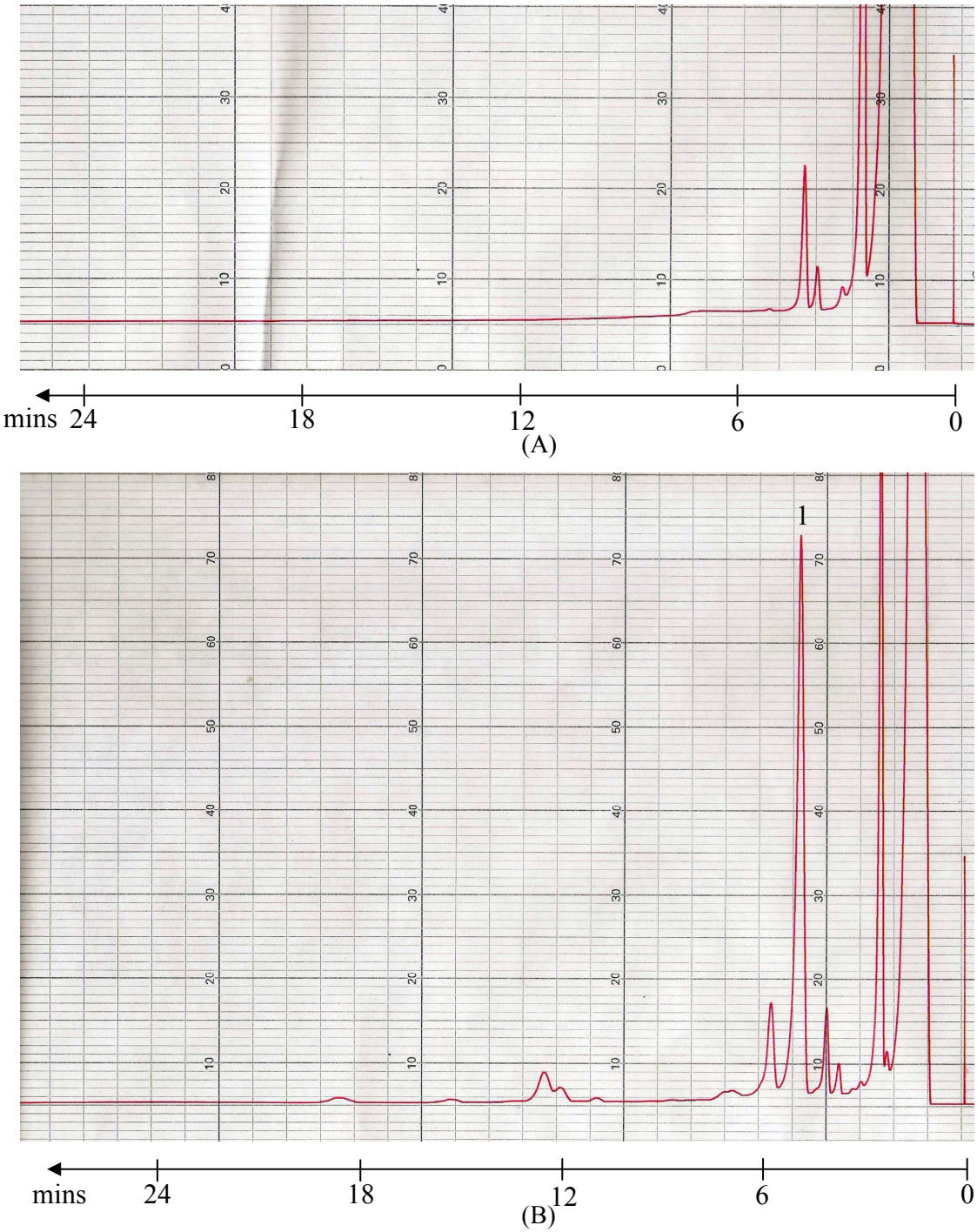

Figure 5.55 HPLC chromatogram of kanamycin-tetraDNS derivative, HPLC conditions: mobile phase is acetonitrile: Milli-Q-water (70:30) C8-luna column, flow rate 1 mL/min, fluorescence detector at λ_{ex} = 330 nm, λ_{ex} = 510 nm. (A) The chromatogram of blank (B) The chromatogram shows peak 1 = kanamycin-tetraDNS derivative at Rt = 4.9 min.

Table 5.8 Summary of HR-ESI-MS from dansylation.

DNS derivatives	Molecular Formula	HR-ESI-MS calculated	HR-ESI-MS found
Aspartic acid-monoDNS $C_{16}H_{18}N_2O_6S$	$C_{16}H_{19}N_2O_6S$ $(M+H)^+$	367.0964	367.0942
Piperidine-monoDNS $C_{17}H_{22}N_2O_2S$	$C_{17}H_{23}N_2O_2S$ $(M+H)^+$	319.1475	319.1472
Piperazine-monoDNS $C_{16}H_{21}N_3O_2S$	$C_{16}H_{22}N_3O_2S$ $(M+H)^+$	320.1437	320.2235
Piperazine-diDNS $C_{28}H_{32}N_4O_4S_2$	$C_{28}H_{33}N_4O_4S_2$ $(M+H)^+$ $C_{28}H_{34}N_4O_4S_2$ $(M+2H)^{2+}$	553.1938 277.1011	553.1911 277.1009
1,4-Diaminobutane-monoDNS $C_{16}H_{23}N_3O_2S$	$C_{16}H_{24}N_3O_2S$ $(M+H)^+$	322.1589	322.1562
1,4-Diaminobutane-diDNS $C_{28}H_{34}N_4O_4S_2$	$C_{28}H_{35}N_4O_4S_2$ $(M+1)^+$	555.2094	555.2091
1,7-Diaminoheptane-monoDNS $C_{19}H_{29}N_3O_2S$	$C_{19}H_{30}N_3O_2S$ $(M+H)^+$	364.2053	364.2036
1,7-Diaminoheptane-diDNS $C_{31}H_{40}N_4O_4S_2$	$C_{31}H_{41}N_4O_4S_2$ $(M+H)^+$	597.25564	597.2250
1,12-Diaminododecane-diDNS $C_{36}H_{50}N_4O_4S_2$	$C_{36}H_{52}N_4O_4S_2$ $(M+2H)^{2+}$	334.1696	334.1708
Spermidine-triDNS $C_{43}H_{52}N_6O_6S_3$	$C_{43}H_{53}N_6O_6S_3$ $(M+H)^+$	845.3183	845.3163
	$C_{43}H_{52}N_6NaO_6S_3$ $(M+Na)^+$	867.3003	867.2992
N-(4-Aminobutyl) hexahydropyrimidine-monoDNS $C_{20}H_{30}N_4O_2S$	$C_{20}H_{31}N_4O_2S$ $(M+H)^+$	391.2162	391.2148
N-(4-Aminobutyl) hexahydropyrimidine-diDNS $C_{32}H_{41}N_5O_4S_2$	$C_{32}H_{42}N_5O_4S_2$ $(M+H)^+$	624.2678	624.2676
Spermine-tetraDNS $C_{58}H_{70}N_8O_8S_4$	$C_{58}H_{71}N_8O_8S_4$ $(M+H)^+$	1135.4272	1135.4241
	$C_{58}H_{70}N_8NaO_8S_4$ $(M+Na)^+$	1157.4097	1157.4061
1,4-(Dihexahydropyrimidine) butane-diDNS $C_{36}H_{48}N_6O_4S_2$	$C_{36}H_{49}N_6O_4S_2$ $(M+H)^+$	693.3251	693.3275
1-(Hexahydropyrimidine)-5-aza-aminooctane-triDNS $C_{47}H_{59}N_7O_6S_3$	$C_{47}H_{59}N_7O_6S_3$ $(M+H)^+$	914.3767	914.3772
	$C_{47}H_{59}N_7NaO_6S_3$ $(M+Na)^+$	936.3586	936.3560
N^4,N^9-Oleoyl spermine-monoDNS $C_{58}H_{101}N_4O_4S_2$	$C_{58}H_{102}N_4O_4S_2$ $(M+H)^+$	964.7647	964.7666
N^4,N^9-Didecanoyl spermine-diDNS $C_{54}H_{84}N_6O_6S_2$	$C_{54}H_{85}N_6O_6S_2$ $(M+H)^+$	977.5972	977.5947
N^4-Decanoyl-N^9-cholesteryl carbamate spermine-mono DNS $C_{60}H_{99}N_5O_5S$	$C_{60}H_{100}N_5O_5S$ $(M+H)^+$	1002.7440	1002.7434
	$C_{60}H_{99}N_5NaO_5S$ $(M+Na)^+$	1024.7264	1024.7357
N^4,N^9-Digeranoyl spermine-monoDNS $C_{42}H_{65}N_5O_4S$	$C_{42}H_{66}N_5O_4S$ $(M+H)^+$	736.4830	736.4850

N^4,N^9-Dioctadecanoyl spermine-monoDNS $C_{58}H_{105}N_5O_4S$	$C_{58}H_{106}N_5O_4S$ $(M+H)^+$	968.7965	968.7984
Kanamycin-tetra DNS $C_{66}H_{80}N_8O_{19}S_4$	$C_{66}H_{81}N_8O_{19}S_4$ $(M+H)^+$	1417.4500	1417.4496

Conclusions of DNS Cl derivatization

DNS Cl reacts with primary and secondary amines with the result of full derivatization if the molar ratio to DNS Cl is enough, resulting in diDNS derivatives for diamines such as 1,4-diaminobutane, 1,5-diaminopentane, 1,7-diaminoheptane, triDNS derivative for spermidine and tetraDNS derivative for spermine. However, the monoDNS derivative of each diamine was obtained when we used lower DNS Cl ratios whilst investigating the phenomenon of fluorescence yield. Peaks in HPLC chromatograms from spermine-tetraDNS derivatives are eluted after 30 min even when a C8 column was used (with isocratic mobile phase of acetonitrile: Milli-Q-water = 70:30) due to the hydrophobic nature of the molecule and its high molecular weight. However, by converting spermine into 1,4-dihexahydropyrimidine-butane (the dihexahydropyrimidine derivative of spermine) before dansylation, the retention time was reduced to ~19 min. The excess of DNS Cl reagent was destroyed using a solution of alanine. Polyamines were analysed on an Reversed-phase ODS Hypersil, ODS luna, C8 luna column with an isocratic mobile phase mixture of acetonitrile and Milli-Q-water at a flow rate of 1 mL/min with fluorescence detection at excitation and emission wavelength of 330 and 510 nm, respectively and UV detection at λ_{max} = 330 nm. The reaction time of DNS Cl at 20^{o}C gave a lower yield than at 60^{o}C and it is better to set the temperature at 60^{o}C rather than at room temperature which might vary.

Several advantages of DNS Cl derivatization are: its high degree of reproducibility, precision, sensitivity and the high stability of the derivatives. However, when compared with other derivatization methods, DNS Cl requires more time than the others. The DNS Cl derivatization might not be suitable for large molecules. If the molecule has many reactive amino groups, then when it is (poly)-labelled with DNS Cl the product is more lipophilic and therefore slower to elute from the HPLC column. In this study, the simultaneous use of two detectors connected in series for the determination of polyamine-DNS derivatives, to detect both UV and fluorescence benefits in not missing a peak that might detected by only one detector, thus increasing the reliability of the method. On the basis of peak size, fluorescence detection showed higher sensitivity for amine-DNS derivatives. However, both detectors were shown to be accurate and produced calibration curves of good linearity.

CHAPTER 6: THERMOSPERMINE SYNTHESIS

Spermidine (3.4) and spermine (3.4.3) are major polyamines in most organisms. Spermine is probably present in all eukaryotes; however, it is rare in prokaryotes or might be replaced by thermine (norspermine, 3.3.3) and thermospermine (3.3.4) *e.g.* in certain species of thermophilic bacteria. *Thermus thermophilus* is an extreme thermophile and the major polyamines in this bacterium, grown under the optimal conditions at 80^0C, are thermine and thermospermine (Figure 6.1) (Oshima, 1979).

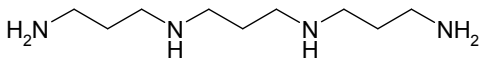

Thermine (3.3.3)

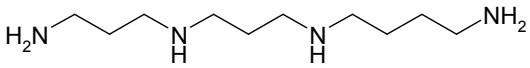

Thermospermine (3.3.4)

Figure 6.1 Thermine ($C_9H_{24}N_4$) has a 3.3.3 methylene distribution, one methylene less than spermine (3.4.3), Thermospermine ($C_{10}H_{26}N_4$) with its 3.3.4 methylene arrangement is an isomer of spermine (3.4.3).

Thermus aquaticus is a species of thermophillus that thrives at 70^0C. It is the source of the heat-resistant enzyme Taq DNA polymerase, one of the most important enzymes in molecular biology due to its use in the polymerase chain reaction (PCR) DNA amplification technique.

Using current methods, thermine (3.3.3) and thermospermine (3.3.4) are difficult to distinguish from spermine (3.4.3) (Oshima, 1983; Knott *et al.*, 2007). It is also possible that some literature reports of spermine biosynthesis may in fact be partly or wholly due to thermospermine (Hamana and Matsuzaki, 1984; Hosoya *et al.*, 2004). Thus, thermospermine has been synthesised in order to develop improved methods for its separation from spermine and their analysis. The synthesis started with spermidine (3.4) and used the method of Ganem and Chantrapromma (1983) (Figure 6.2).

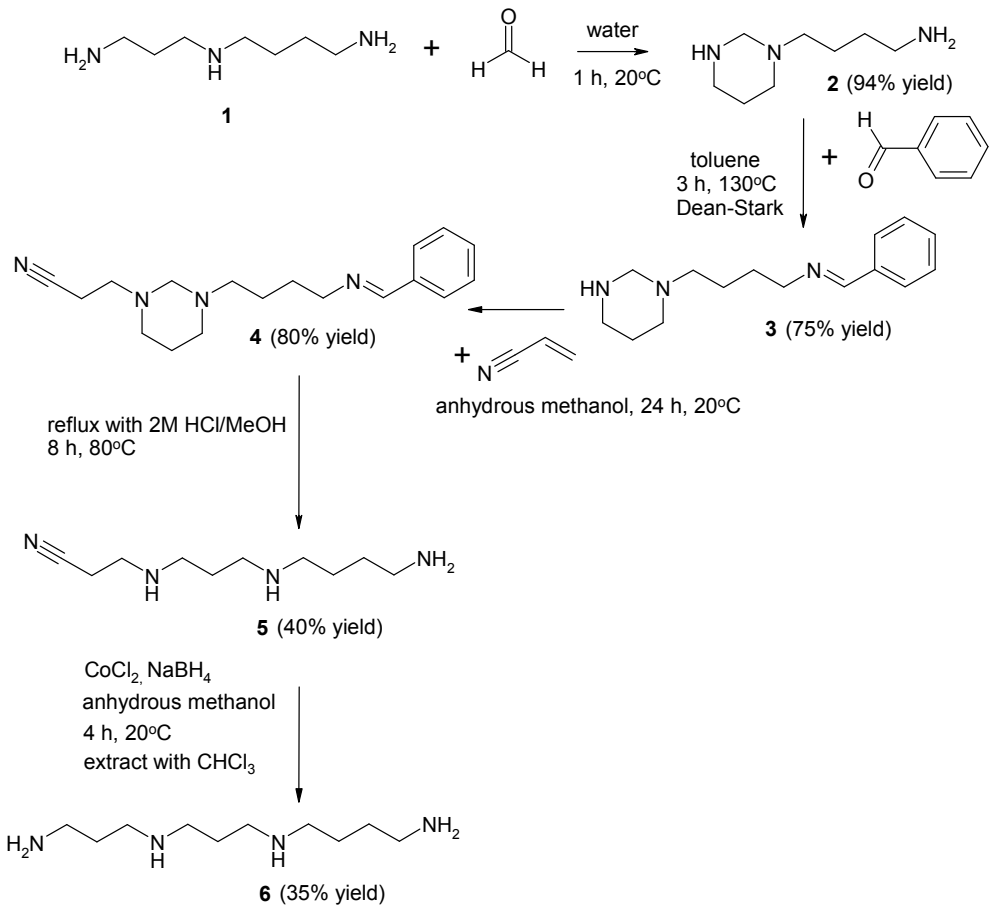

Figure 6.2 Thermospermine synthesis (Method 1).

Method 1 step 1 *N*-(4-Aminobutyl)hexahydropyrimidine (2)

N-(4-Aminobutyl)hexahydropyrimidine (**2**) was prepared by the reaction of spermidine and formaldehyde (equal mole ratios) to give the stable hexahydropyrimidine ring as a viscous oily liquid which displayed a molecular weight greater than that of spermidine by the desired 12 mass units (found 158.1630, $C_8H_{20}N_3$ requires m/z $[M+H]^+$ = 158.1657). The product obtained from formaldehyde (2 equiv.) gave the HR-ESI-MS (Figure 6.3). This spectrum shows a peak at m/z 158.1630 (required = 158.1657) corresponding to the $[M+H]^+$ ion derived from *N*-(4-aminobutyl)hexahydropyrimidine (**2**) together with a trace peak at m/z 146.1673 (required = 146.1657) corresponding to the $[M+H]^+$ ion of the starting material spermidine. However, the major peak was at m/z 170.1635 (required = 170.1657) which corresponds to the $[M+H]^+$ ion of the *N-(N′*-methylene-4-iminobutyl)-hexahydropyrimidine (**13**) (Figure 6.4) which had an additional molecule of formaldehyde reacted at the remaining primary amino group.

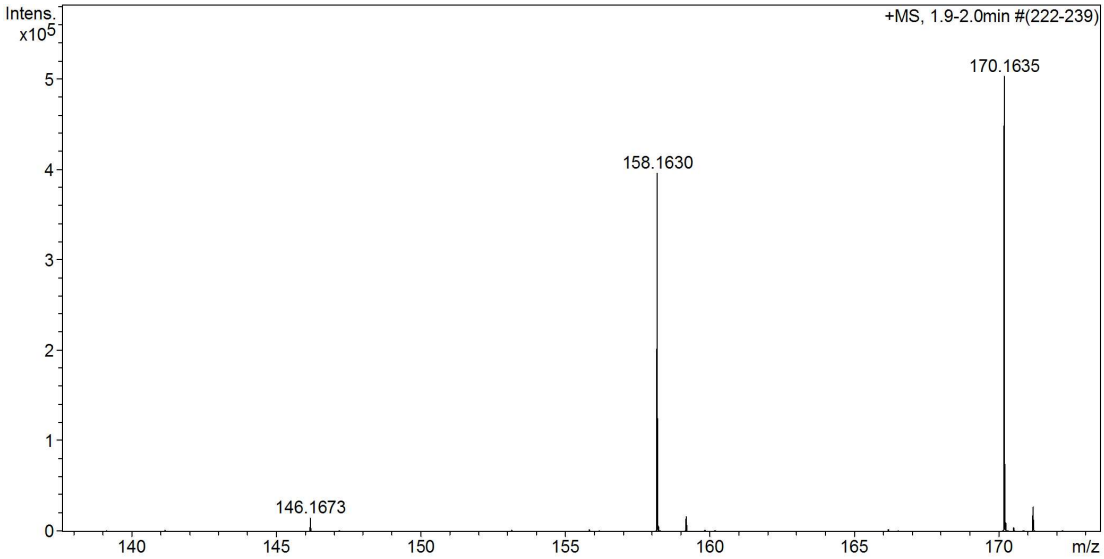

Figure 6.3 HR-ESI-MS spectrum of spermidine (**1**) (M.W. = 145.1579, $C_7H_{19}N_3$) expected m/z $[M+H]^+$ ion = 146.1657 (found = 146.1673), *N*-(4-aminobutyl) hexahydropyrimidine (**2**) (M.W. = 157.1579, $C_8H_{19}N_3$) expected m/z $[M+H]^+$ ion = 158.1657 (found = 158.1630), *N-(N'*-methylene-4-iminobutyl)-hexahydropyrimidine (**13**) (M.W. = 169.1579, $C_9H_{19}N_3$) expected m/z $[M+H]^+$ ion = 170.1657 (found = 170.1635).

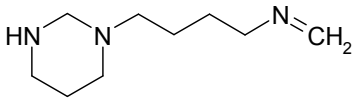

13

Figure 6.4 *N-(N'*-Methylene-4-iminobutyl)-hexahydropyrimidine (**13**), $C_9H_{19}N_3$ (M.W = 169.1579).

Even with 1.1 equiv. of formaldehyde a small peak of m/z = 170.1648 (required = 170.1657) was observed (Figure 6.5), but was virtually eliminated when 0.9 equiv. of formaldehyde were used (Figure 6.6). The reaction were examined in different mole ratio of formaldehyde, the results were obtained (Table 6.1). The desired product, *N*-(4-aminobutyl) hexahydropyrimidine (**2**), was examined by NMR spectroscopy (Figures 6.7, 6.8, and 6.9) and the peaks were assigned.

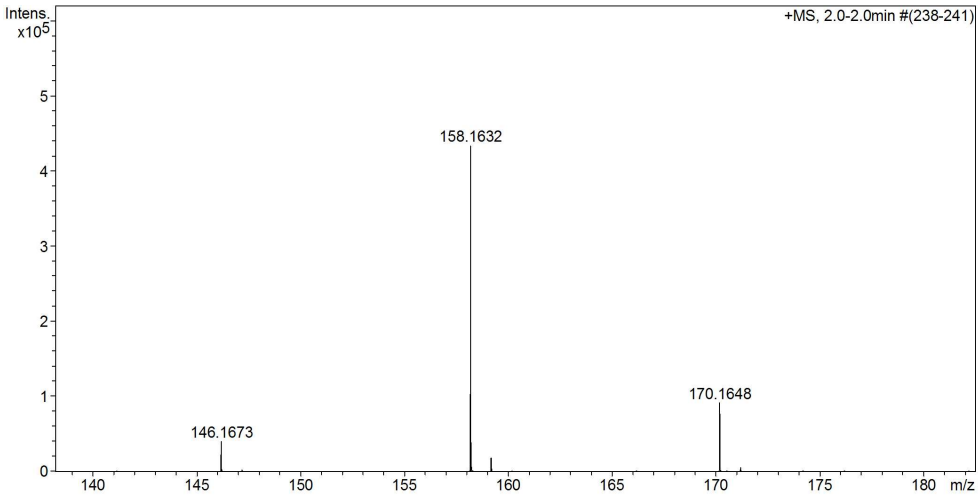

Figure 6.5: HR-ESI-MS spectrum of products by the reaction of 1.1 equiv. of formaldehyde against spermidine. The spectrum shows spermidine (**1**) (M.W. = 145.1579, $C_7H_{19}N_3$) expected m/z $[M+H]^+$ ion = 146.1657 (found = 146.1673), *N*-(4-aminobutyl) hexahydropyrimidine (**2**) (M.W. = 157.1579, $C_8H_{19}N_3$) expected m/z $[M+H]^+$ ion = 158.1657 (found = 158.1632), *N-(N'*-methylene-4-iminobutyl)-hexahydropyrimidine (**13**) (M.W. = 169.1579, $C_9H_{19}N_3$) expected m/z $[M+H]^+$ ion = 170.1657 (found = 170.1648).

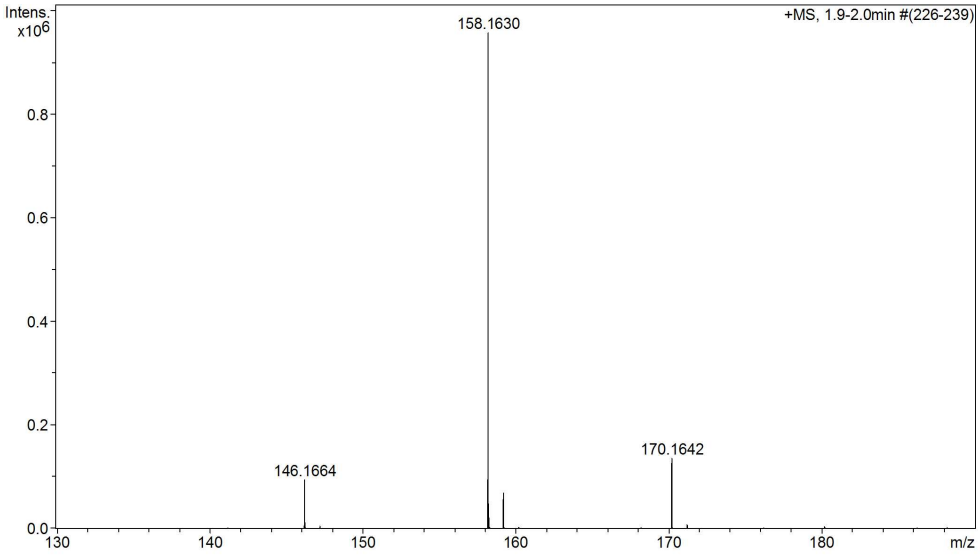

Figure 6.6 HR-ESI-MS spectrum of products by the reaction of 0.9 equiv. of formaldehyde against spermidine. The spectrum shows spermidine (**1**) (M.W. = 145.1579, $C_7H_{19}N_3$) expected m/z $[M+H]^+$ ion = 146.1657 (found = 146.1664), *N*-(4-aminobutyl) hexahydropyrimidine (**2**) (M.W. = 157.1579, $C_8H_{19}N_3$) expected m/z $[M+H]^+$ ion = 158.1657 (found = 158.1630), *N-(N'*-methylene-4-iminobutyl)-hexahydropyrimidine (**13**) (M.W. = 169.1579, $C_9H_{19}N_3$) expected m/z $[M+H]^+$ ion = 170.1657 (found = 170.1642).

Table 6.1 Comparison of the amount of the desired product *N*-(4-aminobutyl) hexahydropyrimidine (**2**) at expected m/z $[M+H]^+$ ion = 158.1657: *N-(N′*-methylene-4-iminobutyl)-hexahydropyrimidine (**13**) at expected m/z $[M+H]^+$ ion = 170.1657; starting material spermidine (**1**) at expected m/z $[M+H]^+$ ion = 146.1657 when prepared using different ratios of formaldehyde to spermidine.

mole ratio of formaldehyde to spermidine	(**1**)	(**2**)	(**13**)
2.0 equiv.	1.8%	43.2%	55.0%
1.1 equiv.	7.1%	76.1%	16.8%
0.9 equiv.	7.6%	81.4%	11.0%

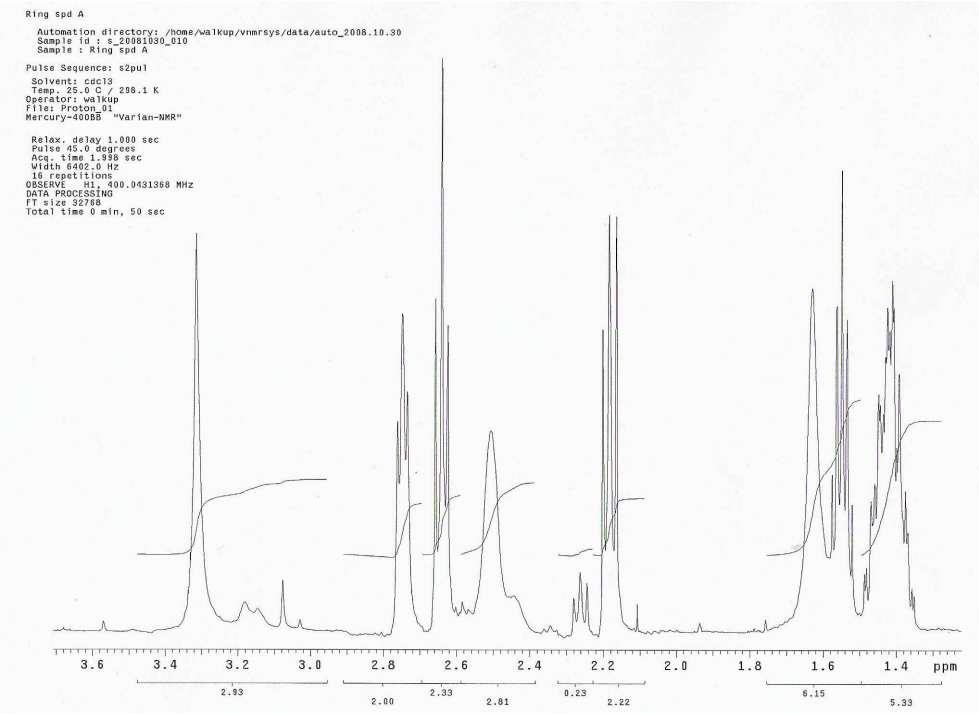

Figure 6.7 Expansion of ^{1}H-NMR spectrum (400 MHz, $CDCl_3$) of *N*-(4-aminobutyl) hexahydropyrimidine (**2**).

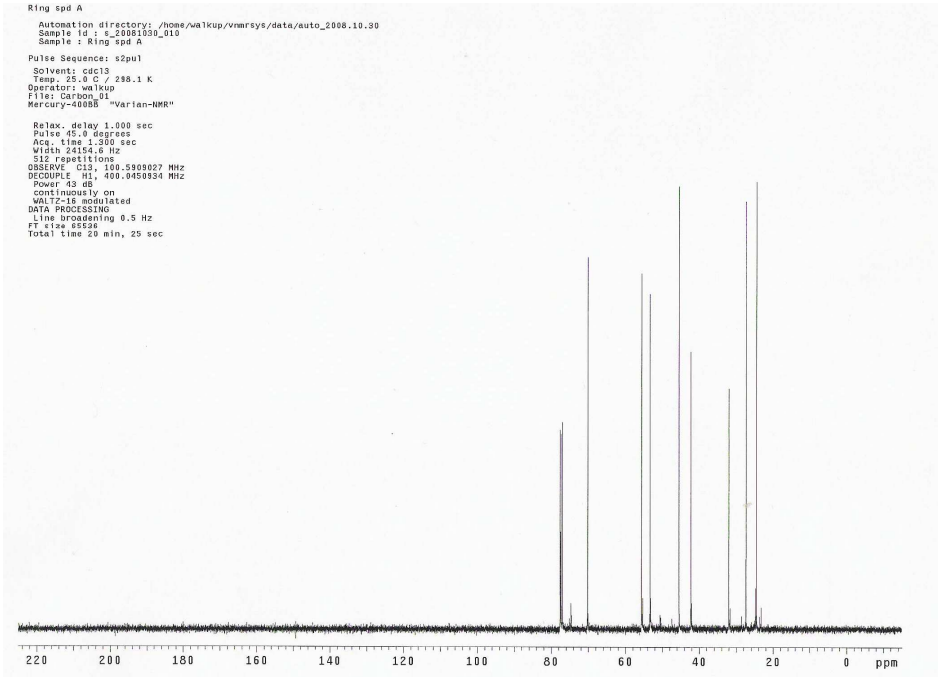

Figure 6.8 ^{13}C-NMR spectrum (100 MHz, $CDCl_3$) of *N*-(4-aminobutyl) hexahydropyrimidine (**2**).

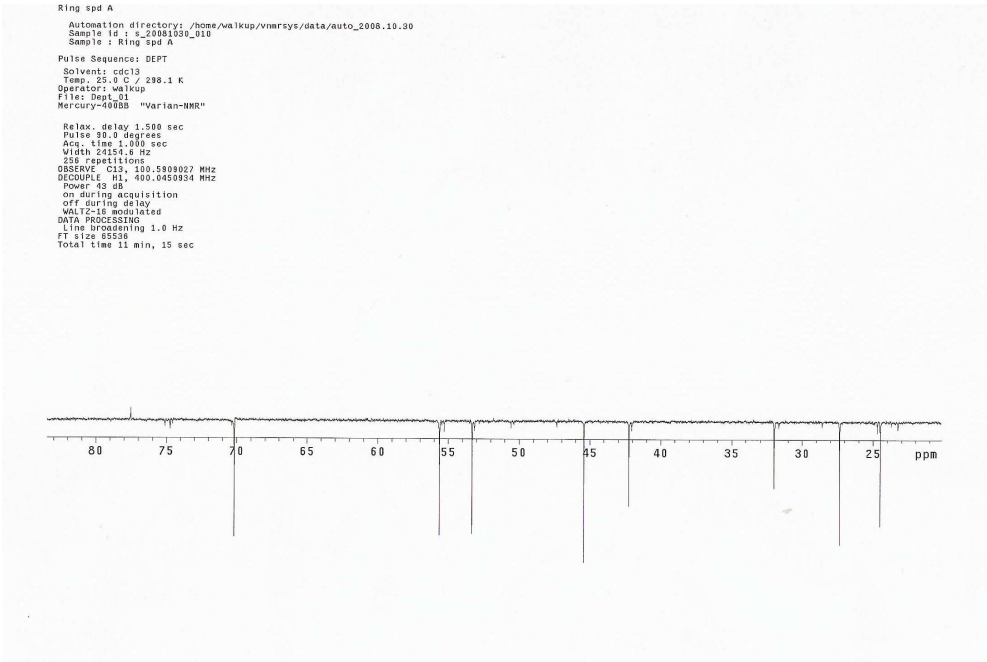

Figure 6.9 ^{13}C-NMR DEPT spectrum (100 MHz, $CDCl_3$) of *N*-(4-aminobutyl) hexahydropyrimidine (**2**).

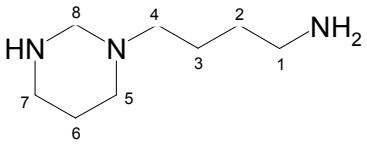

δ_H ($CDCl_3$) (400 MHz) 3.29 (2H, s, C(8)H_2), 2.73 (2H, m C(1)H_2), 2.64 (2H, m, C(7)H_2), 2.44 (1H, s, NH), 2.62 (2H, m, C(4)H_2), 2.17 (2H, b, C(5)H_2), 1.62 (2H, s, NH_2), 1.54 (2H, p, C(3)H_2), 1.41 (4H, m, C(2) H_2, C(6)H_2).

δ_C ($CDCl_3$) (100 MHz) 24.15 (C(6)), 26.96 (C(3)), 31.47 (C(2)), 41.72 (C(1)), 44.99 (C(7)), 52.94 (C(4)), 55.24 (C(5)), 69.74 (C(8)).

After *N*-(4-aminobutyl) hexahydropyrimidine (**2**) was obtained, the protection of the primary amine by using BOC (tert-Butyl carbamates) was considered. However, BOC reacts with both primary (Figure 6.10) and secondary amines (Figure 6.11) of *N*-(4-aminobutyl) hexahydropyrimidine (**2**) and yielded a mixture of mono- and diBOC products as confirmed by HR-ESI-MS (Figure 6.12).

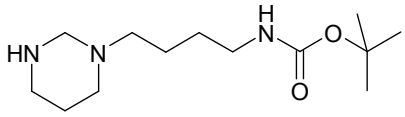

Figure 6.10 *N*-(4-Aminobutyl) hexahydropyrimidine (**2**) monoBOC derivative.

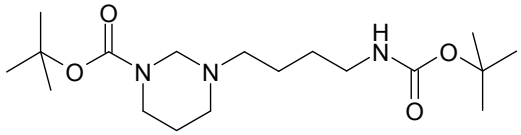

Figure 6.11 *N*-(4-Aminobutyl)hexahydropyrimidine (**2**) diBOC derivative.

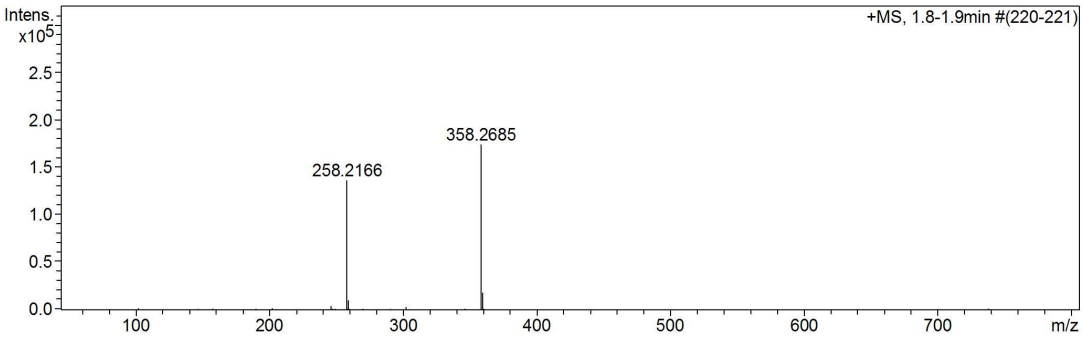

Figure 6.12 HR-ESI-MS spectrum of *N*-(4-aminobutyl) hexahydropyrimidine (**2**) with mono BOC on primary amine (M.W. = 257.2103, $C_{13}H_{27}N_3O_2$) expected m/z $[M+H]^+$ ion = 258.2181 (found = 258.2166) and *N*-(4-aminobutyl) hexahydropyrimidine (**2**) with diBOC (M.W. = 357.2627, $C_{18}H_{35}N_3O_4$) expected m/z $[M+H]^+$ ion = 358.2706 (found = 358.2685).

Method 1 step 2 Protection of primary amine group of *N*-(4-aminobutyl) hexahydropyrimidine (2) by the method of Ganem.

N-(4-Aminobutyl) hexahydropyrimidine (**2**) was reacted with benzaldehyde which is a selective protecting group for the remaining primary amine to obtain 4-(*N*-benzylideneaminobutyl)hexahydropyrimidine (**3**) (Figure 6.13).

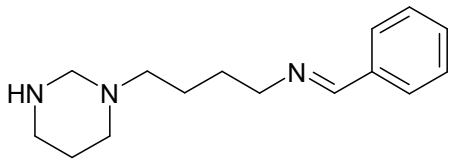

Figure 6.13 4-(*N*-Benzylideneaminobutyl)hexahydropyrimidine (**3**), $C_{15}H_{23}N_3$ (M.W = 245.1892).

HR-ESI-MS of 4-(*N*-benzylideneaminobutyl)hexahydropyrimidine (**3**) (Figure 6.14) shows the presence of an ion at m/z 246.1970 (found = 246.1945) corresponding to $[M+H]^+$ ion of this compound but also apparently a large peak at m/z = 158.1657 (found = 158.1628) for unreacted starting material. Another possibility is that this peak (m/z = 158.1657) arose from deprotection of the product when the MS solution was made up.

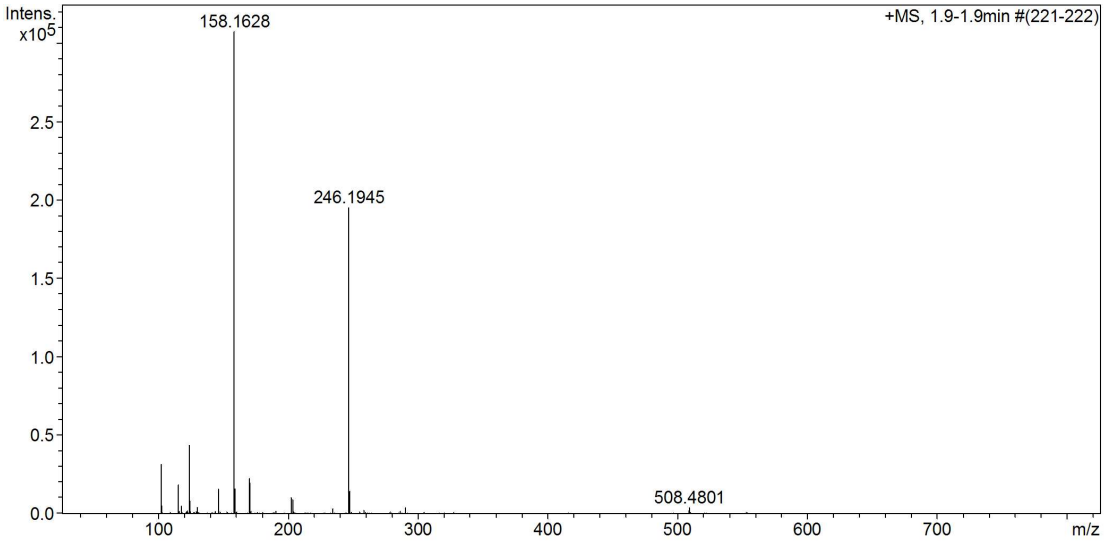

Figure 6.14 HR-ESI-MS spectrum of *N*-(4-aminobutyl)hexahydropyrimidine (**2**) (M.W. = 157.1579, $C_8H_{19}N_3$) expected m/z $[M+H]^+$ ion = 158.1657 (found = 158.1628) and the desired product of 4-(*N*-benzylideneaminobutyl) hexahydropyrimidine (**3**) (M.W. = 245.1892, $C_{15}H_{23}N_3$) expected m/z $[M+H]^+$ ion = 246.1970 (found = 246.1945).

The product was examined by NMR.

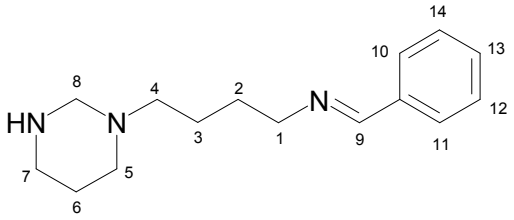

δ_H ($CDCl_3$) (400 MHz) 8.24 (H, s, C(9) H), 7.68 (2H, m, C(10)H, C(11)H), 7.37 (3H, m, C(12)H, C(13)H, C(14)H), 3.58 (2H, t, C(1)H_2), 3.07 (2H, s C(8)H_2), 2.55 (2H, t, C(7)H_2), 2.48 (2H, t, C(4)H_2), 2.34 (2H, t, C(5)H_2), 1.67 (2H, m, C(3)H_2), 1.58 (4H, m, C(2) H_2, C(6)H_2).

Dansylation method 2 (Chapter 2, page 45) was also used to investigate the purity of the 4-(*N*-benzylideneaminobutyl)hexahydropyrimidine (**3**). The HPLC chromatogram (Figure 6.17) showed the main peak at Rt = 6.4 min. HR-ESI-MS showed mainly 4-(*N*-benzylideneaminobutyl)hexahydropyrimidine (**3**)-monoDNS derivative (Figure 6.15, HR-ESI-MS as Figure 6.19) with a trace amount of *N*-(4-aminobutyl) hexahydropyrimidine (**2**)-monoDNS derivative (Figure 6.16, HR-ESI-MS as Figure 6.18). This might be evidence for the loss of the benzylidine group prior to MS because from the previous study *N*-(4-aminobutyl) hexahydropyrimidine (**2**) forms the diDNS derivative. Thus it appears that the primary amino group was still protected when the dansylation reaction was carried out.

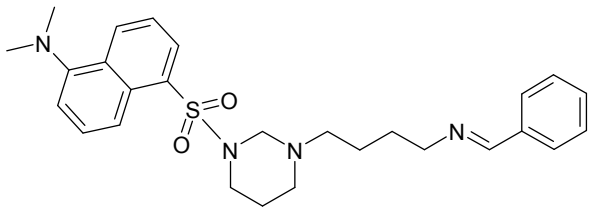

Figure 6.15 4-(*N*-Benzylideneaminobutyl)hexahydropyrimidine (**3**)-monoDNS derivative.

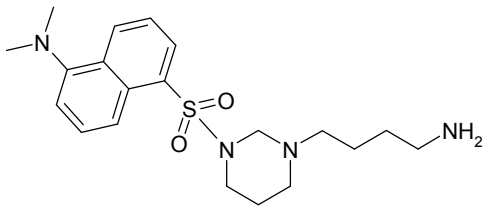

Figure 6.16 *N*-(4-Aminobutyl)hexahydropyrimidine (**2**)-monoDNS derivative.

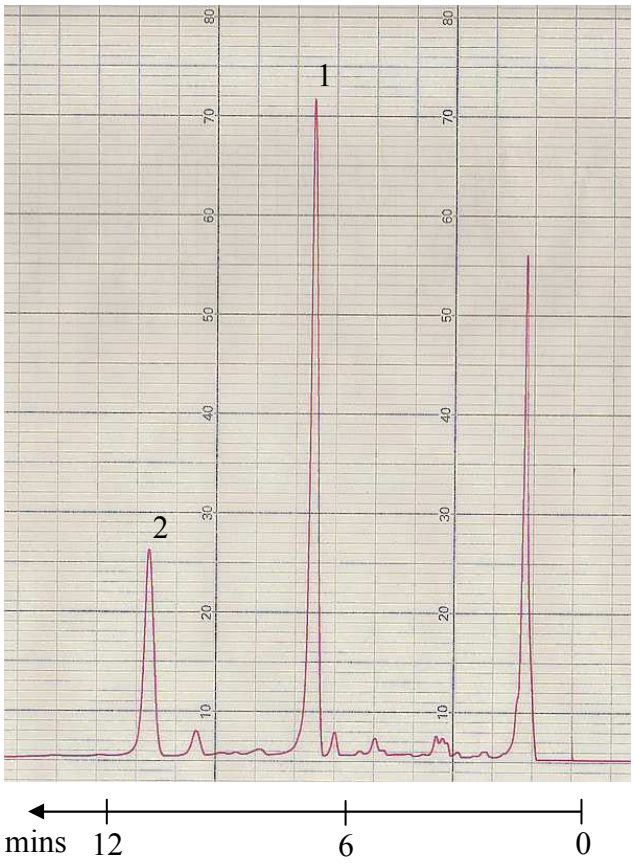

Figure 6.17 HPLC chromatogram of 4-(N-benzylideneaminobutyl)hexahydropyrimidine (3)-monoDNS derivative. HPLC conditions: mobile phase is acetonitrile: Milli-Q-water (70:30), C8-luna column, flow rate 1 mL/min, fluorescence detector at λ_{ex} = 330 nm, λ_{em} = 510 nm. The chromatogram shows peak 1 = 4-(N-benzylideneaminobutyl)hexahydro-pyrimidine (3)-monoDNS derivative at Rt = 6.4 min, peak 2 = spermidine triDNS derivative at Rt = 11.0 min.

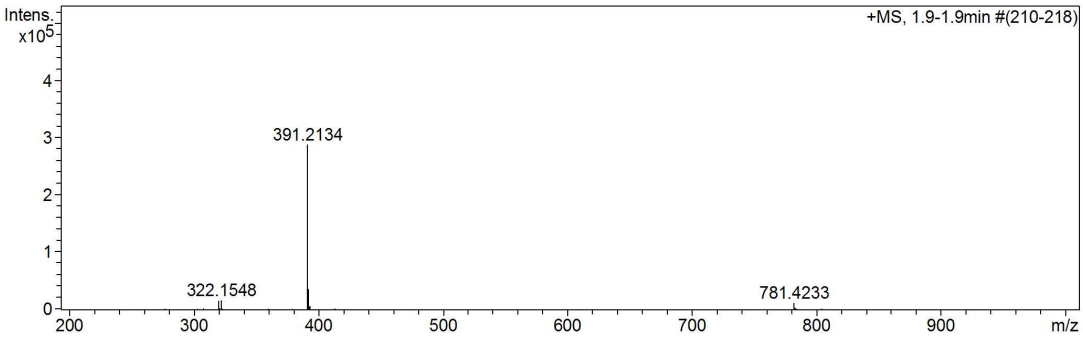

Figure 6.18 HR-ESI-MS spectrum of *N*-(4-aminobutyl)hexahydropyrimidine (**2**) – monoDNS derivative (M.W. = 390.2089, $C_{20}H_{30}N_4O_2S$) expected m/z $[M+H]^+$ ion = 391.2168 (found = 391.2134) and dimer ion m/z $[2M+H]^+$ ion = 781.4346 (found = 781.4233).

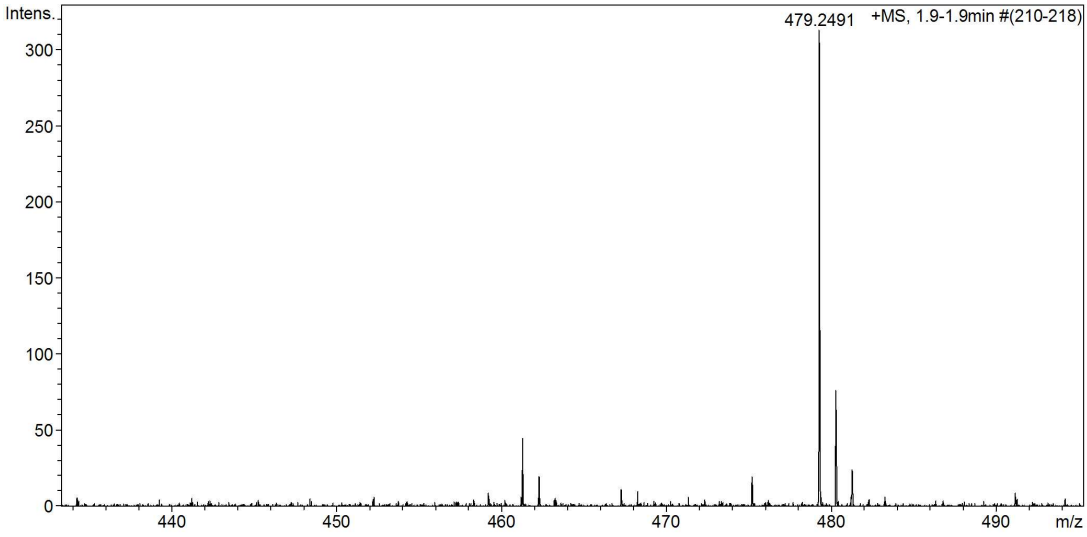

Figure 6.19 HR-ESI-MS spectrum the desired product of 4-(*N*-benzylideneaminobutyl)-hexahydropyrimidine (**3**)-monoDNS (M.W. = 478.2403, $C_{27}H_{34}N_4O_2S$) expected m/z $[M+H]^+$ ion = 479.2481 (found = 479.2491) (this figure was expanded from Figure 6.18).

Method 1 step 3 Michael addition of acrylonitrile

N^1-(*N*-Benzylidene-(1-hexahydropyrimidinebutyl)-N^3-propionitrile (**4**) was prepared by Michael addition of the unprotected secondary amine of 4-(*N*-benzylideneaminobutyl)-hexahydropyrimidine (**3**) with acrylonitrile to yield N^1-(*N*-benzylidene-(1-hexahydro-pyrimidinebutyl)-N^3-propionitrile (**4**) (Figure 6.20) (80% yield).

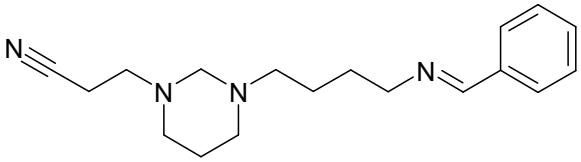

Figure 6.20: N^1-(*N*-Benzylidene-(1-hexahydropyrimidinebutyl)-N^3-propionitrile (**4**), $C_{18}H_{26}N_4$ (M.W = 298.2157).

By HR-ESI-MS spectra (Figure 6.22), the desired product was found at m/z $[M+1]^+$ ion = 299.2201. However, a contamination of $C_{11}H_{22}N_4$ (the possible structures shown in Figure 6.21) was also found at m/z $[M+1]^+$ ion = 211.1895. Depending upon whether the benzylidine group was lost when the sample was prepared for MS or whether it was absent in the starting material.

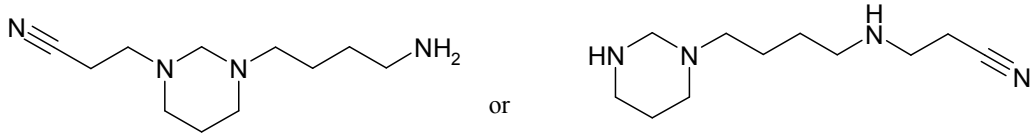

Figure 6.21 $C_{11}H_{22}N_4$ (M.W = 210.1844).

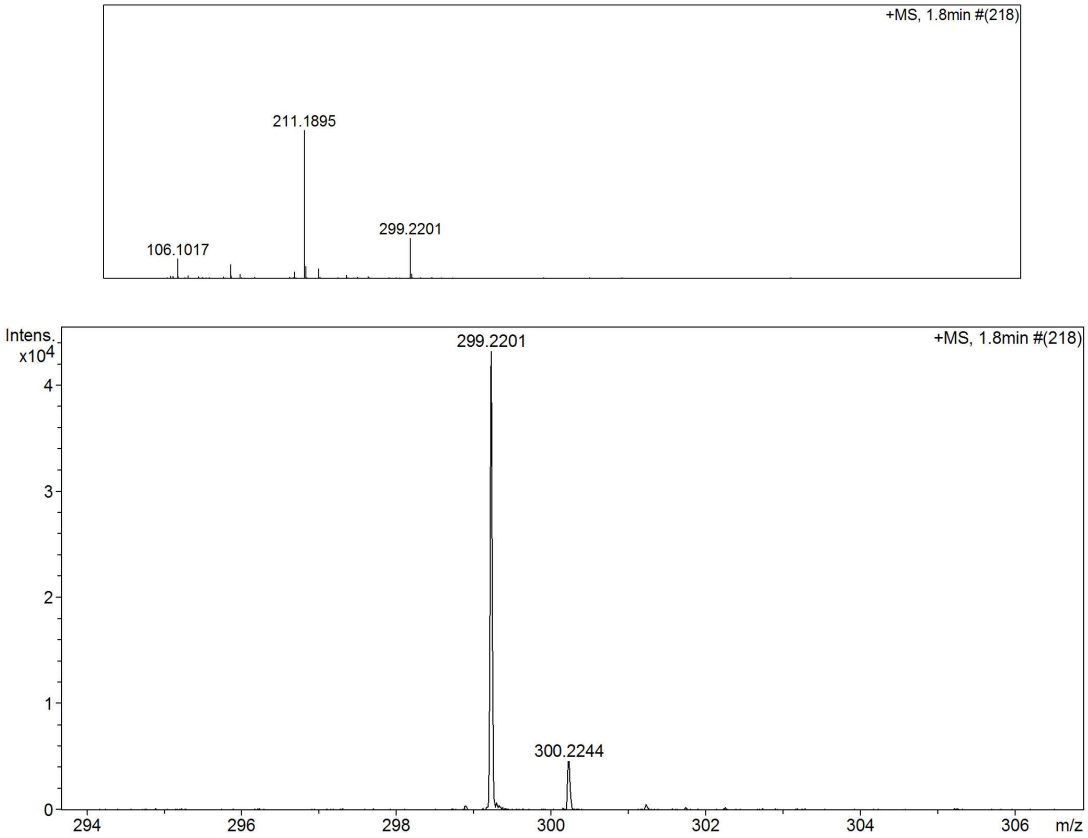

Figure 6.22 HR-ESI-MS spectra of the desired product of N^1-(*N*-benzylidene-(1-hexahydropyrimidinebutyl)-N^3-propionitrile (**4**) (M.W = 298.2157, $C_{18}H_{26}N_4$), expected m/z $[M+H]^+$ = 299.2235 (found = 299.2201) and a contamination product (Figure 6.26) at M.W = 210.1844, $C_{11}H_{22}N_4$, expected m/z $[M+H]^+$ ion = 211.1922 (found = 211.1895).

Method 1 step 4 Deprotection of the amino groups

Both the protection functions were removed simultaneously by heating under reflux with 2M HCl in methanol to yield 12-amino-4,8-diaza-dodecanenitrile (**5**) (Figure 6.23) which was confirmed by HR-ESI-MS (Figure 6.24) and the structure was confirmed by NMR (Figure 6.25, 6.26).

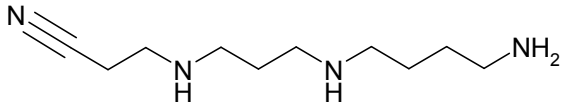

Figure 6.23 12-Amino-4,8-diaza-dodecanenitrile (**5**), $C_{10}H_{22}N_4$ (M.W. = 198.1844).

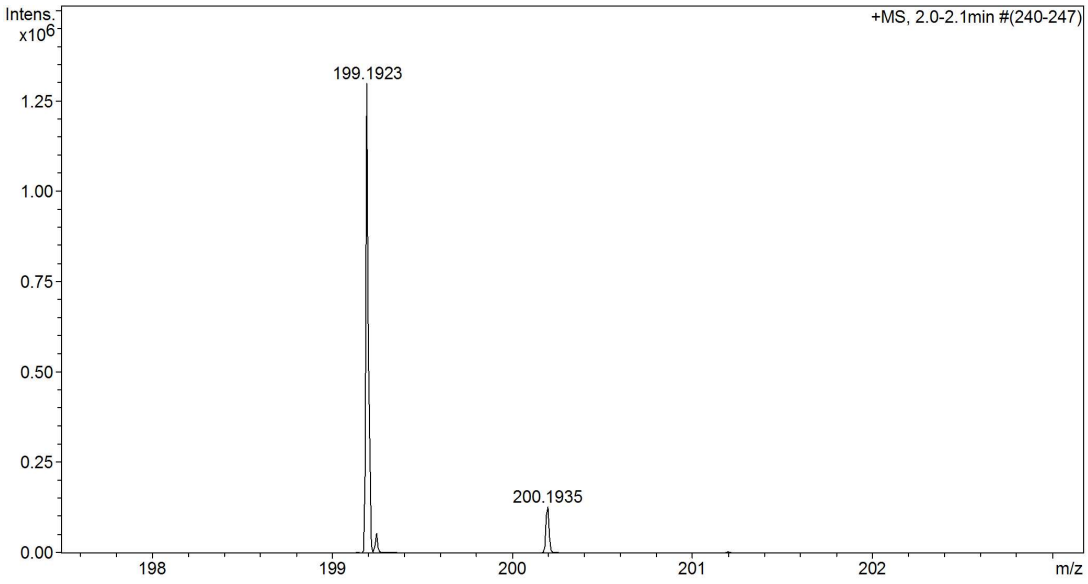

Figure 6.24 HR-ESI-MS spectra of desired product 12-amino-4,8-diaza-dodecanenitrile (**5**), (M.W. = 198.1844, $C_{10}H_{22}N_4$) expected m/z $[M+H]^+$ ion = 199.1923 (found = 199.1923).

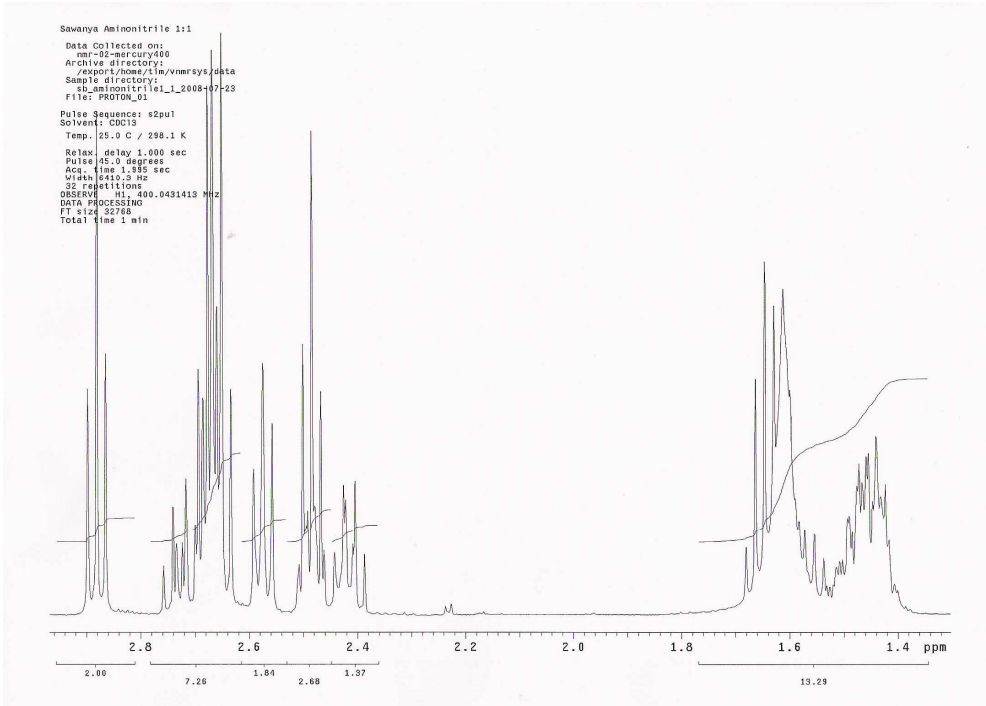

Figure 6.25 Expansion ^{1}H-NMR (400 MHz, $CDCl_3$) spectra of 12-amino-4,8-diaza-dodecanenitrile (**5**).

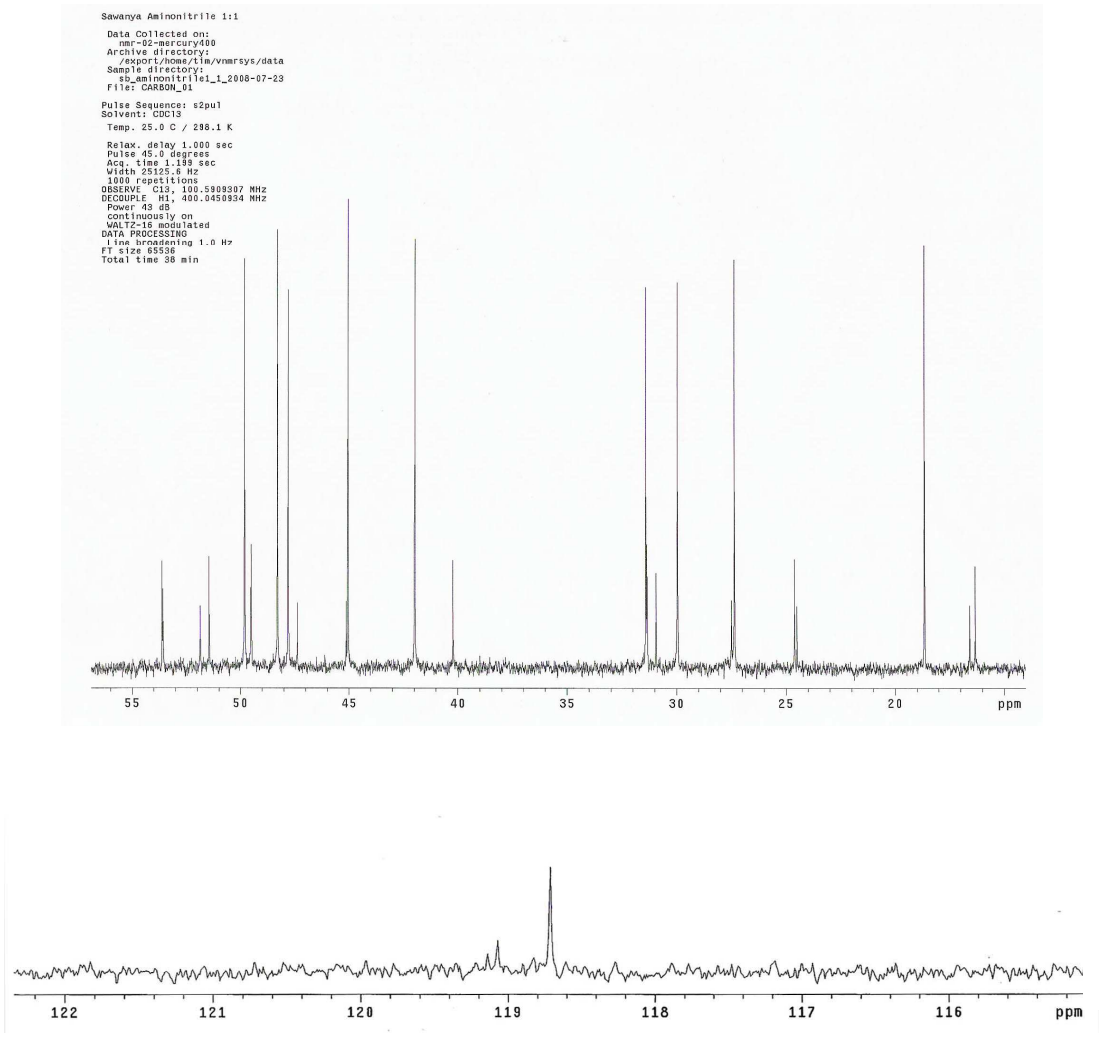

Figure 6.26 Expansion of ^{13}C-NMR (100 MHz, $CDCl_3$) spectra of 12-amino-4,8-diaza-dodecanenitrile (**5**).

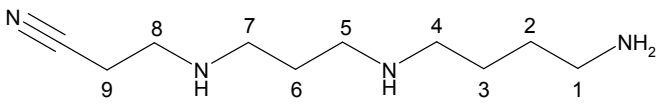

δ_H ($CDCl_3$) (400 MHz) 2.88 (2H, t, C(9) H_2), 2.67 (4H, m, C(5)H_2, C(7)H_2), 2.57 (2H, t, C(8)H_2), 2.48 (2H, m, C(1)H_2), 2.46 (2H, m, C(4)H_2), 1.65 (4H, m, C(2)H_2, C(6)H_2), 1.44 (2H, m, C(3)H_2).

δ_C ($CDCl_3$) (100 MHz) 18.64, 27.34, 29.95, 31.40, 41.96, 45.05, 47.81, 48.29, 49.80, 118.71.

Step 5: Thermospermine

$CoCl_2$ catalyzed reduction of the 12-amino-4,8-diaza-dodecanenitrile (**5**) by sodium borohydride yielded the desired thermospermine, 1,12-diamino-4,8-diazadodecane, (**6**) (Figure 6.27) as a yellowish oily liquid. HR-ESI-MS (Figure 6.28) showed a major peak at m/z = 203.2236 corresponding to the $[M+H]^+$ ion of spermine and thermospermine.

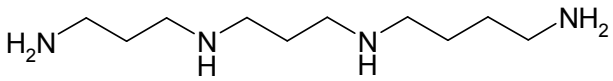

Figure 6.27 Thermospermine, $C_{10}H_{26}N_4$ (M.W = 202.2157).

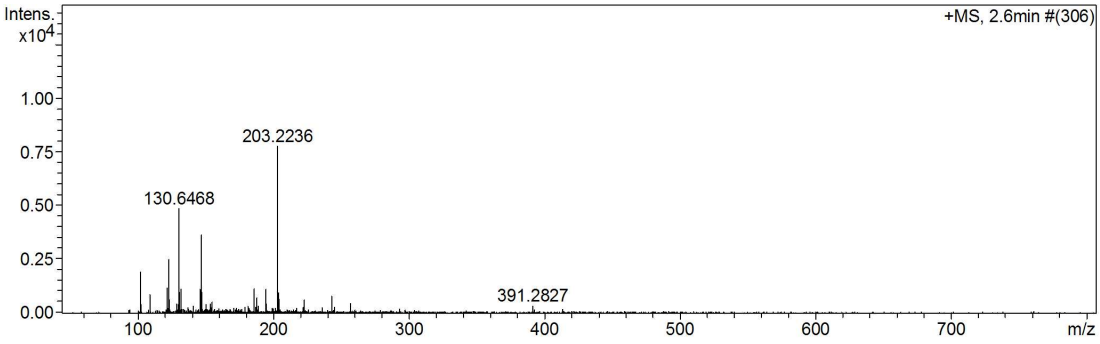

Figure 6.28 HR-ESI-MS spectrum of desired product thermospermine, (M.W. = 202.2157, $C_{10}H_{26}N_4$) expected m/z $[M+H]^+$ ion = 203.2236 (found = 203.2236).

Method 2 Thermospermine synthesis by using phthalimide as the protecting group.

The alternative method of thermospermine synthesis was done by using phthalimide as the protecting group (Figure 6.29).

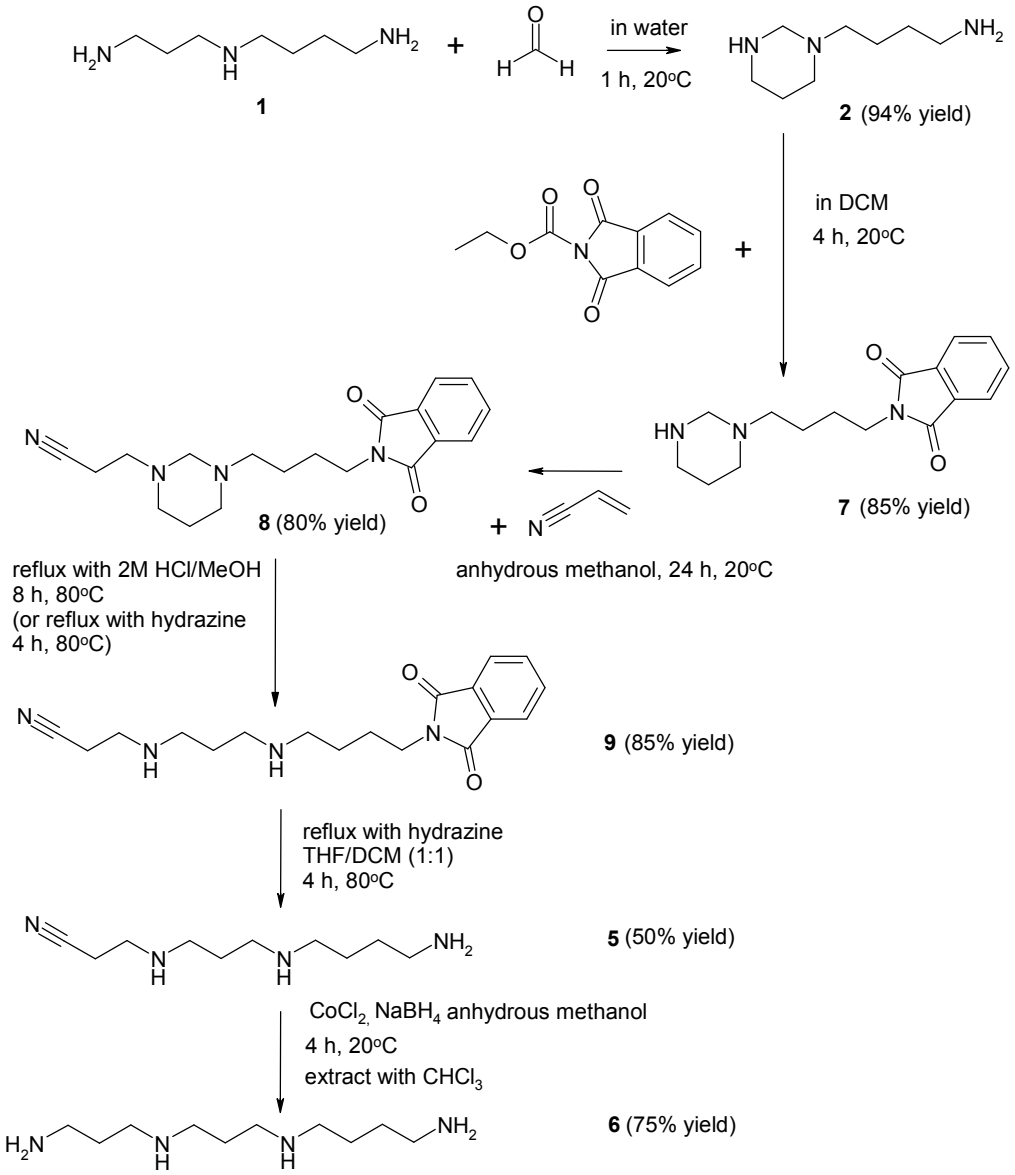

Figure 6.29 Thermospermine synthesis (method 2).

Method 2 step 1 *N*-(4-Aminobutyl)hexahydropyrimidine (2)

N-(4-Aminobutyl)hexahydropyrimidine (2) was prepared by the reaction of spermidine and formaldehyde as in method 1 step 1.

Method 2 step 2 2-(*N*-Butylhexahydropyrimidine)isoindoline-1,3-dione

N-(4-Aminobutyl)hexahydropyrimidine (**2**) was reacted with phthalimide which is a selective protecting group for the remaining primary amine to obtain the 2-(*N*-butyl-hexahydropyrimidine) isoindoline-1,3-dione (**7**) (Figure 6.30) which was confirmed by HR-ESI-MS (Figure 6.31) and by NMR (Figure 6.32).

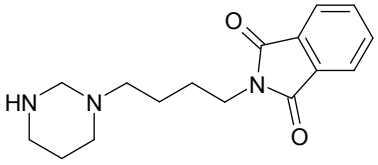

Figure 6.30 2-(*N*-Butylhexahydropyrimidine)isoindoline-1,3-dione (**7**), $C_{16}H_{21}N_3O_2$ (M.W = 287.1634).

δ_H ($CDCl_3$) (400 MHz) 7.846 (2H, m, C(10) H, C(11)H), 7.814 (2H, m, C(9)H, C(12)H), 4.101 (2H, s, C(8)H_2), 3.703 (2H, t, C(1)H_2), 3.204 (2H, t C(7)H_2), 3.015 (2H, t, C(4)H_2), 2.898 (2H, t, C(5)H_2), 1.912 (2H, quin, C(3)H_2), 1.824 (2H, quin, C(2)H_2), 1.695 (2H, quin, C(6) H_2).

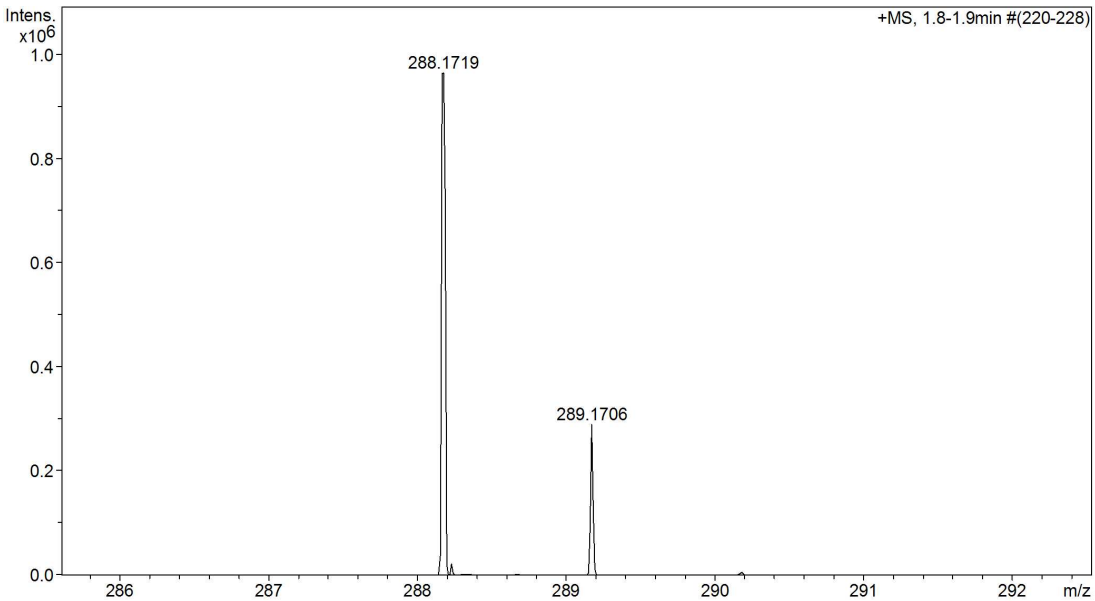

Figure 6.31 HR-ESI-MS spectrum of 2-(*N*-butylhexahydropyrimidine)isoindoline-1,3-dione (**7**) (M.W. = 287.1634, $C_{16}H_{21}N_3O_2$) expected m/z $[M+H]^+$ ion = 288.1712 (found = 288.1719).

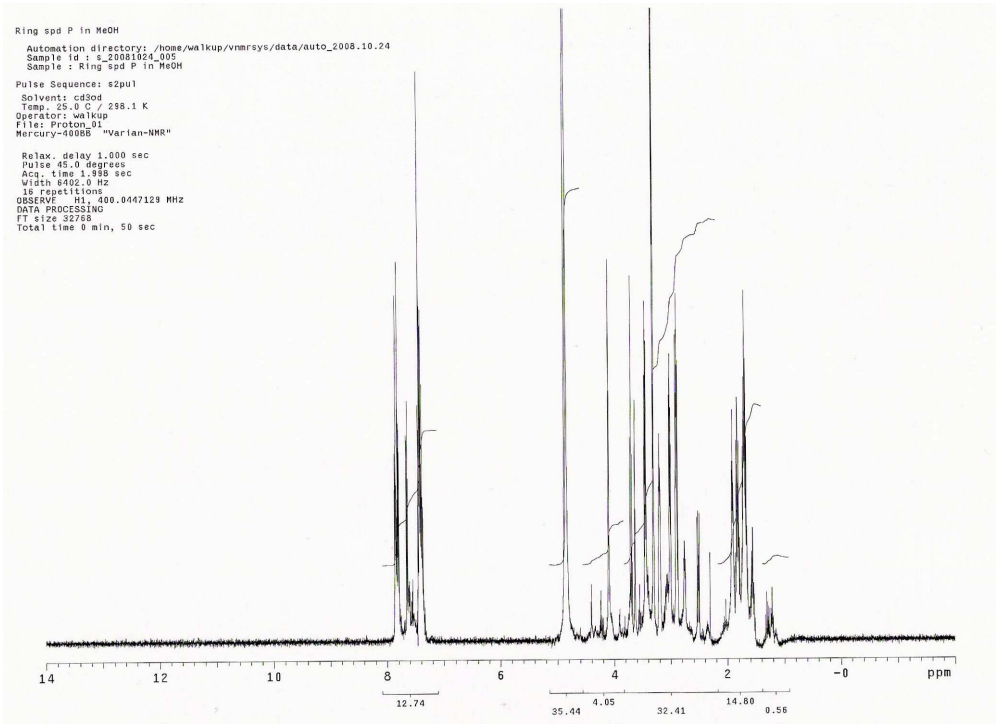

Figure 6.32 ^{1}H NMR of 2-(*N*-butylhexahydropyrimidine)isoindoline-1,3-dione (**7**).

Method 2 step 3 Adding acrylonitrile to 2-(*N*-butylhexahydropyrimidine) isoindoline-1,3-dione (7)

2-(N^{1}-Butylhexahydropyrimidine)-isoindoline-1,3-dione-N^{3}-propionitrile (**8**) was prepared by Michael addition of the unprotected secondary amine of 2-(*N*-butylhexahydropyrimidine)isoindoline-1,3-dione (**7**) by acrylonitrile (80% yield) (Figure 6.33). This amine was confirmed by HR-ESI-MS (Figure 6.34) and examined by NMR (Figure 6.35, 6.36, 6.37).

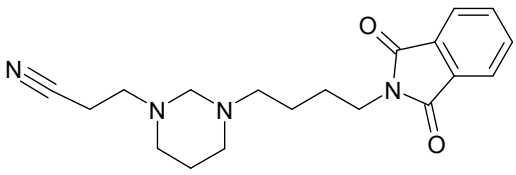

Figure 6.33 2-(N^{1}-Butylhexahydropyrimidine)-isoindoline-1,3-dione-N^{3}-propionitrile (**8**), $C_{19}H_{24}N_4O_2$ (M.W = 340.1899).

δ_H ($CDCl_3$) (400 MHz) 7.804 (2H, m, C(10) H, C(11)H), 7.691 (2H, m, C(9)H, C(12)H), 3.659 (2H, m, C(8)H_2), 3.659 (2H, t, C(1)H_2), 2.863 (2H, t, C(14)H_2), 2.732 (2H, m,

$C(13)H_2$), 2.683 (2H, m, $C(4)H_2$), 2.490 (4H, m, $C(5)H_2$, $C(7)H_2$), 1.850 (2H, quin, $C(3)H_2$), 1.683 (2H, quin, $C(2)H_2$), 1.567 (2H, m, $C(6)H_2$).

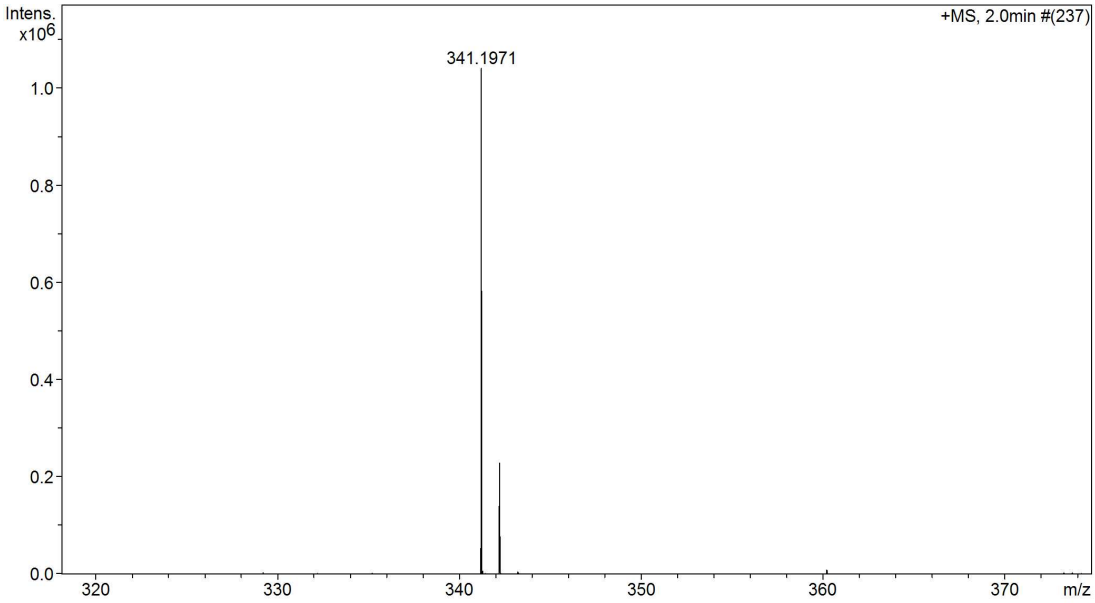

Figure 6.34 HR-ESI-MS spectrum of 2-(N^1-butylhexahydropyrimidine)-isoindoline-1,3-dione-N^3-propionitrile (**8**), (M.W. = 340.1899, $C_{19}H_{24}N_4O_2$) expected m/z $[M+H]^+$ ion = 341.1977 (found = 341.1971).

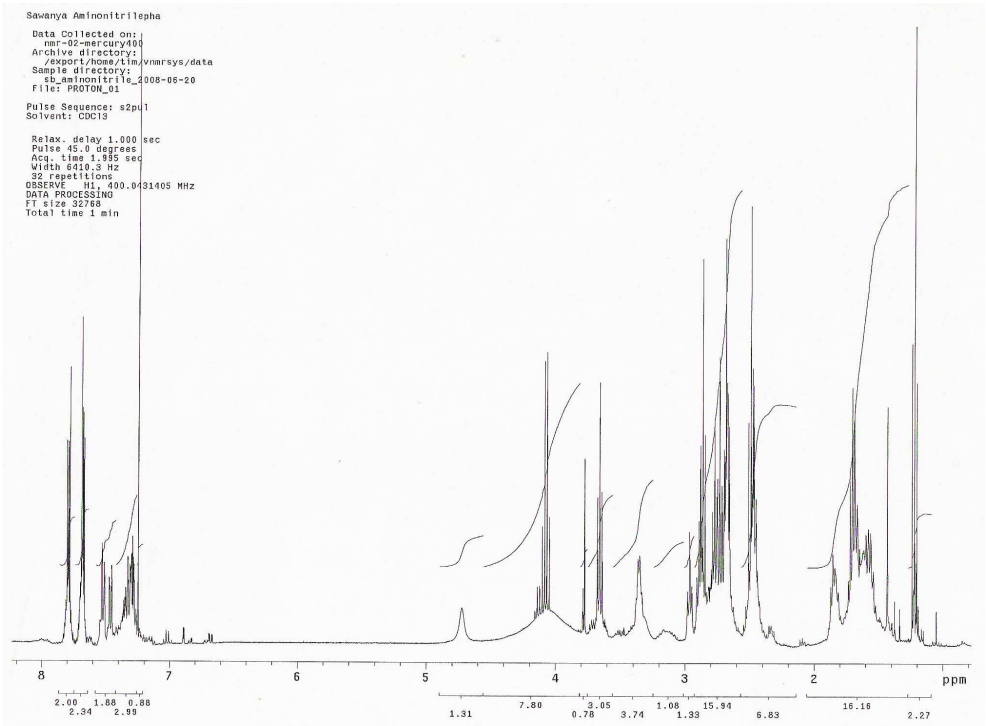

Figure 6.35 ^{1}H NMR of 2-(N^1-butylhexahydropyrimidine)-isoindoline-1,3-dione-N^3-propionitrile (**8**).

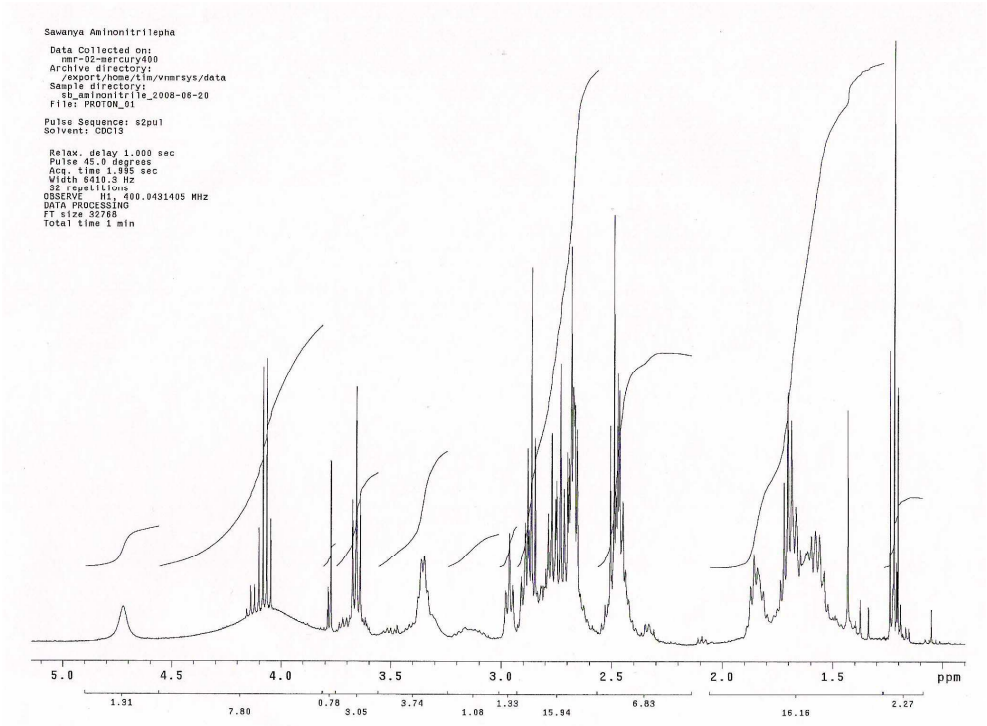

Figure 6.36 Expansion of ^{1}H NMR of 2-(N^{1}-butylhexahydropyrimidine)-isoindoline-1,3-dione-N^{3}-propionitrile (**8**).

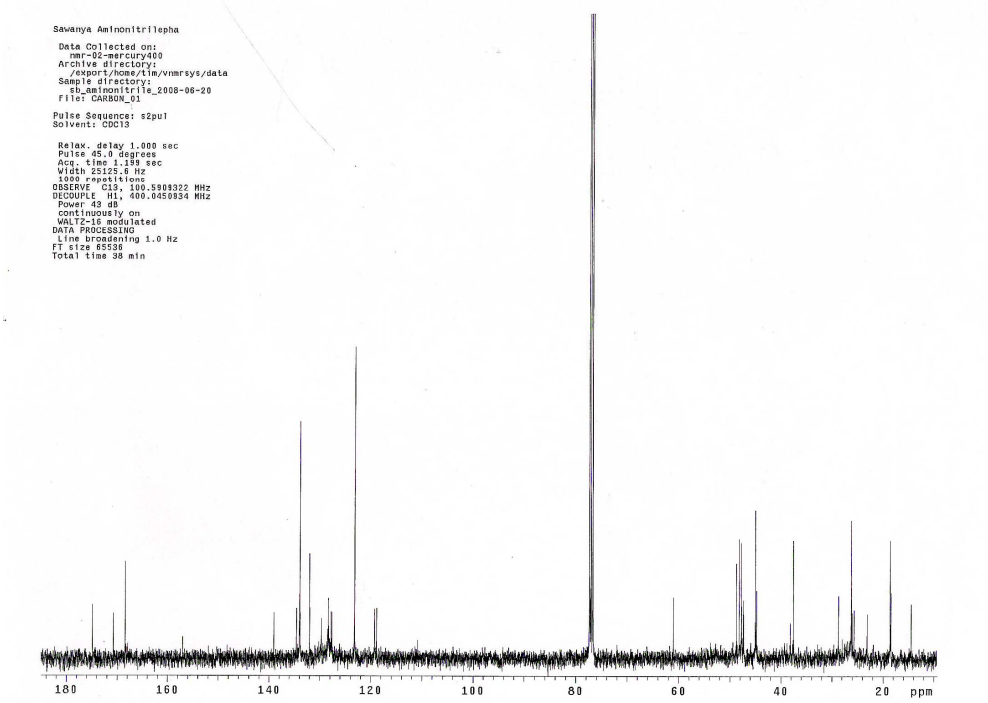

Figure 6.37 ^{13}C NMR of 2-(N^{1}-butylhexahydropyrimidine)-isoindoline-1,3-dione-N^{3}-propionitrile (**8**).

Method 2 step 4 Deprotection of the hexahydropyrimidine ring of 2-(N^1-butylhexahydropyrimidine)-isoindoline-1,3-dione-N^3-propionitrile (8)

By reflux with 2 M HCl-methanol (15 mL) at 80°C for 8 h., the methylene group from hexahydropyrimidine ring of 2-(N^1-butylhexahydropyrimidine)-isoindoline-1,3-dione-N^3-propionitrile (**8**) was removed to yield 12-(1,3-dioxoisoindolin-2-yl)-4,8-diaza-dodecanenitrile (**9**) (Figure 6.38) (85% yield).

HR-ESI-MS spectrum of 12-(1,3-dioxoisoindolin-2-yl)-4,8-diaza-dodecanenitrile (**9**) (M.W. = 328.1899, $C_{18}H_{24}N_4O_2$) expected m/z $[M+H]^+$ ion = 329.1977 (found = 329.1965) and also found 2-(N^1-butylhexahydropyrimidine)-isoindoline-1,3-dione-N^3-propionitrile (**8**) (M.W. = 340.1899, $C_{19}H_{24}N_4O_2$) expected m/z $[M+H]^+$ ion = 341.1977 (found = 341.2005).

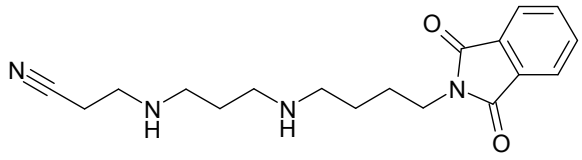

Figure 6.38 12-(1,3-Dioxoisoindolin-2-yl)-4,8-diaza-dodecanenitrile (**9**), $C_{18}H_{24}N_4O_2$ (M.W. = 328.1899).

Method 2 step 5 Removal of the phthalimide group to give 12-amino-4,8-diaza-dodecanenitrile (5)

12-(1,3-Dioxoisoindolin-2-yl)-4,8-diaza-dodecanenitrile (**9**) was treated with hydrazine monohydrate in CH_2Cl_2/ THF (1:1) and reflux for 4 h at 80°C to yield 12-amino-4,8-diaza-dodecanenitrile (**5**) (50% yield) (Figure 6.39). This amine was confirmed by HR-ESI-MS.

HR-ESI-MS spectra of desired product 12-amino-4,8-diaza-dodecanenitrile (**5**), (M.W. = 198.1844, $C_{10}H_{22}N_4$) expected m/z $[M+H]^+$ ion = 199.1923 (found = 199.1920)

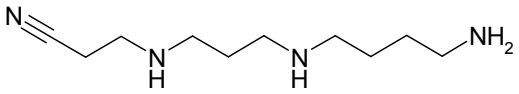

Figure 6.39 12-Amino-4,8-diaza-dodecanenitrile (**5**), $C_{10}H_{22}N_4$ (M.W. = 198.1844).

Dansylation (Chapter 2, page 45) was used to investigated 12-amino-4,8-diaza-dodecanenitrile (**5**). The HPLC chromatogram of 12-amino-4,8-diaza-dodecanenitrile (**5**)-triDNS derivative was obtained (Figures 6.40 and 6.41), the derivative was eluted at 12.5 min (HPLC conditions: C-8 luna column, mobile phase: acetonitrile: Milli-Q-water (70:30), flow rate = 1 mL/min) and confirmed by HR-ESI-MS (Figures 6.42 and 6.43).

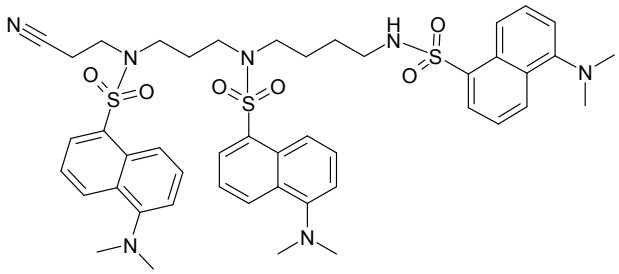

Figure 6.40 12-Amino-4,8-diaza-dodecanenitrile (**5**)-triDNS derivative.

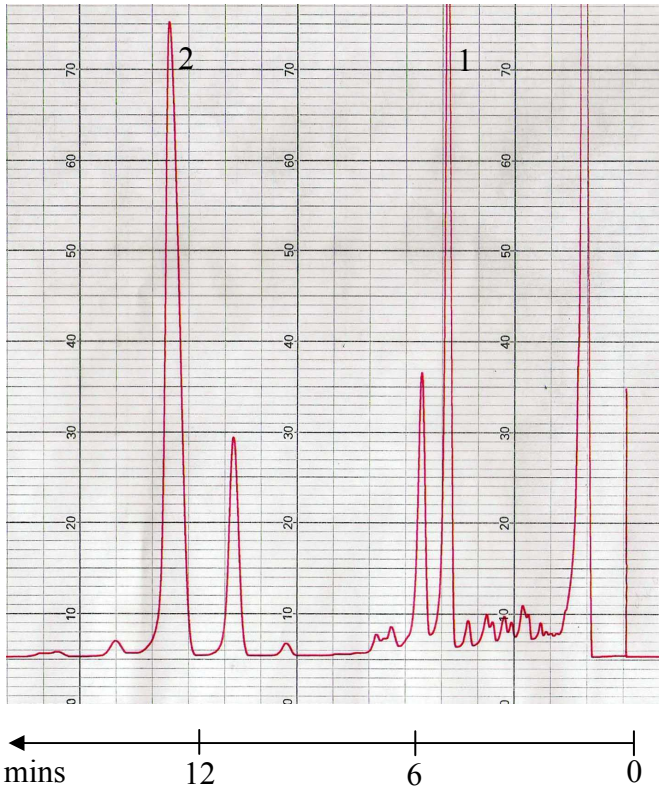

Figure 6.41 HPLC chromatogram of 12-amino-4,8-diaza-dodecanenitrile (**5**)-DNS derivative. HPLC conditions: mobile phase is acetonitrile: Milli-Q-water (70:30), C8-luna column, flow rate 1 mL/min, fluorescence detector at λ_{ex} = 330 nm, λ_{em} = 510 nm. The chromatogram shows peak 1 = 12-amino-4,8-diaza-dodecanenitrile (**5**)-diDNS derivative at Rt = 5.0 min, peak 2 = 12-amino-4,8-diazadodecanenitrile (**5**)-triDNS derivative at Rt = 12.5 min.

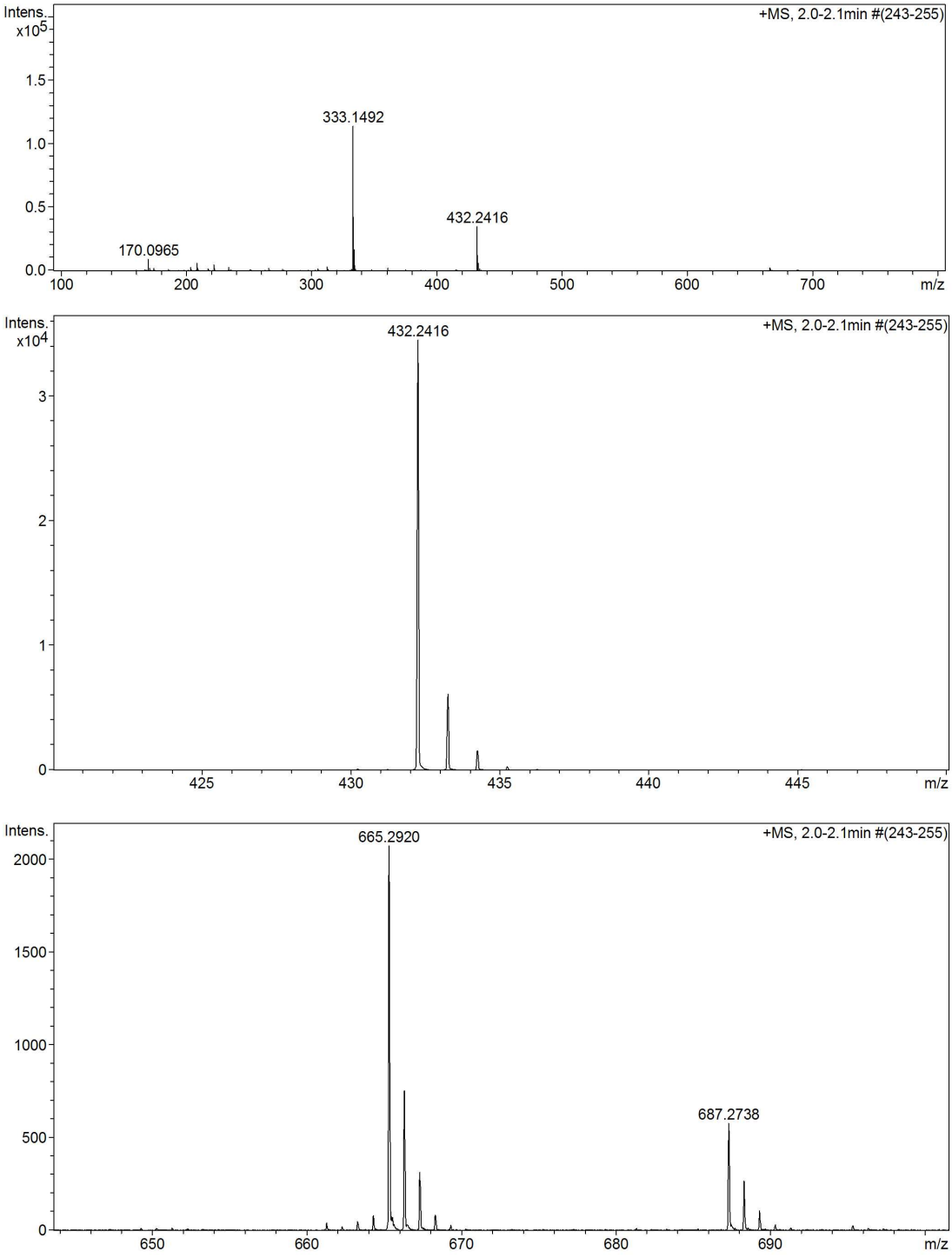

Figure 6.42 HR-ESI-MS spectra of 12-amino-4,8-diaza-dodecanenitrile (**5**)-monoDNS derivative (M.W. = 431.2355, $C_{22}H_{33}N_5O_2S$) expected m/z $[M+H]^+$ ion = 432.2433 (found = 432.2416) and 12-amino-4,8-diaza-dodecanenitrile (**5**)-diDNS derivative (M.W. = 664.2865, $C_{34}H_{44}N_6O_4S_2$) expected m/z $[M+H]^+$ ion = 665.2943 (found = 665.2920).

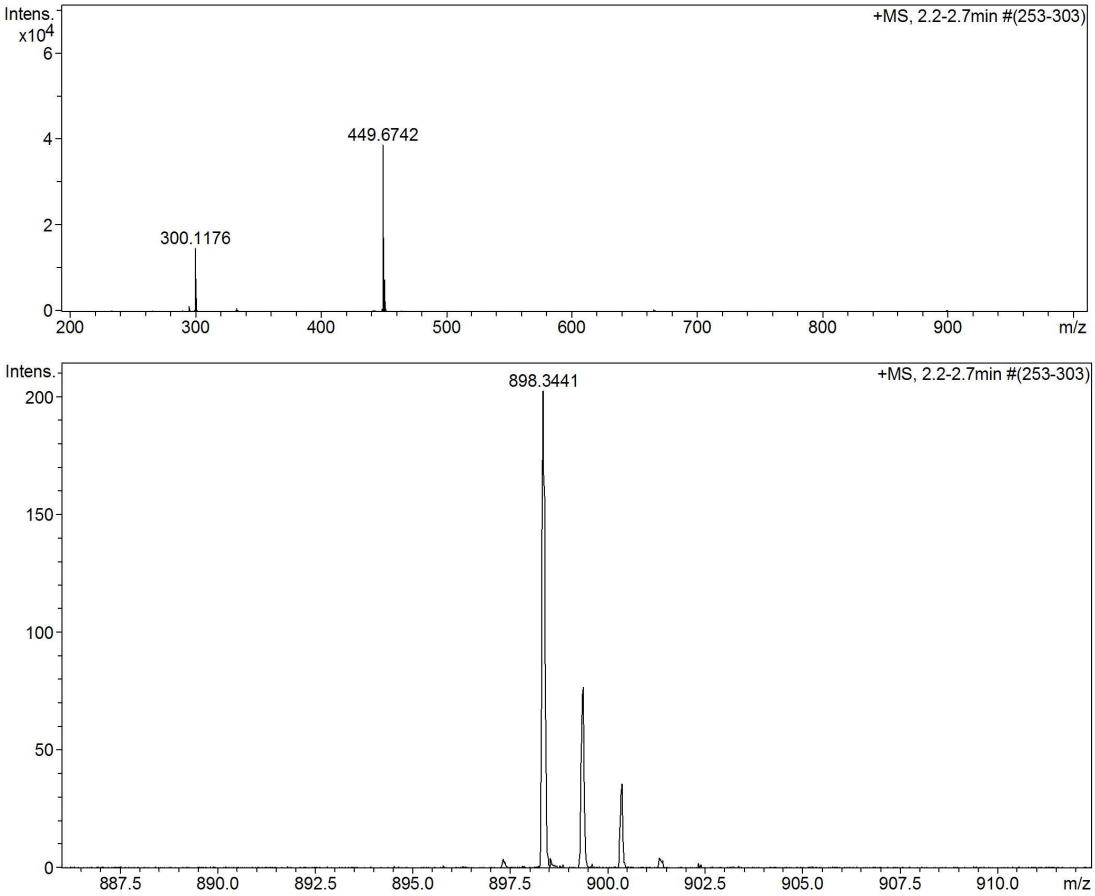

Figure 6.43 HR-ESI-MS spectra of 12-amino-4,8-diaza-dodecanenitrile (**5**)-triDNS derivative (M.W. = 897.3376, $C_{46}H_{55}N_7O_6S_3$) expected m/z $[M+H]^+$ ion = 898.3454 (found = 898.3441) and doubly charged $[M+2H]^{2+}$ ion = 449.6766 (found = 449.6742) (at Rt = 12.5 min).

Method 2 step 6 Thermospermine

The last step is to reduce triple bond of nitrile of 12-amino-4,8-diaza-dodecanenitrile (**5**) to obtain thermospermine by using sodium borohydride. The molecular weight of the desired thermospermine was confirmed by HR-ESI-MS (Figure 6.44).

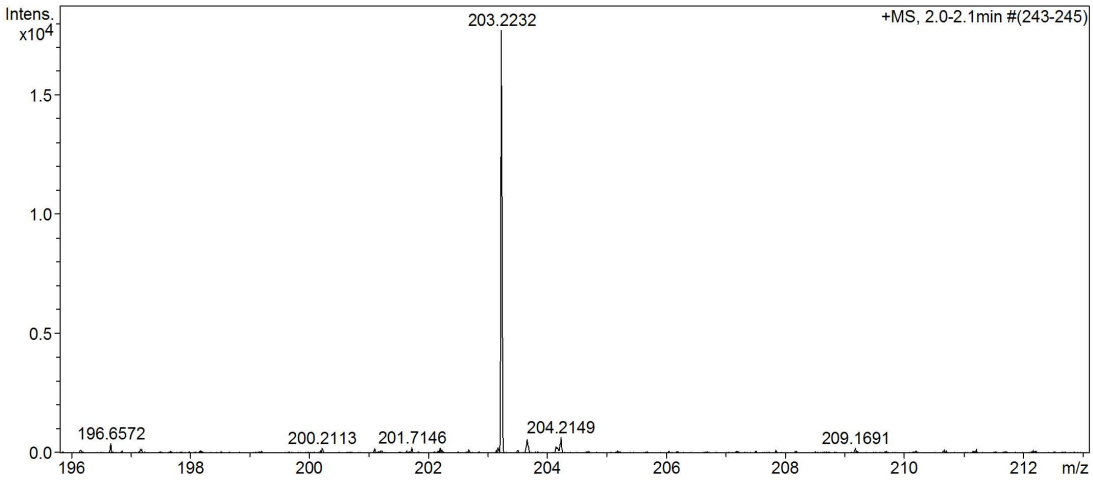

Figure 6.44 HR-ESI-MS spectrum of desired product thermospermine, (M.W. = 202.2157, $C_{10}H_{26}N_4$) expected m/z $[M+H]^+$ ion = 203.2236 (found = 203.2232) and doubly charged ion $[M+2H]^{2+}$ = 102.1156 (found = 102.1130).

Method 2 alternative step 4 Alternative deprotection method for 12-amino-4,8-diaza-dodecanenitrile (5) by simultaneous removal of phthalimide and hexahydropyrimidine from 2-(*N*^{1}-butylhexahydropyrimidine)-isoindoline-1,3-dione-*N*^{3}-propionitrile (8)

2-(*N*^{1}-Butylhexahydropyrimidine)-isoindoline-1,3-dione-*N*^{3}-propionitrile (**8**) was treated with hydrazine monohydrate in CH_2Cl_2/ THF (1:1) and reflux for 4 h at 80^{o}C to remove the phthalimide group to yield 3-(*N*^{1}-(4-aminobutyl) hexahydropyrimidine)propanenitrile (Figure 6.45). This amine was confirmed by HR-ESI-MS (Figure 6.46).

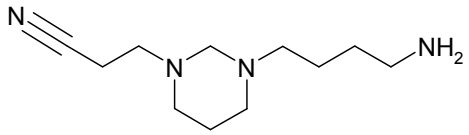

Figure 6.45 3-(*N*^{1}-(4-Aminobutyl) hexahydropyrimidine)propanenitrile, $C_{11}H_{22}N_4$ (M.W. = 210.1844).

From this MS result, it suggested that the deprotection reaction of the phthalimide group by hydrazine monohydrate simultaneously removed the methylene from the hexahydropyrimidine ring of *N*-(4-aminobutyl) hexahydropyrimidine (**2**). This result was confirmed by removal of hexahydropyrimidine ring from *N*-(4-aminobutyl) hexahydropyrimidine (**2**) by the same method (Figure 6.47). The HR-ESI-MS of this starting material, *N*-(4-aminobutyl) hexahydropyrimidine (**2**) was confirmed as M.W. of = *N*-(4-aminobutyl) hexahydropyrimidine (**2**) = 157.1579 ($C_8H_{19}N_3$) expected m/z $[M+H]^+$ ion =

158.1657 (found = 158.1640). The product of spermidine (**1**), M.W. = 145.1579 ($C_7H_{19}N_3$) was confirmed by HR-ESI-MS as expected m/z $[M+H]^+$ ion = 146.1657 (found = 146.1638) which was obtained from the reaction of hydrazine.

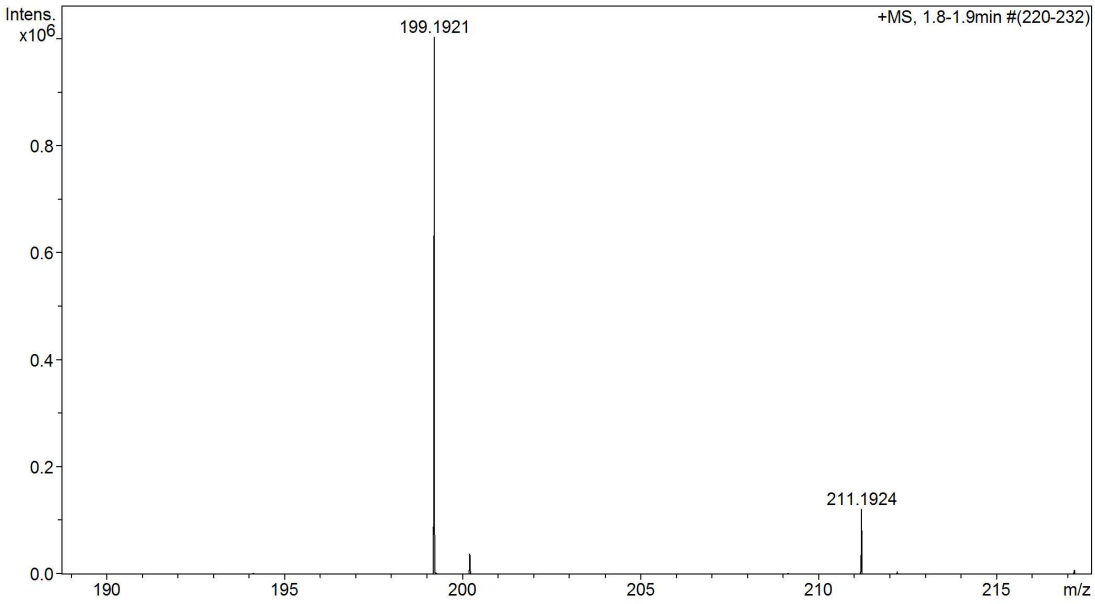

Figure 6.46 HR-ESI-MS spectrum of 3-(N^1-(4-aminobutyl) hexahydropyrimidine) propanenitrile (M.W. = 210.1844, $C_{11}H_{22}N_4$) expected m/z $[M+H]^+$ ion = 211.1923 (found = 211.1924) and also found 12-amino-4,8-diaza-dodecanenitrile (**5**), (M.W. = 198.1844, $C_{10}H_{22}N_4$) expected m/z $[M+H]^+$ ion = 199.1923 (found = 199.1921).

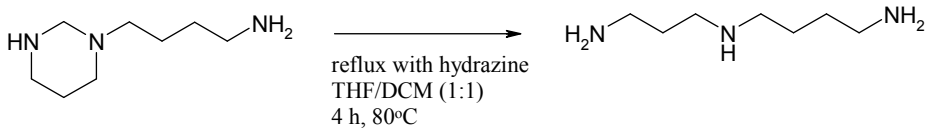

Figure 6.47 Scheme of removal of hexahydropyrimidine ring from *N*-(4-aminobutyl) hexahydropyrimidine (**2**).

Thermospermine synthesised by method 1 has a problematic step at step 2 when using benzaldehyde as the protecting group which the environment needed to be dry, a small amount of water will cleave the benzaldehyde group. Thus, the risk of getting incomplete reaction started from this step. By using phthalimide as the protecting group in method 2 step 2, the reaction was set at milder conditions (at 20°C) and gave more yield of desired product. By alternative way of remove the protecting group by method 2 step 4, the yield of the aminonitrile, 12-amino-4,8-diaza-dodecanenitrile (**5**) was increased (75% yield).

Spermine and Thermospermine

A comparison of the NMR spectra between spermine and thermospermine was performed. The NMR of spermine is shown in Figures 6.48, 6.49 and 6.50 and the NMR of thermospermine in Figures 6.51, 6.52 and 6.53.

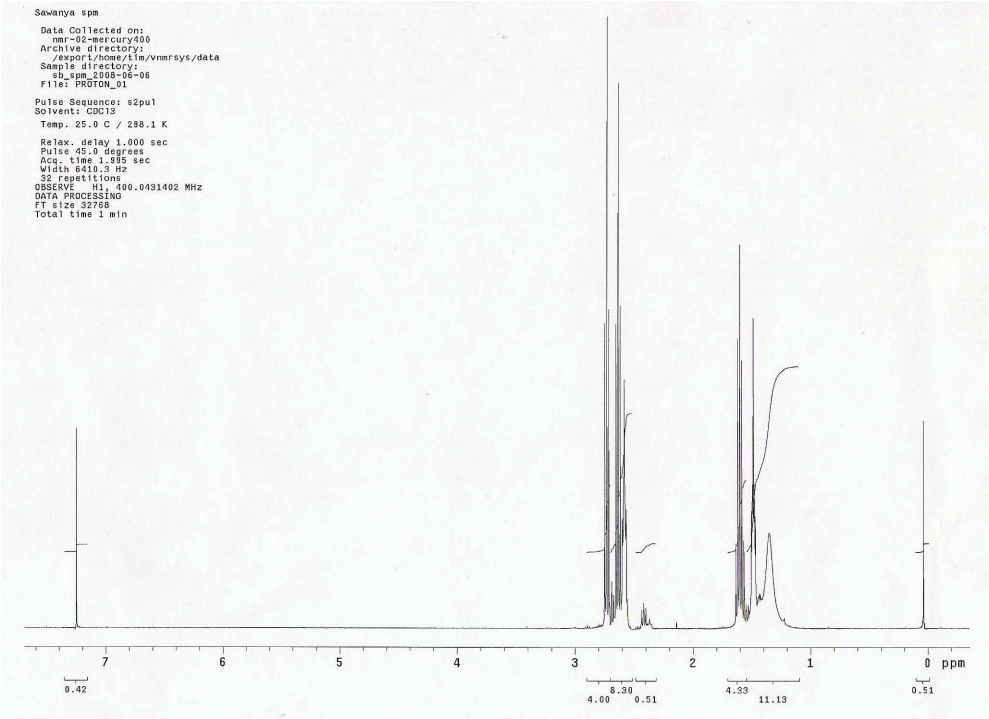

Figure 6.48 ^{1}H NMR of spermine.

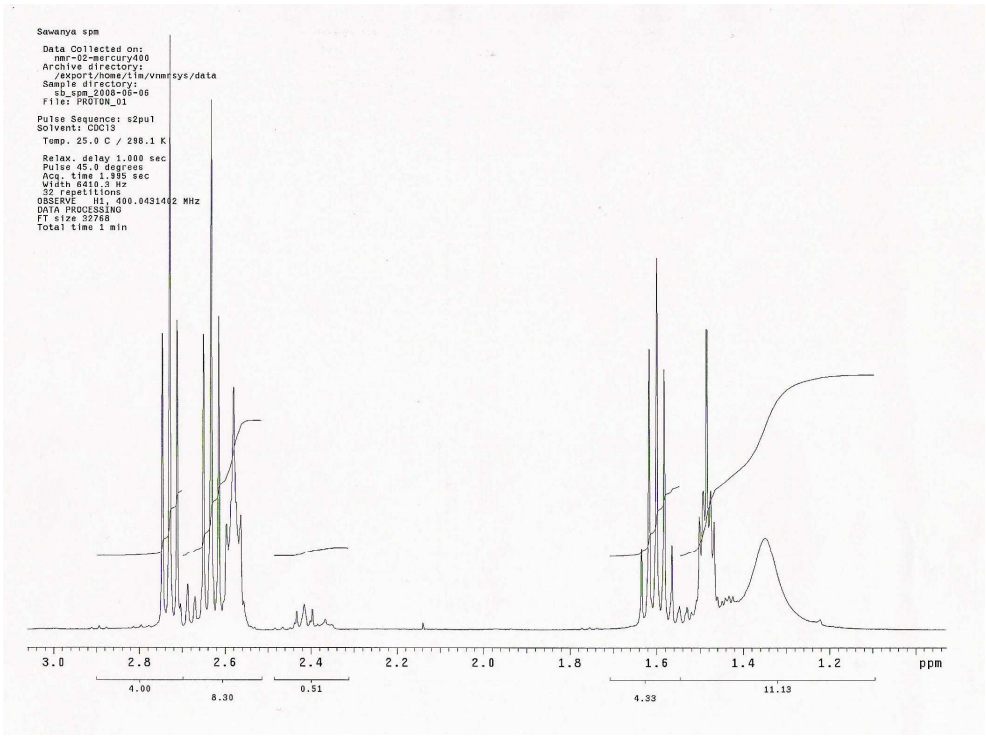

Figure 6.49 ^{1}H NMR of spermine.

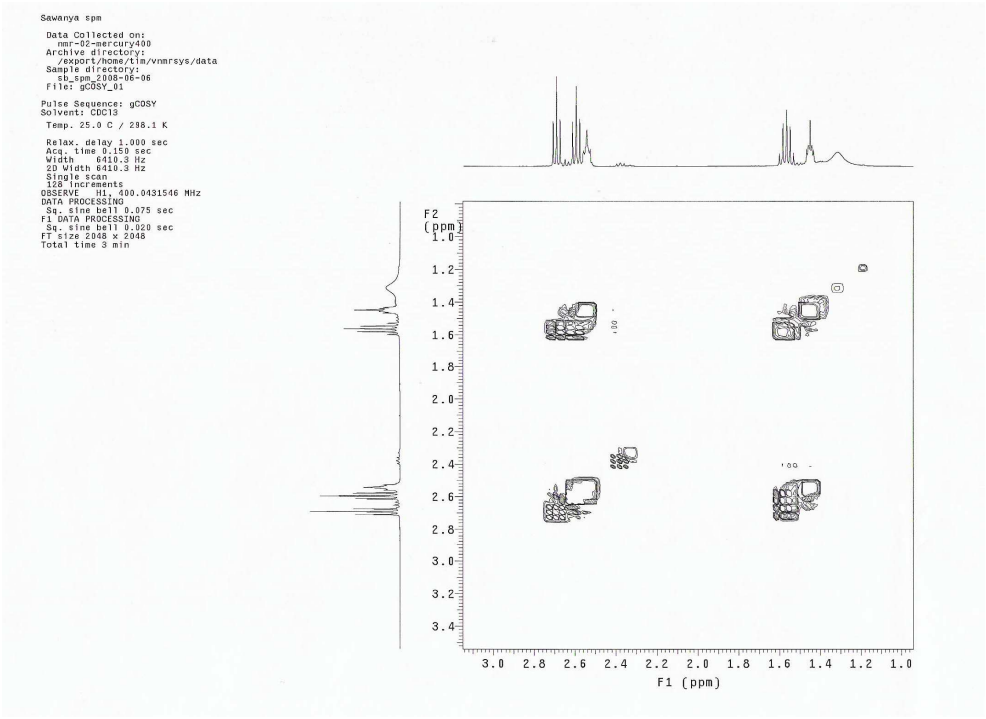

Figure 6.50 COSY of spermine.

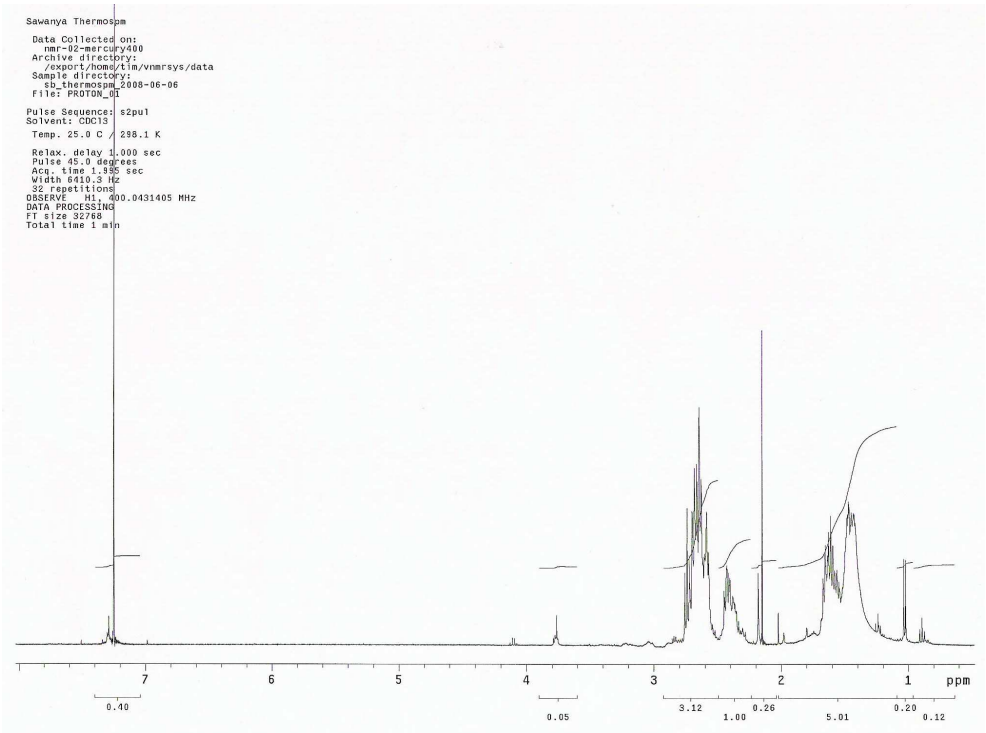

Figure 6.51 ^{1}H NMR of thermospermine.

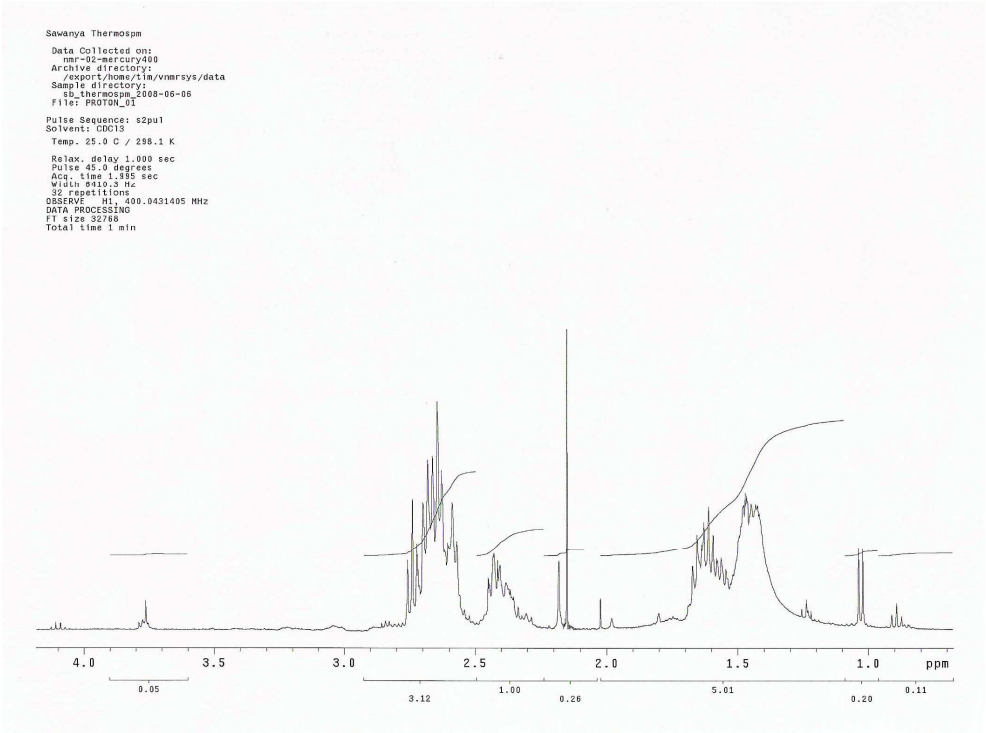

Figure 6.52 ^{1}H NMR of thermospermine.

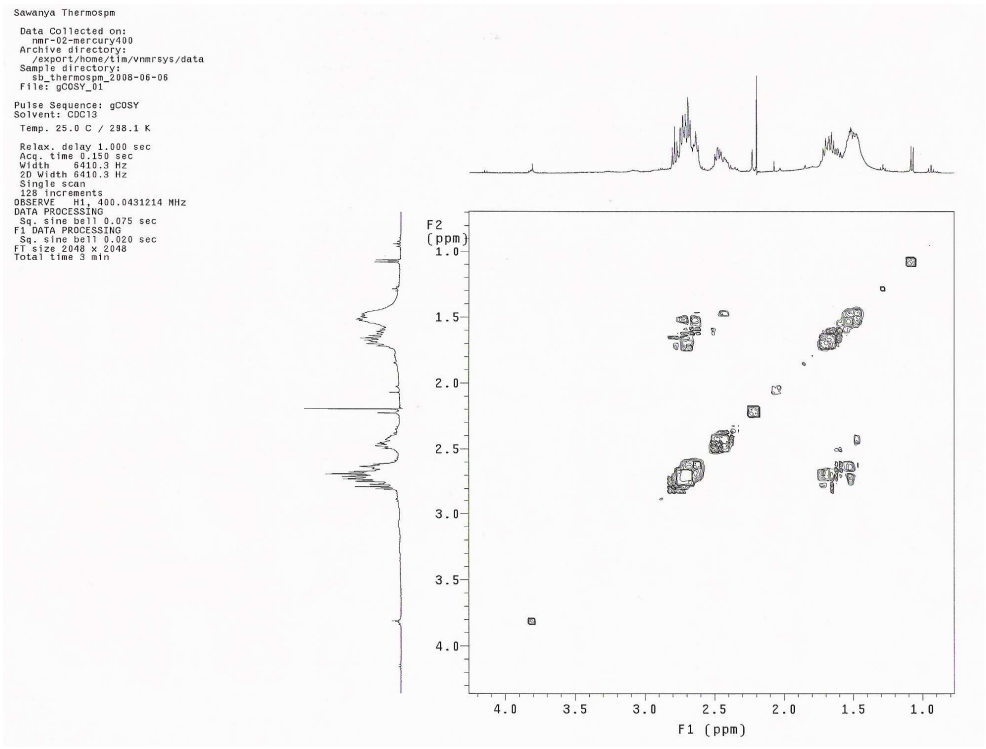

Figure 6.53 COSY NMR of thermospermine.

Analysis of Thermospermine and Spermine

Method 1 Analysis by HR-ESI-MS

Hexahydropyrimidine derivative of spermine

Dihexahydropyrimidine rings derivative of spermine, 1,4-(dihexahydropyrimidine)butane (**11**) was prepared by the reaction of spermine (**10**) against formaldehyde (2 equiv.) (Figure 6.54) and the result was confirmed by HR-ESI-MS (Figure 6.55).

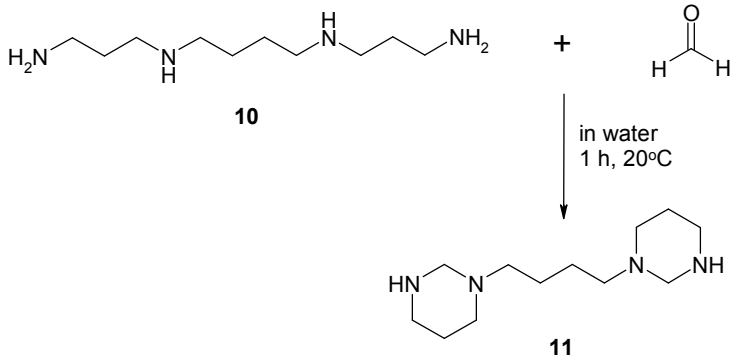

Figure 6.54 1,4-(Dihexahydropyrimidine) butane (**11**) synthesis.

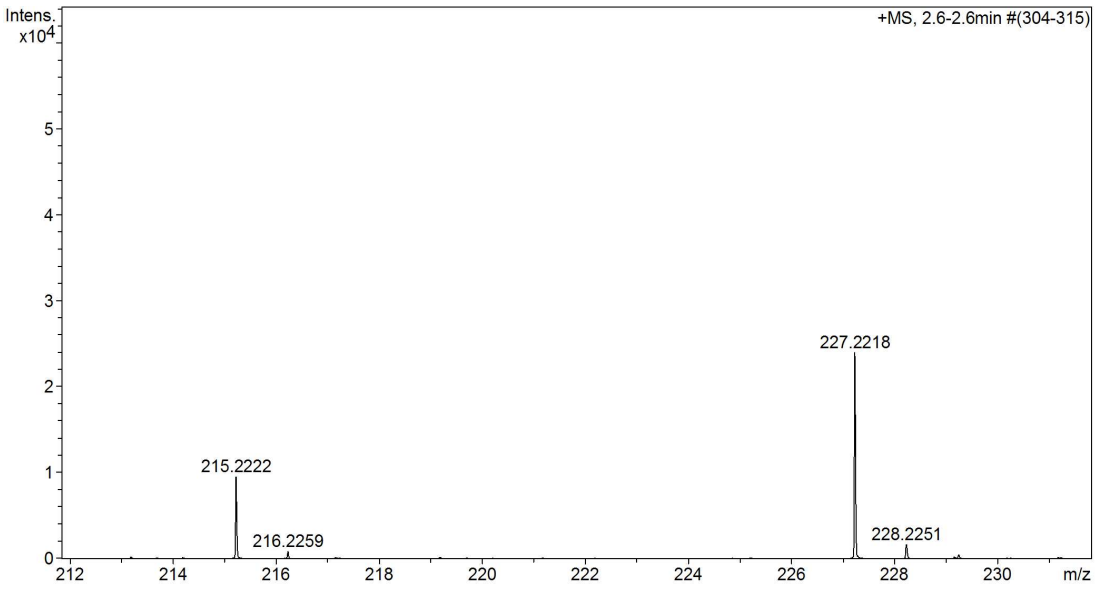

Figure 6.55 HR-ESI-MS spectrum of desired product 1,4-dihexahydropyrimidine-butane (**11**) (M.W. = 226.2157, $C_{12}H_{26}N_4$) expected m/z $[M+H]^+$ ion = 227.2236 (found = 227.2218) and doubly charged ion $[M+2H]^{2+}$ = 114.1157 (found = 114.1181) also found was the product of incomplete reaction where spermine had been derivatized with only one hexahydropyrimidine ring, 1-hexahydropyrimidine-5-aza-8-aminooctane (M.W. = 214.2157, $C_{11}H_{26}N_4$) expected m/z $[M+H]^+$ ion = 215.2236 (found = 215.2222)

From this result, it is concluded that the reaction of spermine (**10**) with formaldehyde (2 equiv.) was not complete so the mole ratio of formaldehyde was increased to 2.5 equiv. and the result was confirmed by HR-ESI-MS (Figure 6.56).

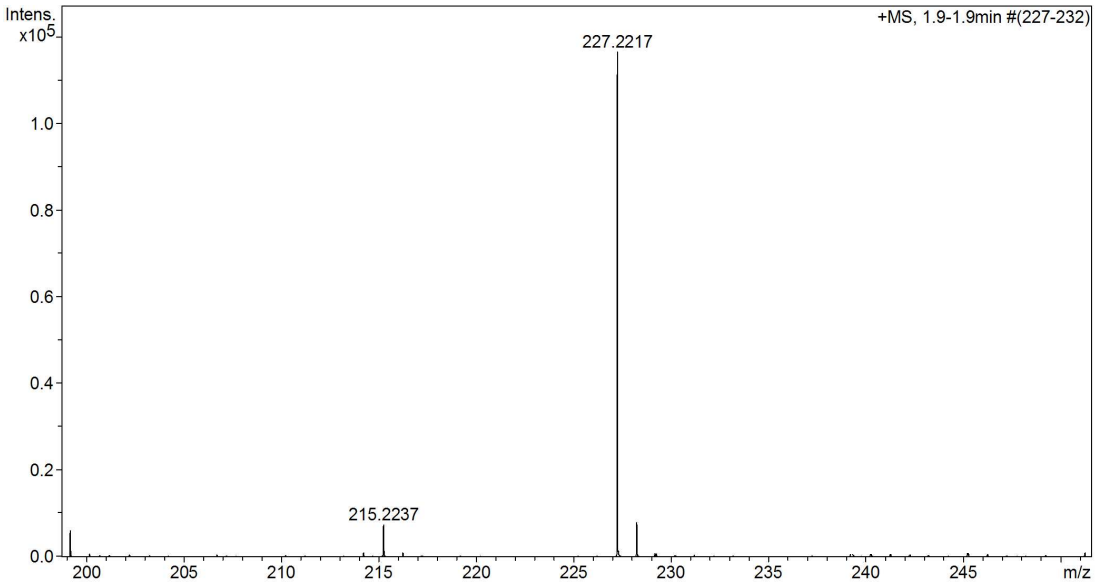

Figure 6.56 HR-ESI-MS spectra of desired product 1,4-(dihexahydropyrimidine) butane (**11**) (M.W. = 226.2157, $C_{12}H_{26}N_4$) expected m/z $[M+H]^+$ ion = 227.2236 (found = 227.2217) also found was the product of incomplete reaction where spermine had been derivatized with only one hexahydropyrimidine ring, 1-hexahydropyrimidine-5-aza-8-aminooctane (M.W. = 214.2157, $C_{11}H_{26}N_4$) expected m/z $[M+H]^+$ ion = 215.2236 (found = 215.2237).

The mole ratio of formaldehyde was increased to 2.5 equiv., however, the m/z $[M+H]^+$ ion = 215.2236 was still obtained. It is possible that this value of $[M+H]^+$ ion at 215.2236 arose from hexahydropyrimidine ring of thermospermine, 1-(hexahydropyrimidine)-4-aza-aminooctane (**12**), which means that thermospermine might contaminate in the commercial spermine.

Hexahydropyrimidine derivative of thermospermine

Hexahydropyrimidine ring derivative of thermospermine, 1-(hexahydropyrimidine)-4-aza-aminooctane (**12**) was prepared by the reaction of thermospermine (**6**) against formaldehyde 0.1 mL (2 equiv.) (Figure 6.57). The product was confirmed by HR-ESI-MS (Figure 6.58).

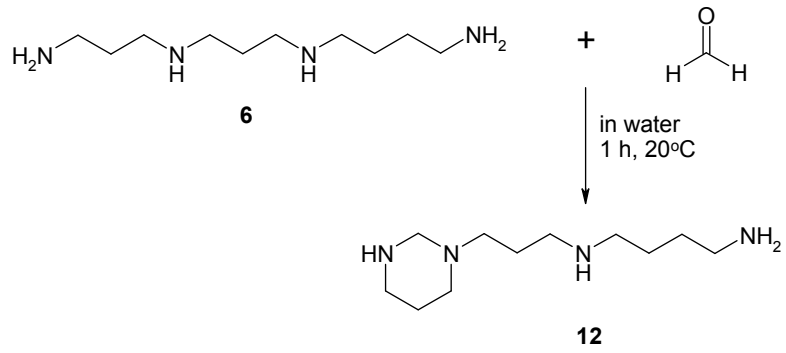

Figure 6.57 1-(Hexahydropyrimidine)-4-aza-aminooctane (**12**) synthesis.

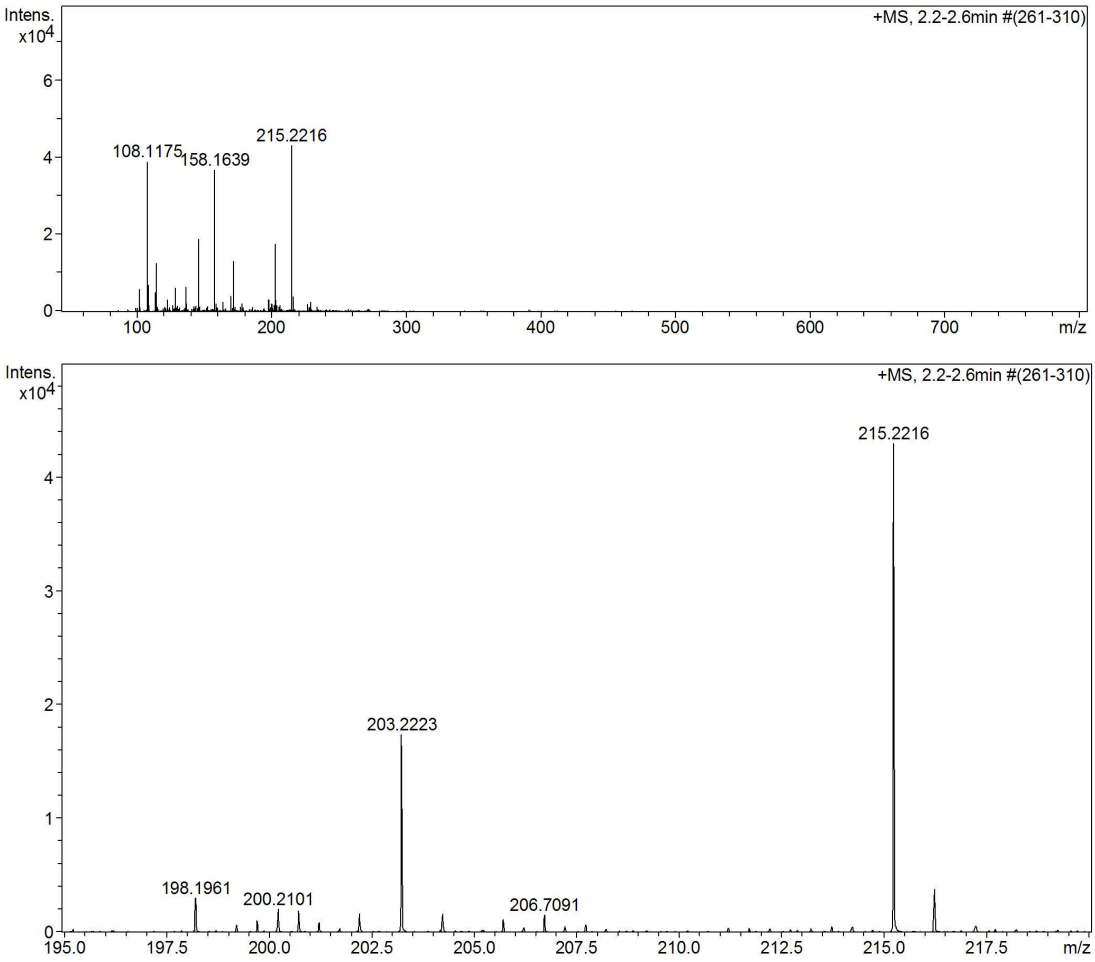

Figure 6.58 HR-ESI-MS spectra of desired product 1-(hexahydropyrimidine)-4-aza-aminooctane (**12**) (M.W. = 214.2157, $C_{11}H_{26}N_4$) expected m/z $[M+H]^+$ ion = 215.2236 (found = 215.2216) and doubly charged ion $[M+2H]^{2+}$ = 108.1157 (found = 108.1175) also the starting material of thermospermine (**6**), (M.W. = 202.2157, $C_{10}H_{26}N_4$) expected m/z $[M+H]^+$ ion = 203.2236 (found = 203.2223) and peak of *N*-(4-aminobutyl) hexahydropyrimidine (**2**) (M.W. = 157.1579, $C_8H_{19}N_3$), expected m/z $[M+H]^+$ ion = 158.1657 (found = 158.1639).

From the result of HR-ESI-MS, it suggested that not all of thermospermine was converted to $N^1$1-(hexahydropyrimidine)-4-aza-aminooctane (**12**), as the MS showed peak at $[M+H]^+$ ion = 203.2236 of the starting material and also the peak of *N*-(4-aminobutyl) hexahydropyrimidine (**2**) at $[M+H]^+$ ion = 158.1657, however, the peak of 1,4-(dihexahydropyrimidine)butane (**11**) not found.

Method 2: Analysis by the reaction with dideuteriated formaldehyde.

Spermidine

The reaction of spermidine (**1**) with dideuteriated formaldehyde gave the desired product of *N*-(4-aminobutyl) hexahydropyrimidine dideuteriated but this reaction might give the other possible product (Figure 6.59), the presence of both products were confirmed by HR-ESI-MS (Figure 6.60).

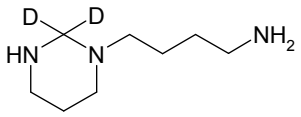

N-(4-Aminobutyl) hexahydropyrimidine-2,2-dideuteriate

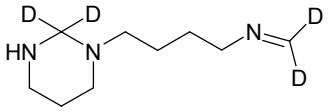

N-(4-(Dideuterioratedmetyl-1-ene)iminobutyl)-hexahydropyrimidine-2,2-dideuteriate

Figure 6.59 The products from the reaction of spermidine (**1**) with dideuteriated formaldehyde.

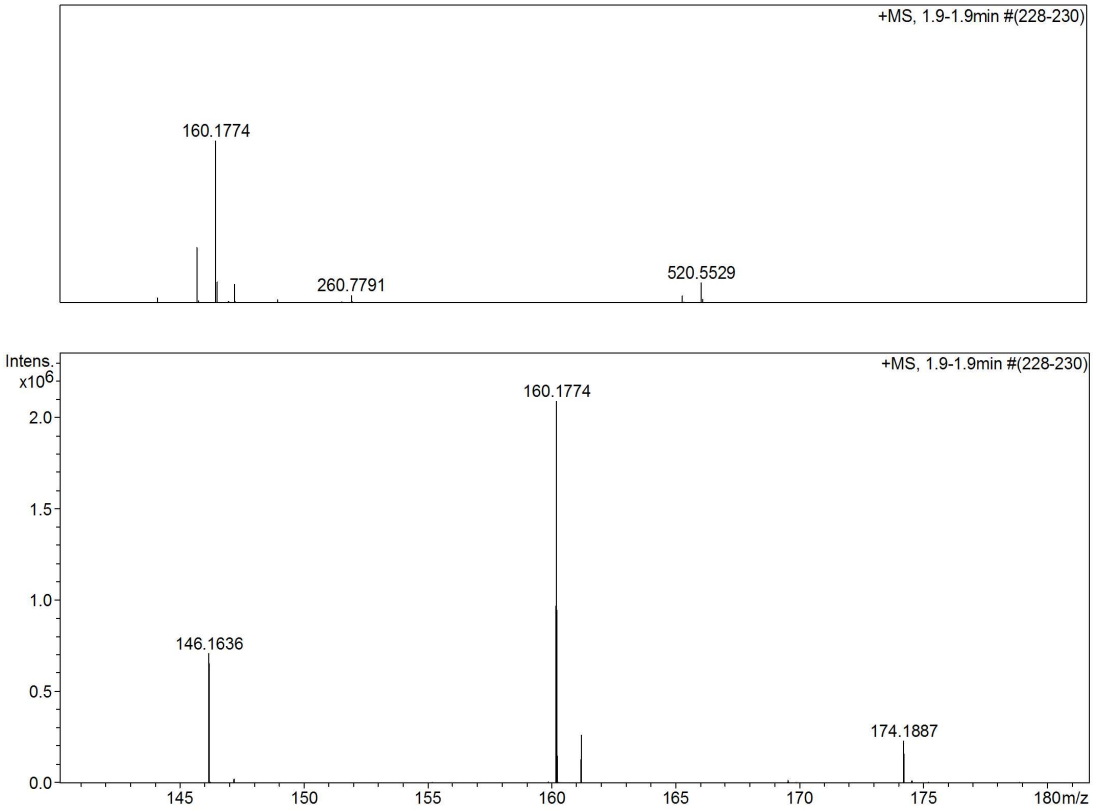

Figure 6.60 HR-ESI-MS spectra of spermidine (**1**) (M.W. = 145.1548, $C_7H_{15}N_3D_2$) expected m/z $[M+H]^+$ ion = 146.1626 (found = 146.1636), and the peak of *N*-(4-aminobutyl) hexahydropyrimidine dideuteriate (M.W. = 159.1704, $C_8H_{17}N_3D_2$) expected m/z $[M+H]^+$ ion = 160.1783 (found = 160.1774) and the peak of *N*-(4-(1-ine dideuteriorated)-aminobutyl)-hexahydropyrimidine dideuteriate (M.W. = 173.1829, $C_9H_{15}N_3D_4$) expected m/z $[M+H]^+$ ion = 174.1908 (found = 174.1887)

The result showed the desired product of *N*-(4-aminobutyl) hexahydropyrimidine dideuteriate at m/z $[M+H]^+$ ion = 160.1783 as the main peak and the expected peak of *N*-(4-(1-ine dideuteriated)-aminobutyl)-hexahydropyrimidine dideuteriate at m/z $[M+H]^+$ ion = 174.1908, however, there was another peak at m/z $[M+H]^+$ ion = 146.1626 which might be from the contamination of 3, 3 amine (Figure 6.61) from the commercial spermidine.

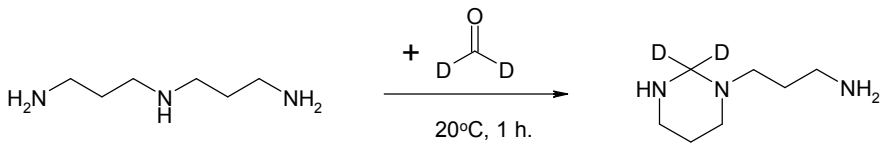

Figure 6.61 The reaction between spermidine and dideuteriated formaldehyde.

Spermine

Spermine was reacted with dideuteriated formaldehyde to obtain the desired product 1,4-dihexahydropyrimidine-2,2,2′,2′-tetradeuterio-butane (Figure 6.62) confirmed by HR-ESI-MS (Figure 6.63). The mole ratio of dideuteriated formaldehyde used was 2.5 equiv., however, the m/z $[M+H]^+$ ion = 217.2361 was obtained. It is possible that in the commercial spermine contains thermospermine which will give the same $[M+H]^+$ ion value.

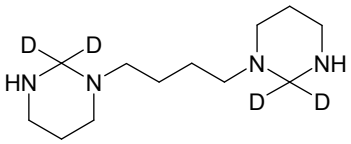

Figure 6.62 1,4-Dihexahydropyrimidine-2,2,2′,2′-tetradeuterio-butane (spermine-di-2,2,2′,2′-dideuterohexahydropyrimidine).

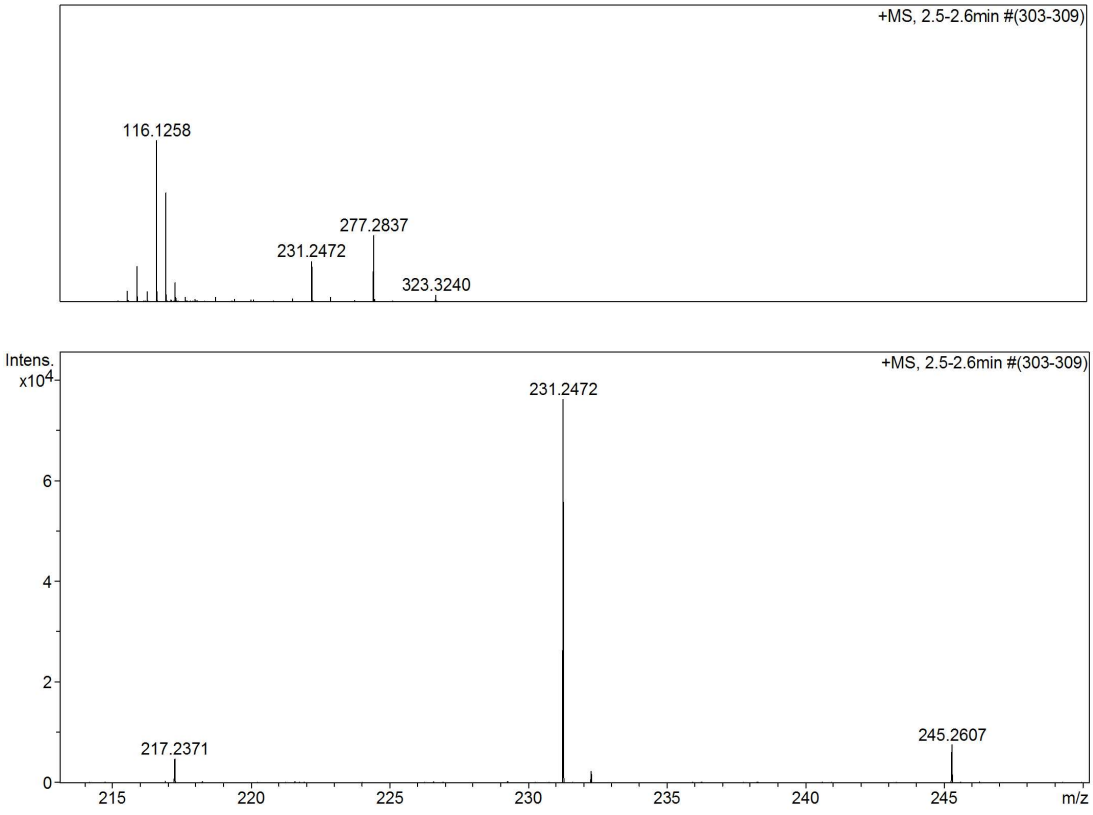

Figure 6.63 HR-ESI-MS spectra of 1,4-(dihexahydropyrimidine-2,2,2′,2′-tetradeuterio) butane (M.W. = 230.2408, $C_{12}H_{22}N_4D_4$) expected m/z $[M+H]^+$ ion = 231.2486 (found = 231.2472), doubly charged ion of $[M+2H]^{2+}$ at 116.1282 (found = 116.1258) and also the trace of $C_{11}H_{24}N_4D_2$, M.W. = 216.2283 expected m/z $[M+H]^+$ ion = 217.2361 (found = 217.2371).

Thermospermine

The reaction of thermospermine with dideuteriate formaldehyde was carried out and the desired product of 1-(hexahydropyrimidine dideuterio)-4-aza-aminooctane was obtained (Figure 6.64) which was confirmed by HR-ESI-MS (Figure 6.65). The HR-ESI-MS showed the major peak of the desired product, 8-(1-hexahydropyrimidine-2,2-dideuteri)-4-aza-aminooctane, at $[M+H]^+$ ion = 217.2361 but also found the contamination of 1,4-(dihexahydropyrimidine-2,2,2′,2′-tetradeuterio) butane at $[M+H]^+$ ion = 231.2486. Which indicates that thermospermine is not pure.

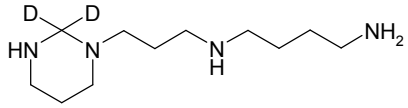

Figure 6.64 8-(1-Hexahydropyrimidine-2,2-dideuterio)-4-aza-aminooctane.

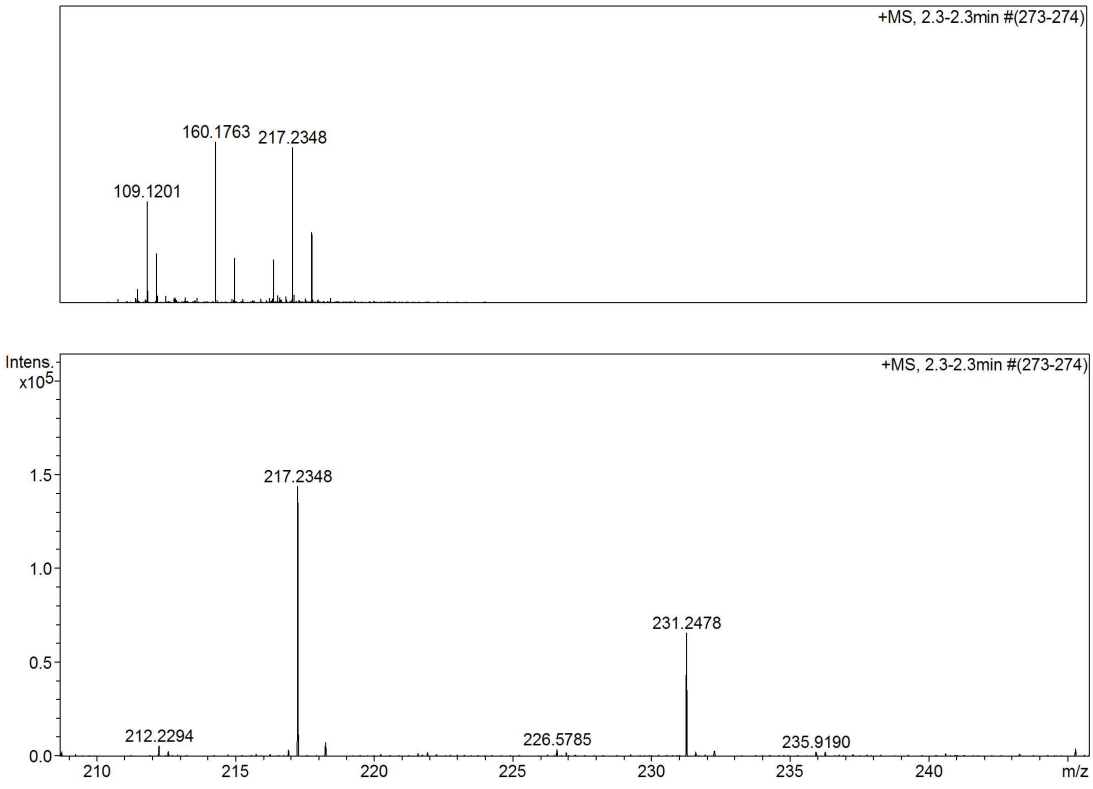

Figure 6.65 HR-ESI-MS spectra of 8-(1-hexahydropyrimidine-2,2-dideuterio)-4-aza-aminooctane (M.W. = 216.2283, $C_{11}H_{24}N_4D_2$) expected m/z $[M+H]^+$ ion = 217.2361 (found = 217.2348) doubly charged ion $[M+2H]^{2+}$ = 109.1219 (found = 109.1201) also found the peak of contamination of 8-(1-hexahydropyrimidine-2,2-dideuteri)-4-aza-aminooctane (M.W. = 230.2408, $C_{12}H_{22}N_4D_4$) expected m/z $[M+H]^+$ ion = 231.2486 (found = 231.2478).

Method 3 By the reaction of formaldehyde: dideuteriated formaldehyde (1:1).

Spermidine

Formaldehyde: dideuteriated formaldehyde (1:1) solution was used to react with spermidine in equal mole ratio, the desired products were the mixture of *N*-(4-aminobutyl)hexahydro-pyrimidine (**2**) and *N*-(4-aminobutyl) hexahydropyrimidine dideuteriate which were confirmed by HR-ESI-MS (Figure 6.66).

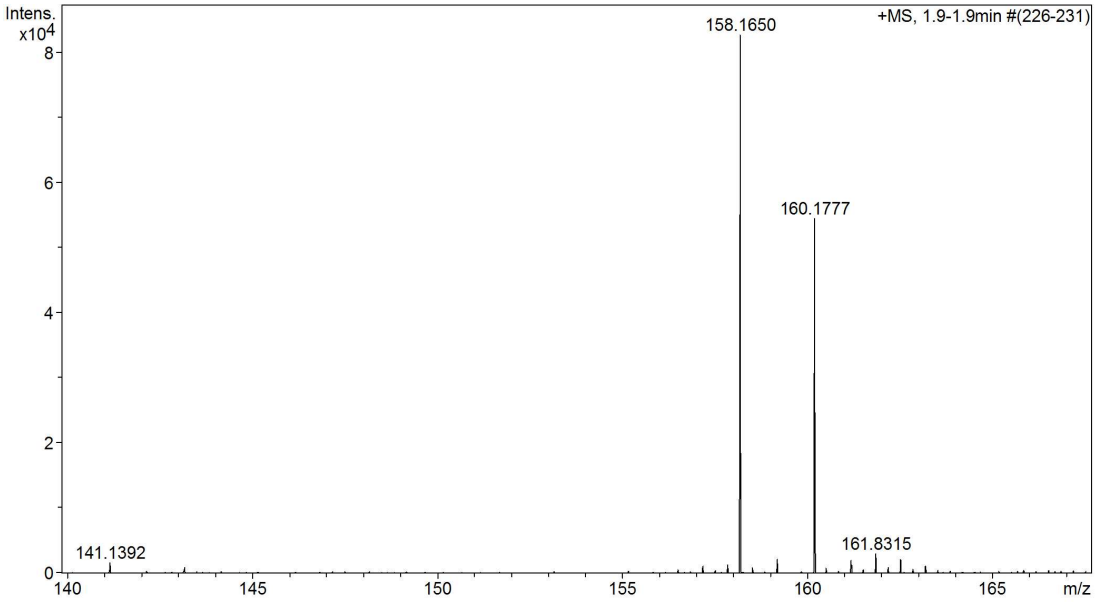

Figure 6.66 HR-ESI-MS spectrum of *N*-(4-aminobutyl) hexahydropyrimidine (**2**) (M.W. = 157.1579, $C_8H_{19}N_3$) expected m/z $[M+H]^+$ ion = 158.1657 (found = 158.1650) and *N*-(4-aminobutyl) hexahydropyrimidine dideuteriate (M.W. = 159.1704, $C_8H_{17}N_3D_2$) expected m/z $[M+H]^+$ ion = 160.1783 (found = 160.1777).

Spermine

The possible products from the reaction of spermine against formaldehyde: dideuteriated formaldehyde (1:1) solution (2 equiv.) was shown in Figure 6.67 and confirmed by HR-ESI-MS (Figure 6.68).

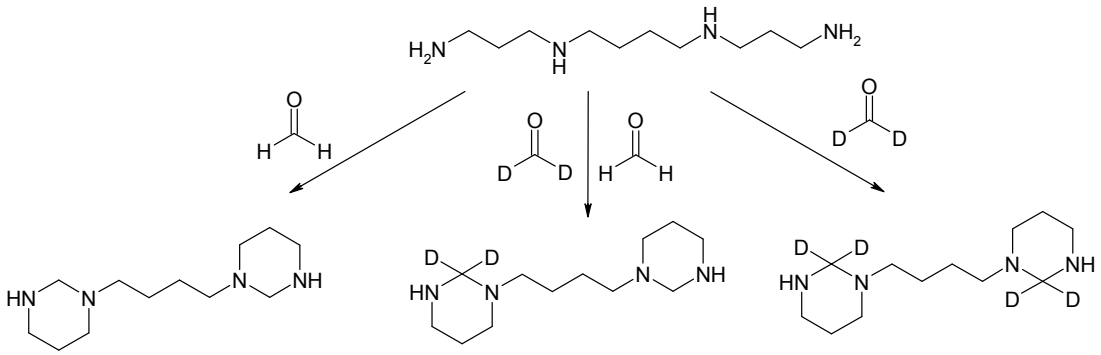

Figure 6.67 The possible products from the reaction of spermine against formaldehyde: dideuteriated formaldehyde (1:1) solution (2 equiv.).

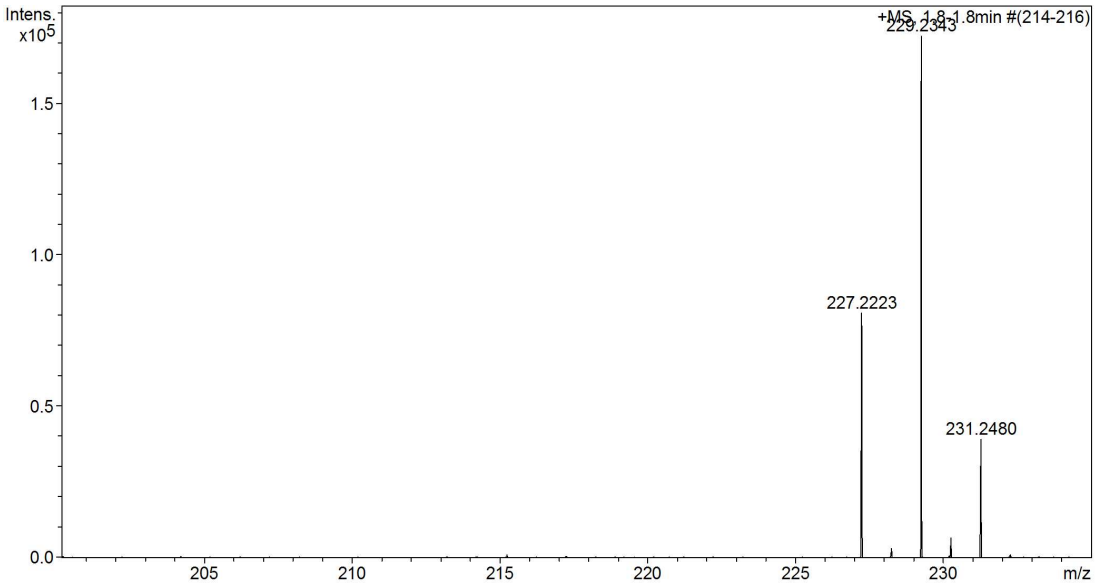

Figure 6.68 HR-ESI-MS spectrum of desired product 1,4-(dihexahydropyridine)butane(**11**) (M.W. = 226.2157, $C_{12}H_{26}N_4$) expected m/z $[M+H]^+$ ion = 227.2236 (found = 227.2223), the product of 1-(hexahydropyrimidine)-5-aza-aminooctane (M.W. = 228.2283, $C_{12}H_{24}N_4D_2$) expected m/z $[M+H]^+$ ion = 229.2361 (found = 229.2343) 1,4-(dihexahydropyrimidine tetradeuteriate) butane (M.W. = 230.2408, $C_{12}H_{22}N_4D_4$) expected m/z $[M+H]^+$ ion = 231.2486 (found = 231.2480).

Thermospermine

The possible products from the reaction of thermospermine against formaldehyde: dideuteriated formaldehyde (1:1) solution (2 equiv.) was shown in Figure 6.69 and confirmed by HR-ESI-MS (Figure 6.70).

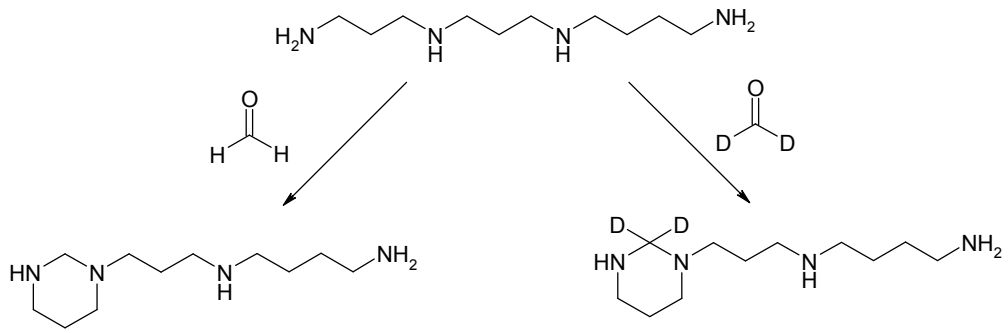

Figure 6.69 The possible products from the reaction of thermospermine against formaldehyde: dideuteriated formaldehyde (1:1) solution (2 equiv.).

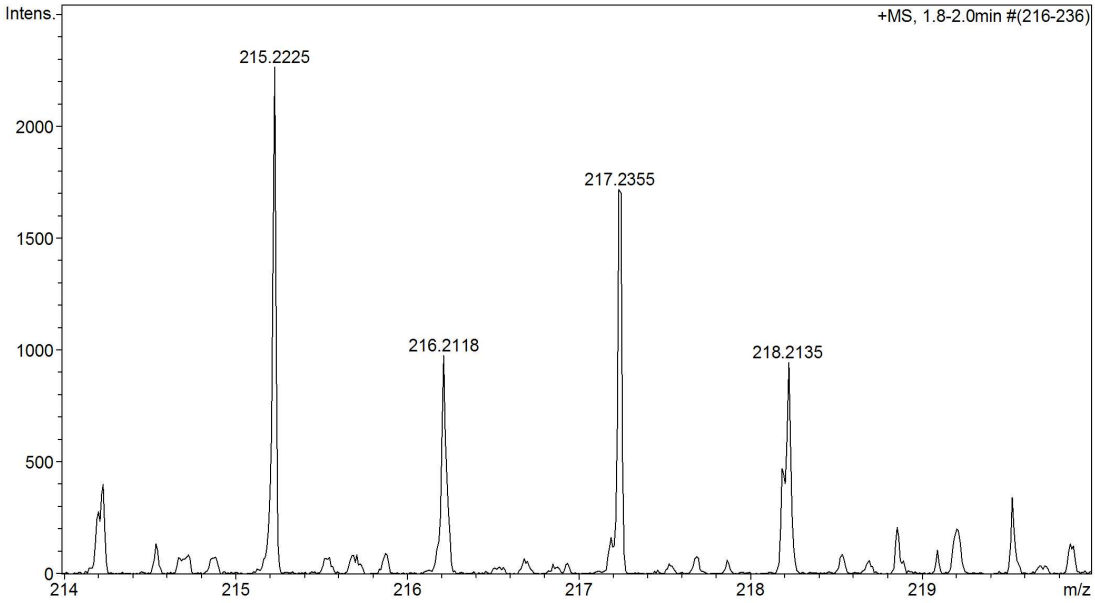

Figure 6.70 HR-ESI-MS spectra of desired product 1-(hexahydropyrimidine)-4-aza-aminooctane (**12**) (M.W. = 214.2157, $C_{11}H_{26}N_4$) expected m/z $[M+H]^+$ ion = 215.2236 (found = 215.2225) and 1-(hexahydropyrimidine dideuteriate)-4-aza-aminooctane (M.W. = 216.2283, $C_{11}H_{24}N_4D_2$) expected m/z $[M+H]^+$ ion = 217.2361 (found = 217.2355).

Method 4 By labelling the thermospermine and hexahydropyrimidine ring of thermospermine with dansyl chloride. Later, method 2 of dansylation was used to investigate these products.

Spermidine

N-(4-Aminobutyl) hexahydropyrimidine (**2**) reacts with DNS Cl to give *N*-(4-aminobutyl) hexahydropyrimidine (**2**)-diDNS derivative (Figure 6.71). HPLC chromatogram of this

product showed shorter retention time than spermidine (**1**)-triDNS derivative (Figure 6.72). The elution of *N*-(4-aminobutyl) hexahydropyrimidine (**2**)-diDNS derivative was confirmed by HR-ESI-MS (Figure 6.73).

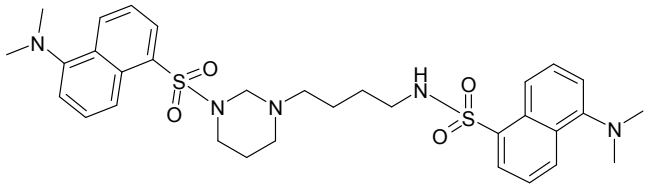

Figure 6.71 *N*-(4-Aminobutyl) hexahydropyrimidine (**2**)-diDNS derivative (M.W. = 623.2599, $C_{32}H_{41}N_5O_4S_2$)

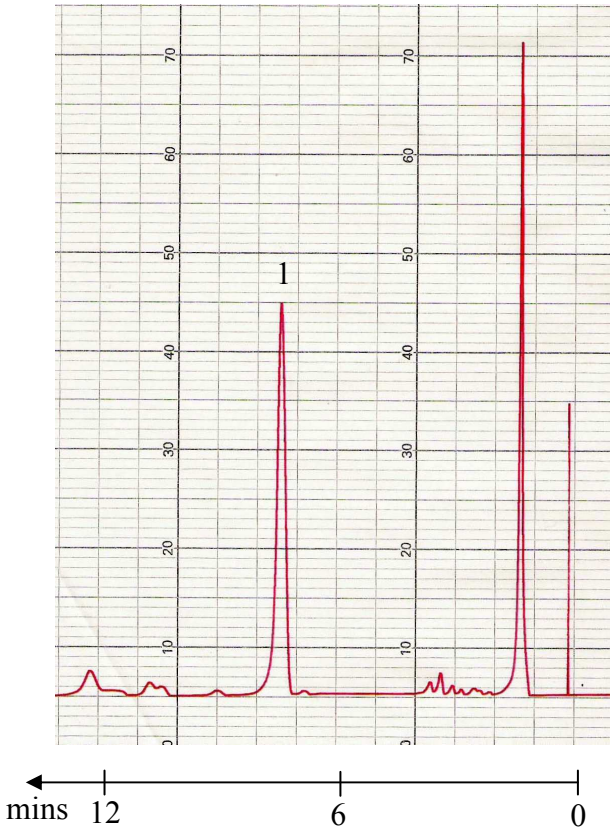

Figure 6.72 HPLC chromatogram of *N*-(4-aminobutyl) hexahydropyrimidine (**2**)-diDNS derivative. HPLC conditions: mobile phase is acetonitrile: Milli-Q-water (70:30), C8-luna column, flow rate 1 mL/min, fluorescence detector at λ_{ex} = 330 nm, λ_{em} = 510 nm. The chromatogram shows peak 1 = *N*-(4-aminobutyl) hexahydropyrimidine (**2**)-diDNS derivative at Rt = 7.0 min, peak 2 = spermidine-triDNS derivative at Rt = 11.5 min.

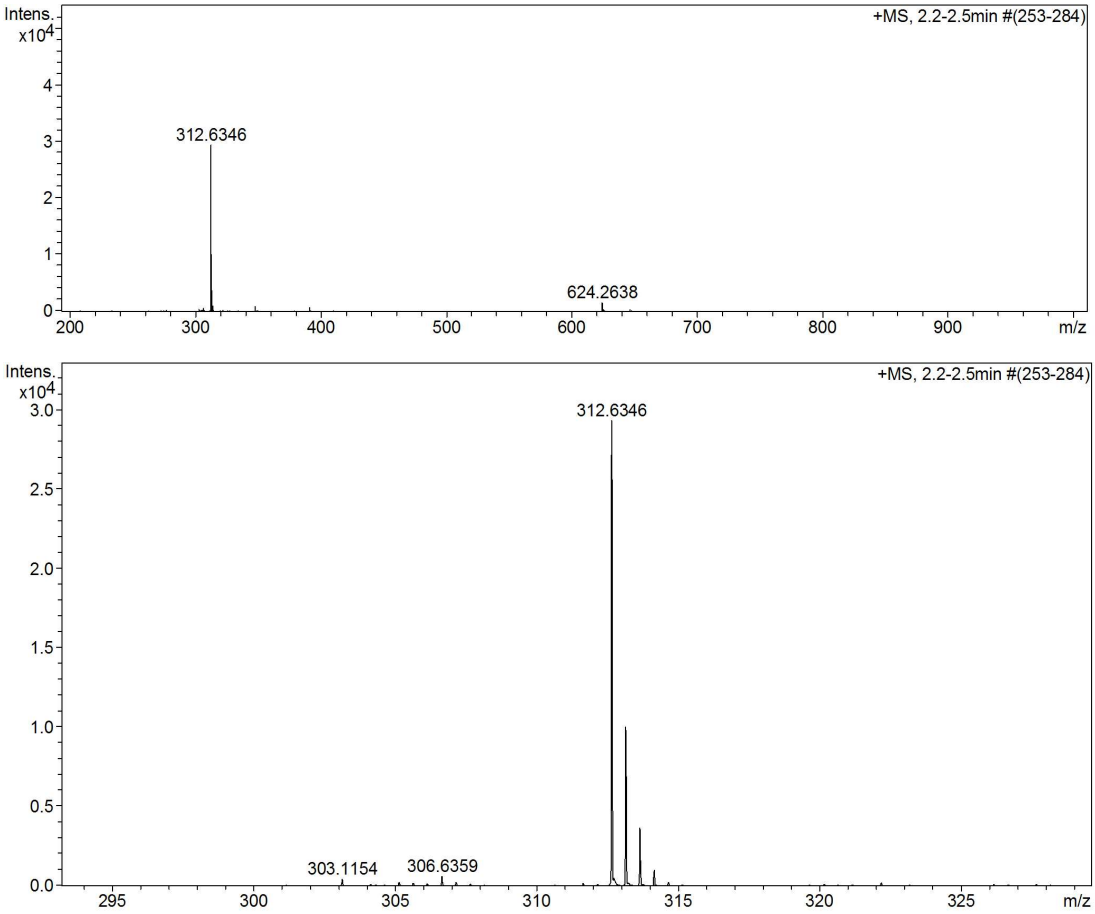

Figure 6.73 HR-ESI-MS spectra of *N*-(4-aminobutyl) hexahydropyrimidine (**2**)-diDNS derivative (M.W. = 623.2599, $C_{32}H_{41}N_5O_4S_2$) expected m/z $[M+H]^+$ ion = 624.2678 (found = 624.2638) and doubly charged ion $[M+2H]^{2+}$ = 312.6378 (found = 312.6346).

Spermine and thermospermine

Spermine and thermospermine react with DNS Cl to give the same molecular weight derivatives as tetraDNS derivatives (Figure 6.74) which both cannot be distinguished by HR-ESI-MS (Figure 6.76) or by HPLC chromatogram (Figure 6.75) as they will be eluted at the same retention time (at 30 min, HPLC conditions: mobile phase is acetonitrile: Milli-Q-water (70:30), C8-luna column, flow rate 1 mL/min). However, by the reaction with formaldehyde, spermine will be changed into 1,4-(dihexahydropyrimidine)butane (**11**) which reacts with only two moiety of DNS Cl while thermospermine will be changed into 1-(hexahydropyrimidine)-4-aza-aminooctane (**12**) which reacts with three moiety of DNS Cl. Thus, by this method, spermine and thermospermine will be distinguished by HPLC.

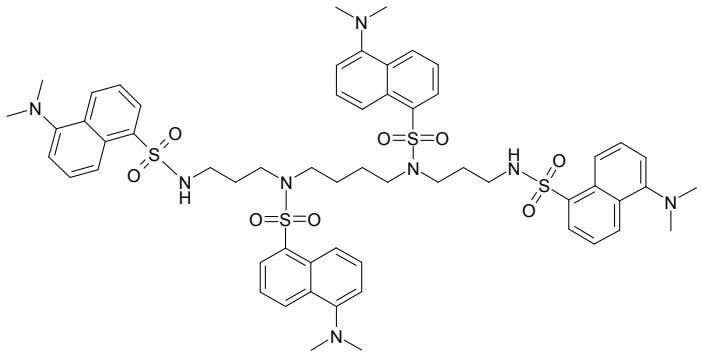

(A) Spermine-tetraDNS derivative

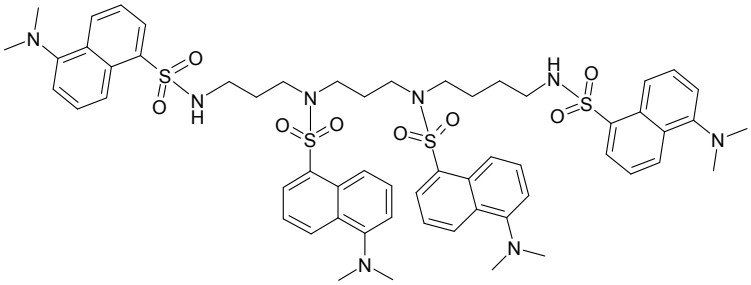

(B) Thermospermine-tetraDNS derivative

Figure 6.74 The tetraDNS derivatives of (A) spermine and (B) thermospermine, both have the same molecular formula $C_{58}H_{70}N_8O_8S_4$, M.W. = 1134.4199.

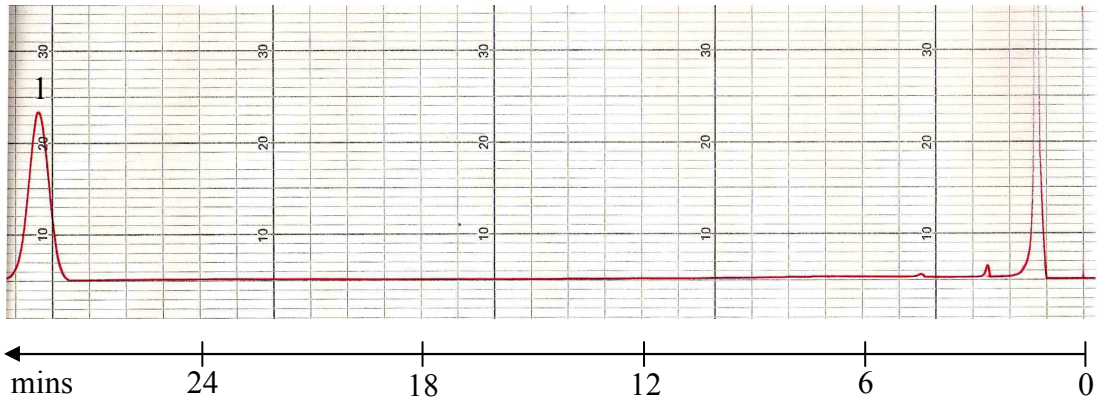

Figure 6.75 HPLC chromatogram of spermine-tetraDNS derivative. HPLC conditions: mobile phase is acetonitrile: Milli-Q-water (70:30), C8-luna column, flow rate 1 mL/min, fluorescence detector at λ_{ex} = 330 nm, λ_{em} = 510 nm. The chromatogram shows peak 1 = spermine-tetraDNS derivative at Rt = 28.5 min.

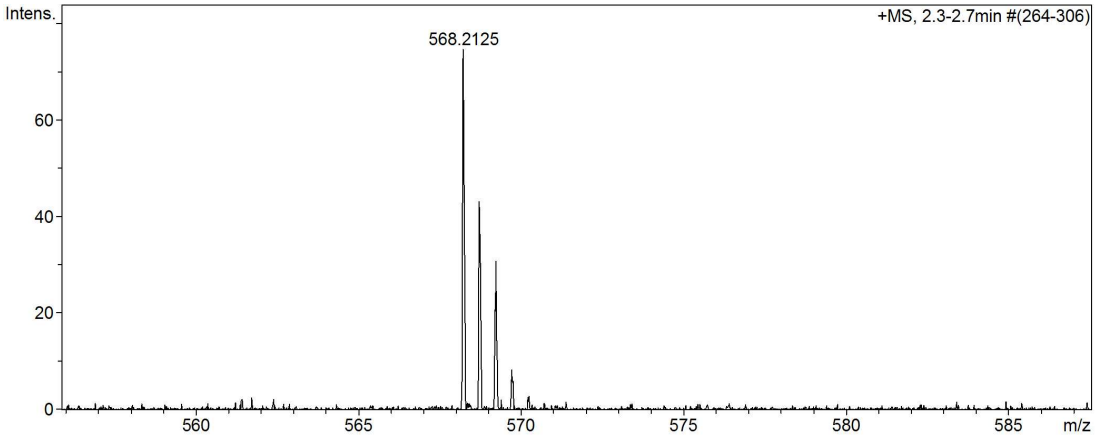

Figure 6.76 HR-ESI-MS spectrum of spermine or thermospermine-tetraDNS derivative (M.W. = 1134.4199, $C_{58}H_{70}N_8O_8S_4$) expected m/z $[M+H]^+$ ion = 1135.4277 and doubly charged ion $[M+2H]^{2+}$ = 568.2177 (found = 568.2125).

When spermine reacts with formaldehyde, two possible products could be obtained. One possible product contains one ring of hexahydropyrimidine and another one from the completed reaction which adds two methylene groups to spermine yield 1,4-(dihexahydropyrimidine)butane (**11**). The reaction of formaldehyde with thermospermine leads to production of 1-(hexahydropyrimidine)-4-aza-aminooctane (**12**). Both one ring of hexahydropyrimidine of spermine and 1-(hexahydropyrimidine)-4-aza-aminooctane (**12**) react with DNS Cl reagent to yield triDNS derivatives which both have the same molecular weight. Thus, HPLC chromatogram cannot differentiate these two molecules. So it is necessary to get the reaction complete to obtain only one product of 1,4-(dihexahydropyrimidine)butane (**11**) from the reaction of spermine against formaldehyde.

1,4-(Dihexahydropyrimidine)butane (**11**) reacted with DNS Cl to yield 1,4-(dihexahydropyrimidine)butane (**11**)-diDNS derivative (Figure 6.77). HPLC chromatogram of this derivative was obtained (Figure 6.78) and confirmed the elution at Rt = 10 min by HR-ESI-MS (Figure 6.79).

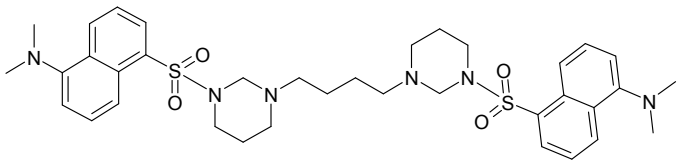

Figure 6.77 1,4-(Dihexahydropyrimidine)butane (**11**)-diDNS derivative.

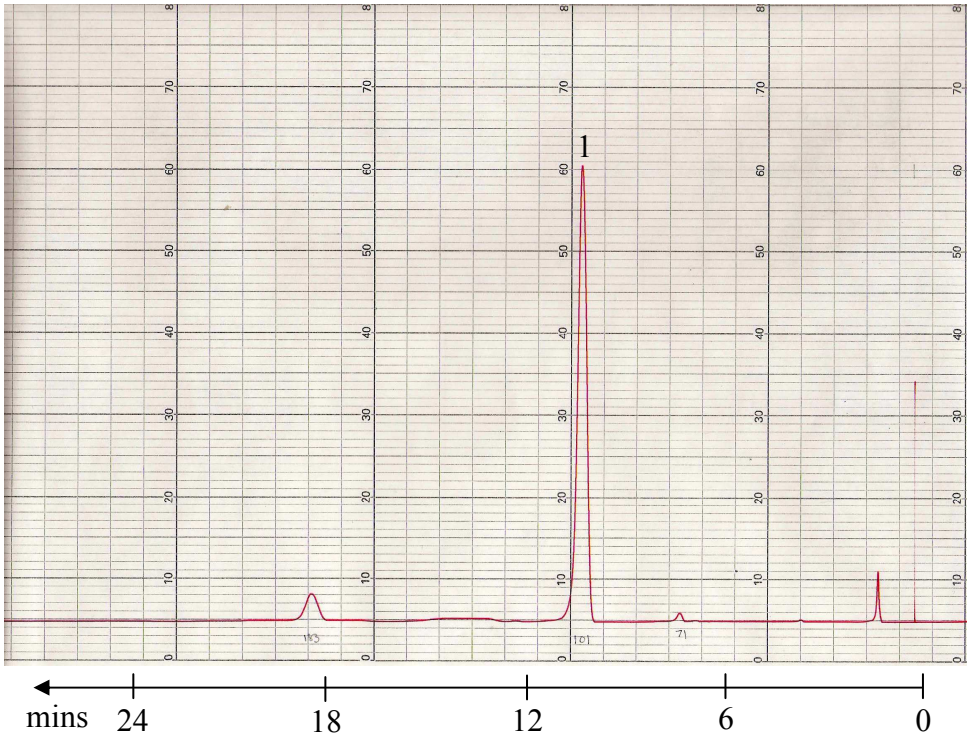

Figure 6.78 HPLC chromatogram of 1,4-(dihexahydropyrimidine)butane (**11**)-diDNS derivative. HPLC conditions: mobile phase is acetonitrile: Milli-Q-water (70:30), C8-luna column, flow rate 1 mL/min, fluorescence detector at λ_{ex} = 330 nm, λ_{em} = 510 nm. The chromatogram shows peak 1 = 1,4-(dihexahydropyrimidine)butane (**11**)-diDNS derivative at Rt = 10.0 min.

By dansylation thermospermine, the peak of 1-(hexahydropyrimidine)-4-aza-aminooctane (**12**)-triDNS derivative was eluted at Rt = 18 min (HPLC condition; C-8 luna, mobile phase: acetonitrile: Milli-Q-water (70: 30) flow rate = 1 mL/min). HPLC chromatogram is shown in Figure 6.80, the elution was confirmed by HR-ESI-MS (Figure 6.81).

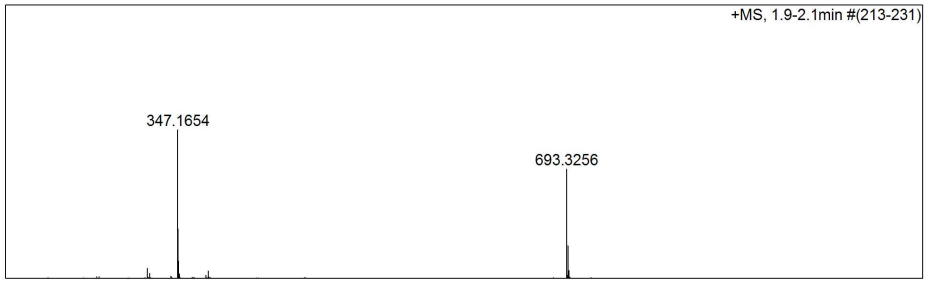

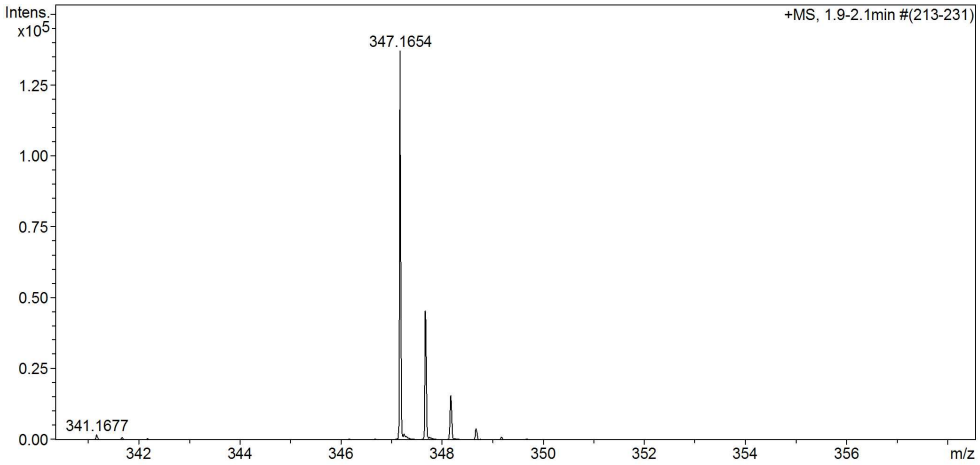

Figure 6.79 HR-ESI-MS spectra of 1,4-(dihexahydropyrimidine)butane (**11**)-diDNS derivative (M.W. = 692.3178, $C_{36}H_{48}N_6O_4S_2$) expected m/z $[M+H]^+$ ion = 693.3256 (found = 693.3256) and doubly charged ion $[M+2H]^{2+}$ = 347.1667 (found = 347.1654).

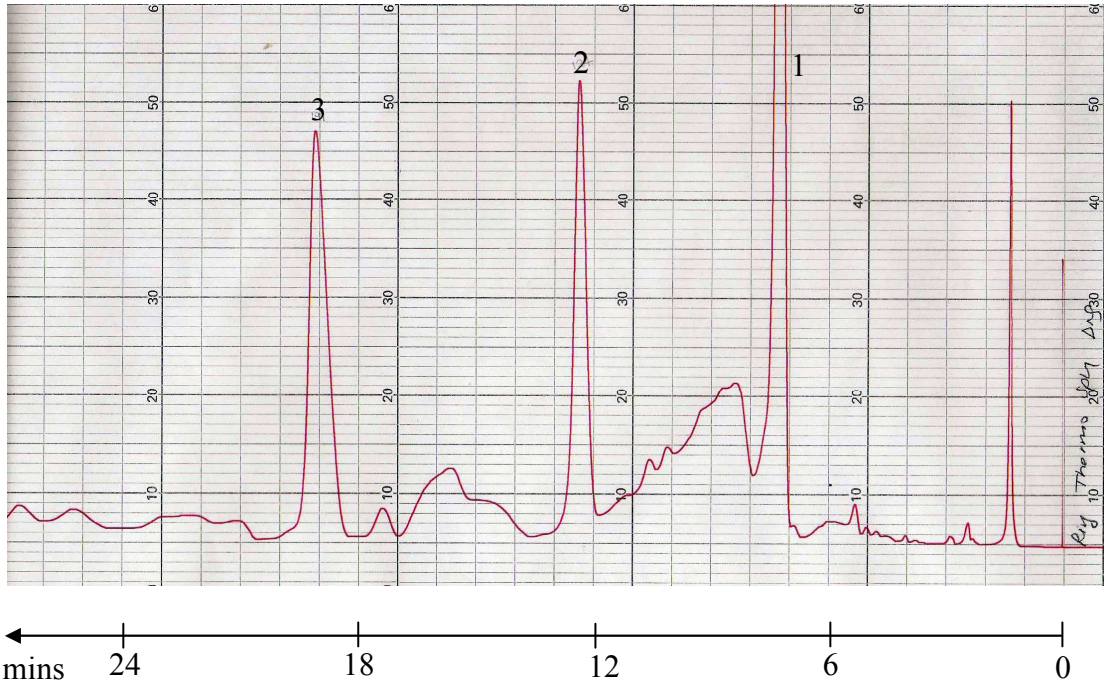

Figure 6.80 HPLC chromatogram of 1-(hexahydropyrimidine)-4-aza-aminooctane (**12**)-triDNS derivative. HPLC conditions: mobile phase is acetonitrile: Milli-Q-water (70:30), C8-luna column, flow rate 1 mL/min, fluorescence detector at λ_{ex} = 330 nm, λ_{em} = 510 nm. The chromatogram shows peak 1 = *N*-(4-aminobutyl) hexahydropyrimidine (**2**)-diDNS derivative at Rt = 7.0 min, peak 2 = 1,4-(dihexahydropyrimidine)butane (**11**)-diDNS derivative at Rt = 12.0 min, peak 3 = 1-(hexahydropyrimidine)-4-aza-aminooctane (**12**)-triDNS derivative at Rt = 19.0 min.

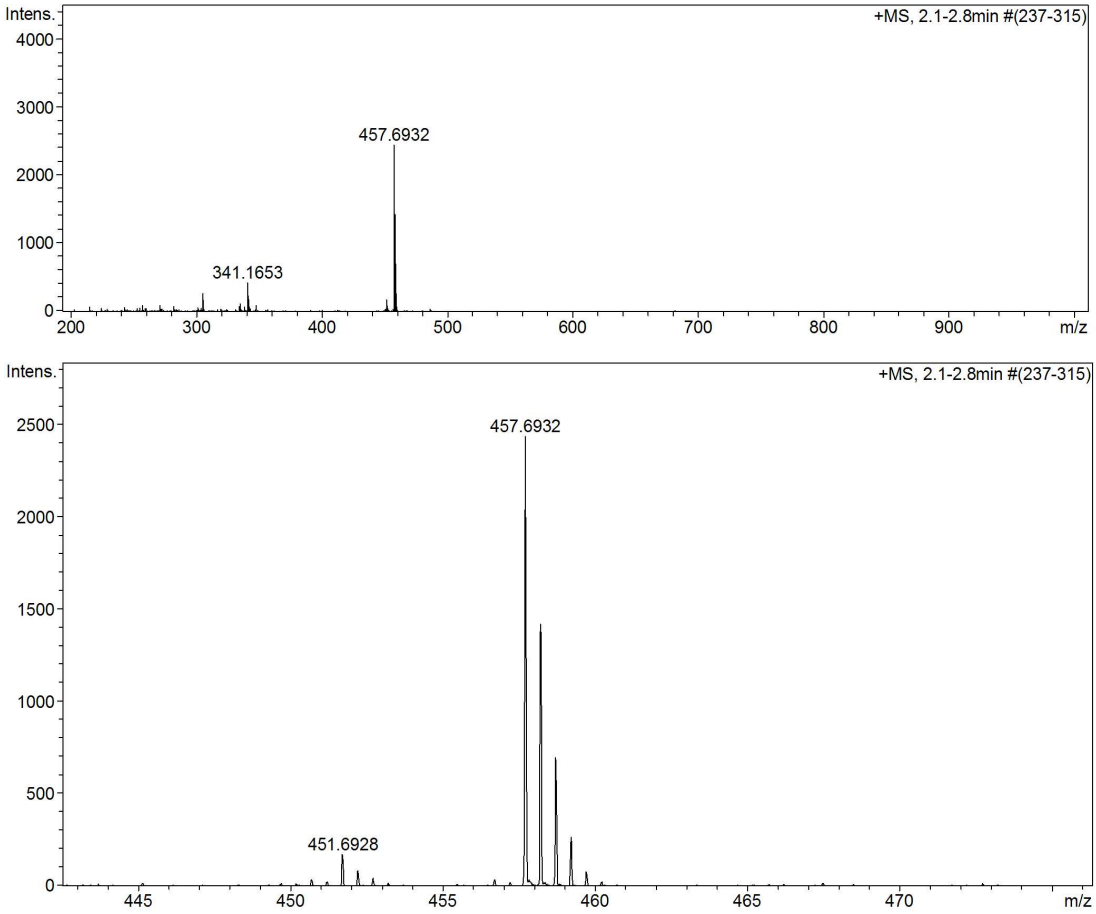

Figure 6.81 HR-ESI-MS spectra of 1-(hexahydropyrimidine)-4-aza-aminooctane (**12**)-triDNS derivative (M.W. = 913.3689, $C_{47}H_{59}N_7O_6S_3$) expected m/z $[M+H]^+$ ion = 914.3767 and doubly charged ion $[M+2H]^{2+}$ = 457.6923 (found = 457.6932).

1,4-(Dihexahydropyrimidine tetradeuterio)butane was reacted with DNS Cl to obtain the diDNS derivative (Figure 6.82) and injected onto HPLC. After purification by HPLC the identity of the homogenous product was confirmed by HR-ESI-MS (Figure 6.83).

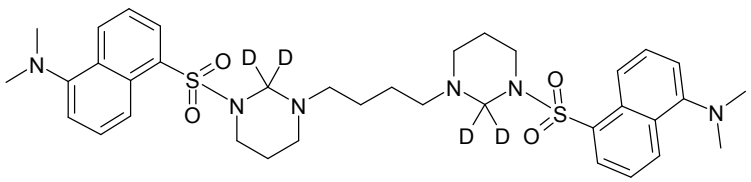

Figure 6.82 1,4-(Dihexahydropyrimidine tetradeuterio)butane-diDNS derivative.

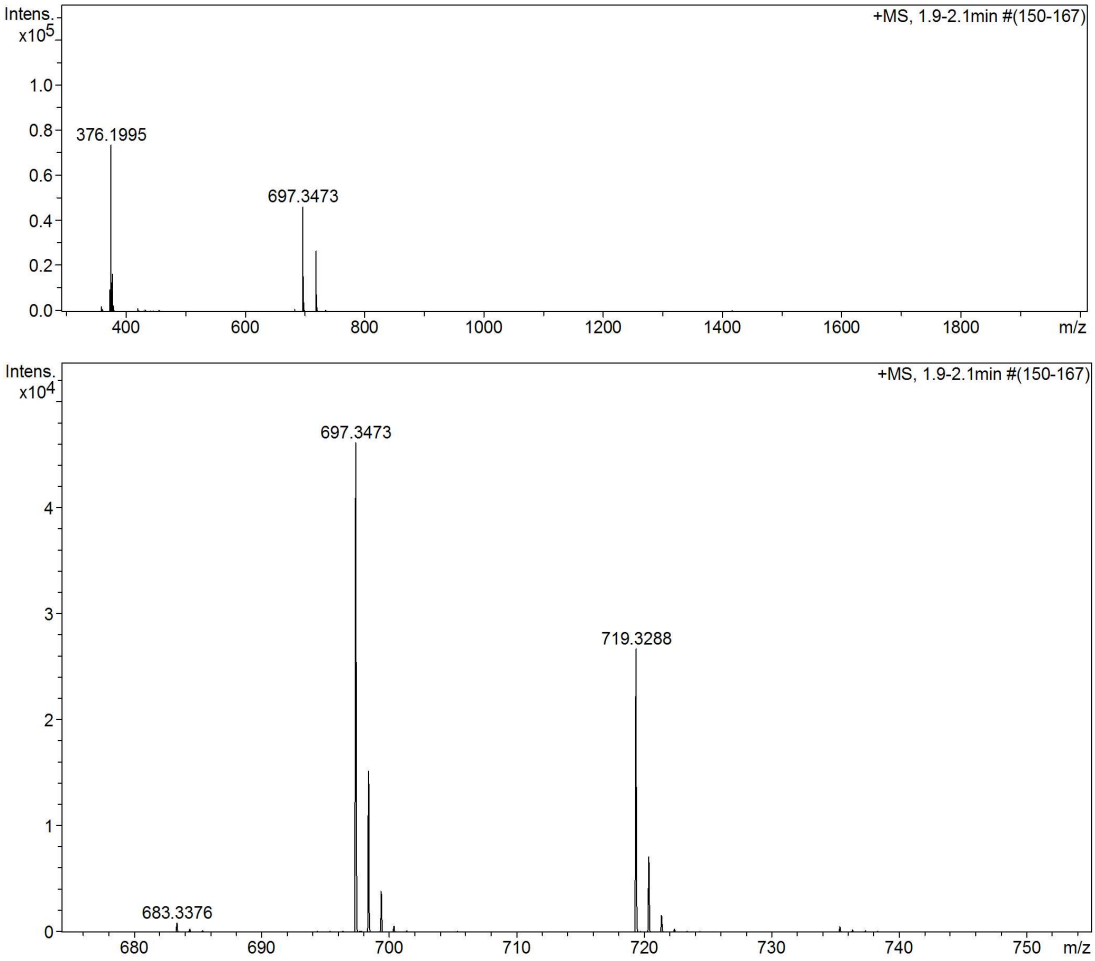

Figure 6.83 HR-ESI-MS spectra of 1,4-(dihexahydropyrimidine tetradeuterio)butane-diDNS derivative (M.W. = 696.3429, $C_{36}H_{44}N_6O_4S_2D_4$) expected m/z $[M+H]^+$ ion = 697.3508 (found = 697.3473) and $[M+Na]^+$ = 719.3327 (found = 719.3288).

1-(Hexahydropyrimidine dideuterio)-4-aza-aminooctane was reacted with DNS Cl to obtain the triDNS derivative (Figure 6.84) and injected onto HPLC. The chromatogram was obtained and was confirmed by HR-ESI-MS (Figure 6.85).

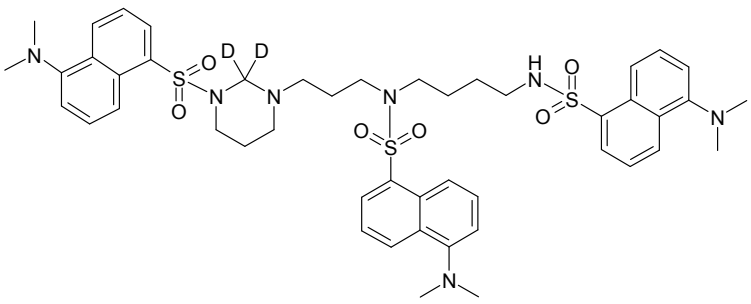

Figure 6.84 1-(Hexahydropyrimidine dideuterio)-4-aza-aminooctane–triDNS derivative.

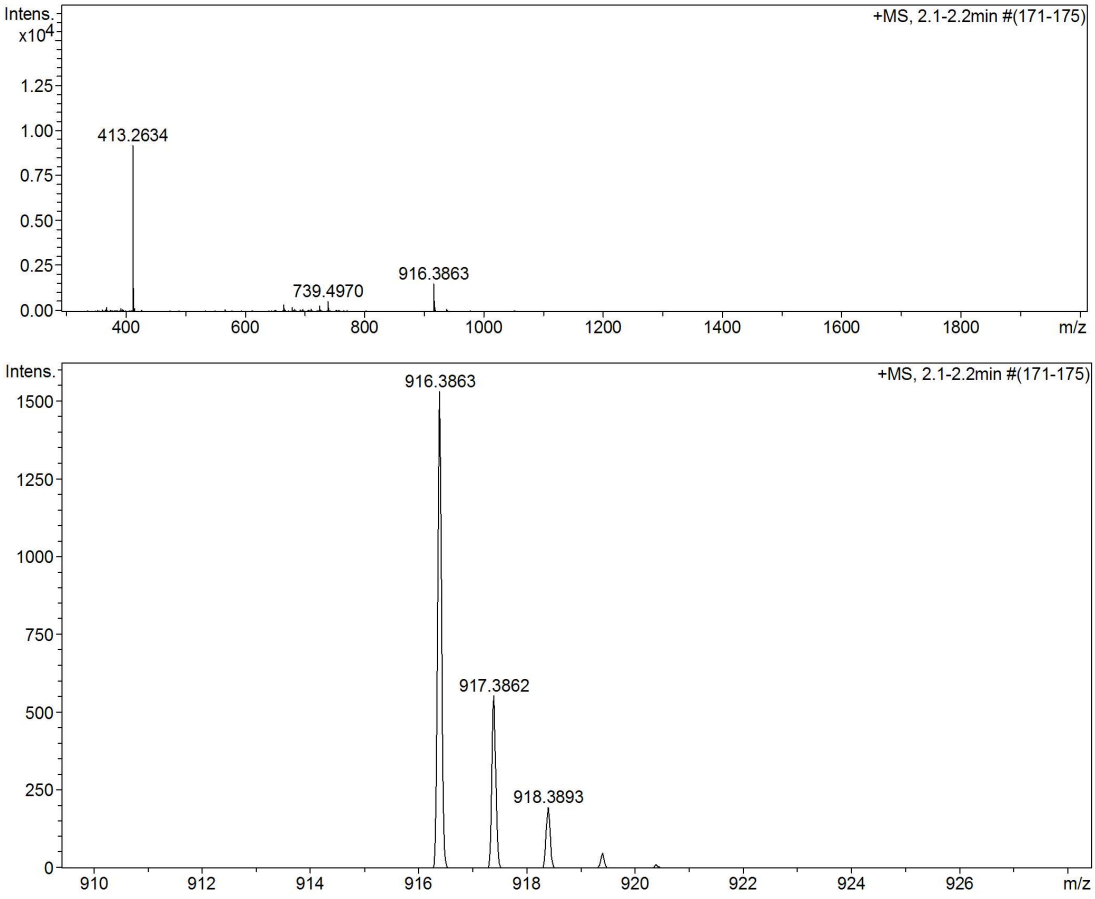

Figure 6.85 HR-ESI-MS spectra of 1-(hexahydropyrimidine-2,2- dideuterio)-4-aza-aminooctane–triDNS derivative (M.W. = 915.3814, $C_{47}H_{57}N_7O_6S_3D_2$) expected m/z $[M+H]^+$ ion = 916.3892 (found = 916.3863).

The analysis of spermidine, spermine and thermospermine were examined. The reaction to turn these molecules into hexahydropyrimidine derivatives was proved by HR-ESI-MS. Moreover, in the case of spermine and thermospermine, their hexahydropyrimidine derivatives were separated well after labelling with the fluorophores which can be visualized by the different retention time from HPLC chromatograms and also the retention times were shorter than their original molecules (spermidine, spermine and thermospermine).

General conclusions

The increasing interest in natural and synthetic polyamines, and investigations into their roles in physiological and biochemical processes, has led to a need for the development of simpler and more efficient methods for their quantitative and qualitative determination.

The difficulties encountered in identifying and measuring the quantity of *e.g.* cellular polyamines are especially that the only reactive centres are the amine groups. Aliphatic mono-, di- and polyamines do not have chemical structures that permit their investigation by UV spectrophotometry as they lack chromophores. Thus, for many analytical techniques, the sensitivity of detection of these amines depends on derivatization reactions. Specificity is also limited by the quality of the chromatographic separation procedures with these basic molecules.

The most widely employed procedures for the detection and determination of separated primary and secondary amines are TLC visualised with ninhydrin reagent. The use of fluorescamine as a spray reagent enables the analysis of these amines in picomole amounts. Other techniques include ion-exchange and ion-paired RP-HPLC combined with pre- or post-column derivatization and UV or fluorescence monitoring. However, these methods have been replaced by more sensitive and specific techniques, pre-column derivatization followed by RP-HPLC separation is now the preferred method for the separation and quantitation of polyamines.

A number of reagents have been used for the pre-chromatographic derivatization of polyamines. Among many suitable reagents, 5-dimethylaminonaphthalene-1-sulfonyl chloride (DNS Cl), fluorescamine, 9-fluorenylmethyl carbamate (FMOC Cl) and *o*-phthalaldehyde/mercaptoethanol (OPA/MCE) have been widely applied for pre-chromatographic derivatization of polyamines. Many factors influence the derivatization procedures for amines such as the pH value of the reaction, concentration of the reagents, reaction temperature and reaction time.

In this research, attempts have been make to optimize the derivatization methods of different fluorophores with respect to the time duration, temperature, pH of the reactions. In addition, the HPLC mobile phase has been optimized to achieve good base-line resolution and to increase the sensitivity of the amine detection by RP-HPLC. Furthermore, the studies investigate the chemical reaction of these fluorophores with biogenic polyamines and

synthetic intermediates using mass spectrometry to confirm the chemical identity of the derivatives.
The ideal fluorophore reagent should react rapidly and quantitatively under mild conditions. The reagent should give only a single, stable derivative per amine. The derivatives should be detectable with high sensitivity and the reagent itself or its degradation products should not interfere with the chromatographic separation.

In this work, four fluorophores have been used for labelling polyamines *i.e.* OPA/MCE, fluorescamine, FMOC-Cl and DNS Cl. The first two fluorophores are more selective reagents, reacting only with primary amines in contrast with the latter two acid chlorides which react with both primary and secondary amino groups.

1,7-Diaminoheptane forms the di-derivatives of OPA/MCE while this diamine forms only a mono-fluorescamine derivative. This might due to the bulky molecule of fluorescamine itself creating a steric hindrance to further reaction.

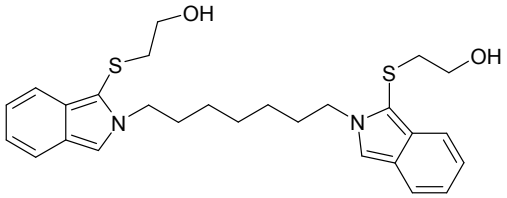

1,7-Diaminoheptane-diOPA/MCE derivative

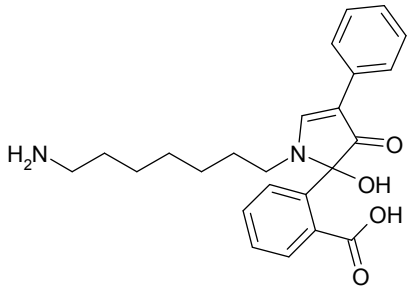

1,7-Diaminoheptane monofluorescamine derivative

With these amines, two protons need to be lost from the nitrogen atom in order to create the closed five-membered ring which is isoindole when OPA/MCE is used and oxidised pyrrole when fluorescamine is used. Thus those reagents are specific for primary amines.
Fluorescent molecules tend to be rigid molecules with delocalized electron systems which in

these cases are the lone pair electrons on the nitrogen atoms that delocalize in the aromatic ring. These electronic properties give these derivatives high fluorescence intensity.
The application of OPA/MCE is more advantageous than using fluorescamine as the derivatives of OPA/MCE have a relatively high quantum yield in comparison with the derivatives of fluorescamine. However, the derivatives formed by OPA/MCE are not very stable, especially polyamines containing unreacted secondary amino groups *e.g.* spermidine and spermine. Some disadvantages of pre-column derivatization by OPA/MCE are that the process of derivatization needs to be more carefully controlled in the reaction conditions to achieve good reproducibility because of poor stability and also the difficulties in reagent preparation.

Although the stability of both spermidine-diOPA/MCE derivatives and spermine-diOPA/MCE derivative were low, the spermidine-diOPA/MCE derivative was more stable, perhaps due to the lower number of secondary amino functional groups in the molecule. Protecting these secondary amines of spermidine and spermine with FMOC Cl after OPA/MCE, enabled the molecule to be fully derivatized as spermidine-diOPA/MCE-monoFMOC and spermine-diOPA/MCE-diFMOC.

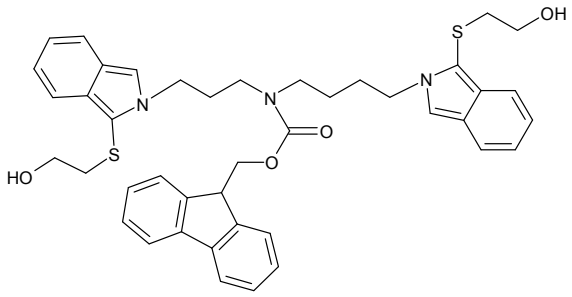

Spermidine-diOPA/MCE-monoFMOC

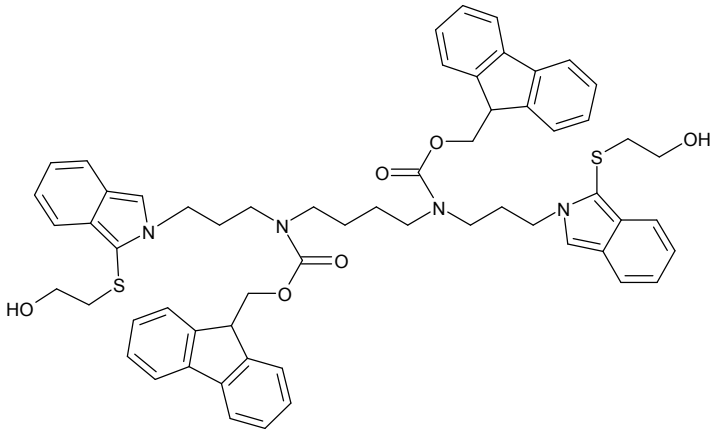

Spermine-diOPA/MCE-diFMOC

The derivatization products of spermidine-diOPA/MCE-monoFMOC and spermine-diOPA/MCE-diFMOC gave HPLC peaks with good symmetrical shape and efficient derivatization in terms of increased fluorescent responses and better reproducibility.

The OPA/MCE method for aminoglycosides is easy and simple to perform. The reaction time (10 min) is also practical, and no extraction process is needed. The derivatives of aminoglycosides-OPA/MCE are more stable than those of the simple (model) aliphatic amines. The HR-ESI-MS suggested that the derivative of kanamycin and OPA/MCE was kanamycin-triOPA/MCE instead of the expected tetra-OPA/MCE. Furthermore, the HR-ESI-MS analysis of the derivative peak showed neomycin-pentaOPA/MCE instead of the expected hexaOPA/MCE as with kanamycin-triOPA/MCE. This might due to the steric effect of the two amine groups on the same 2-deoxy streptamine ring allowing only one molecule of OPA/MCE to react at one of the amine positions of this ring.

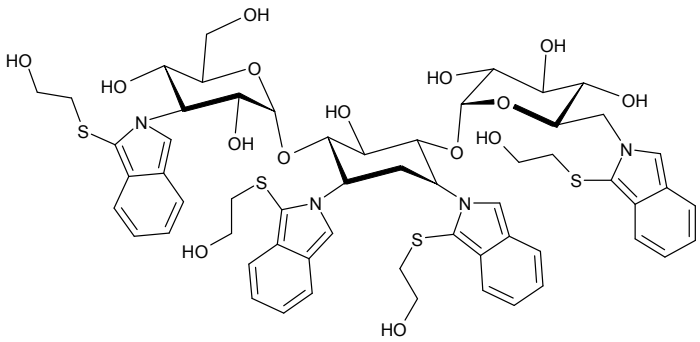

The expected kanamycin tetra-OPA/MCE

Fluorescamine reacts in seconds with amines in borate buffer and unreacted reagent is hydrolyzed in water to yield a non-fluorescent product. The many complicated peaks that are obtained by using this reagent arise from its structure which is chiral and thus, if the reactant also is a chiral molecule, then diastereoisomeric products often give rise to more than one peak by HPLC.

In contrast with the selective fluorophores above, the acid chloride reagents DNS Cl and FMOC Cl react with both primary and secondary amines.

9-Fluorenylmethyl chloroformate (FMOC-Cl) reacts rapidly only with primary and secondary amine groups forming stable and highly fluorescent derivatives under mild conditions. The resulting carbamate derivatives exhibit high fluorescent responses and are stable at 20^{o}C for several days. The disadvantage of FMOC is that it also reacts with water,

to give fluorescent FMOC-OH which displays similar HPLC behaviour and may therefore interfere with some of the HPLC peaks of amine-FMOC derivatives. Also, the FMOC Cl reagent is fluorescent and, as it is used in excess, this can distort or complicate the quantitative (and qualitative) analysis. FMOC Cl gave fully derivatized amines with linear polyamines such as the diFMOC of 1,7-diaminoheptane.

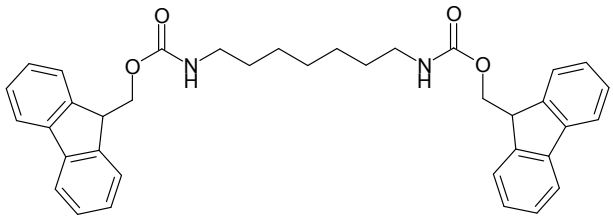

1,7-Diaminoheptane-diFMOC

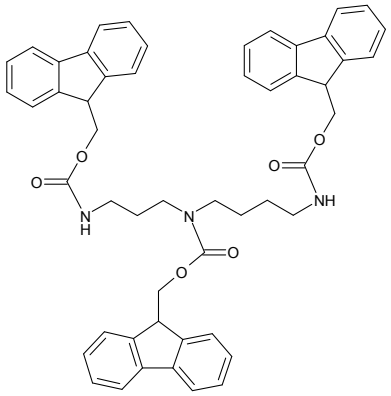

Spermidine-triFMOC

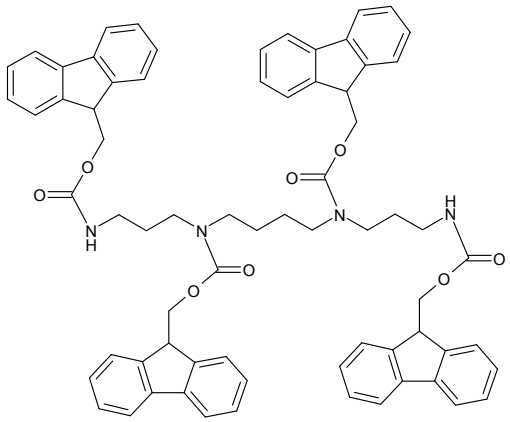

Spermine-tetraFMOC

The FMOC derivatization method was then applied to kanamycin, and the elution of kanamycin-FMOC derivatives was confirmed by HR-ESI-MS as mainly the desired tetrasubstituted derivative in contrast with the kanamycin-triOPA/MCE described above.

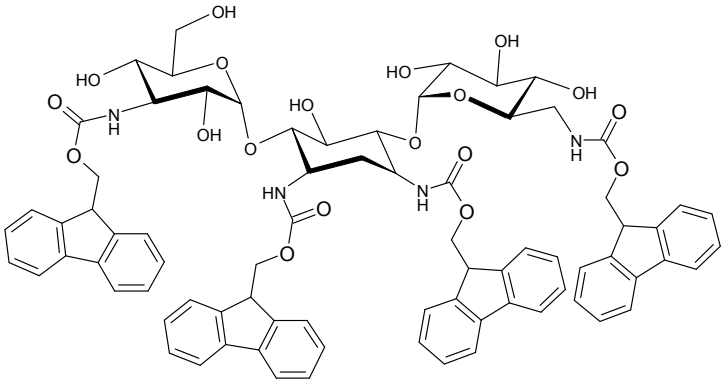

Kanamycin-tetraFMOC

Compared with using OPA/MCE, kanamycin was fully labelled by FMOC Cl. This might due to the reactivity of the FMOC Cl or the flexibility of the linker between the kanamycin nitrogen and the fluorophores. With OPA/MCE, the amine nitrogen atom is built into the fluorophores in a reaction with several steps.

DNS Cl reacts with primary and secondary amines with the result of full derivatization if the molar ratio of DNS Cl is sufficiently high (10-fold or greater excess). DiDNS derivatives form for diamines such as 1,7-diaminoheptane, the triDNS derivative for spermidine, and the tetraDNS derivative for spermine.

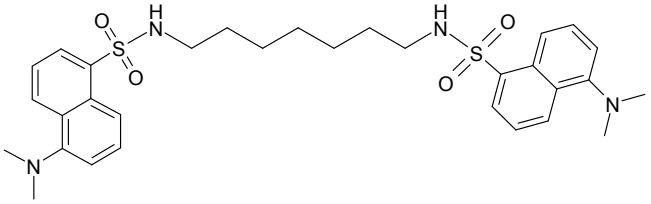

1,7-Diaminoheptane-diDNS

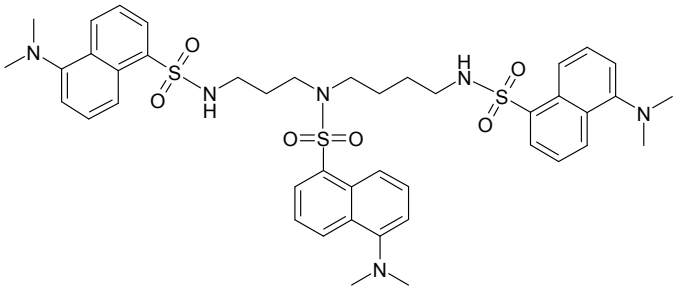

Spermidine-triDNS

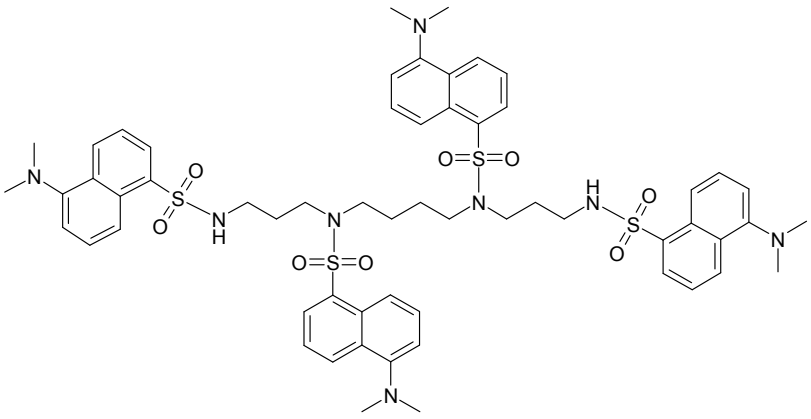

Spermine-tetraDNS

The monoDNS derivatives of a series of simple aliphatic diamines were prepared for investigation of the fluorescence yield. These monoDNS derivatives were prepared by reducing the mole ratio of DNS Cl (to 2-fold) to yield single derivatives.

The OPA/MCE, FMOC Cl and DNS Cl analysis methods were applied to the determination of lipopolyamines with potential in non-viral gene therapy, polyamine conjugates such as N^4,N^9-dioleoylspermine, neochol and also intermediate molecules which were synthesized in the Blagbrough research group. By careful control of the dansylation reaction conditions, most of these compounds yielded only a monoDNS derivative probably due to steric hindrance.

Within the series of fluorophores the relative fluorescence yields of mono- and multiple derivatized amines were determined by measurement of the fluorescent intensity versus UV absorption of the HPLC eluent collected from peaks of the amine-fluorophore derivatives (confirmed by HR-ESI-MS). Ideally, the slope for each sample is proportional to that sample's fluorescence quantum yield. Amine-difluorophore derivatives and amine-trifluorophore derivatives should present the same slope as amine-derivatives. However the results showed that all the amine-difluorophore derivatives have similar slopes in their group but a lower in values than the amine-monofluorophore derivative. For the amine-trifluorophore derivative, the slope is even lower than the slope of the amine-difluorophore derivatives. Thus, the fluorescence intensity did not increase in proportion to the number of fluorophores that were attached to the polyamine, so two or more fluorophores tethered in close proximity interfere with (quench) the fluorescence process. However, it is possible to use the slope for predicting how many fluorophores are attached to a specific polyamine.

Thermospermine (3.3.4), a regioisomer of spermine (3.4.3) was synthesised from spermidine (3.4) as the starting material. The reaction of spermidine and formaldehyde created *N*-(4-aminobutyl)hexahydropyrimidine, this step forming a six-membered ring leaves one primary amine unreacted with four methylene carbons from the stable hexahydropyrimidine ring.

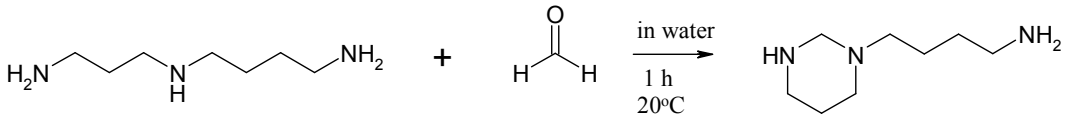

spermidine (3.4)

N-(4-aminobutyl)hexahydropyrimidine

After this step, a selective primary amine protecting groups benzaldehyde (to form an imine) and phthalimide were added to *N*-(4-aminobutyl) hexahydropyrimidine. These two protecting groups were then compared.

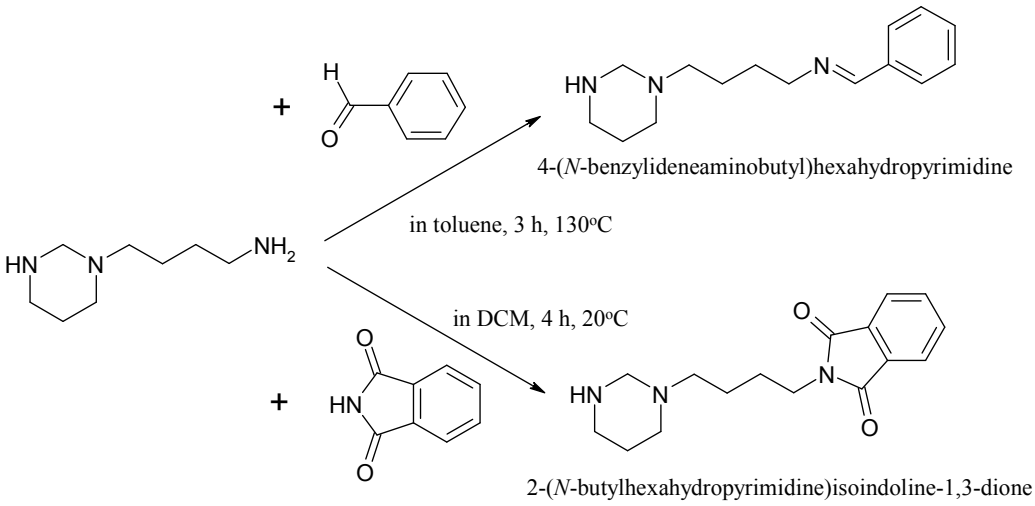

The phthalimide protecting group was added under milder reaction conditions and gave a higher yield than benzaldehyde. Acrylonitrile was added to secondary amine group using the same condition for both starting materials. After that, deprotection of the protecting group and removal of CH_2 from the hexahydropyrimidine were applied in one step. The final step was reduction of the nitrile group using sodium borohydride to obtain the desired thermospermine (3.3.4).

FMOC and dansyl derivatives of spermine (3.4.3) and thermospermine (3.3.4) were not separate by HPLC. By the reaction of formaldehyde, the two isomers yield different products which can be separated by HPLC after labelling with any fluorophores. By using dideuteriated formaldehyde to react with spermine and thermospermine, the expected molecular weight was confirmed by HR-ESI-MS.

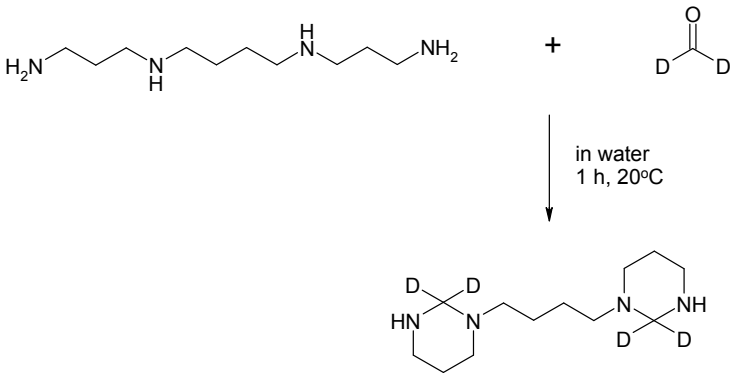

Reaction of spermine with dideuteriated formaldehyde

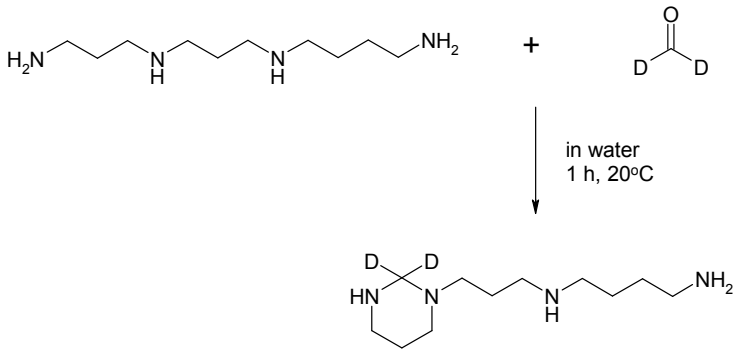

Reaction of thermospermine with dideuteriated formaldehyde

In conclusion, these studies have proven by experiment the benefits of using different fluorophores to label polyamines which allow them to be detected by simple isocratic HPLC systems. The relative fluorescence yield of mono-, di- and tri-derivatives of different fluorophores showed two aspects. Firstly, that the di- or tri-fluorophore derivatives have lower fluorescence yield than the mono-fluorophore derivative which means that the two (or more) fluorophores when tethered in close proximity interfere with (quench) the fluorescence process. Secondly, that plots of fluorescence intensity and UV absorbance can used to predict the relative of the number of fluorophores that are bound to polyamines which also tell about the behaviour of the fluorophores. In these studies, the optimum conditions of derivatization of polyamines by four fluorophores and optimum isocratic HPLC conditions were developed. We have shown that a simple isocratic HPLC system combined with some chemical reaction and derivatization by fluorophores can separate the two isomers of spermine and thermospermine. By reacting dideuteriated formaldehyde with spermine and thermospermine then directly using HR-ESI-MS is a simple alternative way of analysis to distinguish between these two isomers.

REFERENCES

Adams, E., Roelants, W., Paepe, R.D., Roets, E., Hoogmartens, J., 1998. Analysis of gentamicin by liquid chromatography with pulsed electrochemical detection. J. Pharm. 18, 689-698.

Adamou, R., Coly, A., Douabale, E., Saleck, M., Gaye-Seye, M., Tine, A., 2005. Fluorimetric determination of histamine in fish using micellar media and fluorescamine as labelling reagent. J. Fluoresc. 15, 679-688.

Anhalt, J., 1977. Assay of gentamicin in serum by high-pressure liquid chromatography. Antimicrob. Agents Chemother. 11, 651-655.

Allison, L., Mayer, G., Shoup, R., 1984. *o*-Phthalaldehyde derivatives of amines for high-speed liquid chromatography/electrochemistry. Anal. Chem. 56, 1089-1096.

Bachrach, U., Cohen, I., 1961. Spermidine in bacteria cell. J. Gen. Microbiol. 26, 1-9.

Bank, R.A., Jansen, E.J., Beekman, B., te Koppele, J.M., 1996. Amino acid analysis by reverse-phase high-performance liquid chromatography: Improved derivatization and detection conditions with 9-fluorenylmethyl chloroformate. Anal. Biochem. 240, 167-176.

Bakowski, M.T., Toseland, P.A., Wicks, J.F., Trounce, J.R., 1981. A rapid gas chromatographic method for the determination of plasma polyamines and its application to the prediction of tumor response to chemotherapy. Clin. Chim. Acta 110, 273-286.

Bartos, D., Campbell, R.A., Bartos, F., Grettie, D.P., 1975. Direct determination of polyamines in human serum by radioimmunoassay. J. Cancer Res. 35, 2056-2060.

Bauza, T.; Blaise, A.; Daumas, F.; Cabanis, J. C., 1995. Determination of biogenic amines and their precursor amino acids in wines of the Vallee du Rhone by high-performance liquid chromatography with pre-column derivatization and fluorimetric detection. J. Chromatogr. A. 707, 373-379.

Bayermann, M., Bienert, M, Niedrich, H., Carpino, L.A., Sadat-Aalaee, D., 1990. Rapid continuous peptide synthesis via FMOC amino acid chloride coupling and 4 (aminomethyl) piperidine deblocking. J. Org. Chem. 55, 721-728.

Beninati, S., Sartori, C., Argento-Ceru, M. P., 1977. A new method for qualitative and quantitative determination of di- and polyamines in animal tissues by gas-liquid chromatography. Anal. Biochem. 80, 101-107.

Belal, F., Abdine, H., Al-Majed, A., Khalil, N., 2002. Spectrofluorimetric determination of vigabatrin and gabapentin in urine and dosage forms though derivatization with fluorescamine. J. Pharm. Biomed. Anal. 27, 253-260.

Benson, J., Hare, P., 1975. *o*-Phthalaldehyde: fluorogenic detection of primary amines in the picomole range. Comparison with fluorescamine and ninhydrin. Proc. Nat. Acad. Sci. U.S.A. 72, 619-622.

Bernsteina, H., Müller, M., 1995. Increased immunostaining for L-ornithine decarboxylase occurs in neocortical neurons of Alzheimer's disease patients. Neurosci. Lett. 186, 123-126.

Beyer, C., van der Ende, A., 1983. Improved separation procedure for urinary di- and polyamines by means of thin-layer chromatography. Clin. Chim. Acta 129, 211-214.

Bloomfield, V.A., 1991. Condensation of DNA by multivalent cations-condensations on mechanism. Biopolymers. 31, 1471-1481.

Boffey, G.C., Martin, G.M., 1974, A new solvent system for the thin-layer chromatographic separation of the Dansyl derivatives of some biogenic amines. J. Chromatogr. 90, 178-180.

Bollinger, J.M. Jr., Kwon, D.S., Huisman, G.W., Kolter. R., Walsh, C.T., 1995. Glutathionylspermidine metabolism in Escherichia coli. Purification, cloning, overproduction, and characterization of a bifunctional glutathionylspermidine synthetase/amidase. J. Biol. Chem. 270, 14031-14041.

Bolliger, A., 1935. The volumetric microdetermination of spermine in semen. Med. J. Aust. 2, 784-787.

Bouchereau, A., Aziz, A., Larher, F., Martin-Tanguy, J., 1999. Polyamines and environmental challenges: recent development. Plant. Sci. 140, 103-125.

Bremer, H.J., Kohne, E., 1971. Excretion of diamines in human urine. 2. Cadaverine, putrescine, 1,3-diaminopropane, 2,2'-dithiobis (ethylamine) and spermidine in urine of patients with cystinuria and cystinulysinuria. Clin. Chem. Acta 32, 407-418.

Brooks, J.B., Moore, W.E., 1969. Gas chromatographic analysis of amine and other compounds produced by several species of Clostridium. Can. J. Microbiol. 15, 1433-1447.

Buteau, C., Duischaever, C.L., Ashton, G.C., 1984. High-performance liquid chromatographic detection and quantitation of amines in must and wine. J. Chromatogr. A. 284, 201-210.

Carpino, L.A., Han, G.Y, 1970. The 9-fluorenylmethoxycarbonyl function, a new base-sensitive amino-protecting group. J. Am. Chem. Soc. 92, 5748-5749.

Carpino, L.A., Han, G.Y, 1972. 9-Fluorenylmethoxycarbonyl amino-protecting group. J. Org. Chem. 37, 3404-3409.

Carpino, L.A., Sadat-alaee, D., Beyermann, M., 1990. Tris(2-aminoethyl)amine as substitute for 4-(aminomethyl)piperidine in the FMOC/polyamine approach to rapid peptide synthesis J. Org. Chem. 55, 1673-1675.

Carteni-Farina, M., Porcelli, M., Cacciapuoti, G., De Rosa, M., Gambacorta, A., Grant, W.D., Ross, M.N.M., 1985. Polyamines in halophilic agrobacteria. FEMS Microbiol. Lett. 65, 269-274.

Cesur, N., Apak, T., Aboul-Enein, Y., Ozkirimli, S., 2002. LC determination of aminoglutethimide enantiomers as dansyl and fluorescamine derivatives in tablet formulations. J. Pharm. Biomed. Anal. 28, 487-492.

Chen, R.F., 1967. Fluorescence of Dansyl amino acids in organic solvents and protein solutions. Arch. Biochem. Biophys. 120, 609-620.

Chesnov, S., Bigler, L., Bienz, S., Hesse, M., 2002. Detection and characterization of natural polyamines by high-performance liquid chromatography-atmospheric pressure chemical ionization (electrospray ionization) mass spectrometry. Eur. J. Mass Spectr. 8, 1-16.

Childs, A.C., Metha, D.J., Gerner, E.W., 2003. Polyamine-dependent gene expression. Cell. Mol. Life. Sci. 60, 1394–1406.

Choi, M.H., Kim, K., Chung, B.C., 2000. Determination of hair polyamines as *N*-ethoxycarbonyl-*N*-pentafluoropropionyl derivatives by gas chromatography-mass spectrometry. J. Chromatogr. A. 897, 295–305.

Clements, L., Hilbish, T., 1991. Comparison of fluorescamine and *o*-phthalaldehyde methods for measuring amino acid exchange in marine organisms. Limnol. Oceanogr. 36, 1463-1471.

Conca, R., Bruzzoniti, M.C., Mentasti, E., Sarzanini, C., Hajos, P., 2001. Ion chromatographic separation of polyamines: putrescine, spermidine and spermine. Anal. Chim. Acta 439, 107–114.

David, V., Ionescu, M., Dumitrescu, V., 2001. Determination of cycloserine in human plasma by high-performance liquid chromatography with fluorescence detection, using derivatization with p-benzoquinone. J. Chromatogr. B Biomed. Sci. Appl. 761, 27-33

Debernar, S., Weigele, M., Toome, V., Manhart, K., Leimgrub, W., Bohlen, P., Stein, S., Udenfrie, S., 1974. Studies on reaction of fluorescamine with primary amines. Arch. Biochem. Biophys. 163, 390-399.

Deng, H., Bloomfield, V.A., Benevides, J.M., Thomas, G.J. Jr., 2000. Structural basis of polyamine-DNA recognition: spermidine and spermine interactions with genomic B-DNAs of different GC content probed by Raman spectroscopy. Nucleic Acids Res. 28, 3379-3385.

Dorhout, B., Kingna, A.W., de Hoog, E., Muskiet, F.A.J., 1997. Simultaneous determination of polyamines, N-acetylated polyamines and the polyamine analogues BE-3-3-3 and BE 4-4-4-4 by capillary chromatography with nitrogen phosphorus detection. J. Chromatogr. B. 700, 23-30.

Dong, Y., Le Quesne, P. W., 2002. Total synthesis of magnolamide. Heterocycles 56, 221-225.

Dubin, D.T., Rosenthal, S.M., 1960. The acetylation of polyamines in *Escherichia coli*. J. Biol. Chem. 235, 776-782.

Dudley, H.W., Rosenheim, M.C., Rosenheim, O., 1924. The chemical constitution of spermine. 1. The isolation of spermine from animal tissues, and the preparation of its salts. Biochem. J. 18, 1263-1272.

Dudley, H.W., Rosenheim, O., 1925. CXLVII. The chemical constitution of spermine II. The methylation of spermine. Biochem. J. 19, 1032-1033.

Dudley, H.W., Rosenheim, O., 1925. Notes on spermine. Biochem. J. 19, 1034-1036.

Dudley, H.W., Rosenheim, O., Starling, W.W., 1926. The chemical constitution of spermine III. Structure and synthesis. Biochem. J. 20, 1082-1094.

Dudley, H.W., Rosenheim, O., Starling, W.W., 1927.The constitution and synthesis of spermine, a newly discovered base isolated from animal tissues. Biochem. J. 21, 97-103.

Dutcher, D., Hosansky, N., Donin, M.N., Wintersteiner, O., 1951. Neomycin B and C, and some of their degradation products. J. Am. Chem. Soc. 73, 1384-1385.

Eijk, H., Rooyakkers, D., Deutz, N., 1996. Automated determination of polyamines by high-performance liquid chromatography with simple sample preparation. J. Chromatogr. A. 730, 115-120.

Einarsson, S., Josefsson, B., Lagerkvist, S., 1983. Determination of amino acids with 9-fluorenylmethyl chloroformate and reversed-phase high-performance liquid chromatography. J. Chromatogr. 282, 609-618.

Emonds, A., Driessen, O., 1983. Determination of polyamines in plasma by capillary gas chromatography and some applications, Methods. Find. Exp. Clin. Pharmacol. 5, 391-396.

Ekegren, T., Gomes-Trolin, C., 2005. Determination of polyamines in human tissues by precolumn derivatization with 9-fluorenylmethyl chloroformate and high-performance liquid chromatography. Anal. Biochem. 338, 179-185.

Ekegren, T., Gomes-Trolin, C., Nygren, I., Askmark, H., 2004. Maintained regulation of polyamines in spinal cord from patients with amyotrophic lateral sclerosis. J. Neurol. Sci. 222, 49-53.

Ernestus, R.I., Röhn, G., Schröder, R., Els, T., Klekner, A., Paschen, W., Klug, N., 2001. Polyamine metabolism in brain tumours: Diagnostic relevance of quantitative biochemistry. J. Neurol. Neurosurg Psychiatry. 71, 88-92.

Essers, L., 1984. An automated high-performance liquid-chromatographic method for the determination of aminoglycosides in serum using pre-column sample cleanup and derivatization. J. Chromatogr. 305, 345-352.

Fernandez-Ramos, J., Garcia-Campana, A., Ales-Barrero, F., Bosque-Sendra, J., 2006. Determination of gentamycin in pharmaceutical formulations using peroxyoxalate chemiluminescent detection in flow-injection analysis. Talanta 69, 763-768.

Fleisher, J.H., Russell, D.H., 1975. Estimation of urinary diamines and polyamines by thin-layer chromatography. J. Chromatogr. 110, 335-340.

Fischer, F.G., Bohn, H, 1957. Uber die bestimmung von spermin, spermidine and anderen biogenen aminen nach papierelektrophoretischer abtrennung und ihre mengenverhaltnisse in tierischen organen. Hoppe-Seyl. Z. 308, 108-115.

Fourmy, D., Recht, M. I., Puglisi, J. D., 1998. Binding of neomycin-class aminoglycoside antibiotics to the A-site of 16 S rRNA. J. Mol. Biol. 277, 347-362.

Fransson, B., Almeide, M.L.S., Grehn, L., Ragnarsson, U., 1990. Separation of spermidine derivatives by reversed-phase high-performance liquid chromatography using a UV-absorbing counter ion. J. Chromatogr. 508, 229-231.

Fu, S., Zou, X., Wang, X., Liu, X., 1998. Determination of polyamines in human prostate by high-performance in human prostate by high-performance liquid chromatography with fluorescence detection. J. Chromatagr. B. 709, 297-300.

Fujihara, S., Nakashima, T., Kurogochi, Y., 1983, Determination of polyamines in human blood by electron-capture gas-liquid chromatography. J. Chromatogr. 277, 53-60.

Fujimoto, T., Tawa, R., Hirose, S., 1988. Fluorometric determination of sisomicin, an aminoglycoside antibiotic, in dried blood spots on filter-paper by reversed-phase high-performance liquid chromatography with pre-column derivatization. Chem. Pharm. Bull 36, 1571-1574.

Fujiwara, K., Asada, H., Kitagawa, T., Yamamoto, K., Ito, T., Tsuchiya, R., Sohda, M., Nakamura, N., Hara, K., Tomonaga, Y., Ichimaru, M., Takahashi, S., 1983. Preparation of

polyamine antibody and its use in enzyme immunoassay of spermine and spermidine with β-D-galactosidase as a label. J. Immunol. Methods 61, 217-226.

Funk, G., Hunt, C., Epps, D., Brown, P., 1986. Use of a rapid and highly sensitive fluorescamine-based procedure for the assay of plasma lipoproteins. J. Lipid Res. 27, 792-795.

Gaboriau, F., Havouis, R., Moulinoux, J., Delcros, J., 2003. Atmospheric pressure chemical ionization-mass spectrometry method to improve the determination of dansylated polyamines. Anal. Biochem. 318, 212-220.

Ganem, B., Chantrapromma, K., 1983. Preparation of Thermospermine, Methods Enzymol. 94, 416-418.

Gao, C.X., Krull, I.S., Trainor, T., 1990. Determination of aliphatic amines in air by on-line solid-phase derivatization with HPLC-UV/FL. J. Chrom. Sci. 28, 102-108.

Geall, A.J., Taylor, R.J., Earll, M.E., Eaton, M.A.W., Blagbrough, I.S., 2000. Synthesis of cholesteryl polyamine carbamates: pK_a studies and condensation of calf thymus DNA. Bioconjug. Chem. 11, 314-326.

Gehrke, C.W., Kuo, K.C., Zumwatt, R.W., Waalkes, T.P., 1974. Determination of polyamines in human urine by an automated ion-exchange method. J. Chromatogr. 89, 231-238.

Genus, J., Orriach, M., Swennen, R., Zhu, G., Panis, B., Compernolle, F., Auweraer, M., 2006. Simultaneous liquid chromatography determination of polyamines and arylalkyl monoamines. Anal. Biochem. 354, 127-131.

Gosule, L.C., Schellman, J.A., 1976. Compact form of DNA induced by spermidine. Nature. 259, 333-335.

Greger, H., Hadacek, F., Hofer, O., Wurz, G., Zechner, G., 1993. Different types of sulphur-containing amides from Glycosmis cf. chlorosperma. Phytochemistry 32, 933-936.

Greger, H., Pacher, T., Vajrodaya, S., Bacher, M., Hofer, O., 2000. Infraspecific variation of sulfur-containing bisamides from Aglaia leptantha. J. Nat. Prod. 63, 616-620.

Greger, H., Pacher, T., Brem, B., Bacher, M., Hofer, O., 2001. Insecticidal flavaglines and other compounds from Fijian Aglaia species. Phytochemistry 57, 57-64.

Greene, T.W., Wuts, P.G.M., 1991. Protective Groups in Organic Synthesis 2nd edn. Wiley, New York. 69-71.

Guarino, L.A., Cohen, S.S., 1979. Proc. Nat. Acad. Sci. U.S.A. 76, 3184-3188.

Gugliucci, A., 2004. Polyamines as clinical laboratory tools. Clin. Chim. Acta 344, 23-35.

Gustavsson, B., Betner, L., 1990. Fully automated amino acid analysis for protein and peptide hydrolysates by precolumn derivatization with 9-fluorenyl methylchloroformate and 1-aminoadamantane. J. Chromatogr. 507, 67-77.

Hamana, K., Matsuzaki, S., 1992. Polyamines as a chemotaxonomic marker in bacterial systematics. Crit. Rev. Microbiol. 18, 261-283.

Hamana, K., Matsuzaki, S., Niitsu, M., Samejima, K., 1994. Distribution of unusual polyamines in aquatic plants and gramineous seeds. Can. J. Bot. 72, 1114-1120.

Hamana, K., Hamana, H., Niitsu, M., Samejima, K., Sakane, T., Yokota, A., 1994. Occurrence of tertiary and quaternary branched polyamines in thermophilic archaebacteria. Microbios 79, 109-119.

Hamana, K., Hamana, H., Niitsu, M., Samejima, K., Sakane, T., Yokota, A., 1993. Tertiary and quaternary branched polyamines distributed in thermophilic *Saccharococcus* and *Bacillus*. Microbios 75, 23-32.

Hamana, K., Niitsu, M., Samejima, K., Matsuzaki, S., 1991. Linear and branched pentaamines, hexaamines and heptaamines in seeds of *Vicia sativa*. Phytochemistry 30, 3319-3322.

Hamana, K., Matsuzaki, S., 1984. Unusual polyamines in slime molds *Physarum polycephalum* and *Dictyostelium discoideum*. J. Biochem. 95, 1105-1110.

Hamana, K., Matsuzaki, S., Niitsu, M., Samejima, K., 1990. Synthesis of novel polyamines in *Paracoccus, Rhodobacter* and *Micrococcus*. FEMS Microbiol. Lett. 67, 267-274.

Hamana, K., Matsuzaki, S., Niitsu, M., Samejima, K., 1989. Polyamine distribution and the potential to form novel polyamines in phytopathogenic agrobacteria. FEMS Microbiol. Lett. 65, 269-274.

Harrison, G.A., 1931. Spermine in human tissues. Biochem. J. 25, 1885-1892.

Harrison, G.A., 1933. The approximate determination of spermine in single human organs. Biochem. J. 27, 1152-1156.

Hawel III, L., Byus, C.V., 2002. A streamlined method for the isolation and quantitation of nanomole levels of exported polyamines in cell culture media. Anal. Biochem. 311, 127-132.

Heby, O., Andersson, G., 1978. Simplified micro-method for the quantitative analysis of putrescine, spermidine and spermine in urine. J. Chromatogr. 145, 73-80.

Heby, O., Persson, L., Rentala, M., 2007. Targeting the polyamine biosynthetic enzymes: a promising approach to therapy of African sleeping sickness, Chagas' disease, and leishmaniasis. Amino Acids. 33, 359–366

Herbst, E.J., Weaver, R.H., Keister, D.J., 1958. The reaction and cell composition: Diamines and polyamines. Arch. Biochem. Biophys. 75, 171-177.

Hesse, M., 2005. The Encyclopedia of Mass Spectrometry, Volume Ed. N. M. M. Nibbering, Eds. M. L. Gross and R. M. Caprioli, Elsevier, Amsterdam. 4, 417-423.

Hosoya, R., Hamana, K., Niitsu, M., Itoh, T., 2004. Polyamine analysis for chemotaxonomy of thermophilic eubacteria: Polyamine distribution profiles within the orders *Aquificales*, *Thermotogales*, *Thermodesulfobacteriales*, *Thermales*, *Thermoanaerobacteriales*, *Clostridiales* and *Bacillales*. J. Gen. Appl. Microbiol. 50, 271-287.

Imai, K., 1975. Fluorimetric assay of dopamine, norepinephine and their 3-O-methyl metabolites by using fluorescamine. J. Chromatogr. 105, 135-140.

Jänne, J., Pösö, H., Raina, A., 1978. Polyamines in rapid growth and cancer. Biochim. Biophys. Acta 473, 241-293.

Jänne, J., Alhonen, L., Pietilä, M., Keinänen, T.A., 2004. Genetic approaches to the cellular functions of polyamines in mammals. Eur. J. Biochem. 271, 877-894.

Jiang, X., 1990. Determination of polyamines in urine of normal human and cancer patients by capillary gas chromatography. Biomed. Chromatogr. 4, 73-77.

Kaale, E., Goidsenhoven, E., Schepdael, A., Roets, E., Hoogmartens, J., 2001. Electrophoretically mediated microanalysis of gentamicin with in-capillary derivatization and UV detection. Electrophoresis. 22, 2746-2754.

Kai, M., Ogata, T., Haraguchi, K., Ohkura, Y., 1979. High-performance liquid chromatographic determination of free and total polyamines in human serum as fluorescamine derivatives. J. Chromatogr.163, 151-160.

Kamei, S., Ohkubo, A., Saito, S., Takagi, S., 1989. Polyamine detection system for high-performance liquid chromatography involving enzymatic and chemiluminescent reactions. Anal. Chem. 61, 1921-1924.

Khuhawar, M.Y., Memon, A.A., Jaipal, P.D., Bhanger, M.I., 1999. Capillary gas chromatographic determination of putrescine and cadaverine in serum of cancer patients using trifluoroacetylacetone as derivatizing reagent. J. Chromatogr. 723, 17-24.

Khuhawar, M.Y., Qureshi, G.A., 2001. Polyamines as cancer markers: Applicable separation methods. J. Chromatogr. B Biomed. Sci. Appl. 764, 385-407.

Kimberly, M.M., Goldstein, J.H., 1981. Determination of pKa values and total proton distribution pattern of spermidine by C-13 nuclear magnetic-resonance titrations. Anal. Chem. 53, 789-793.

Kirschbaum, J., Luckas, B., Beinert, W.D., 1994. HPLC analysis of biogenic-amines and amino-acids in food-after automatic precolumn derivatization with 9-fluorenylmethyl chloroformate. Am. Lab. 10, 28C-28H.

Knott, J.M., Römer, P., Sumper, M., 2007. Putative spermine syntheses from *Thalassiosira pseudonana* and *Arabidopsis thaliana* synthesize thermospermine rather than spermine. FEBS. Lett. 581, 3081-3086.

Koole, L.H., Moody, H.M., Broeders, N., Quaedflieg, P., Kuijpers, W.H.A., Vangenderen, M.H.P., Coenen, A., Vanderwal, S., Buck, H.M., 1989. Synthesis of phosphate-methylated DNA fragments using 9-fluorenylmethoxycarbonyl as transient base protecting group. J. Org. Chem. 54, 1657-1664.

Kumar, A., Altabella, T., Taylor, M., Tiburcio, A.F., 1997. Recent advances in polyamine research. Trends. Plant. Sci. 2, 124-130.

Kutlan, D., Presits, P., Molnar-Perl, I., 2002. Review Behavior and characteristic of amine derivatives obtained with *o*-phthalaldehyde/3-mercaptopropionic acid and with *o*-phthalaldehyde/N-acetyl-L-cysteine reagents. J. Chromatogr. A. 949, 235-248.

Lavizzari, T., Veciana-Nogues, M., Bover-Cid, S., Marine-Font, A, Vidal-Carou, M., 2006. Improved method for the determination of biogenic amines and polyamines in vegetable

products by ion-pair high-performance liquid chromatography. J. Chromatogr. A. 1129, 67-72.

Lecaroz, C., Campanero, M., Gamazo, C., Blanco-Prieto, M., 2006. Determination of gentamicin in different matrices by a new sensitive high-performance liquid chromatography-mass spectrometric method. Antimicrob. Agents Chemother. 58, 557-563.

Lee, K.S., Drescher, D.G., 1979. Derivatization of cysteine and cystine for fluorescence amino-acid analysis with the ortho-phthaldialdehyde-2-mercaptoethanol reagent. J. Biol. Chem., 254, 6248-6251.

Lewenhoeck, A., 1678. Observations D Anthonii Lewenhoeck de natis e semine genitali animalculis. Phil. Trans. Roy. Soc. London. 12, 1040-1043.

Liquori, A.M., Costantino, L., Crescerai, V., Elia, V., Giglio, E., Puliti, R., DeSantis Savino, M., Vitagliano, V. 1967. Complexes between DNA and polyamines: a molecular model. J. Mol. Biol. 24, 113-122.

Lindroth, P., Mopper, K., 1979. High-performance liquid-chromatographic determination of subpicomole amounts of amino-acids by precolumn fluorescence derivatization with ortho-phthaldialdehyde. Anal. Chem. 51, 1667-1674.

Liu, K., Fu, H., Bei, Q., Luan, S., 2000. Inward potassium channel in guard cells as a target for polyamine regulation of stomatal movements. Plant. Physiol. 124, 1315-1326.

Lopez, M.R.; Alvarez, M.J.G.; Ordieres, A.J.M.; Blanco, P.T., 1996. Determination of dimethylamine in groundwater by liquid chromatography and precolumn derivatization with 9-fluorenylmethylchloroformate. J. Chromatogr. A. 721, 231-239.

Louhou, Z., Zotou, A., 2003. A comparative survey of the simultaneous ultraviolet and fluorescence detection in the RP-HPLC determination of dansylated biogenic amines in alcoholic beverages. Chromatographia 58, 579-585.

Lozanov, V., Petrov, S., Mitev, V., 2004. Simultaneous analysis of amino acid and biogenic polyamines by high-performance liquid chromatography after pre-column derivatization with N-(9-fluorenylmethoxycarbonyloxy)succinimide. J. Chromatogr. A. 1025, 201-208.

Luo, J., Fuell, C., Parr, A., Hill, L., Bailey, P., Elliott, K., Fairhurst, S.A., Martin, C., Michael, A.J., 2009. A novel polyamine acyl transferase responsible for the accumulation of spermidine conjugates in *Arabidopsis* seed. The Plant Cell 21, 318-333.

Madaj, E., Jacobs, W., 1987. Aldehyde-promoted decomposition of 1-(alkylthiol)-2-alkylisoindoles. J. Org. Chem., 52, 3464-3466.

Madhubala, R., 1998. Thin-layer chromatographic method for assaying polyamines. Methods Mol. Biol. 79, 131-136.

Malmberg, R.L., Watson, M.B., Galloway, G.J., Yu, W., 1998. Molecular genetic analyses of plant polyamines. Crit. Rev. Plant. Sci. 17, 199-224.

Mandelstam, J., 1956. Factors affecting the passage of basic amino acids into coliform bacteria. Biochim. Biophys. Acta 22, 313-323.

Mandelstam, J., 1956. Inhibition of bacterial growth by selective interference with the passage of basic amino acids into the cell. Biochim. Biophys. Acta 22, 324-328.

Manov, N., Tzouros, M., Bigler, L., Bienz, S., 2004. Solid-phase synthesis of ^{15}N-labeled acylpentamines as reference compounds for the MS/MS investigation of spider toxins. Tetrahedron 60, 2387-2391.

Martin, F., Maudinas, B., Gadal, P., 1982. Separation of *o*-phthalaldehyde derivatives of free amino acids from plant tissues by isocratic reverse-phase high-performance liquid chromatography. Ann. Bot. 50, 401-406.

Maruszak, W., 1999. analysis of aliphatic amines by micellar electrokinetic chromatography. J. High. Resol. Chromatogr. 22, 126-128.

Mascher, H., Kikuta, C., 1998. Determination of amoxicillin in human serum and plasma by high-performance liquid chromatography and on-line postcolumn derivatization. J. Chromatogr. A. 812, 221-226.

Martell, A.E., Smith, R.M., Motekaitis, R.J., 1997. Critically selected stability constants of metal complexes database. NIST standard reference database. 4.

Mays, D., Van Apeldoorn, J., Lauack, G., 1976. High-performance liquid chromatographic determination of kanamycin. J. Chromatogr. 120, 93-102.

McGregor, R.F., Sharon, M.S., Atkinson, M., Johnson, D.E., 1976. An improved isolation procedure for the gas chromatographic analysis of urinary polyamines. Prep. Biochem. 6, 403-419.

Mendez, E., Matas, R., Soriano, F., 1985. Complete automatization of peptide maps by reversed-phase liquid-chromatography using ortho-phthalaldehyde pre-column derivatization. J. Chromatogr. 323, 373-382.

Middlebrooks, B.L., Toom, P.M., Douglas, W.L., Harrison, R.E., McDowell, S., 1988. Effects of storage time and temperature on the microflora and amine development in Spanish mackerel (Scomberorus maculatus). J. Food Sci. 53, 1024-1029

Minocha, R., Long, S., 2004. Simultaneous separation and quantitation of amino acids and polyamines of forest tree tissues and cell cultures within a single high-performance liquid chromatography run using dansyl derivatization. J. Chromatogr. A. 1035, 63-73.

Moinard, C., Cynober, L., de Bandt, J.P., 2005. Polyamines: Metabolism and implications in human diseases. Clin Nutr. 24, 184-197.

Molnar-Perl, I., 2005. Quantitation of amino acids and amines by chromatography, J. Chrom. Libr. 70, 606-647.

Moore, K.S., Wehrli, S., Roder, H., Rogers, M., Forrest, J.N., McCrimmon, D., Zasloff, M., 1993. Squalamine - an aminosterol antibiotic from the shark. Proc. Nat. Acad. Sci. U.S.A. 90, 1354-1358.

Moye, H.A., Boning A.J. Jr., 1979. A versatile fluorogenic labelling reagent for primary and secondary amines: 9-fluorenylmethyl chloroformate. Anal. Lett. 12, 25-35.

Muskiet, F.A.J., van den Berg, G.A., Kingma, A.W., Fremouw-Ottevangers, D.C., Halie, M.R., 1984. Total polyamines and their non-α-amino acid metabolites simultaneously determined in urine by capillary gas chromatography, with nitrogen-phosphorus detector; and some clinical applications. Clin. Chem. 30, 687-695.

Nakamura, H., Pisano, J., 1976. Derivatization of compounds at the origin of thin-layer plates with fluorescamine. J. Chromatogr. 121, 33-40.

Nakamura, H., Takagi, K., Tamura, Z., Yoda, R., Yamamoto, Y., 1984. Stepwise fluorometric determination of primary and secondary amines by liquid chromatography after derivatization with 2-methoxy-2,4-diphenyl-3(2H)-furanone. Anal. Chem. 56, 919-922.

Neadle, D.J., Pollit, R.J., 1965. The formation of l-dimethylaminonaphthalene-5-sulphonamide during the preparation of 1-dimethylaminonaphthalene-5-sulphonylamino-acids. Biochem. J. 97, 607-608.

Oertel, R., Neumeister, V., Kirch, W., 2004. Hydrophilic interaction chromatography combined with tandem-mass spectrometry to determine six aminoglycosides in serum. J. Chromatogr. A. 1058, 197-201.

Oguri, S., Yoneya, Y., Mizunuma, M., Fugiki, Y., Otsuka, K., Terube, S., 2002. Selective detection of amines using capillary electrochromatography with an on-column derivatization technique. Anal. Chem. 74, 3463-3469.

Omasch, F., Aikens, D., Bunce, S., Schwartz, H., Nairn, D., Hurwitz, C., 1984. The interactions between nucleic acids and polyamines: III. Microscopic protonation constants of spermidine. Biophys. Chem. 19, 245-253.

O'Reilly, E., Lanza, J., 1995. Fluorescamine: a rapid and inexpensive method for measuring total amino acids in nectars. Ecology 76, 2656-2660.

Osby, O., Martin, M., Ganem, B., 1984. An exceptionally mild deprotection of phthalimides. Tetrahedron Lett. 25, 2093-2096.

Oshima T., 1979, New polyamine, thermospermine, 1,12-diamino-4,8-diazadodecane, from an extreme thermophile. J. Biol. Chem. 254, 8720-8722.

Oshima T., 1983, Novel polyamines in Thermus thermophilus: Isolation, identification, and chemical synthesis. Methods Enzymol. 94, 401-411.

Palmer, B.N., Powell, H.K.J., 1974. Polyamine complexes with seven-membered chelate rings: complex formation of 3-azaheptane-1,7-diamine, 4-azaoctane-1,8-diamine (spermidine), and 4,9-diazadodecane-1,12-diamine (spermine) with copper (II) and hydrogen ions in aqueous solution. J. Chem. Soc. Dalton 19, 2089–2092.

Patchett, M.L., Monk, C.R., Daniel, R.M., Morgan, H.W., 1988. Determination of agmatine, arginine, citrulline and ornithine by reversed-phase liquid-chromatography using automated pre-column derivatization with ortho-phthalaldehyde. J. Chromatogr. B Biomed. Sci. Appl. 425, 269-276.

Price, J.R., Metz, P.A., Veening, H., 1987. HPLC of 9-fluorenylmethylchloroformate-polyamine derivatives with fluorescence detection. Chromatographia. 24, 795-790.

Raspaud, E., Chaperon, I., Leforestier, A., Livolant, F., 1999. Spermine-induced aggregation of DNA, nucleosome and chromatin. Biophys. J. 77, 1547-1555.

Rattenbury, J. M., Lax, P. M., Blau, K., Sandler, M., 1979, Separation and quantification of urinary di-and polyamines by chromatography with electron capture detection. Clin. Chim. Acta 95, 61-67.

Razin, S., Rozansky, R., 1957. The responsibility of spermine for the antibacterial action of human semen. J. Lab. Clin. Med. 49, 877-881.

Rosenheim, O., 1924. The isolation of spermine phosphate from semen and testis. Biochem. J. 18, 1253-1263.

Rosenthal, S. M., Tabor, C. W., 1958. The pharmacology of spermine and spermidine. Distribution and excretion. J. Pharmacol. 116, 131-138.

Roth, M., Hampai, A., 1973. Column chromatography of amino-acids with fluorescence detection. J. Chromatogr. 83, 353-356.

Roth, M., 1971. Fluorescence reaction for amino acids. Anal. Chem. 43, 880-882.

Sadain, S.K., Koropchak, J.A., 1999. Condensation nucleation light scattering detection for biogenic amines separated by ion-exchange chromatography. J. Chromatogr. A. 844, 111-118.

Sagirli, O., Ersoy, L., 2004. An HPLC method for the determination of lisinopril in human plasma and urine with fluorescence detection. J. Chromatogr. B. 809, 159-165.

Saifah, E, Puripattanavong, J., Likhitwitayawuid, K., Cordell, J. A., Chai, H., Pezzuto, J. M., 1993. Bisamides from Aglaia species: Structure analysis and potential to reverse drug resistance with cultured cells. J. Nat. Prod. 56, 473-477.

Saifah, E, Suparakchinda, N., 1998. Bis-amide from *Aglaia rubiginosa*. Planta Med. 64, 682.

Saifah, E, Suttisri, R., Shamsub, S., Pengsuparp, T., Lipipun, V., 1999. Bis-amide from *Aglaia edulis*. Phytochemistry 52, 1085-1088.

Sairam, R. K., Tyagi, A., 2004. Physiology and molecular biology of salinity stress tolerance in plants. Curr. Science 86, 407-421.

Saito,K., Horie,M., Nose,N., Nakagomi,K., Nakazawa,H., 1992. Determination of polyamines in foods by liquid chromatography with on-column fluorescence derivatization. Anal. Sci. 8, 675-680.

Salem, N., Zuman, P., 2006. Comparison of solution chemistries of ortho-phthaldehyde and 2,3-napthalenedicarboxaldehyde. Anal. Chem.78, 7802-7808.

Salem, N., Andreescu, S., Zuman, P., 2007. Existence and reactivity of three forms of orthophthalaldehyde in aqueous solution. polarographic, voltammetric and spectrophotometric study. J. Phys. Chem. A. 111, 4658-4670.

Samejima, K., Kawase, M., Sakamoto, S., Okada, M., Endo, Y., 1976. A sensitive fluorimetric method for the determination of aliphatic diamines and polyamines in biological materials by high-speed liquid chromatography. Anal. Biochem. 76, 392-406.

Samejima, K., 1974. Separation of fluorescamine derivatives of aliphatic diamines and polyamines by high-speed liquid chromatography. J. Chromatogr. 96, 250-254.

Schäfer, A., Benz, H., Fiedler, W., Guggisberg, A., Bienz, S., Hesse, M., 1994. Polyamine toxins from the venom of spiders and wasps. Alkaloids. Chem. Biol. 45, 1-125.

Schreiner, P., 1878. Ueber eine neue organische basis in thierischen organism. Liebigs Ann. 194, 68-84

Schuster, R., 1988. Determination of amino acids in biological, pharmaceutical, plant and food samples by automated pre-column derivatization and high-performance liquid chromatography. J. Chromatogr. B. Biomed. Sci. Appl. 431, 271-284.

Seiler, N.; Knodgen, B.; Eisenbeiss, F., 1978. Determination of di-and polyamines by high-performance liquid chromatographic separation of their 5-dimethylaminonaphthalene-1-sulfonyl derivatives. J. Chromatogr. 145, 29-39.

Seiler N., Wiechmann M., 1965. Determination of amines on the 10-10-mole scale. Separation of 1-dimethylamino-naphthalene-5-sulfonyl amides by thin-layer chromatography. Experientia, 21, 203-204.

Seiler N., Wiechmann M., 1966. Quantitative bestimmung von aminen und aminosauren als 1-dimethylamino-naphthalin-5-sulfonsaureamide auf dunnschichtchromatogrammen. Fresenius. Z Anal. Chem., 220, 109-127.

Seiler N., 1970. Use of the dansyl reaction in biochemical analysis. Methods Biochem. Anal., 18, 259-337.

Seiler, N, Schmidt, G.T., Schneide, H. H., 1973. 5-Di-N-butylaminonaphthalene-1-sulphonyl chloride-new reagent for fluorescence labelling of amines, amino-acids and peptides. J. Chromatogr. 84, 95-107.

Sheppeck II, J.E., Kar, H., Hong. H., 2000. A convenient and scalable procedure for removing the FMOC group in solution. Tetrahedron Lett. 41, 5329-5333.

Skelley, A., Mathies, R., 2003. Chiral separation of fluorescamine-labeled amino acids using microfabricated capillary electrophoresis devices for extraterrestrial exploration. J. Chromatogr. A. 1021, 191-199.

Silverman, M., Evans, E.A. Jr., 1943. The effects of spermidine and other polyamines on the growth inhibition of *Escherichia coli* by atabrine. J. Biol. Chem. 150, 265-266.

Simons, S., Johnson, D., 1976. The structure of fluorescent adduct formed in the reaction of *o*-phthalaldehyde and thiols with amines. J. Am. Chem. Soc. 98, 7098-7099.

Simons, S., Johnson, D., 1977. Ethanethiol: a thiol conveying improved properties to the fluorescent product of *o*-phthalaldehyde and thiols with amines. Anal. Biochem., 82, 250-254.

Simons, S., Johnson, D., 1978. Reaction of o-phthalaldehyde and thiols with primary amines formation of 1-Alkyl (and aryl)thio-2-alkylisoindoles. J. Org. Chem. 43, 705-725.

Simpson, R., Spriggle, J., Veening, H., 1983. Off-line liquid chromatographic-mass spectrometric studies of *o*-phthalaldehyde-primary amine derivatives. J. Chromatogr. A. 261, 407-414.

Slemr, J., Beyermann, K., 1984. Determination of biogenic amines in meat by combined ion-exchange and capillary gas chromatography. J. Chromatogr. 283, 241-250.
Smith, R.G., Daves, G.D. Jr., 1977. Gas-chromatography mass spectrometry mass-spectrometry analysis of polyamines using deuterated analogs as internal standards. Biomed. Mass Spectr. 4, 146-151.

Sneath, P.H.A., 1995. Putrescine as an essential growth factor for a mutant of *Aspergillus nidulans*. Nature 175, 818.

Stead, D.A., Richards, R.M.E., 1996. Sensitive fluorimetric determination of gentamicin sulfate in biological matrices using solid-phase extraction, pre-column derivatization with 9-fluorenylmethyl chloroformate and reversed-phase high-performance liquid chromatography J. Chromatogr. B 675, 295-302

Stein, S., Bohlen, P., Udenfriend, S., 1974. Studies on the reaction of fluorescamine with primary amines. Arch. Biochem, Biophys. 163, 390-399.

Still, W.C., Kahn, M., Mitra, A., 1978. Rapid chromatographic technique for preparative separation with moderate resolution. J. Org. Chem. 43, 2923-2925.

Stobaugh, J.F., Repta, A.J., Sternson, L.A., Garren, K.W., 1983. Factors affecting the stability of fluorescent isoindoles derived from reaction of ortho-phthalaldehyde and hydroxyalkylthiols with primary amines. Anal. Biochem. 135, 495-504.

Stockert, J., Blazquez, A., Galaz, S., Juarranz, A., 2008. A mechanism for the fluorogenic reaction of amino groups with fluorescamine and MDPF. Acta Histochem. 110, 333-340.

Stoev, G., Michailova, A., 2000. Quantitative determination of sulphonamide residues in foods of animal origin by high-performance liquid chromatography with fluorescence detection. J. Chromatogr. A. 871, 37-42.

Suzuki, S., Kobayashi, K., Noda, J., Suzuki, T., Takama, K., 1990. Simultaneous determination of biogenic amines by reversed-phase high-performance liquid chromatography. J. Chromatogr. 508, 225-228.

Tabor, C.W., 1962. Stabilization of protoplasts and spheroplasts by spermine and other polyamines. J. Bacteriol. 83, 1101-1111.

Tabor, C.W., Tabor, H., 1984. Polyamines. Annu. Rev. Biochem. 53, 749-790.

Tabor, C.W., Tabor, H., 1985. Polyamines in Microorganisms. Microbiol. Rev. 49, 81-99.

Tabor, H., Rosenthal, S.M., Tabor, C.W., 1958. Biosynthesis of spermidine and spermine from putrescine and methionine. J. Biol. Chem. 233, 907-914.

Takao, K., Miyatake, S., Fukazawa, K., Wada, M., Sugita, Y., Shirahata, A., 2008. Measurement of spermidine/spermine-N1-acetyltransferease activity by high-performance liquid chromatography with N1-dansylnorspermine as the substrate. Anal. Biochem. 376, 277-279.

Takeda, Y., Samejima, K., Nagano, K., Watanabe, M., Sugeta, H., Kyogoku, Y., 1983. Simultaneous determination of biogenic amines by reversed-phase high-performance liquid chromatography. Eur. J. Biochem. 130, 383-389.

Tawa, R., Matsunaga, H., Fujimoto, T., 1998. High-performance liquid chromatographic analysis of aminoglycoside antibiotics. J. Chromatogr. A. 812, 141-150.

Teti, D., Visalli, M., McNair, H., 2002. Analysis of polyamines as markers of (patho)physiological conditions. J. Chromatogr. B. Analyt. Technol. Biomed. Life. Sci. 781, 107-149.

Thomas , T., Thomas , T.J., 2003. Polyamine metabolism and cancer. J. Cell. Mol. Med. 7, 113-126.

Tonin, G.S., Wheeler, C.T., Crozier, A., 1991. A simple and sensitive high performance liquid chromatography procedure for the analysis of polyamines, Abst. 14th Int. Conf. Plant Growth substances, Amsterdam, 70.

Toumadje, A. Richardson, D.G., 1988. Endogenous polyamine concentrations during development, storage and ripening of pear fruits. Phytochemistry 27, 335-338.

Trepman, E., Chen, R., 1980. Fluorescence stopped-flow study of the *o*-phthalaldehyde reaction. Arch. Biochem. Biophys. 204, 524-532.

Tsukamoto, S., Kato, H., Hirota, H., Fusetani, N., 1996, Stellettadine A: a new acylated bisguanidinium alkaloid which induces larval metamorphosis in Ascidians from a marine sponge Stelletta sp. Tetrahedron Lett. 37, 5555-5556.

Udenfriend, S., Stein, S., Bohlen, P., Dairman, W., Leimgruber, W., Weigele, M., 1972. Fluorescamine-a reagent for assay of amino-acids, peptides, proteins, and primary amines in picomole range. Science 178, 871-872.

Umekage, S., Ueda, T., 2006. Spermidine inhibits transient and stable ribosome subunit dissociation. FEBS. Lett. 580, 1222-1226.

van den Berg, G.A., Muskiet, F.A.J., Kingma, A.W., van der Slik, W., Halie, M.R., 1986, Simultaneous gas-chromatographic determination of free and acetyl-conjugated polyamines in urine. Clin. Chem. 32, 1930-1937.

Varady, W.S., Rajur, S.B., Nicewonger, R.B., Guo, M.J., Ditto, L., 2000. Fast and quantitative high-performance liquid chromatography method for the determination of 9-fluorenyl-methoxycarbonyl release from solid-phase synthesis resins. J. Chromatogr. A. 869, 171-179.

Veening, H., Pitt, W., Jones, G., 1974. Ion-exchange chromatographic separation and fluorometric detection of urinary polyamines. J. Chromatogr. 90, 129-139.

Vidal-Carou, C., Lahoz-Portoles, F., Bover-Cid, S., Marine-Font, A., 2003, Ion-pair high-performance liquid chromatographic determination of biogenic amines and polyamines in wine and other alcoholic beverages. J. Chromatogr. A. 998, 235-241.

Waksman, S.A., Lechevalier, H.A., 1949. Neomycin, a new antibiotic active against streptomycin-resistant bacteria, including tuberculosis organisms. Science 109, 305-307.

Walden, R., Cordeiro, A., Tiburcio, A.F., 1997. Polyamines: small molecules triggering pathways in growth and development. Plant Physiol. 113, 1009-1013.

Wallace, H.M., Fraser, A.F., Hughes, A., 2003. A perspective of polyamine metabolism. Biochem. J. 376, 1-14.

Wallace, H.M., Niiranen, K., 2007. Polyamine analogues - an update. Amino Acids. 33, 261-265.

Wang, G.Y.S., Graziani, E., Waters, B., Pan, W., Li, X., McDermott, J., Meurer, G., Saxena, G., Andersen, R.J., Davies, J., 2000. Novel natural products from soil DNA libraries in a Streptomycete host. Org. Lett. 2, 2401-2404.

Watanabe, S., Kusama-Eguchi, K., Kobayashi, H., Igarashi, K., 1991. Estimation of polyamine binding to macromolecules and ATP in bovine lymphocytes and rat liver. J. Biol. Chem. 266, 20803-20809.

Weaver, R.H., Herbst, E.J., 1958. Metabolism of diamines and polyamines in microorganisms. J. Biol. Chem. 231, 637-646.

Weber G., 1952. Polarization of the fluorescence of macromolecules. 2. Fluorescent conjugates of ovalbumin and bovine serum albumin. Biochem. J. 51, 155-167.

Weigele, M., Debernado, S.L., Tengi, J.P., Leimgruber, W., 1972. A novel reagent for the fluorometric assay of primary amines. J. Am. Chem. Soc. 94, 5927-5928.

Wettlaufer, S.H., Weinstein, L.H., 1988. Quantitation of polyamines using thin-layer chromatography and image analysis. J. Chromatogr. 441, 361-366.

Wienen, F., Holzgrabe, U., 2002. Characterization of paramomycin sulphate by capillary electrophoresis with UV detection after pre-capillary derivatization. Chromatographia 55, 327-331.

Wong, O., Sternson, L., Schowen, R., 1985. Reaction of *o*-phthalaldehyde with alanine and thiols: Kinetics and mechanism. J. Am. Chem. Soc. 107, 6421-6422.

Wortham, B.W., Patel, C.N., Oliveira, M.A., 2007. Polyamines in bacteria: pleiotropic effects yet specific mechanisms. Adv. Exp. Med. Biol. 603, 106-115.

Wrede, F., 1924. Zur kenntnis des spermins III. Hoppe-Seyl. Z. 138, 119-135.

Wrede, F., 1925. Ueber die aus dem menschlichen sperma isolierte base spermin. Dtsch. Med. Wschr. 51, 24.

Wrede, F., 1926. Zur kenntnis des spermins IV. Hoppe-Seyl. Z. 153, 291-312.

Wrede, F., Banik, E., 1923. Zur kenntnis des spermins II. Uber die von schreiner aus dem sperma isolierte base. Hoppe-Seyl. Z. 131, 38-53.

Wrede, F., Fanselow, H., Strack, E., 1926. Information on the spermine. V Zur kenntnis des spermins V. Hoppe-Seyl. Z. 161, 66-73.

Wrede, F., Fanselow, H., Strack, E., 1926. Information on the spermine. VI Zur kenntnis des spermins VI. Hoppe-Seyl. Z. 163, 219-228.

Yamamoto, S., Yokogawa, M., Wakamatsu, K., Kataoka, H., Makita, M., 1982. Gas chromatographic method for the determination of urinary acetylpolyamines. J. Chromatogr. B 233, 29-38.

Yamamoto, S., Kobayashi, T., Suemoto, Y., Makita, M., 1984. An improved gas chromatographic method for the determination of urinary acetylpolyamines. Chem. Pharm. Bull. 32, 1878-1884.

Yoshitake, M., Nohta, H., Yoshida, H., Yoshitake, T., Todoroki, K., Yamaguchi, M., 2006. Selective determination of native fluorescent bioamines though precolumn derivatization and liquid chromatography using intramolecular fluorescence resonance energy transfer detection. Anal. Chem. 78, 920-927.

Yu, H. J., Chen, C. C., Shieh, B. J., 1998. Two new constituents from the leaves of *Magnolia coco*. J. Nat. Prod. 61, 1017-1019.

Yu, Z., Li, W., Brunk, U.T., 2003. 3-Aminopropanal is a lysosomotropic aldehyde that causes oxidative stress and apoptosis by rupturing lysosomes. APMIS. 111, 643-652.

Zhan, W., Wang, T., Li, S., 2000. Derivatization, extraction and concentration of amino acids and peptides by using organic/aqueous phases in capillary electrophoresis with fluorescence detection. Electrophoresis 21, 3593-3599.

Zhou, Y., Yang, W., Zhhang, L., Wang, Z., 2007. Determination of kanamycin A in animal feeds by solid phase extraction and high performance liquid chromatography with pre-column derivatization and fluorescence detection. J. Liq. Chromatogr. Relat. Technol. 30, 1603-1615.

Appendix

Four Abstracts (three Posters and one Oral) from these studies were presented at the following international meetings:

Analytical Research Forum 2007, RSC, Glasgow, UK;

The Interface of Chemistry and Biology in the Omics Era 2007, The Sixth Princess Chulabhorn International Science Congress, Bangkok, Thailand;

Bioorganic Chemistry 2008, RSC, Bath, UK;

British Pharmaceutical Conference (BPC) 2008, Manchester, UK.

Poster presentation at RSC, Analytical Research Forum 2007.
University of Strathclyde, Glasgow, UK. 16 – 18 July 2007.

PHARMACEUTICAL ANALYSIS OF POLYAMINES AND AMINOGLYCOSIDES

Sawanya Buranaphalin, Dr I S Blagbrough, Dr M G Rowan**

Department of Pharmacy and Pharmacology, University of Bath, Bath BA2 7AY

prsisb@bath.ac.uk

Fluorescence derivatives have long been used in the polyamines which lack chromophores in their molecules. In this study, fluorescence derivatization was extended to examine partially protected polyamines, aminoglycosides and synthetic intermediates in the preparation of complex lipophilic polyamine compounds required for non-viral gene delivery investigations. Fluorescence spectroscopy and poly-derivatization with a panel of extrinsic fluorophores (e.g. dansyl chloride, *o*-phthalaldehyde, 9-fluorenylmethoxycarbonyl chloride and fluorescamine derivatives) will enable optimization of synthetic routes in with analysis of intermediates. A variety of natural products which contain several amine functional groups: 2 (putrescine, cadaverine), 3 (spermidine), 4 (spermine, kanamycin), 5 (tobramycin, paromomycin), up to 6 (neomycin) and also synthetic intermediates such as diphthalimido spermine, trifluoroacetate spermine, tri-Boc spermine were examined.

After derivatization, the di- and polyamines were separated by the reversed-phase high performance liquid chromatography (RP-HPLC) on the ODS column (150 x 4 mm I.D., 5 μm) using suitable isocratic systems, a flow rate of 1 ml min^{-1} and fluorescence detection. Where necessary, the contaminants, produced during the derivatization reaction, were almost eliminated by extraction steps. The identity of fluorescent derivatives was confirmed by liquid chromatography-mass spectrometry to monitor for partial derivatization of polyamino compounds.

The results show that synthesis of polyamine derivatives in quantitative yield depends on the time of reaction, the temperature and the ratio of fluorophore reagent. A number of model chromatographic separations of polyamine-fluorophores were achieved. Linearity of derivatization was calculated for amines and regression coefficient ranged from 0.968 to 0.999. The repeatability of the method was good. In some cases, the derivatization reactions failed to yield the desired products due to incompatibility of the reaction conditions with protecting groups present in the substrate. Relative quantum yields of the polyamine-fluorophores derivatives also examined to determine the effect of intramolecular quenching which was appeared to give less fluorescence intensity in some polyamine-fluorophores derivatives. This methodology will provide a useful way to analyse semi-synthetic analogues of those natural products which are being developed as vehicles for non-viral gene delivery.

Acknowledgements: Thai Government Collaborative Research Network.

Poster presentation at The Sixth Princess Chulabhorn International Science Congress, Bangkok Thailand. 25-29 November 2007.
The Interface of Chemistry and Biology in the Omics Era: Drug Discovery #19 NP.

ANALYSIS OF LINEAR AND BRANCHED POLYAMINE NATURAL PRODUCT CONJUGATES FOR EFFICIENT BIOPHARMACEUTICAL DELIVERY

Sawanya Buranaphalin, Michael G. Rowan, and Ian S. Blagbrough
Department of Pharmacy and Pharmacology, University of Bath, Bath BA2 7AY, U.K.

The development of the innovative, nano- and biotechnologies for drug delivery, together with the use of natural products and their conjugates in drug discovery and as biomarkers make the application of linear polyamines, e.g. spermidine and spermine, and aminoglycosides (branched naturally occurring polyamines e.g. neomycin with 6 amines) important as pharmaceutical leads for the efficient delivery of biopharmaceuticals e.g. siRNA delivery and DNA delivery for gene therapy.

Our continuing research on organic nano-bioparticles as vehicles for non-viral gene delivery has afforded a library of semi-synthetic polyamine conjugates which are efficient at DNA condensation and DNA delivery. These compounds e.g. N^4,N^9- dioleoyl-spermine and a cholesteryl neomycin conjugate have been synthesized in our laboratories. However, their quantitative analysis is challenging as they lack any chromophore. In order to analyse these polyamine-containing molecules, fluorescence derivatization was used. We have developed methods for poly-derivatization with a panel of extrinsic fluorophores (e.g. dansyl chloride, *o*-phthalaldehyde, 9-fluorenylmethoxycarbonyl chloride and fluorescamine) followed by HPLC with fluorescence and UV absorption detection. These methods enable optimization of synthetic routes with analysis of intermediates.

Reaction and chromatographic conditions were optimized with each of the above fluorophores using a series of model mono- and diamines and finally applied to natural and semi-synthetic polyamines. Linear responses were obtained over the concentration range (0.01-1.0 mM). The relative quantum yields of the polyamine-fluorophore derivatives were examined to determine the effect of intramolecular quenching. This methodology will provide a useful way to analyse semi-synthetic analogues of these important natural products which are being developed as efficient vehicles for non-viral gene delivery.

We thank the CRN for financial support (studentship to SB).

Poster presentation at RSC Bioorganic Meeting, University of Bath. 31 March 2008. Poster Abstract #23.

ANALYSIS OF LINEAR AND BRANCHED POLYAMINE NATURAL PRODUCT CONJUGATES FOR EFFICIENT BIOPHARMACEUTICAL DELIVERY

Sawanya Buranaphalin, Michael G. Rowan, and Ian S. Blagbrough
Department of Pharmacy and Pharmacology, University of Bath, Bath BA2 7AY, U.K.

Investigation of organic nano-bioparticles as vehicles for non-viral gene delivery has afforded a library of semi-synthetic polyamine conjugates which are efficient at DNA condensation and DNA delivery. We are continuing our studies with compounds containing linear polyamines, e.g. spermidine and spermine which are then applied to drug delivery. However, their quantitative analysis is challenging as they lack any chromophore.[1] In order to analyse these polyamine-containing molecules, fluorescence derivatization has been applied.

One aim of this study was to extend fluorescence derivatization to examine partially protected polyamines and synthetic intermediates in the preparation of complex lipophilic polyamine conjugates required for non-viral gene delivery investigations.

We have developed methods for poly-derivatization with a panel of extrinsic fluorophores (e.g. dansyl chloride,[1] OPA (*o*-phthalaldehyde),[2] FMOC (9-fluorenylmethoxycarbonyl chloride)[2,3] and fluorescamine) followed by HPLC with both fluorescence and UV absorption detection. The target analytes, e.g. natural and semi-synthetic polyamines, possess multiple amino-functions, primary and secondary including some which are sterically hindered. The reaction and chromatographic conditions were optimized for each fluorophore using a series of model mono- and diamines and finally applied to the linear and branched polyamine natural product conjugates. The methods we have developed enable the analytical optimization of synthetic routes. Our results show that synthesis of polyamine derivatives in quantitative yield depends on the reaction conditions: time, temperature, and the molar ratio of derivatization reagent to substrate amine. The chemical structures of the resulting derivatives were confirmed by off-line high resolution electrospray ionization mass spectrometry (HR ESI-MS). Linear responses were obtained over the concentration range (0.01-1.0 mM). The relative quantum yields of the polyamine-fluorophore derivatives were examined to determine the effect of intramolecular quenching.

Off-line MS analysis of the reaction products demonstrated complete derivatization of both primary and secondary amino groups with dansyl and FMOC fluorescent derivatives and of primary amine groups for OPA and fluorescamine derivatives. Dansyl derivatization of polyamines showed no apparent steric hindrance. Under the HR ESI-MS ionization conditions used, the expected $[M+H]^+$ and also the doubly charged $[(M+2H)/2]^{++}$ ions were often observed with dansyl derivatives, presumably because this fluorophore contains basic amino groups that can be protonated easily, whereas FMOC derivatives gave predominantly $[M+Na]^+$ ions. The OPA reaction with polyamines is rapid, but the products have poor stability. The derivatization of polyamines with fluorescamine gave multiple products (HPLC analysis). In summary, this methodology to detect and quantify polyamines and their conjugates provides a useful way to analyse semi-synthetic analogues of these important natural products which are being developed as efficient vehicles for non-viral gene delivery and as anti-cancer lead compounds where quantitative analysis is important.

We acknowledge the CRN for financial support (studentship to SB) and we also thank the EPSRC National Mass Spectrometry Centre (Swansea) for rapid and efficient HR MS analytical services.

1. Minocha R., Long S., *J. Chromatogr. A*, 2004, **1035**, 63-73.
2. Koros A., Hanczko R., Jambor A., Qian Y., Perl A., Molnar-Perl I., *J. Chromatogr. A*, 2007, **1149**, 46-55.
3. Lozanov V., Petrov S., Mitev V., *J. Chromatogr. A* 2004, **1025,** 201-208.

Oral Presentation at British Pharmaceutical Conference (BPC) Manchester. Pharmacy in the 21st Century, Adding years to life and life to years. 7 – 9 September 2008.
This was awarded the Prize for the Best Oral Presentation.

ANALYSIS OF LINEAR AND BRANCHED POLYAMINE NATURAL PRODUCT CONJUGATES FOR EFFICIENT BIOPHARMACEUTICAL DELIVERY

Sawanya Buranaphalin, Michael G. Rowan, and Ian S. Blagbrough
Department of Pharmacy and Pharmacology, University of Bath, Bath BA2 7AY, U.K.

Objectives:
The applications of linear polyamines, e.g. spermidine and spermine and branched polyamines e.g. aminoglycosides as the innovative biotechnologies for drug delivery are continuing researched in our group. The organic nano-bioparticles as vehicles for non-viral gene delivery has afforded a library of semi-synthetic polyamine conjugates which are efficient at DNA condensation and DNA delivery. However, their quantitative analysis is challenging as they lack any chromophore[1]. In order to analyse these polyamine-containing molecules, fluorescence derivatization was used.

Methods:
We have developed methods for poly-derivatization with a panel of extrinsic fluorophores (e.g. dansyl chloride[2], *o*-phthalaldehyde, 9-fluorenylmethoxycarbonyl chloride[3] and fluorescamine) followed by HPLC with fluorescence and UV absorption detection. These methods enable optimization of synthetic routes with analysis of intermediates. Reaction and chromatographic conditions were optimized with each of the above fluorophores using a series of model mono- and diamines and finally applied to natural and semi-synthetic polyamines. The resulted derivatives were confirmed by off-line high resolution electrospray ionization mass spectrometry. Linear responses were obtained over the concentration range (0.01-1.0 mM). The relative quantum yields of the polyamine-fluorophore derivatives were examined to determine the effect of intramolecular quenching.

Results:
The results show that synthesis of polyamine derivatives in quantitative yield depends on the time of reaction, the temperature and the ratio amount of the labels chromophore. Protonated polyamines e.g. putrescine, spermidine and spermine are polycations when made the derivatization of these molecules with the chromophore. Off-line MS analysis of the reaction products demonstrated complete derivatization of both primary and secondary amino groups with dansyl and FMOC fluorescence derivatives and of primary amine groups for OPA and fluorescamine derivatives. Under the ionization condition used the derivatives showed bivalent cation $[(M+2H)/2]^{++}$ in addition to monovalent ions $(M+H)^{+}$ with Dansyl derivatives because this chromophore contain basic amino groups that can be protonated easily whereas FMOC derivatives gave prominent [M+Na]+ ions. Derivatization of polyamines showed no apparent steric hindrance. OPA reaction is rapid but the products have poor stability. The derivatization with fluorescamine gave multiple products with polyamines and chiral compounds due to the presence of a chiral cetre in the fluorophore

Conclusions:
This methodology will provide a useful way to analyse semi-synthetic analogues of these important natural products which are being developed as efficient vehicles for non-viral gene delivery.

We thank the CRN for financial support (studentship to SB).

References:
1. Minocha R., Long S., (2004) *J. Chromatogr. A* **1035**: 63-73.
2. Lozanov V., Petrov S., Mitev V., (2004) *J. Chromatogr. A* **1025**: 201- 208.
3. Koros A., Hanczko R., Jambor A., Qian Y., Perl A., Molnar-Perl I., (2007) *J. Chromatogr. A* **1149**: 46-55.